

# 6

## APPLIED ELECTROMAGNETICS

In Chapter 2 we set our goal to learn how to interpret Maxwell's equations and the associated constitutive relations and to use them to discuss various applications. In the preceding chapters we achieved the first task, namely that of introducing and understanding Maxwell's equations,

$$\nabla \cdot \mathbf{D} = \rho$$

$$\nabla \cdot \mathbf{B} = 0$$

$$\nabla \times \mathbf{E} = -\frac{\partial \mathbf{B}}{\partial t}$$

$$\nabla \times \mathbf{H} = \mathbf{J} + \frac{\partial \mathbf{D}}{\partial t}$$

and the various related concepts. We now have the basic electromagnetic theory necessary to venture into the realm of applied electromagnetic theory to which this chapter serves as an introduction. The topics of applied electromagnetic theory are varied, but perhaps the most important among them are concerned with the field basis of circuit theory and with electromagnetic waves. This is reflected in the topics covered in this chapter.

# PART I. Statics, Quasistatics, and Distributed Circuits

## 6.1 Poisson's Equation

Maxwell's equations for the static electric field are given by

$$\nabla \cdot \mathbf{D} = \rho \quad (6-1)$$

$$\nabla \times \mathbf{E} = 0 \quad (6-2)$$

In view of (6-2),  $\mathbf{E}$  can be expressed as the gradient of a scalar potential  $V$  as we learned in Section 2.12. Thus we have

$$\mathbf{E} = -\nabla V \quad (6-3)$$

and

$$\mathbf{D} = \epsilon \mathbf{E} = -\epsilon \nabla V \quad (6-4)$$

Substituting (6-4) into (6-1), we obtain

$$\nabla \cdot \epsilon \nabla V = -\rho$$

or

$$\nabla V \cdot \nabla \epsilon + \epsilon \nabla^2 V = -\rho \quad (6-5)$$

where  $\nabla^2 V$  is the Laplacian of  $V$ . Equation (6-5) is the differential equation for the electrostatic potential  $V$  in a region of volume charge density  $\rho$ . If we assume that  $\epsilon$  is a constant in the region,  $\nabla \epsilon$  is equal to zero so that (6-5) reduces to

$$\nabla^2 V = -\frac{\rho}{\epsilon} \quad (6-6)$$

Equation (6-6) is known as Poisson's equation. If the medium is charge free, then  $\rho = 0$  and (6-6) reduces to

$$\nabla^2 V = 0 \quad (6-7)$$

which is known as Laplace's equation. In this section we discuss the applications of Poisson's equation by considering two examples.

**EXAMPLE 6-1.** Charge is distributed with uniform density  $\rho_0$  C/m<sup>3</sup> throughout a sphere of radius  $a$  centered at the origin. It is desired to find the electrostatic potential and hence the electric field intensity both inside and outside the sphere by using Poisson's equation for  $r < a$  and Laplace's equation for  $r > a$ .

From Poisson's and Laplace's equations, we have

$$\nabla^2 V = \begin{cases} -\frac{\rho_0}{\epsilon} & \text{for } r < a \\ 0 & \text{for } r > a \end{cases} \quad (6-8)$$

Because of the spherical symmetry of the charge distribution, the potential is a function of  $r$  only. Thus all derivatives of  $V$  with respect to  $\theta$  and  $\phi$  are

zero, so that (6-8) becomes

$$\frac{\partial}{\partial r} \left( r^2 \frac{\partial V}{\partial r} \right) = \begin{cases} -\frac{\rho_0 r^2}{\epsilon} & \text{for } r < a \\ 0 & \text{for } r > a \end{cases} \quad (6-9)$$

Integrating both sides of (6-9) with respect to  $r$  and then dividing by  $r^2$  and integrating again with respect to  $r$ , we obtain

$$V = \begin{cases} -\frac{\rho_0 r^2}{6\epsilon} - \frac{A}{r} + B & \text{for } r < a \\ -\frac{C}{r} + D & \text{for } r > a \end{cases} \quad (6-10)$$

where  $A$ ,  $B$ ,  $C$ , and  $D$  are arbitrary constants of integration.

We now have to evaluate the arbitrary constants  $A$ ,  $B$ ,  $C$ , and  $D$  by using the boundary conditions and other considerations. First, the potential can be arbitrarily set equal to zero at  $r = \infty$ , so that  $D = 0$ . Second, from  $\mathbf{E} = -\nabla V$ , we have

$$\mathbf{E} = \begin{cases} \left( \frac{\rho_0 r}{3\epsilon} - \frac{A}{r^2} \right) \mathbf{i}_r & \text{for } r < a \\ -\frac{C}{r^2} \mathbf{i}_r & \text{for } r > a \end{cases}$$

so that, from Gauss' law, the charge contained within a sphere of radius  $r$  ( $< a$ ) centered at the origin is  $4\pi r^2 \epsilon E_r = 4\pi r^2 \epsilon [(\rho_0 r/3\epsilon) - (A/r^2)]$ . For the charge distribution under consideration, this quantity must approach zero as  $r \rightarrow 0$ . This is possible only if  $A$  is equal to zero. The solution for  $V$  is thus reduced to

$$V = \begin{cases} -\frac{\rho_0 r^2}{6\epsilon} + B & \text{for } r < a \\ -\frac{C}{r} & \text{for } r > a \end{cases} \quad (6-11)$$

Next, we note that, at the boundary  $r = a$ , the potential must be continuous in the absence of an impulse type of discontinuity in the normal component of electric field intensity (such discontinuities can exist in the presence of an electric dipole layer at the surface). Also, at  $r = a$ ,  $D_r$  must be continuous in the absence of a surface charge. Using these two boundary conditions, we have

$$-\frac{\rho_0 a^2}{6\epsilon} + B = -\frac{C}{a} \quad (6-12a)$$

$$\epsilon \frac{\rho_0 a}{3\epsilon} = -\epsilon \frac{C}{a^2} \quad (6-12b)$$

Solving (6-12a) and (6-12b) for  $B$  and  $C$  and substituting in (6-11), we obtain

the required solution for  $V$  as

$$V = \begin{cases} -\frac{\rho_0 r^2}{6\epsilon} + \frac{\rho_0 a^2}{2\epsilon} & \text{for } r < a \\ \frac{\rho_0 a^3}{3\epsilon r} & \text{for } r > a \end{cases} \quad (6-13)$$

The corresponding solution for  $\mathbf{E}$  is

$$\mathbf{E} = \begin{cases} \frac{\rho_0 r}{3\epsilon} \mathbf{i}_r & \text{for } r < a \\ \frac{\rho_0 a^3}{3\epsilon r^2} \mathbf{i}_r & \text{for } r > a \end{cases} \quad (6-14)$$

We note that this solution is in agreement with the result of Example 2-6. ■

In the preceding example we illustrated the method of solving for the potential for a given charge distribution, using Poisson's and Laplace's equations. However, Poisson's equation is more useful for another class of problems, in which the charge distribution is the quantity to be determined. We now consider an example of this type.

**EXAMPLE 6-2.** A simplified model of a vacuum diode consists of two parallel conducting plates occupying the planes  $x = 0$  and  $x = d$ , between which an electric field is established by maintaining a potential difference of  $V_0$  volts as shown in Fig. 6.1. The plate at the lower potential is called the cathode and the plate at the higher potential is called the anode. The cathode is heated so that it emits electrons into the space between the plates, to be collected by the anode and thereby establish a current flow. Let us assume for simplicity that (a) the electrons are emitted from the cathode with zero

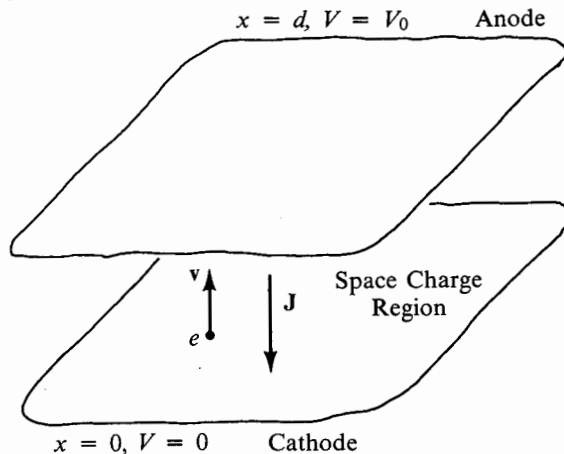


**Fig. 6.1.** Simplified model of a vacuum diode.

initial velocity and (b) the number of electrons emitted from the cathode is limited not by the cathode temperature but by the space charge between the cathode and the anode. For steady current flow under these conditions, the electric field at the cathode is zero. If it were some nonzero value and directed towards the cathode, the electrons would be emitted from the cathode with some acceleration and the current would then be temperature limited but not space-charge limited. (In the actual case, the field intensity is slightly nonzero and directed towards the cathode, since no electrons would leave the cathode otherwise.) If the field intensity were some nonzero value and directed towards the anode, there would be no space charge, since the electrons could not leave the cathode. It is desired to find the potential distribution and hence the space charge distribution between the cathode and the anode.

Let  $V$  be the potential at a distance  $x$  from the cathode, which is considered to be at zero potential. Then the work done by the electric field in moving an electron through a distance  $x$  from the cathode is equal to  $|e|V$ , where  $e$  is the charge of the electron. This work must be equal to the kinetic energy acquired by the electron. Thus, denoting  $\mathbf{v} = v(x)\mathbf{i}_x$  as the velocity of the electron, we have

$$|e|V = \frac{1}{2}mv^2 \quad (6-15)$$

where  $m$  is the electronic mass. From (6-15), we get  $v = \sqrt{2|e|V/m}$  so that

$$\mathbf{v} = \sqrt{\frac{2|e|V}{m}}\mathbf{i}_x \quad (6-16)$$

If  $\rho(x)$  is the density of the space charge constituted by the electrons, the current density  $\mathbf{J}$  is given by

$$\mathbf{J} = \rho\mathbf{v} = \rho\sqrt{\frac{2|e|}{m}}V^{1/2}\mathbf{i}_x \quad (6-17)$$

For steady current flow,

$$\mathbf{J} = J_0\mathbf{i}_x \quad (6-18)$$

where  $J_0$  is a constant. Comparing the right sides of (6-17) and (6-18) we obtain

$$\rho = J_0\sqrt{\frac{m}{2|e|}}V^{-1/2}$$

From Poisson's equation, we now have

$$\frac{d^2V}{dx^2} = -\frac{\rho}{\epsilon_0} = -\left[\frac{J_0}{\epsilon_0}\sqrt{\frac{m}{2|e|}}\right]V^{-1/2} = kV^{-1/2} \quad (6-19)$$

where  $k = -(J_0/\epsilon_0)\sqrt{m/2e}$  is a constant. Equation (6-19) is the differential equation for  $V$  in the region between the cathode and the anode. To solve for  $V$ , we multiply the left and right sides of (6-19) by  $2(dV/dx)dx$  and  $2dV$ ,

respectively, to obtain

$$2 \frac{dV}{dx} d\left(\frac{dV}{dx}\right) = 2kV^{-1/2} dV \quad (6-20)$$

Integrating both sides of (6-20), we get

$$\left(\frac{dV}{dx}\right)^2 = 4kV^{1/2} + A$$

where  $A$  is the constant of integration to be evaluated from the boundary condition for  $dV/dx$  at the cathode. But  $dV/dx$  is the negative of the electric field intensity. Since the electric field intensity as well as the potential are zero at the cathode,  $A$  is equal to zero. Thus

$$\frac{dV}{dx} = 2\sqrt{k} V^{1/4}$$

or

$$V^{-1/4} dV = 2\sqrt{k} dx \quad (6-21)$$

Integrating both sides of (6-21), we obtain

$$\frac{4}{3} V^{3/4} = 2\sqrt{k} x + B$$

where  $B$  is the constant of integration. To evaluate  $B$ , we note that  $V = 0$  for  $x = 0$ . Hence  $B = 0$ , giving us

$$V = \left(\frac{3}{2}\sqrt{k} x\right)^{4/3}$$

Finally, from the condition that  $V = V_0$  for  $x = d$ , we have

$$V_0 = \left(\frac{3}{2}\sqrt{k} d\right)^{4/3}$$

so that

$$V = V_0 \left(\frac{x}{d}\right)^{4/3} \quad (6-22)$$

Equation (6-22) is the required solution for the potential between the two plates. The electric field intensity is given by

$$\mathbf{E} = -\nabla V = -\frac{\partial V}{\partial x} \mathbf{i}_x = -\frac{4}{3} \frac{V_0}{d} \left(\frac{x}{d}\right)^{1/3} \mathbf{i}_x$$

The space charge density is given by

$$\rho = \epsilon_0 \nabla \cdot \mathbf{E} = \epsilon_0 \frac{\partial E_x}{\partial x} = -\frac{4}{9} \frac{\epsilon_0 V_0}{d^2} \left(\frac{x}{d}\right)^{-2/3}$$

The current density is given by

$$\mathbf{J} = \rho \sqrt{\frac{2|e|}{m}} V^{1/2} \mathbf{i}_x = -\frac{4}{9} \epsilon_0 \sqrt{\frac{2|e|}{m}} \frac{V_0^{3/2}}{d^2} \mathbf{i}_x$$

This equation is known as the Child–Langmuir law. The negative sign for  $\mathbf{J}$  arises from the fact that the current flow is opposite to the direction of motion of the electrons.

## 6.2 Laplace's Equation

A very important class of problems encountered in practice are those for which the charges are confined to the surfaces of conductors. For such problems, either the charge distribution on the surfaces of the conductors, or the potentials of the conductors, or a combination of the two are specified and the problem consists of finding the potential and hence the electric field in the charge-free region bounded by the conductors. Obviously, the potential in the charge-free region satisfies Laplace's equation

$$\nabla^2 V = 0 \quad (6-7)$$

assuming  $\epsilon$  to be constant. Hence the solution consists of finding a potential that satisfies Laplace's equation and the specified boundary conditions. Since the right side of Laplace's equation is zero irrespective of the boundary conditions, we can obtain a general solution for the potential that satisfies a particular simplified form of Laplace's equation once and for all. The general solution consists of arbitrary constants of integration, which are evaluated by using the boundary conditions for the specific problem.

Let us consider the cartesian coordinate system. In the general case for which the potential is a function of all three coordinates  $x$ ,  $y$ , and  $z$ , Laplace's equation is given by

$$\frac{\partial^2 V}{\partial x^2} + \frac{\partial^2 V}{\partial y^2} + \frac{\partial^2 V}{\partial z^2} = 0 \quad (6-23)$$

However, if the potential is a function of only one of the coordinates, say  $x$ , and independent of the other two, we obtain a simplified version of Laplace's equation as

$$\frac{\partial^2 V}{\partial x^2} = \frac{d^2 V}{dx^2} = 0 \quad (6-24)$$

Integrating (6-24) with respect to  $x$  twice, we obtain

$$V = Ax + B \quad (6-25)$$

where  $A$  and  $B$  are the arbitrary constants of integration. Equation (6-25) is the general solution for the electrostatic potential in a charge-free region for the case in which the potential is a function of  $x$  only. In other words, all problems for which the potential varies with  $x$  only but having different boundary conditions must have solutions of the form given by (6-25). Only the values of the arbitrary constants  $A$  and  $B$  differ from one problem to the other. Thus, having found the general solution once and for all, it is a matter of fitting the given boundary conditions to evaluate the arbitrary constants for obtaining the particular solution to the problem. Let us consider a simple example.

**EXAMPLE 6-3.** Two parallel conducting plates occupying the planes  $x = 0$  and  $x = d$  are kept at potentials  $V = 0$  and  $V = V_0$ , respectively, as shown in

Fig. 6.2. We wish to find the solution for the potential and hence for the electric field intensity between the plates and evaluate the charge densities on the plates.

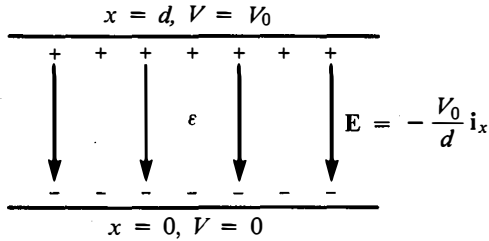


Fig. 6.2. Two parallel perfectly conducting plates separated by a dielectric of permittivity  $\epsilon$  and kept at potentials  $V = 0$  and  $V = V_0$ .

The general solution for the potential between the two plates is given by (6-25). The boundary conditions are

$$V = 0 \quad \text{for } x = 0$$

$$V = V_0 \quad \text{for } x = d$$

Substituting these boundary conditions in (6-25), we have

$$0 = A(0) + B \quad \text{or} \quad B = 0$$

$$V_0 = A(d) + B = A(d) + 0 \quad \text{or} \quad A = \frac{V_0}{d}$$

Thus the required solution for the potential is

$$V = \frac{V_0}{d}x \quad 0 < x < d$$

The electric field intensity is given by

$$\mathbf{E} = -\nabla V = -\frac{\partial V}{\partial x}\mathbf{i}_x = -\frac{V_0}{d}\mathbf{i}_x \quad 0 < x < d$$

The field is shown sketched in Fig. 6.2. The surface charge densities on the two plates are given by

$$[\rho_s]_{x=0} = [\mathbf{D}]_{x=0} \cdot \mathbf{i}_x = -\frac{\epsilon V_0}{d}\mathbf{i}_x \cdot \mathbf{i}_x = -\frac{\epsilon V_0}{d}$$

$$[\rho_s]_{x=d} = [\mathbf{D}]_{x=d} \cdot (-\mathbf{i}_x) = \left(-\frac{\epsilon V_0}{d}\mathbf{i}_x\right) \cdot (-\mathbf{i}_x) = \frac{\epsilon V_0}{d} \quad \blacksquare$$

**EXAMPLE 6-4.** Let the region between the two plates in Example 6-3 consist of two dielectric media having permittivities  $\epsilon_1$  for  $0 < x < t$  and  $\epsilon_2$  for  $t < x < d$  as shown in Fig. 6.3. It is desired to find the solutions for the potentials in the two regions  $0 < x < t$  and  $t < x < d$ .

Since the permittivities of the two regions are different, the solutions for the potentials in the two regions must be different although having the same general form as given by (6-25). We therefore choose different arbitrary constants for the two different regions. Thus the general solutions for the



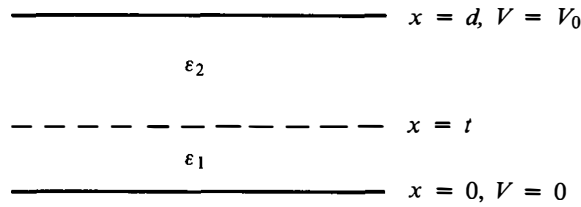


**Fig. 6.3.** Two parallel perfectly conducting plates separated by two dielectric media of permittivities  $\epsilon_1$  and  $\epsilon_2$  and kept at potentials  $V = 0$  and  $V = V_0$ .

potentials in the two regions are

$$V_1 = A_1x + B_1 \quad 0 < x < t \quad (6-26a)$$

$$V_2 = A_2x + B_2 \quad t < x < d \quad (6-26b)$$

The boundary conditions specified in the problem are

$$V_1 = 0 \quad \text{for } x = 0 \quad (6-27a)$$

$$V_2 = V_0 \quad \text{for } x = d \quad (6-27b)$$

However, we have four arbitrary constants  $A_1, B_1, A_2,$  and  $B_2$  to be determined. Hence we need two more boundary conditions. Obviously, we turn our attention to the boundary  $x = t$  between the two dielectrics for these two conditions, which are

$$V_1 = V_2 \quad \text{for } x = t \quad (6-27c)$$

and

$$D_{x_1} = D_{x_2}$$

or

$$\epsilon_1 \frac{\partial V_1}{\partial x} = \epsilon_2 \frac{\partial V_2}{\partial x} \quad \text{for } x = t \quad (6-27d)$$

Substituting the four boundary conditions (6-27a)–(6-27d) into (6-26a) and (6-26b), we obtain

$$0 = A_1(0) + B_1$$

$$V_0 = A_2(d) + B_2$$

$$A_1(t) + B_1 = A_2(t) + B_2$$

$$\epsilon_1 A_1 = \epsilon_2 A_2$$

Solving these four equations for the four arbitrary constants and substituting the resulting values in (6-26a) and (6-26b), we find the required solutions for  $V_1$  and  $V_2$  as

$$V_1 = \frac{\epsilon_2 x}{\epsilon_2 t + \epsilon_1(d-t)} V_0 \quad 0 < x < t$$

$$V_2 = \frac{\epsilon_2 t + \epsilon_1(x-t)}{\epsilon_2 t + \epsilon_1(d-t)} V_0 \quad t < x < d$$

The potential at the interface  $x = t$  is

$$\frac{\epsilon_2 t}{\epsilon_2 t + \epsilon_1 (d - t)} V_0 \quad \blacksquare$$

Thus far we have considered the one-dimensional case for which the potential is a function of  $x$  only. The one-dimensional problems for which the potentials are a function of  $y$  only and  $z$  only are not any different from the case considered, since the differential equations for  $V$  are the same as (6-24) except that  $x$  is replaced by  $y$  or  $z$ . Thus there is only one one-dimensional problem in the cartesian coordinate system although there are three coordinates. Considering the three commonly used coordinate systems, that is, cartesian, cylindrical, and spherical coordinate systems and arguing in this manner, we note that there are only five different one-dimensional problems in all although there are nine coordinates. There is not much to be gained by considering in detail the remaining four one-dimensional problems. Hence we simply list in Table 6.1 the general solutions for each case, a particular set of boundary conditions and the corresponding particular solution. It is left as an exercise (Problem 6.3) for the student to verify these.

**TABLE 6.1.** General Solutions for One-Dimensional Laplace's Equations and Particular Solutions for Particular Sets of Boundary Conditions

<i>Coordinate with Which <math>V</math> Varies</i>	<i>General Solution</i>	<i>Boundary Conditions</i>	<i>Particular Solution</i>
$x$	$Ax + B$	$V = 0, x = 0$ $V = V_0, x = d$	$\frac{V_0 x}{d}$
$r$ (cylindrical)	$A \ln r + B$	$V = 0, r = a$ $V = V_0, r = b$	$\frac{V_0}{\ln b/a} \ln \frac{r}{a}$
$\phi$	$A\phi + B$	$V = 0, \phi = 0$ $V = V_0, \phi = \alpha$	$\frac{V_0}{\alpha} \phi$
$r$ (spherical)	$\frac{A}{r} + B$	$V = 0, r = a$ $V = V_0, r = b$	$\frac{V_0}{(1/b) - (1/a)} \left( \frac{1}{r} - \frac{1}{a} \right)$
$\theta$	$A \ln \left( \tan \frac{\theta}{2} \right) + B$	$V = 0, \theta = \alpha$ $V = V_0, \theta = \beta$	$V_0 \frac{\ln [(\tan \theta/2)/(\tan \alpha/2)]}{\ln [(\tan \beta/2)/(\tan \alpha/2)]}$

Before we take up the discussion of Laplace's equation in two dimensions, we consider briefly the use of analogy in solving magnetic field problems involving permanent magnetization. From Maxwell's curl equation for the static magnetic field, we have, for a region free of true currents, that is, for  $\mathbf{J} = 0$ ,

$$\nabla \times \mathbf{H} = 0$$

We can then express  $\mathbf{H}$  as the gradient of a scalar magnetic potential  $V_m$ ,

that is,

$$\mathbf{H} = -\nabla V_m \quad (6-28)$$

Substituting  $\mathbf{B} = \mu_0(\mathbf{H} + \mathbf{M})$  in Maxwell's divergence equation for  $\mathbf{B}$ , we have

$$\nabla \cdot \mathbf{B} = \nabla \cdot \mu_0(\mathbf{H} + \mathbf{M}) = 0$$

or

$$\nabla \cdot \mathbf{H} = -\nabla \cdot \mathbf{M} \quad (6-29)$$

Substituting (6-28) into (6-29), we obtain

$$\nabla^2 V_m = \nabla \cdot \mathbf{M} \quad (6-30)$$

Comparing (6-28) and (6-30) with (6-3) and (6-6), respectively, we observe the following analogy:

$$\mathbf{H} \longleftrightarrow \mathbf{E} \quad (6-31a)$$

$$V_m \longleftrightarrow V \quad (6-31b)$$

$$\nabla \cdot \mathbf{M} \longleftrightarrow -\frac{\rho}{\epsilon} \quad (6-31c)$$

If  $\mathbf{M}$  is discontinuous at a boundary, then  $\nabla \cdot \mathbf{M}$  results in an impulse function. To find the appropriate analogy, we consider a rectangular box of infinitesimal volume  $\Delta v$  and enclosing a portion of the boundary at which  $\mathbf{M}$  is discontinuous as shown in Fig. 6.4. Then we have

$$\int_{\Delta v} \nabla \cdot \mathbf{M} \, dv \longleftrightarrow - \int_{\Delta v} \frac{\rho}{\epsilon} \, dv$$

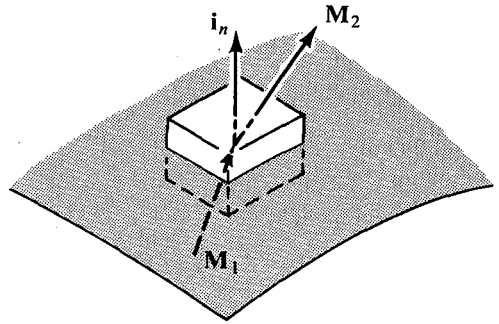


**Fig. 6.4.** For showing that a discontinuity in  $\mathbf{M}$  at a boundary is analogous to a surface charge density.

From the divergence theorem,  $\int_{\Delta v} \nabla \cdot \mathbf{M} \, dv$  is equal to  $\oint_S \mathbf{M} \cdot \mathbf{i}_n \, dS$ , where  $S$  is the surface area of the box. Now, if we let the box shrink to the boundary, this integral becomes  $(\mathbf{M}_2 - \mathbf{M}_1) \cdot \mathbf{i}_n \Delta S$  whereas  $\int_{\Delta v} (\rho/\epsilon) \, dv$  becomes  $(\rho_s/\epsilon) \Delta S$ , where  $\Delta S$  is the surface area on the boundary to which the box shrinks and  $\rho_s$  is the surface charge density. Thus we have

$$(\mathbf{M}_2 - \mathbf{M}_1) \cdot \mathbf{i}_n \Delta S \longleftrightarrow -\frac{\rho_s}{\epsilon} \Delta S$$

or

$$(\mathbf{M}_2 - \mathbf{M}_1) \cdot \mathbf{i}_n \leftrightarrow -\frac{\rho_s}{\epsilon} \quad (6-31d)$$

Making use of the analogy indicated by (6-31a)–(6-31d), we can solve magnetostatic problems involving permanent magnetization. Let us consider an example.

**EXAMPLE 6-5.** The region  $0 < x < d$  is occupied by a medium characterized by the magnetization vector  $\mathbf{M} = M_0 \mathbf{i}_x$ , where  $M_0$  is a constant, as shown in Fig. 6.5(a). It is desired to find  $\mathbf{H}$  and  $\mathbf{B}$  both inside and outside the region  $0 < x < d$ .

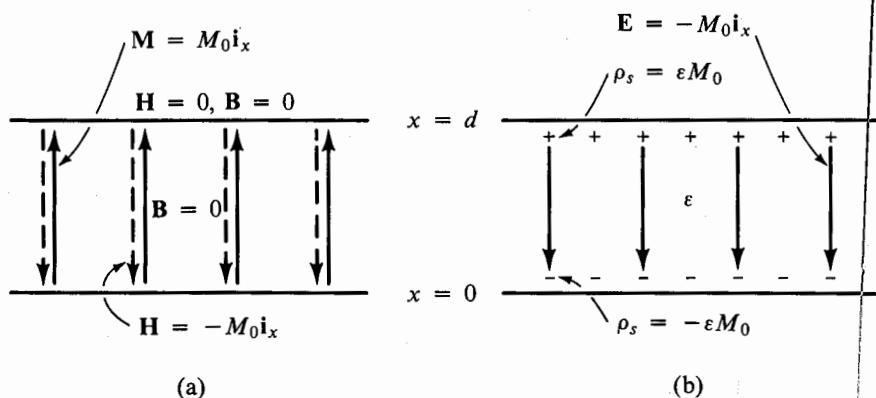


**Fig. 6.5.** (a) A medium characterized by magnetization vector  $\mathbf{M} = M_0 \mathbf{i}_x$ . (b) Electrostatic analog of (a).

Since there are no true currents associated with the medium, we can use the analogy developed above. For the given  $\mathbf{M}$ ,  $\nabla \cdot \mathbf{M} = 0$  so that the analogous volume charge density is zero. However,

$$(\mathbf{M}_2 - \mathbf{M}_1) \cdot \mathbf{i}_n = \begin{cases} (0 - M_0 \mathbf{i}_x) \cdot (-\mathbf{i}_x) = M_0 & \text{for } x = 0 \\ (0 - M_0 \mathbf{i}_x) \cdot \mathbf{i}_x = -M_0 & \text{for } x = d \end{cases}$$

The analogous surface charge density is therefore given by

$$\rho_s = \begin{cases} -\epsilon M_0 & \text{for } x = 0 \\ \epsilon M_0 & \text{for } x = d \end{cases}$$

From the solution to Example 6-3, the electrostatic potential and the electric field intensity for this surface charge distribution are

$$V = M_0 x$$

$$\mathbf{E} = \begin{cases} -M_0 \mathbf{i}_x & 0 < x < d \\ 0 & \text{otherwise} \end{cases}$$

The surface charge distribution and the electric field lines are shown in Fig. 6.5(b). Now, from (6-31a), the required magnetic field intensity is given by

$$\mathbf{H} = \begin{cases} -M_0 \mathbf{i}_x & 0 < x < d \\ 0 & \text{otherwise} \end{cases}$$

The corresponding magnetic flux density is

$$\begin{aligned} \mathbf{B} = \mu_0(\mathbf{H} + \mathbf{M}) &= \begin{cases} \mu_0(-M_0 \mathbf{i}_x + M_0 \mathbf{i}_x) & 0 < x < d \\ \mu_0(0 + 0) & \text{otherwise} \end{cases} \\ &= 0 \quad \text{everywhere} \end{aligned}$$

These are shown in Fig. 6.5(a). ■

We now consider the solution of Laplace's equation in two dimensions. If the potential is a function of the two coordinates  $x$  and  $y$  and independent of  $z$ , then it satisfies the equation

$$\frac{\partial^2 V}{\partial x^2} + \frac{\partial^2 V}{\partial y^2} = 0 \quad (6-32)$$

Equation (6-32) is a partial differential equation in two dimensions  $x$  and  $y$ . The technique by means of which it is solved is known as the "separation of variables" technique. It consists of assuming that the solution for the potential is the product of two functions, one of which is a function of  $x$  only and the second, a function of  $y$  only. Denoting these functions to be  $X$  and  $Y$ , respectively, we have

$$V(x, y) = X(x) Y(y) \quad (6-33)$$

Substituting this assumed solution into the differential equation, we obtain

$$Y \frac{d^2 X}{dx^2} + X \frac{d^2 Y}{dy^2} = 0 \quad (6-34)$$

Dividing both sides of (6-34) by  $XY$  and rearranging, we get

$$\frac{1}{X} \frac{d^2 X}{dx^2} = -\frac{1}{Y} \frac{d^2 Y}{dy^2} \quad (6-35)$$

The left side of (6-35) involves  $x$  only whereas the right side involves  $y$  only. Thus Eq. (6-35) states that a function of  $x$  only is equal to a function of  $y$  only. A function of  $x$  only other than a constant cannot be equal to a function of  $y$  only other than the same constant for all values of  $x$  and  $y$ . For example,  $2x$  is equal to  $4y$  for only those pairs of values of  $x$  and  $y$  for which  $x = 2y$ . But we are seeking a solution which is good for all pairs of  $x$  and  $y$ . Thus the only solution which satisfies (6-35) is that each side of (6-35) must be equal to a constant. Denoting this constant as  $\alpha^2$ , we have

$$\frac{d^2 X}{dx^2} = \alpha^2 X \quad (6-36a)$$

and

$$\frac{d^2Y}{dy^2} = -\alpha^2 Y \quad (6-36b)$$

Note that we have obtained two ordinary differential equations involving the separate independent variables  $x$  and  $y$ , respectively, starting with the partial differential equation involving both of the variables  $x$  and  $y$ . It is for this reason that the method is known as the separation of variables technique. The constant  $\alpha^2$  is known as the separation constant.

For a nonzero  $\alpha^2$ , the solutions for Eq. (6-36a) must be functions of  $x$  which when differentiated twice result in the same functions multiplied by  $\alpha^2$ . The functions that satisfy this property are the exponential functions  $e^{\alpha x}$  and  $e^{-\alpha x}$ . Since (6-36a) is a linear differential equation, the general solution consists of a superposition of the two solutions multiplied by arbitrary constants. For  $\alpha^2 = 0$ , the solution for (6-36a) can be obtained by integrating it twice. Thus

$$X(x) = \begin{cases} Ae^{\alpha x} + Be^{-\alpha x} & \text{for } \alpha \neq 0 \\ A_0x + B_0 & \text{for } \alpha = 0 \end{cases} \quad (6-37a)$$

where  $A, B, A_0$ , and  $B_0$  are the arbitrary constants. Similarly, for  $\alpha^2 \neq 0$ , the solutions for Eq. (6-36b) must be functions of  $y$  which when differentiated twice result in the same functions multiplied by  $-\alpha^2$ . The functions that satisfy this property are  $\cos \alpha y$  and  $\sin \alpha y$ . Again, since (6-36b) is a linear differential equation, the general solution consists of a superposition of the two solutions multiplied by arbitrary constants. For  $\alpha^2 = 0$ , the solution for (6-36b) can be obtained by integrating it twice. Thus

$$Y(y) = \begin{cases} C \cos \alpha y + D \sin \alpha y & \text{for } \alpha \neq 0 \\ C_0y + D_0 & \text{for } \alpha = 0 \end{cases} \quad (6-37b)$$

where  $C, D, C_0$ , and  $D_0$  are the arbitrary constants. Substituting (6-37a) and (6-37b) into (6-33), we obtain the required solution for (6-32) as

$$V(x, y) = \begin{cases} (Ae^{\alpha x} + Be^{-\alpha x})(C \cos \alpha y + D \sin \alpha y) & \text{for } \alpha \neq 0 \\ (A_0x + B_0)(C_0y + D_0) & \text{for } \alpha = 0 \end{cases} \quad (6-38)$$

We now consider an example of the application of (6-38).

**EXAMPLE 6-6.** Let us consider the idealized problem of an infinitely long rectangular slot cut in a semiinfinite plane conducting slab held at zero potential as shown in Fig. 6.6. With reference to the coordinate system shown in the figure, assume that a potential distribution given by  $V = V_0 \sin(\pi y/b)$ , where  $V_0$  is a constant, is created at the mouth  $x = a$  of the slot by the application of a potential to an appropriately shaped conductor away from the mouth of the slot not shown in the figure. It is desired to find the potential distribution in the slot.

The problem is two dimensional in  $x$  and  $y$  and hence the general solution

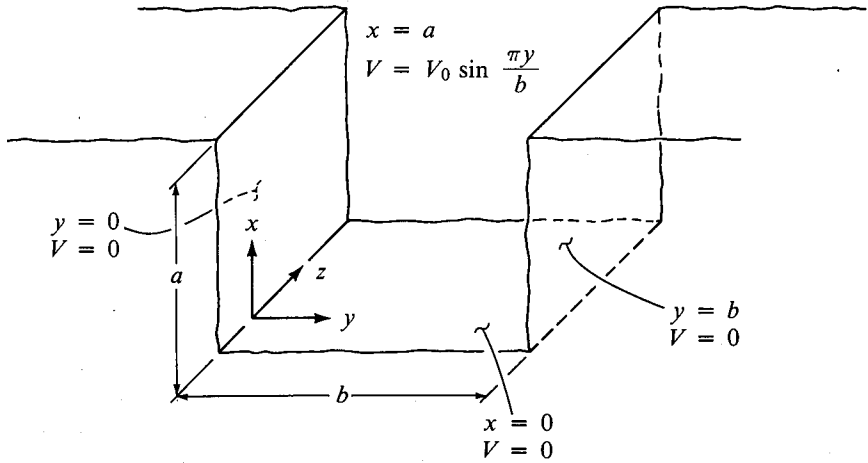


Fig. 6.6. An infinitely long rectangular slot cut in a semiinfinite plane conducting slab at zero potential. The potential at the mouth of the slot is  $V_0 \sin(\pi y/b)$  volts.

for  $V$  is given by (6-38). The boundary conditions are

$$V = 0 \quad y = 0, 0 < x < a \quad (6-39a)$$

$$V = 0 \quad y = b, 0 < x < a \quad (6-39b)$$

$$V = 0 \quad x = 0, 0 < y < b \quad (6-39c)$$

$$V = V_0 \sin \frac{\pi y}{b} \quad x = a, 0 < y < b \quad (6-39d)$$

The solution corresponding to  $\alpha = 0$  does not fit the boundary conditions since  $V$  is required to be zero for two values of  $y$  and in the range  $0 < x < a$ . Hence we can ignore that solution and consider only the solution for  $\alpha \neq 0$ . Applying the boundary condition (6-39a), we have

$$0 = (Ae^{\alpha x} + Be^{-\alpha x})(C) \quad \text{for } 0 < x < a$$

The only way of satisfying this equation for a range of values of  $x$  is by setting  $C = 0$ . Next, applying the boundary condition (6-39c), we have

$$0 = (A + B)D \sin \alpha y \quad \text{for } 0 < y < b$$

This requires that  $(A + B)D = 0$ , which can be satisfied by either  $D = 0$  or  $A + B = 0$ . However,  $D = 0$  results in a trivial solution of zero for the potential. Hence we set

$$A + B = 0 \quad \text{or} \quad B = -A$$

Thus the solution for  $V$  reduces to

$$\begin{aligned} V(x, y) &= (Ae^{\alpha x} - Ae^{-\alpha x})D \sin \alpha y \\ &= A' \sinh \alpha x \sin \alpha y \end{aligned} \quad (6-40)$$

where  $A' = 2AD$ . Next, applying boundary condition (6-39b) to (6-40), we have

$$0 = A' \sinh \alpha x \sin \alpha b \quad \text{for } 0 < x < a$$

To satisfy this equation without obtaining a trivial solution of zero for the potential, we set

$$\sin \alpha b = 0$$

or

$$\alpha b = n\pi \quad n = 1, 2, 3, \dots$$

$$\alpha = \frac{n\pi}{b} \quad n = 1, 2, 3, \dots \quad (6-41)$$

Since several values of  $\alpha$  given by (6-41) satisfy the boundary condition, several solutions are possible for the potential. To take this fact into account, we write the solution as the superposition of all these solutions multiplied by different arbitrary constants. In this manner we obtain

$$V(x, y) = \sum_{n=1,2,3,\dots}^{\infty} A'_n \sinh \frac{n\pi x}{b} \sin \frac{n\pi y}{b} \quad \text{for } 0 < y < b \quad (6-42)$$

Finally, applying the boundary condition (6-39d) to (6-42), we get

$$V_0 \sin \frac{\pi y}{b} = \sum_{n=1,2,3,\dots}^{\infty} A'_n \sinh \frac{n\pi a}{b} \sin \frac{n\pi y}{b} \quad \text{for } 0 < y < b \quad (6-43)$$

On the right side of (6-43), we have an infinite series of sine terms in  $y$  whereas on its left side, we have only one sine term in  $y$ . Equating the coefficients of the sine terms having the same arguments, we obtain

$$A'_n \sinh \frac{n\pi a}{b} = \begin{cases} V_0 & \text{for } n = 1 \\ 0 & \text{for } n \neq 1 \end{cases}$$

or

$$A'_1 = \frac{V_0}{\sinh(\pi a/b)}$$

$$A'_n = 0 \quad \text{for } n \neq 1$$

Substituting this result in (6-42), we obtain the required solution for  $V$  as

$$V(x, y) = V_0 \frac{\sinh(\pi x/b)}{\sinh(\pi a/b)} \sin \frac{\pi y}{b} \quad (6-44)$$

Having found the solution, it is always worthwhile to check if it satisfies Laplace's equation and the given boundary conditions to make sure that no error was made in obtaining the solution. The above solution does satisfy these two criteria. ■

If the solution, irrespective of how it is obtained, satisfies Laplace's equation and the specified boundary conditions, it is *the* solution according to the uniqueness theorem. To prove this theorem, let us assume to the contrary that two solutions  $V_1$  and  $V_2$  are possible for the same problem.



Then each of these must satisfy Laplace's equation so that

$$\nabla^2 V_1 = 0 \quad (6-45a)$$

$$\nabla^2 V_2 = 0 \quad (6-45b)$$

The difference  $V_d = V_1 - V_2$  must also satisfy Laplace's equation. Thus

$$\nabla^2 V_d = \nabla^2(V_1 - V_2) = \nabla^2 V_1 - \nabla^2 V_2 = 0 \quad (6-46)$$

Also, both  $V_1$  and  $V_2$  must satisfy the same boundary conditions, so that

$$[V_d]_S = [V_1 - V_2]_S = [V_1]_S - [V_2]_S = 0 \quad (6-47)$$

where  $S$  represents the boundary surface. Now, using the vector identity

$$\nabla \cdot (VA) = V \nabla \cdot \mathbf{A} + \nabla V \cdot \mathbf{A}$$

we have

$$\nabla \cdot (V_d \nabla V_d) = V_d \nabla^2 V_d + |\nabla V_d|^2 \quad (6-48)$$

Integrating both sides of (6-48) throughout the volume enclosed by the boundary  $S$ , we have

$$\int_{\text{vol}} (\nabla \cdot V_d \nabla V_d) dv = \int_{\text{vol}} (V_d \nabla^2 V_d) dv + \int_{\text{vol}} |\nabla V_d|^2 dv \quad (6-49)$$

However, from the divergence theorem and from (6-47),

$$\int_{\text{vol}} (\nabla \cdot V_d \nabla V_d) dv = \oint_S (V_d \nabla V_d) \cdot d\mathbf{S} = 0$$

Also, noting that  $\nabla^2 V_d = 0$  in accordance with (6-46), Eq. (6-49) reduces to

$$\int_{\text{vol}} |\nabla V_d|^2 dv = 0 \quad (6-50)$$

Since  $|\nabla V_d|^2$  is positive everywhere, the only way that (6-50) can be satisfied is if  $|\nabla V_d|^2$  is equal to zero throughout the volume of interest. Thus

$$\nabla V_d = 0$$

or

$$V_d = V_1 - V_2 = \text{constant} \quad (6-51)$$

However,  $V_d$  is equal to zero on the boundaries and hence the constant on the right side of (6-51) must be zero, giving us  $V_1 = V_2$  throughout the volume of interest and thereby proving the uniqueness theorem.

**EXAMPLE 6-7.** The rectangular slot of Fig. 6.6 is covered at the mouth  $x = a$  by a conducting plate which is kept at a potential  $V = V_0$ , a constant, making sure that the edges touching the corners of the slot are insulated as shown by the cross-sectional view in Fig. 6.7(a). We wish to find the potential in the slot for this new boundary condition.

Since the boundary conditions (6-39a)–(6-39c) remain the same, all we have to do to find the required solution for the potential is to substitute

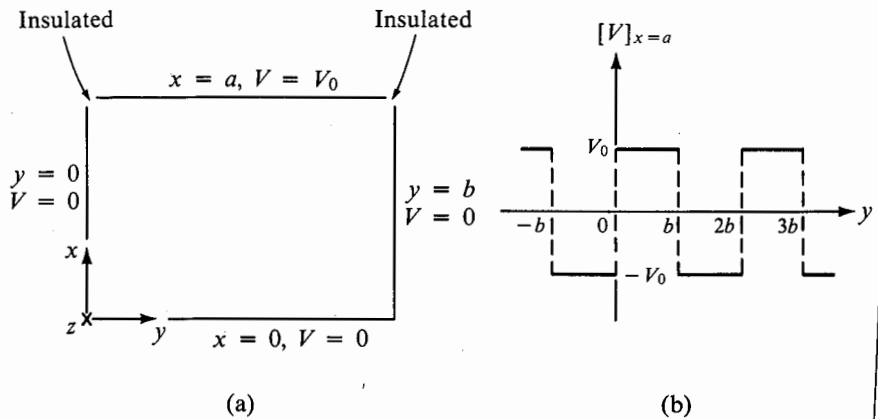


Fig. 6.7. (a) Cross section of an infinitely long rectangular slot cut in a semiinfinite plane conducting slab held at zero potential and covered at the mouth by a conducting plate held at a potential of  $V_0$  volts. (b) Choice of potential to create an odd periodic function of period  $2b$  in  $y$  for  $[V]_{x=a}$ .

the new boundary condition

$$V = V_0 \quad x = a, 0 < y < b$$

in (6-42) and evaluate the coefficients  $A'_n$ . Thus we have

$$V_0 = \sum_{n=1,2,3,\dots}^{\infty} A'_n \sinh \frac{n\pi a}{b} \sin \frac{n\pi y}{b} \quad \text{for } 0 < y < b \quad (6-52)$$

We have an infinite series of sine terms in  $y$  having periods  $2b/n$  on the right side of (6-52) whereas the left side of (6-52) is a constant. Thus we cannot hope to obtain  $A'_n$  simply by comparing the coefficients of the sine terms having like arguments. If we do so, we get the ridiculous answer of  $V_0 = 0$  and all  $A'_n = 0$  since there is no constant term on the right side and there are no sine terms on the left side. The correct way of evaluating  $A'_n$  is to make use of the so-called orthogonality property of sine functions, which reads

$$\int_{y=0}^p \sin \frac{m\pi y}{p} \sin \frac{n\pi y}{p} dy = \begin{cases} 0 & m \neq n \\ \frac{p}{2} & m = n \end{cases}$$

where  $m$  and  $n$  are integers. Multiplying both sides of (6-52) by  $\sin(m\pi y/b) dy$  and integrating between the limits 0 and  $b$ , we have

$$\int_{y=0}^b V_0 \sin \frac{m\pi y}{b} dy = \int_{y=0}^b \sum_{n=1,2,3,\dots}^{\infty} A'_n \sinh \frac{n\pi a}{b} \sin \frac{n\pi y}{b} \sin \frac{m\pi y}{b} dy \quad (6-53)$$

The integration and summation on the right side of (6-53) can be inter-

changed, giving us

$$\int_{y=0}^b V_0 \sin \frac{m\pi y}{b} dy = \sum_{n=1,2,3,\dots}^{\infty} A'_n \sinh \frac{n\pi a}{b} \int_{y=0}^b \sin \frac{m\pi y}{b} \sin \frac{n\pi y}{b} dy$$

or

$$\frac{V_0 b}{m\pi} (1 - \cos m\pi) = \left( A'_m \sinh \frac{m\pi a}{b} \right) \frac{b}{2}$$

or

$$A'_m = \begin{cases} \frac{4V_0}{m\pi} \frac{1}{\sinh(m\pi a/b)} & \text{for } m \text{ odd} \\ 0 & \text{for } m \text{ even} \end{cases} \quad (6-54)$$

Substituting this result in (6-42), we obtain the required solution for the potential inside the slot as

$$V = \sum_{n=1,3,5,\dots}^{\infty} \frac{4V_0}{n\pi} \frac{\sinh(n\pi x/b)}{\sinh(n\pi a/b)} \sin \frac{n\pi y}{b} \quad (6-55)$$

The above procedure for evaluating the constants  $A'_n$  can also be appreciated by recognizing that the right side of (6-52) is the Fourier series for an odd periodic function in  $y$  having the period  $2b$ . We must then have an odd periodic function of period  $2b$  on the left side of (6-52). To achieve this, we note that, since the solution is for inside the slot only, it is sufficient if we satisfy the boundary condition for  $[V]_{x=a}$  for the range  $0 < y < b$ . We are therefore at liberty to choose  $[V]_{x=a}$  for the remainder of  $y$  so that an odd periodic function of period  $2b$  is obtained. Obviously, the choice must be as shown in Fig. 6.7(b). The evaluation of  $A'_n$  then consists of finding the coefficients of the Fourier series for this function and comparing these with the coefficients of the series on the right side of (6-52). The steps leading from (6-53) to (6-54) are essentially equivalent to this procedure.

Another class of problems for which Laplace's equation is applicable is those involving the determination of steady current in a conducting slab under the application of potential difference between different surfaces of the slab. For the steady-current condition we have

$$\nabla \cdot \mathbf{J}_c = 0$$

where  $\mathbf{J}_c$  is the current density. Replacing  $\mathbf{J}_c$  by  $\sigma \mathbf{E}$ , where  $\sigma$  is the conductivity of the slab, we have

$$\nabla \cdot \sigma \mathbf{E} = 0$$

Substituting for  $\mathbf{E}$  in terms of  $V$ , we get

$$-\nabla \cdot \sigma \nabla V = 0 \quad (6-56)$$

If  $\sigma$  is constant, Eq. (6-56) reduces to

$$\nabla^2 V = 0$$

Thus the potential associated with the steady current flow satisfies Laplace's equation. Hence the solution for this potential can be obtained in exactly the same manner as for the charged conductor problems. In fact, the solution for the potential for a particular steady-current problem can be written down by inspection if the solution for the potential for an analogous charged conductor problem is already known and vice versa. Having found the solution for the potential, the current density can be found by using

$$\mathbf{J}_c = \sigma \mathbf{E} = -\sigma \nabla V \quad (6-57)$$

**EXAMPLE 6-8.** A thin rectangular slab of uniform conductivity  $\sigma_0$  mhos/m has its edges coated with perfectly conducting material. One of the edges is kept at a potential  $V_0$  relative to the other three by appropriate placement of insulators as shown in Fig. 6.8(a). It is desired to find the steady-current distribution in the conductor.

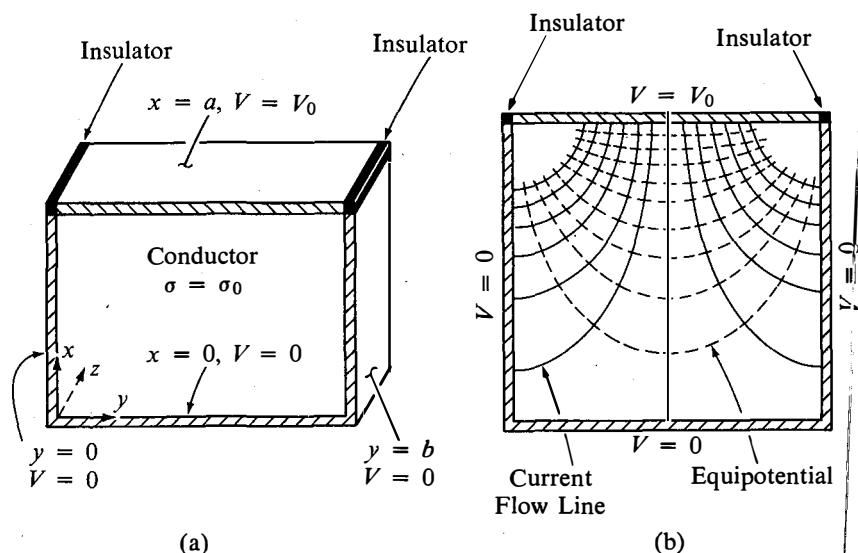


**Fig. 6.8.** (a) A rectangular slab of conductivity  $\sigma_0$  with one of its edges kept at a potential  $V_0$  relative to the other three. (b) Equipotentials and direction lines of current density for the conducting slab for the case  $b/a = 1$ .

The problem is exactly analogous to the rectangular slot problem of Example 6-7. Hence, from the solution for the potential found in that problem and given by (6-55), we obtain the required current density as

$$\begin{aligned} \mathbf{J}_c &= -\sigma_0 \nabla \left( \sum_{n=1,3,5,\dots}^{\infty} \frac{4V_0 \sinh(n\pi x/b)}{n\pi \sinh(n\pi a/b)} \sin \frac{n\pi y}{b} \right) \\ &= -\frac{4V_0 \sigma_0}{b} \sum_{n=1,3,5,\dots}^{\infty} \frac{1}{\sinh(n\pi a/b)} \left( \cosh \frac{n\pi x}{b} \sin \frac{n\pi y}{b} \mathbf{i}_x \right. \\ &\quad \left. + \sinh \frac{n\pi x}{b} \cos \frac{n\pi y}{b} \mathbf{i}_y \right) \end{aligned}$$

The approximate shapes of the equipotentials and the direction lines of  $\mathbf{J}_c$  are sketched in Fig. 6.8(b) for  $b = a$ , that is, for a square conducting slab. ■

We have illustrated the solution of the two-dimensional Laplace's equation in the cartesian coordinates  $x$  and  $y$  and its applications. The technique of solution in the other coordinate systems or even in three dimensions is the same, that is, the separation of variables technique except that we get some complicated functions in certain cases. Hence, instead of pursuing this topic further, we will discuss a numerical method of solving Laplace's equation which is well suited for adaptation to a digital computer. To illustrate the principle behind the method, let us pose the following problem: Supposing we know the potentials  $V_1, V_2, \dots, V_6$  at six points which are equidistant from a point  $P(0, 0, 0)$  and lying on mutually perpendicular axes (which we call  $x, y,$  and  $z$ ) passing through  $P$  as shown in Fig. 6.9, how do we

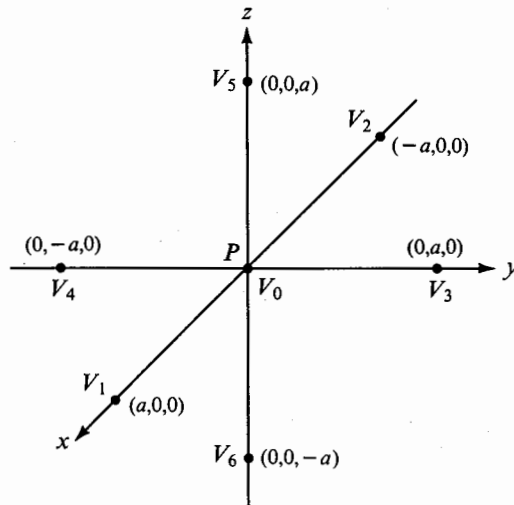


Fig. 6.9. For showing that the potential at a point  $P$  is approximately equal to the average of the potentials at six points equidistant from  $P$  and lying along mutually perpendicular axes through  $P$ .

evaluate approximately the potential at the point  $P$  consistent with Laplace's equation? To answer this question, we recognize that

$$[\nabla^2 V]_P = [\nabla^2 V]_{(0,0,0)} = \left[ \frac{\partial^2 V}{\partial x^2} + \frac{\partial^2 V}{\partial y^2} + \frac{\partial^2 V}{\partial z^2} \right]_{(0,0,0)} = 0 \quad (6-58)$$

However,

$$\begin{aligned}
 \left[ \frac{\partial^2 V}{\partial x^2} \right]_{(0,0,0)} &\approx \frac{1}{a} \left\{ \left[ \frac{\partial V}{\partial x} \right]_{(a/2,0,0)} - \left[ \frac{\partial V}{\partial x} \right]_{(-a/2,0,0)} \right\} \\
 &\approx \frac{1}{a} \left\{ \frac{[V]_{(a,0,0)} - [V]_{(0,0,0)}}{a} - \frac{[V]_{(0,0,0)} - [V]_{(-a,0,0)}}{a} \right\} \\
 &= \frac{1}{a^2} (V_1 - V_0 - V_0 + V_2) \\
 &= \frac{1}{a^2} (V_1 + V_2 - 2V_0)
 \end{aligned} \tag{6-59a}$$

Similarly,

$$\left[ \frac{\partial^2 V}{\partial y^2} \right]_{(0,0,0)} \approx \frac{1}{a^2} (V_3 + V_4 - 2V_0) \tag{6-59b}$$

and

$$\left[ \frac{\partial^2 V}{\partial z^2} \right]_{(0,0,0)} \approx \frac{1}{a^2} (V_5 + V_6 - 2V_0) \tag{6-59c}$$

Substituting (6-59a)–(6-59c) into (6-58) and rearranging, we have

$$V_0 \approx \frac{1}{6} (V_1 + V_2 + V_3 + V_4 + V_5 + V_6) \tag{6-60}$$

Thus the potential at  $P$  is approximately equal to the average of the potentials at the six equidistant points lying along mutually perpendicular axes through  $P$ . The result becomes more and more accurate as the spacing  $a$  becomes less and less. If the potential is a function of two dimensions  $x$  and  $y$  only, we then have  $V_5 = V_6 = V_0$  and (6-60) reduces to

$$V_0 \approx \frac{1}{4} (V_1 + V_2 + V_3 + V_4) \tag{6-61}$$

To illustrate the application of (6-61), we now consider an example.

**EXAMPLE 6-9.** Two sides of an infinitely long box having a right-angled equilateral triangular cross section are kept at zero potential whereas the third side is kept at a potential of 100 volts as shown in Fig. 6.10. The region inside the box is charge free. It is divided into squares and right-angled equilateral triangles as shown in the figure. It is desired to find the potentials at the points  $a$ ,  $b$ , and  $c$  using (6-61).

The solution consists of finding a set of values for the potentials at  $a$ ,  $b$ , and  $c$  which, together with the potentials at points on the boundaries, are consistent with (6-61). By averaging the potentials at  $d$ ,  $f$ ,  $h$ , and  $j$  which are equidistant from  $a$  and lie on mutually perpendicular lines passing through it, we find an initial value of  $\frac{1}{4}(0 + 0 + 0 + 100)$  or 25 volts for the potential at  $a$ . Using this value and the potentials at  $d$ ,  $i$ , and  $j$ , we then find the potential at  $b$  to be  $\frac{1}{4}(25 + 0 + 100 + 100)$  or 56.25. However, we round off all numbers to the nearest tenth of a volt. In rounding off a decimal

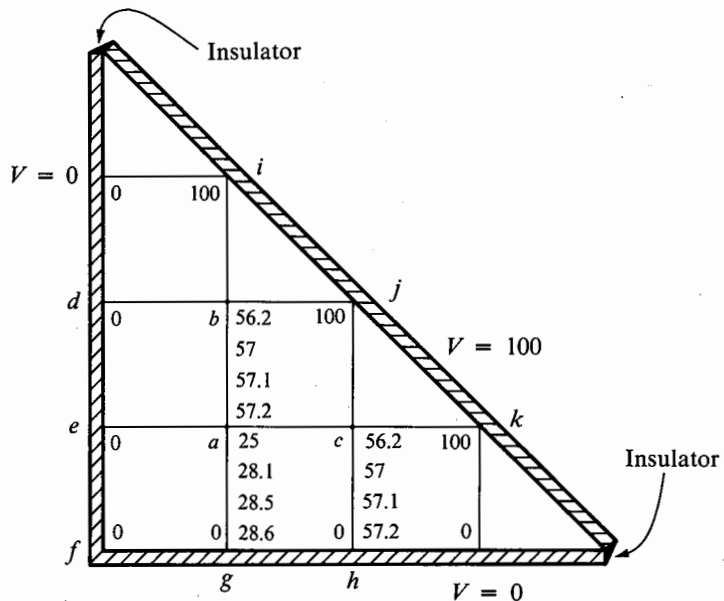


Fig. 6.10. For illustrating a numerical method of solving Laplace's equation.

ending exactly with 5, we increase the previous number by 1 if it is odd and keep it unchanged if it is even. Thus the potential at  $b$  is rounded off to 56.2 volts. Similarly, using the potentials at  $a, j, k$ , and  $h$ , we obtain a value of 56.2 volts for the potential at  $c$ . Since we now have potentials at points  $b$  and  $c$  which together with points  $e$  and  $g$  are closer to point  $a$  than the set of points  $d, f, h$ , and  $j$ , we recompute the potential at  $a$  by averaging the potentials at  $b, c, e$ , and  $g$  to obtain a value of  $\frac{1}{4}(56.2 + 56.2 + 0 + 0) = 28.1$  volts. We now note that the potentials at  $b$  and  $c$  have to be recomputed because they are inconsistent with the newly computed potential at point  $a$  and the potentials at the boundary points. We thus obtain a value of  $\frac{1}{4}(28.1 + 0 + 100 + 100) \approx 57.0$  volts for the potentials at  $b$  and  $c$ . This requires a revision of the potential at  $a$  to  $\frac{1}{4}(57 + 57 + 0 + 0) = 28.5$  volts. This process of iteration is continued until a set of values for the potentials at  $a, b$ , and  $c$  are obtained which, together with the potentials at the boundary points, are consistent with (6-61). The final values obtained in this manner are 28.6, 57.2, and 57.2 volts for  $a, b$ , and  $c$ , respectively. Obviously, these values are approximate because of the finite spacing between the grid points. By dividing the region inside the box into smaller squares and triangles, more accurate values can be obtained. In cases where the potentials at the insulated corners are required for the computation of initial values of potentials at grid points inside, average values of potentials on either side of the corners are used. ■

## 6.3 The Method of Images

We learned in Chapter 5 that a conductor surface is an equipotential. We also learned that the electric field at the conductor surface is entirely normal to it. In fact, these two properties are equivalent. In this section we will make use of this property to develop a method for computing the electric field due to charges in the presence of conductors. This method is called the "method of images." We will illustrate the method of images by means of two examples.

**EXAMPLE 6-10.** A point charge  $Q$  is situated at a distance  $d$  from a grounded infinite plane conductor. We wish to find the electric field due to the point charge and the induced surface charge density on the conductor.

First, let us consider two point charges  $Q$  and  $-Q$  situated at a distance  $2d$  apart as shown in Fig. 6.11. The potential at any point  $P$  located at a distance  $r_1$  from  $Q$  and  $r_2$  from  $-Q$  is given by

$$V = \frac{Q}{4\pi\epsilon r_1} - \frac{Q}{4\pi\epsilon r_2} \quad (6-62)$$

If the point  $P$  lies in the plane normal to and bisecting the line joining the point charges,  $r_1$  is equal to  $r_2$  and the potential is zero. Thus this plane is an equipotential. In particular, it is at zero potential. If we insert an infinite

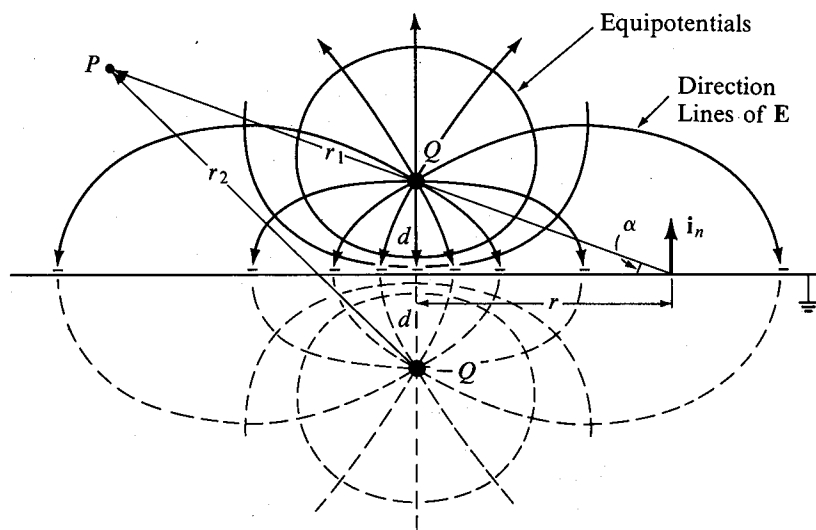


**Fig. 6.11.** For illustrating that the field due to a point charge  $Q$  near a grounded infinite plane conductor is the same as that due to the point charge and an "image" charge ( $-Q$ ) situated at the mirror image of  $Q$  in the plane conductor.



plane conductor into this plane, the field distribution due to the point charges will remain unaltered since the conductor satisfies the boundary condition. Conversely, the field due to a point charge  $Q$  situated at a distance  $d$  from a grounded infinite plane conductor is exactly the same as the field due to the charge  $Q$  plus an "image" charge  $-Q$  situated at the mirror image of  $Q$  in the plane. The direction lines of the electric field intensity and the equipotential surfaces due to the dipole formed by  $Q$  and  $-Q$  can be found by using the methods of Chapter 2. These are sketched in Fig. 6.11. The image charge is only a virtual charge. The field due to the real charge  $Q$  exists only on the side of that charge, with the field lines terminating on the induced charge formed on the surface of the grounded conductor. The virtual nature of the image charge is shown by the broken field lines and equipotentials on the side of the image charge.

The induced surface charge density is equal to the normal component (which is the only component present) of the displacement flux density at the conductor surface. With reference to the geometry shown in Fig. 6.11, the displacement flux density at a point on the conductor surface situated at a distance  $r$  from the projection of  $Q$  onto the surface is given by

$$\begin{aligned} \mathbf{D} &= -2 \frac{Q}{4\pi(d^2 + r^2)} \sin \alpha \mathbf{i}_n \\ &= -\frac{Qd}{2\pi(d^2 + r^2)^{3/2}} \mathbf{i}_n \end{aligned} \quad (6-63)$$

where  $\mathbf{i}_n$  is the unit vector normal to the conductor surface. The induced surface charge density is thus given by

$$\rho_s = \mathbf{D} \cdot \mathbf{i}_n = -\frac{Qd}{2\pi(d^2 + r^2)^{3/2}} \quad (6-64)$$

The total induced surface charge  $Q_i$  is given by

$$\begin{aligned} Q_i &= \int_{\text{conductor surface}} \rho_s dS = \int_{r=0}^{\infty} \int_{\phi=0}^{2\pi} \frac{-Qd}{2\pi(d^2 + r^2)^{3/2}} r dr d\phi \\ &= Q \int_{\alpha=\pi/2}^0 \cos \alpha d\alpha = -Q \end{aligned} \quad (6-65)$$

Thus the total induced surface charge is equal to the image charge. This is to be expected since all field lines ending on the conductor would end on the image charge if the conductor were not present, but an actual charge of  $-Q$  is present at the image point. ■

**EXAMPLE 6-11.** An infinitely long line charge of uniform density  $\rho_{L0}$  C/m is situated parallel to and at a distance  $d$  from the axis of an infinitely long grounded conducting cylinder of radius  $a$  ( $< d$ ) as shown by the cross-sectional view in Fig. 6.12. We wish to find the image charge required for computing the field outside the conducting cylinder.

Let us postulate an infinitely long image line charge of uniform density  $\rho'_{L0}$  at a distance  $b$  from the axis of the conducting cylinder and in the plane containing the axis of the cylinder and the real line charge, as shown in Fig. 6.12. Choosing the line through point  $P_1$  and parallel to the axis of the cylinder

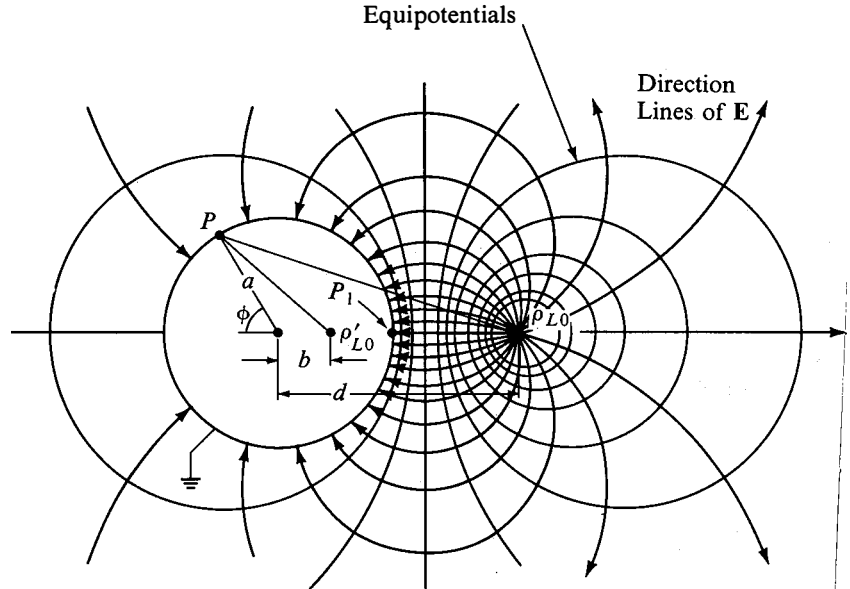


**Fig. 6.12.** For finding the image charge required for computing the field due to a line charge of uniform density parallel to an infinitely long grounded conducting cylinder.

as the reference for zero potential, the potential at any arbitrary point  $P$  on the conductor surface can be written as

$$V = -\frac{\rho_{L0}}{2\pi\epsilon_0} \ln \frac{\sqrt{d^2 + a^2 + 2ad \cos \phi}}{(d - a)} - \frac{\rho'_{L0}}{2\pi\epsilon_0} \ln \frac{\sqrt{b^2 + a^2 + 2ab \cos \phi}}{(a - b)} \quad (6-66)$$

But this quantity must be equal to zero since the conductor is an equipotential and the potential at  $P_1$  is zero. This requires that

$$\rho'_{L0} = -\rho_{L0} \quad (6-67)$$

and

$$\ln \left[ \frac{\sqrt{d^2 + a^2 + 2ad \cos \phi}}{(d - a)} \frac{(a - b)}{\sqrt{b^2 + a^2 + 2ab \cos \phi}} \right] = 0$$

or

$$\frac{\sqrt{d^2 + a^2 + 2ad \cos \phi}}{(d - a)} \frac{(a - b)}{\sqrt{b^2 + a^2 + 2ab \cos \phi}} = 1 \quad (6-68)$$

To find the solution for (6-68), let us consider  $\phi = 0$ . We then have

$$\left(\frac{d+a}{d-a}\right)\left(\frac{a-b}{a+b}\right) = 1$$

or

$$a^2 = bd \quad (6-69)$$

which satisfies (6-68) for all  $\phi$ . Thus, an image line charge of uniform density  $-\rho_{L0}$  and located at a distance  $b = a^2/d$  from the axis of the cylinder satisfies the equipotential requirement for the grounded conducting cylinder. The field outside the cylinder is therefore exactly the same as the field set up by the actual line charge of density  $\rho_{L0}$  at distance  $d$  from the axis and the image line charge of density  $-\rho_{L0}$  at distance  $a^2/d$  from the axis. The direction lines of the electric field intensity and the associated equipotential surfaces can be obtained by the methods learned in Chapter 2. These are shown sketched in Fig. 6.12. It is left as an exercise (Problem 6.15) for the student to show that the total induced surface charge per unit length of the cylinder is equal to the image charge density  $-\rho_{L0}$ . The field inside the cylinder is, of course, equal to zero since the image charge is only a virtual charge. ■

Proceeding in the same manner as in the preceding example, we can obtain the image charge for a point charge near a grounded spherical conductor. If the point charge  $Q$  is situated at a distance  $d$  from the center of the spherical conductor of radius  $a$ , the image charge is a point charge of value  $-Qa/d$ . It lies at a distance  $a^2/d$  from the center of the sphere, along the line joining the center to the charge  $Q$  and on the side of  $Q$ . We leave the derivation as an exercise (Problem 6.16) for the student. The method of images can also be applied for finding fields due to charges in the presence of dielectrics. We will, however, not pursue that topic here.

#### 6.4 Conductance, Capacitance, and Inductance

In Chapter 5 we introduced conductors, dielectrics, and magnetic materials. Let us now consider three different arrangements, each consisting of two parallel perfectly conducting plates as shown in Figs. 6.13(a), (b), and (c). For the structure of Fig. 6.13(a), the medium between the parallel plates is filled with a conducting material of uniform conductivity  $\sigma$ . For the structure of Fig. 6.13(b), the medium between the parallel plates is filled with a perfect dielectric of uniform permittivity  $\epsilon$ . For the structure of Fig. 6.13(c), the two parallel plates are joined at one end of the structure by a perfectly conducting plate and the medium between the plates is filled with a magnetic material of uniform permeability  $\mu$ . Note that free space may be considered as a perfect dielectric of permittivity  $\epsilon_0$  and a magnetic material of permeability  $\mu_0$ . We apply a potential difference of  $V_0$  volts between the parallel plates

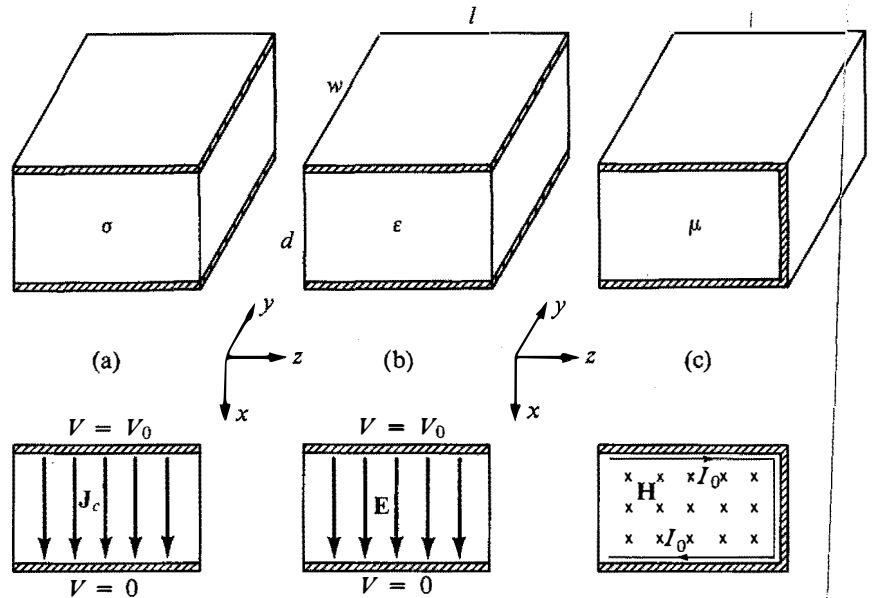


**Fig. 6.13.** Three different structures each consisting of two parallel perfectly conducting plates. The medium between the plates is a conductor for structure (a), a dielectric for structure (b), and a magnetic material for structure (c). The two plates are joined at one end by another perfectly conducting plate for structure (c).

of structures (a) and (b) by connecting appropriate constant voltage sources which are not shown in the figure. We pass a  $z$ -directed surface current  $I_0$  uniformly distributed in the  $y$  direction along the upper plate of structure (c) and return it in the opposite direction along the lower plate by connecting an appropriate constant current source which is not shown in the figure.

The medium between the plates of structure (a) is then characterized by an electric field from the upper to the lower plate and hence by a conduction current in the same direction. The medium between the plates of structure (b) is characterized by an electric field only from the upper to the lower plate and no current. The medium between the plates of structure (c) is characterized by a magnetic field parallel to the plates and towards the direction of advance of a right-hand screw as it is turned in the sense of the current flow. Since the conduction current cannot leave the conductor, it has to be tangential to the conductor surface. This forces the electric field for structure (a) to be in the  $x$  direction. On the other hand, the electric field at the surface of a dielectric need not be tangential to it. This results in fringing of the electric field in the case of structure (b). However, by assuming that

$d$  is very small compared to  $w$  and  $l$ , or by assuming that the structure is actually part of a much larger structure, we can neglect fringing and consider the electric field to be entirely in the  $x$  direction. For the same assumption in the case of structure (c), the magnetic field can be considered to be entirely in the  $y$  direction.

From the result of Example 6-3, the electric field in the case of structures (a) and (b) is then given by

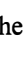
$$\mathbf{E} = \frac{V_0}{d} \mathbf{i}_x \quad (6-70)$$

The current density  $\mathbf{J}_c$  for structure (a) is given by

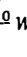
$$\mathbf{J}_c = \sigma \mathbf{E} = \frac{\sigma V_0}{d} \mathbf{i}_x \quad (6-71)$$

The total current  $I_c$  flowing from the upper plate to the lower plate is given by the surface integral of the current density over the cross section of the conductor. However, since the current density is uniform and directed normal to the plates, we can obtain this current by simply multiplying the magnitude of the current density by the area of the plates. Thus

$$I_c = J_c(wl) = \frac{\sigma V_0}{d} wl \quad (6-72)$$

We now define a quantity known as the “conductance” (  ), denoted by the symbol  $G$ , as the ratio of the current flowing from one plate to the other to the potential difference between the plates. From (6-72), the the conductance of the conducting slab arrangement of Fig. 6.13(a) is given by

$$G = \frac{I_c}{V_0} = \frac{\sigma wl}{d} \quad (6-73)$$

We note from (6-73) that the conductance is a function purely of the dimensions of the conductor and its conductivity. The units of conductance are (mhos/meter)(meter<sup>2</sup>/meter) or mhos. The reciprocal of the “conductance” is the “resistance” (  ), which is denoted by the symbol  $R$  and has the units of ohms. Thus

$$R = \frac{V_0}{I_c}$$

or

$$V_0 = I_c R$$

which is the familiar form of Ohm’s law applicable to a finite region of conducting material. The resistance of the slab conductor is given by

$$R = \frac{d}{\sigma wl} = \frac{d}{\sigma A}$$

where  $A$  is the area of the plates.

The phenomenon associated with conduction current is power dissipation. From Chapter 5, the power dissipation density is given by

$$p_d = \mathbf{J}_c \cdot \mathbf{E} = \sigma \mathbf{E} \cdot \mathbf{E} = \sigma E^2 \quad (6-74)$$

Performing volume integration of the power dissipation density over the volume of the conductor of Fig. 6.13(a), we obtain the total power dissipated in the conductor as

$$\begin{aligned} P_d &= \int_{\text{vol}} p_d \, dv = \int_{\text{vol}} \sigma E^2 \, dv \\ &= \int_{\text{vol}} \frac{\sigma V_0^2}{d^2} \, dv \\ &= \frac{\sigma V_0^2}{d^2} (\text{volume of the conductor}) \\ &= \frac{\sigma V_0^2}{d^2} (dwl) = \frac{\sigma wl}{d} V_0^2 = GV_0^2 \end{aligned} \quad (6-75)$$

Equation (6-75) gives the physical interpretation that conductance is the parameter associated with power dissipation in a conductor.

Turning our attention to the structure of Fig. 6.13(b), the displacement flux density is given by

$$\mathbf{D} = \epsilon \mathbf{E} = \frac{\epsilon V_0}{d} \mathbf{i}_x \quad (6-76)$$

The surface charge density on the upper plate is given by

$$[\rho_s]_{x=0} = [\mathbf{D}]_{x=0} \cdot (\mathbf{i}_x) = \frac{\epsilon V_0}{d} \quad (6-77a)$$

The surface charge density on the lower plate is given by

$$[\rho_s]_{x=d} = [\mathbf{D}]_{x=d} \cdot (-\mathbf{i}_x) = -\frac{\epsilon V_0}{d} \quad (6-77b)$$

The total charge on either plate is given by the surface integral of the charge density on that plate over the area of the plate. However, since the charge densities here are uniform, we can obtain the total charge simply by multiplying the charge density by the area of the plate. Thus the magnitude  $Q$  of the charge on either plate is given by

$$Q = \rho_s (wl) = \frac{\epsilon V_0}{d} wl \quad (6-78)$$

We now define a quantity known as the “capacitance” (  $\bullet \text{---} | \text{---} \bullet$  ), denoted by the symbol  $C$ , as the ratio of the magnitude of the charge on either plate to the potential difference between the plates. From (6-78), the capacitance of the dielectric slab arrangement of Fig. 6.13(b) is given by

$$C = \frac{Q}{V_0} = \frac{\epsilon wl}{d} \quad (6-79)$$

We note from (6-79) that the capacitance is a function purely of the dimen-

sions of the dielectric slab and its permittivity. The units of capacitance are (farads/meter)(meter<sup>2</sup>/meter) or farads.

The phenomenon associated with the electric field in a dielectric medium is energy storage. From Chapter 5, the electric stored energy density is given by

$$w_e = \frac{1}{2} \mathbf{D} \cdot \mathbf{E} = \frac{1}{2} \epsilon E^2 \quad (6-80)$$

Performing volume integration of the electric stored energy density over the volume of the dielectric of Fig. 6.13(b), we obtain the total electric stored energy in the dielectric as

$$\begin{aligned} W_e &= \int_{\text{vol}} w_e \, dv = \int_{\text{vol}} \frac{1}{2} \epsilon E^2 \, dv \\ &= \int_{\text{vol}} \frac{1}{2} \frac{\epsilon V_0^2}{d^2} \, dv \\ &= \frac{1}{2} \frac{\epsilon V_0^2}{d^2} (\text{volume of the dielectric}) \\ &= \frac{1}{2} \frac{\epsilon V_0^2}{d^2} (dwl) = \frac{1}{2} \frac{\epsilon wl}{d} V_0^2 = \frac{1}{2} CV_0^2 \end{aligned} \quad (6-81)$$

Equation (6-81) gives the physical interpretation that capacitance is the parameter associated with storage of electric energy in a dielectric.

Turning our attention to the structure of Fig. 6.13(c) and neglecting fringing, the magnetic field intensity between the plates is the same as that due to infinite plane current sheets of densities given by

$$\mathbf{J} = \begin{cases} \frac{I_0}{w} \mathbf{i}_z & \text{for } x = 0 \\ -\frac{I_0}{w} \mathbf{i}_z & \text{for } x = d \end{cases}$$

Hence the magnetic field intensity is uniform between the plates and zero outside the plates, that is,

$$\mathbf{H} = \begin{cases} H_0 \mathbf{i}_y & 0 < x < d \\ 0 & \text{otherwise} \end{cases}$$

From the boundary condition for the tangential magnetic field intensity, the value of  $H_0$  is equal to the surface current density  $I_0/w$  since the field is zero outside the plates. Thus

$$\mathbf{H} = \frac{I_0}{w} \mathbf{i}_y \quad \text{for } 0 < x < d$$


and

$$\mathbf{B} = \mu \mathbf{H} = \frac{\mu I_0}{w} \mathbf{i}_y \quad \text{for } 0 < x < d \quad (6-82)$$

The magnetic flux  $\psi$  linking the current  $I_0$  is given by the surface integral of

the magnetic flux density over the area bounded by any contour along which the current flows. This area is simply the cross-sectional area of the magnetic material normal to the magnetic field lines. Since the magnetic field lines are straight, it may seem like they do not link the current. However, straight lines are circles of infinite radii and hence the magnetic field does link the current. For the structure of Fig. 6.13(c), since the magnetic flux density is uniform, we can obtain the required magnetic flux  $\psi$  by simply multiplying the magnetic flux density by the cross-sectional area normal to it. The quantity  $\psi$  is known as the magnetic flux linkage associated with the current  $I_0$ . Thus

$$\psi = B_y(dl) = \frac{\mu I_0}{w} dl \quad (6-83)$$

We now define a quantity known as the "inductance" (  ), denoted by the symbol  $L$ , as the ratio of the magnetic flux linkage associated with the current  $I_0$  to the current  $I_0$ . From (6-83), the inductance of the magnetic material slab arrangement of Fig. 6.13(c) is given by

$$L = \frac{\psi}{I_0} = \frac{\mu dl}{w} \quad (6-84)$$

We note from (6-84) that the inductance is a function purely of the dimensions of the magnetic material and its permeability. The units of inductance are (henrys/meter)(meter<sup>2</sup>/meter) or henrys.

The phenomenon associated with magnetic field in a magnetic material medium is energy storage. From Chapter 5, the magnetic stored energy density is given by

$$w_m = \frac{1}{2} \mathbf{H} \cdot \mathbf{B} = \frac{1}{2} \mu H^2 \quad (6-85)$$

Performing volume integration of the magnetic stored energy density over the volume of the magnetic material of Fig. 6.13(c), we obtain the total magnetic stored energy in the magnetic material as

$$\begin{aligned} W_m &= \int_{\text{vol}} w_m dv = \int_{\text{vol}} \frac{1}{2} \mu H^2 dv \\ &= \int_{\text{vol}} \frac{1}{2} \frac{\mu I_0^2}{w^2} dv \\ &= \frac{1}{2} \frac{\mu I_0^2}{w^2} (\text{volume of the magnetic material}) \\ &= \frac{1}{2} \frac{\mu I_0^2}{w^2} (dwl) = \frac{1}{2} \frac{\mu dl}{w} I_0^2 = \frac{1}{2} L I_0^2 \end{aligned} \quad (6-86)$$

Equation (6-86) gives the physical interpretation that inductance is the parameter associated with storage of magnetic energy in a magnetic material.

To write general expressions for the conductance, capacitance and inductance in terms of the fields, let us consider the three structures shown



by the cross-sectional views in Figs. 6.14(a), (b), and (c), which consist of identical pairs of parallel, infinitely long, perfect conductors having arbitrary but uniform cross sections. Let the medium between the two conductors of structures (a), (b), and (c) be characterized by uniform conductivity  $\sigma$ ,

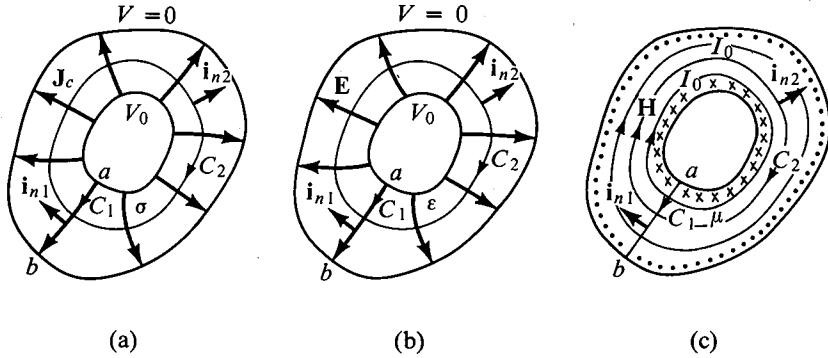


Fig. 6.14. For writing general expressions for (a) conductance, (b) capacitance, and (c) inductance.

uniform permittivity  $\epsilon$ , and uniform permeability  $\mu$ , respectively. As in the case of the structures of Fig. 6.13, we apply a potential difference between the two conductors of structures (a) and (b) and pass a current into the plane of the paper along one conductor of structure (c), returning it out of the plane of the paper along its second conductor. Structures (a) and (b) are then characterized by an electric field whose direction lines originate normal to the inner conductor and terminate normal to the outer conductor. The electric field results in a conduction current in structure (a). Structure (c) is characterized by a magnetic field, whose direction lines lie in the plane of the paper and surround the inner conductor.

Let us now consider unit lengths of the three structures normal to the plane of the paper. We can then write the following quantities:

For structure (a),

$$V_0, \text{ potential difference between the conductors} = \int_a^b \mathbf{E} \cdot d\mathbf{l} \quad (6-87a)$$

$I_c$ , current flowing from the inner to the outer conductor  
= current crossing the area formed by the contour  $C_2$  and length unity in the axial direction

$$= \oint_{C_2} \mathbf{J}_c \cdot \mathbf{i}_{n_2} dl = \sigma \oint_{C_2} \mathbf{E} \cdot \mathbf{i}_{n_2} dl \quad (6-87b)$$

For structure (b),

$$V_0, \text{ potential difference between the conductors} = \int_a^b \mathbf{E} \cdot d\mathbf{l} \quad (6-88a)$$

$Q$ , magnitude of surface charge on either conductor

= displacement flux crossing the area formed by the contour  $C_2$  and length unity in the axial direction

$$= \oint_{C_2} \mathbf{D} \cdot \mathbf{i}_{n_2} dl = \epsilon \oint_{C_2} \mathbf{E} \cdot \mathbf{i}_{n_2} dl \quad (6-88b)$$

For structure (c),

$$I_0, \text{ surface current flowing on either conductor} = \oint_{C_2} \mathbf{H} \cdot d\mathbf{l} \quad (6-89a)$$

$\psi$ , magnetic flux linking the current  $I_0$

= magnetic flux crossing the area formed by the contour  $C_1$  and length unity in the axial direction

$$= \int_a^b \mathbf{B} \cdot \mathbf{i}_{n_1} dl = \mu \int_a^b \mathbf{H} \cdot \mathbf{i}_{n_1} dl \quad (6-89b)$$

From (6-87a)–(6-89b), we can write the general expressions for  $G$ ,  $C$ , and  $\mathcal{L}$  per unit length, denoted by  $\mathfrak{G}$ ,  $\mathfrak{C}$ , and  $\mathfrak{L}$ , as

$$\mathfrak{G} = \frac{I_c}{V_0} = \frac{\sigma \oint_{C_1} \mathbf{E} \cdot \mathbf{i}_{n_2} dl}{\int_a^b \mathbf{E} \cdot d\mathbf{l}} \quad (6-90)$$

$$\mathfrak{C} = \frac{Q}{V_0} = \frac{\epsilon \oint_{C_2} \mathbf{E} \cdot \mathbf{i}_{n_2} dl}{\int_a^b \mathbf{E} \cdot d\mathbf{l}} \quad (6-91)$$

$$\mathfrak{L} = \frac{\psi}{I_0} = \frac{\mu \int_a^b \mathbf{H} \cdot \mathbf{i}_{n_1} dl}{\oint_{C_2} \mathbf{H} \cdot d\mathbf{l}} \quad (6-92)$$

From (6-90) and (6-91), we note that

$$\frac{\mathfrak{G}}{\mathfrak{C}} = \frac{\sigma}{\epsilon} \text{ mhos/farads} \quad (6-93)$$

From the discussion of Section 3.10, the electric field lines of structure (b) and the magnetic field lines of structure (c) are everywhere orthogonal to each other and their magnitudes are proportional, since the conductor cross sections for the two structures are the same. Thus we can write

$$\mathbf{E} = k\mathbf{H} \times \mathbf{i}_z \quad (6-94)$$

where  $k$  is the constant of proportionality and  $\mathbf{i}_z$  is directed into the plane of the paper. Substituting (6-94) into (6-91), we have

$$\begin{aligned} \mathfrak{C} &= \frac{\epsilon \oint_{C_2} k\mathbf{H} \times \mathbf{i}_z \cdot \mathbf{i}_{n_2} dl}{\int_a^b k\mathbf{H} \times \mathbf{i}_z \cdot d\mathbf{l}} \\ &= \frac{\epsilon k \oint_{C_2} \mathbf{H} \cdot \mathbf{i}_z \times \mathbf{i}_{n_2} dl}{k \int_a^b \mathbf{H} \cdot \mathbf{i}_z \times d\mathbf{l}} = \frac{\epsilon \oint_{C_2} \mathbf{H} \cdot d\mathbf{l}}{\int_a^b \mathbf{H} \cdot \mathbf{i}_{n_1} dl} \end{aligned} \quad (6-95)$$

From (6-92) and (6-95), we note that

$$\mathcal{L}\mathcal{E} = \mu\epsilon \text{ henry-farad/m}^2 \quad (6-96)$$

Equations (6-93) and (6-96) provide simple relationships between the conductance per unit length, capacitance per unit length, and inductance per unit length of a structure consisting of two infinitely long, parallel perfect conductors having arbitrary but uniform cross sections. Expressions for these three quantities are listed in Table 6.2 for some common configurations of conductors having the cross sections shown in Fig. 6.15.

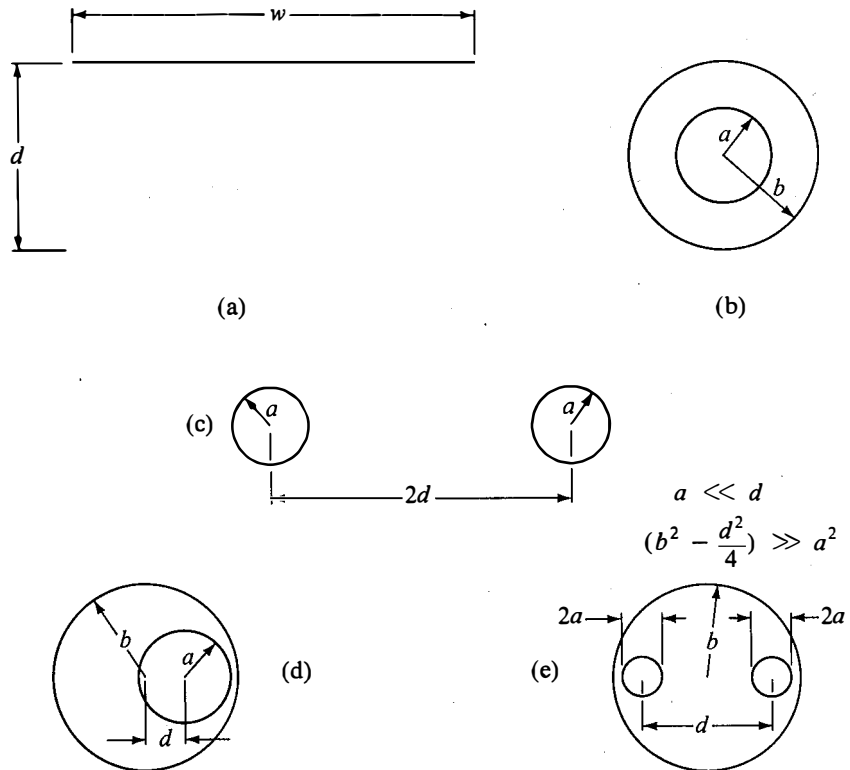


**Fig. 6.15.** Cross sections of some common configurations of parallel infinitely long conductors.

**EXAMPLE 6-12.** It is desired to obtain the conductance, capacitance, and inductance per unit length of the parallel cylindrical wire arrangement of Fig. 6.15(c).

In view of (6-93) and (6-96), it is sufficient if we find one of the three quantities. Hence we choose to find the capacitance per unit length. To do this, we refer to Example 6-11 and Fig. 6.12 and note that placing a cylindrical conductor coinciding with the equipotential cylindrical surface having its axis at a distance  $b$  from the line charge  $\rho_{L0}$  and on the side opposite to the grounded conductor will not alter the field. Hence the field of the parallel wire arrangement of Fig. 6.15(c) is exactly the same as the field due to equal

**TABLE 6.2.** Conductance, Capacitance, and Inductance per Unit Length for Some Structures Consisting of Infinitely Long Conductors Having the Cross Sections Shown in Fig. 6.15

Description	$\mathcal{G}$ , Conductance per Unit Length	$\mathcal{C}$ , Capacitance per Unit Length	$\mathcal{L}$ , Inductance per Unit Length
Parallel plane conductors, Fig. 6.15(a)	$\sigma \frac{w}{d}$	$\epsilon \frac{w}{d}$	$\mu \frac{d}{w}$
Coaxial cylindrical conductors, Fig. 6.15(b)	$\frac{2\pi\sigma}{\ln(b/a)}$	$\frac{2\pi\epsilon}{\ln(b/a)}$	$\frac{\mu}{2\pi} \ln \frac{b}{a}$
Parallel cylindrical wires, Fig. 6.15(c)	$\frac{\pi\sigma}{\cosh^{-1}(d/a)}$	$\frac{\pi\epsilon}{\cosh^{-1}(d/a)}$	$\frac{\mu}{\pi} \cosh^{-1} \frac{d}{a}$
Eccentric inner conductor, Fig. 6.15(d)	$\frac{2\pi\sigma}{\cosh^{-1}\left(\frac{a^2+b^2-d^2}{2ab}\right)}$	$\frac{2\pi\epsilon}{\cosh^{-1}\left(\frac{a^2+b^2-d^2}{2ab}\right)}$	$\frac{\mu}{2\pi} \cosh^{-1} \frac{a^2+b^2-d^2}{2ab}$
Shielded parallel cylindrical wires, Fig. 6.15(e)	$\frac{\pi\sigma}{\ln\left[\frac{d(b^2-d^2/4)}{a(b^2+d^2/4)}\right]}$	$\frac{\pi\epsilon}{\ln\left[\frac{d(b^2-d^2/4)}{a(b^2+d^2/4)}\right]}$	$\frac{\mu}{\pi} \ln \frac{d(b^2-d^2/4)}{a(b^2+d^2/4)}$

and opposite line charges situated as shown in Fig. 6.16. The potential difference between the two points  $A$  and  $B$  is then given by

$$V_0 = 2 \frac{\rho_{L0}}{2\pi\epsilon} \ln \frac{2d - a - b}{a - b} \quad (6-97)$$

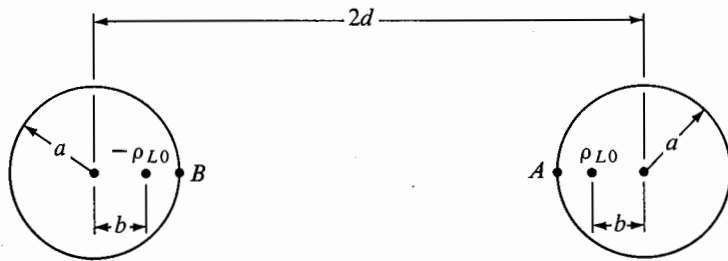


**Fig. 6.16.** For the determination of  $\mathcal{G}$ ,  $\mathcal{L}$ , and  $\mathcal{C}$  for the parallel cylindrical wire arrangement of Fig. 6.15(c).

However, from Example 6-11,

$$b = \frac{a^2}{2d - b}$$

or

$$b = d \pm \sqrt{d^2 - a^2} \quad (6-98)$$

Ignoring the plus sign on the right side of (6-98), since  $b$  has to be less than

$d$ , and substituting for  $b$  in (6-97) we have

$$\begin{aligned} V_0 &= \frac{\rho_{L0}}{\pi\epsilon} \ln \frac{2d - a - d + \sqrt{d^2 - a^2}}{a - d + \sqrt{d^2 - a^2}} \\ &= \frac{\rho_{L0}}{\pi\epsilon} \ln \frac{\sqrt{d^2 - a^2} + (d - a)}{\sqrt{d^2 - a^2} - (d - a)} \\ &= \frac{\rho_{L0}}{\pi\epsilon} \ln \frac{d + \sqrt{d^2 - a^2}}{a} = \frac{\rho_{L0}}{\pi\epsilon} \cosh^{-1} \frac{d}{a} \end{aligned} \quad (6-99)$$

Finally, the capacitance per unit length is given by

$$c = \frac{\rho_{L0}}{V_0} = \frac{\pi\epsilon}{\cosh^{-1}(d/a)} \quad (6-100)$$

which agrees with the expression given in Table 6.2. The corresponding expressions for  $\mathcal{G}$  and  $\mathcal{L}$  obtained by using (6-93) and (6-96), respectively, are given in Table 6.2. ■

For volume current distributions, we have to consider the magnetic field internal to the current distribution in addition to the magnetic field external to it. The inductance associated with the internal field is known as the "internal inductance" as compared to the "external inductance" associated with the external field. The inductance we defined by (6-84) and (6-92) is the external inductance. To obtain the internal inductance, we have to take into account the fact that different flux lines in the volume occupied by the current distribution link different partial amounts of the total current. We will illustrate this by means of an example.

**EXAMPLE 6-13.** A current  $I$  amp flows with uniform volume density  $\mathbf{J} = J_0 \mathbf{i}_z$  amp/m<sup>2</sup> along an infinitely long, solid cylindrical conductor of radius  $a$  and returns with uniform surface density in the opposite direction along the surface of an infinitely long, perfectly conducting cylinder of radius  $b$  ( $> a$ ) and coaxial with the inner conductor. It is desired to find the internal inductance per unit length of the inner conductor.

The cross-sectional view of the conductor arrangement is shown in Fig. 6.17(a). From symmetry considerations, the magnetic field is entirely in the  $\phi$  direction and independent of  $\phi$ . Applying Ampere's circuital law to a circular contour of radius  $r$  ( $< a$ ) as shown in Fig. 6.17(a), we have

$$2\pi r H_\phi = \pi r^2 J_0$$

or

$$\mathbf{H} = H_\phi \mathbf{i}_\phi = \frac{J_0 r}{2} \mathbf{i}_\phi \quad r < a$$

The corresponding magnetic flux density is given by

$$\mathbf{B} = \mu \mathbf{H} = \frac{\mu J_0 r}{2} \mathbf{i}_\phi \quad r < a$$

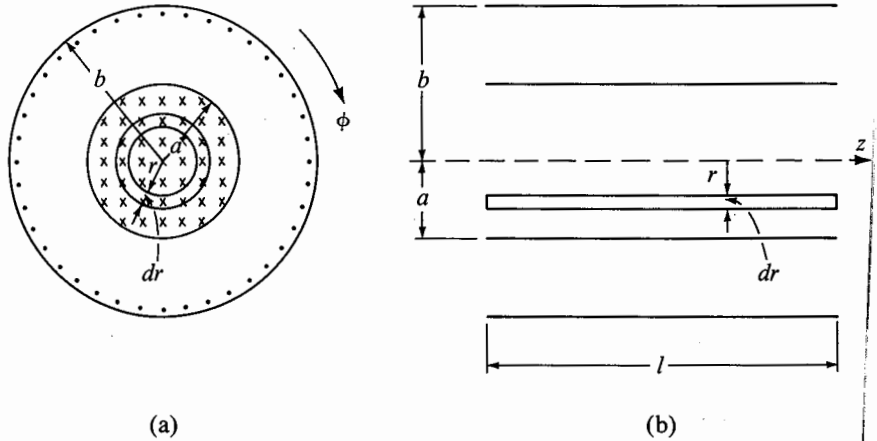


Fig. 6.17. For evaluating the internal inductance per unit length associated with a volume current of uniform density along an infinitely long cylindrical conductor.

where  $\mu$  is the permeability of the conductor. Let us now consider a rectangle of infinitesimal width  $dr$  in the  $r$  direction and length  $l$  in the  $z$  direction at a distance  $r$  from the axis as shown in Fig. 6.17(b). The magnetic flux  $d\psi_i$  crossing this rectangular surface is given by

$$\begin{aligned} d\psi_i &= B_\phi(\text{area of the rectangle}) \\ &= \frac{\mu J_0 r l dr}{2} \end{aligned}$$

where the subscript  $i$  denotes flux internal to the conductor. This flux surrounds only the current flowing within the radius  $r$ , as can be seen from Fig. 6.17(a). Let  $N$  be the fraction of the total current  $I$  linked by this flux. Then

$$\begin{aligned} N &= \frac{\text{current flowing within radius } r (< a)}{\text{total current } I} \\ &= \frac{J_0 \pi r^2}{J_0 \pi a^2} = \left(\frac{r}{a}\right)^2 \end{aligned}$$

The contribution from the flux  $d\psi_i$  to the internal flux linkage associated with the current  $I$  is the product of  $N$  and the flux itself, that is,  $N d\psi_i$ . To obtain the internal flux linkage associated with  $I$ , we integrate  $N d\psi_i$  between the limits  $r = 0$  and  $r = a$ , taking into account the dependence of  $N$  upon  $d\psi_i$ . Thus

$$\psi_i = \int_{r=0}^a N d\psi_i = \int_{r=0}^a \left(\frac{r}{a}\right)^2 \frac{\mu J_0 l r}{2} dr = \frac{\mu J_0 l a^2}{8}$$

Finally, the required internal inductance per unit length is

$$\mathcal{L}_i = \frac{\psi_i}{I} = \frac{(\mu J_0 a^2 / 8)}{(J_0 \pi a^2)} = \frac{\mu}{8\pi} \quad (6-101)$$

Alternatively, we can obtain  $\mathcal{L}_i$  from energy considerations by making use of the result (6-86) that the magnetic stored energy is equal to  $\frac{1}{2}LI^2$ . For  $\mathcal{L}_i$ , we have to consider the energy stored in the volume internal to the current distribution. For unit length of the conductor, this is given by

$$\begin{aligned} W_{mi} &= \int_{\text{vol}} \frac{1}{2} \mu H^2 dv \\ &= \int_{r=0}^a \int_{\phi=0}^{2\pi} \int_{z=0}^1 \frac{1}{2} \mu \left( \frac{J_0 r}{2} \right)^2 r dr d\phi dz = \frac{\pi \mu J_0^2 a^4}{16} \end{aligned}$$

The internal inductance is then given by

$$\mathcal{L}_i = \frac{2W_{mi}}{I^2} = \frac{(\pi \mu J_0^2 a^4 / 8)}{(J_0^2 \pi^2 a^4)} = \frac{\mu}{8\pi}$$

which is the same as (6-101). Finally, to find the total inductance per unit length of the arrangement of Fig. 6.17(a), we have to add the external inductance due to the flux in the region  $a < r < b$  to the internal inductance given by (6-101). This external inductance is given in Table 6.2. ■

From the steps involved in the solution of Example 6-13, we observe that the general expression for the internal inductance is

$$L_{\text{int}} = \frac{1}{I} \int_S N d\psi \quad (6-102a)$$

where  $S$  is any surface through which the internal magnetic flux associated with  $I$  passes. We note that (6-102a) is also good for computing the external inductance since for external inductance  $N$  is independent of  $d\psi$ . Hence

$$L_{\text{ext}} = \frac{N}{I} \int_S d\psi = N \frac{\Psi}{I} \quad (6-102b)$$

In Eq. (6-102b), the value of  $N$  is unity if  $I$  is a surface current as for the structures of Figs. 6.13(c) and 6.14(c). On the other hand, for a filamentary wire wound on a core,  $N$  is equal to the number of turns of the winding in which case  $\psi$  represents the flux through the core, that is, the flux crossing the surface formed by one turn. To explain this, let us consider a two-turn winding  $abcdefghi$  carrying current  $I$  as shown in Fig. 6.18(a) and imagine the flux lines penetrating the surface formed by the two-turn winding. According to definition, the magnetic flux linking  $I$  is the flux crossing the surface formed by the two-turn winding. Let us twist the portion  $cdef$  of the winding and stretch the winding to the shape shown in Fig. 6.18(b). We can now see that the flux lines come from underneath the surface of the first turn ( $abcd$ ), go below the surface of the second turn ( $efgh$ ), and come out of it again as shown in Fig. 6.18(b) so that the flux linking  $I$  is equal to twice the flux passing through one of the surfaces  $abcd$  and  $efgh$ .

The discussion pertaining to inductance thus far has been concerned with "self inductance," that is, inductance associated with a current distribu-

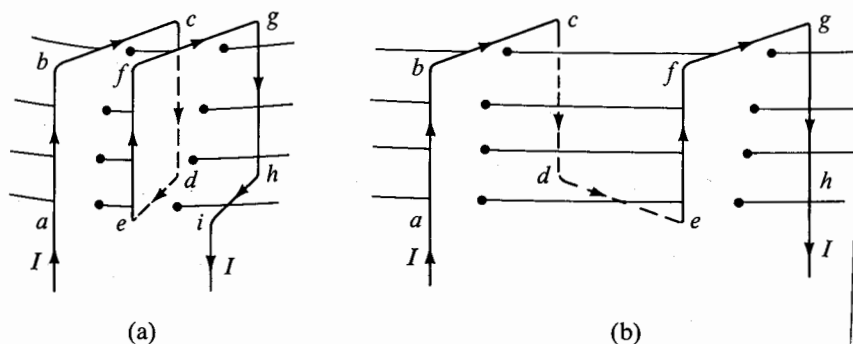


Fig. 6.18. For illustrating that the flux linking a filamentary wire of  $N$  turns is equal to  $N$  times the flux crossing the surface formed by one turn.

tion by virtue of its own flux linking it. On the other hand, if we have two independent currents  $I_1$  and  $I_2$ , we can talk of the flux due to one current linking the second current. This leads to the concept of "mutual inductance." The mutual inductance denoted as  $L_{12}$  is defined as

$$L_{12} = N_1 \frac{\psi_{12}}{I_2} \quad (6-103)$$

where  $\psi_{12}$  is the magnetic flux produced by  $I_2$  but linking one turn of the  $N_1$ -turn winding carrying current  $I_1$ . Similarly,

$$L_{21} = N_2 \frac{\psi_{21}}{I_1} \quad (6-104)$$

where  $\psi_{21}$  is the magnetic flux produced by  $I_1$  but linking one turn of the  $N_2$ -turn winding carrying current  $I_2$ . It is left as an exercise (Problem 6.24) for the student to show that  $L_{21} = L_{12}$ . We will now consider a simple example illustrating the computation of mutual inductance.

**EXAMPLE 6-14.** A single straight wire, infinitely long and carrying current  $I_1$ , lies below to the left and parallel to a two-wire telephone line carrying current  $I_2$ , as shown by the cross-sectional and plan views in Figs. 6.19(a) and 6-19(b), respectively. It is desired to obtain the mutual inductance between the single wire and the telephone line per unit length of the wires. The thickness of the telephone wire is assumed to be negligible.

Choosing a coordinate system with the axis of the single wire as the  $z$  axis and applying Ampere's circuital law to a circular path around the single wire, we obtain the magnetic flux density due to the single wire as

$$\mathbf{B} = \frac{\mu_0 I_1}{2\pi r} \mathbf{i}_\phi$$

The flux  $d\psi_{21}$  crossing a rectangular surface of length unity and width  $dy$



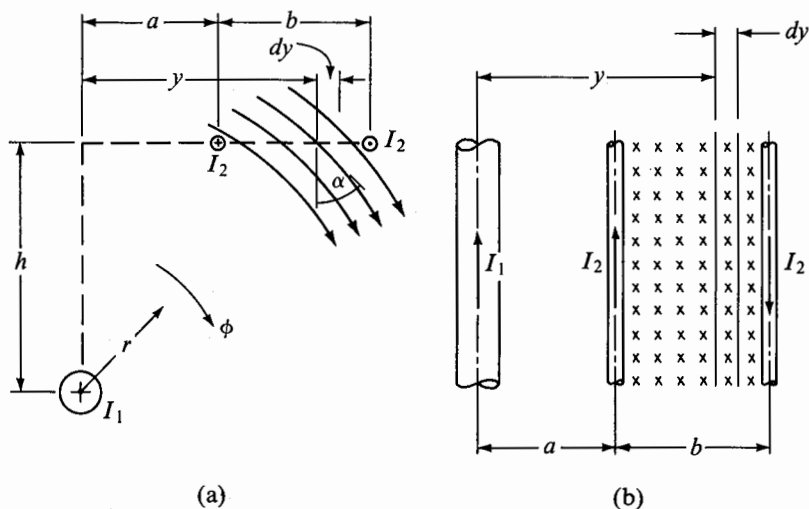


Fig. 6.19. For the computation of mutual inductance per unit length between a two-wire telephone line and a single wire parallel to it.

lying between the telephone wires as shown in Fig. 6.19(b) is then given by

$$d\psi_{21} = B dy \cos \alpha = \frac{\mu_0 I_1 y}{2\pi(h^2 + y^2)} dy$$

where  $\alpha$  is the angle between the flux lines and the normal to the rectangular surface as shown in Fig. 6.19(a). The total flux  $\psi_{21}$  crossing the rectangular surface of length unity and extending from one telephone wire to the other is

$$\begin{aligned} \psi_{21} &= \int_{y=a}^{a+b} d\psi_{21} = \int_{y=a}^{a+b} \frac{\mu_0 I_1 y}{2\pi(h^2 + y^2)} dy \\ &= \frac{\mu_0 I_1}{4\pi} \ln \frac{h^2 + (a+b)^2}{h^2 + a^2} \end{aligned}$$

This is the flux due to  $I_1$  linking  $I_2$  per unit length along the wires. Thus the required mutual inductance per unit length of the wires is given by

$$\mathcal{L}_{21} = \frac{\psi_{21}}{I_1} = \frac{\mu_0}{4\pi} \ln \frac{h^2 + (a+b)^2}{h^2 + a^2} \text{ henrys/m} \quad \blacksquare$$

## 6.5 Magnetic Circuits

Let us consider the two structures shown in Figs. 6.20(a) and (b). The structure of Fig. 6.20(a) is a toroidal conductor of uniform conductivity  $\sigma$  and having a cross-sectional area  $A$  and mean circumference  $l$ . There is an infinitesimal gap  $a-b$  across which a potential difference of  $V_0$  volts is maintained

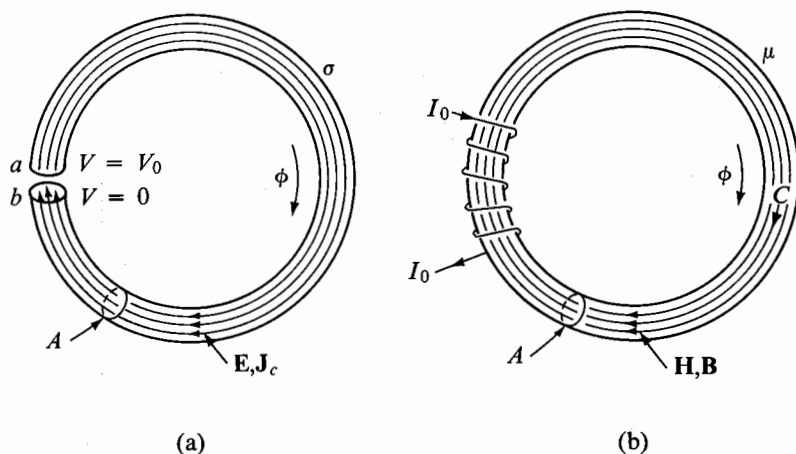


Fig. 6.20. For illustrating the analogy between electric and magnetic circuits.

by connecting an appropriate voltage source. Because of the potential difference, an electric field is established in the toroid and a conduction current results from the higher potential surface  $a$  to the lower potential surface  $b$  as shown in the figure. The structure of Fig. 6.20(b) is a toroidal magnetic core of uniform permeability  $\mu$  and having a cross-sectional area  $A$  and mean circumference  $l$ . A current  $I$  amp is passed through a filamentary wire of  $N$  turns wound around the toroid by connecting an appropriate current source. Because of the current through the winding, a magnetic field is established in the toroid and a magnetic flux results in the direction of advance of a right-hand screw as it is turned in the sense of the current.

Since the conduction current cannot leak into the free space surrounding the conductor, it is confined entirely to the conductor. On the other hand, the magnetic flux can leak into the free space surrounding the magnetic core and hence is not confined completely to the core. However, let us consider the case for which  $\mu \gg \mu_0$ . Applying the boundary conditions at the boundary between a magnetic material of  $\mu \gg \mu_0$  and free space as shown in Fig. 6.21, we have

$$B_1 \sin \alpha_1 = B_2 \sin \alpha_2$$

$$H_1 \cos \alpha_1 = H_2 \cos \alpha_2$$

or

$$\frac{B_1}{H_1} \tan \alpha_1 = \frac{B_2}{H_2} \tan \alpha_2$$

$$\frac{\tan \alpha_1}{\tan \alpha_2} = \frac{\mu_2}{\mu_1} \ll 1$$

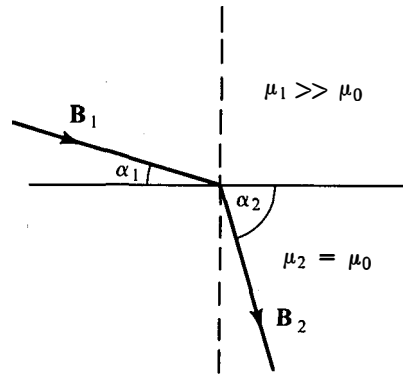


**Fig. 6.21.** Lines of magnetic flux density at the boundary between freespace and a magnetic material of permeability  $\mu \gg \mu_0$ .

Thus  $\alpha_1 \ll \alpha_2$ , and

$$\frac{B_2}{B_1} = \frac{\sin \alpha_1}{\sin \alpha_2} \ll 1$$

For example, if the values of  $\mu_1$  and  $\alpha_2$  are  $1000\mu_0$  and  $89^\circ$ , respectively, then  $\alpha_1 = 3^\circ 16'$  and  $\sin \alpha_1 / \sin \alpha_2 = 0.057$ . We can assume for all practical purposes that the magnetic flux is confined entirely to the magnetic core just as the conduction current is confined to the conductor. The structure of Fig. 6.20(b) is then known as a "magnetic circuit" similar to the "electric circuit" of Fig. 6.20(a).

For the structure of Fig. 6.20(a), we have

$$\nabla \times \mathbf{E} = 0 \quad (6-105a)$$

$$\int_a^b \mathbf{E} \cdot d\mathbf{l} = V_0 \quad (6-105b)$$

$$\mathbf{J}_c = \sigma \mathbf{E} \quad (6-105c)$$

$$I_c = \int_A \mathbf{J}_c \cdot d\mathbf{S} \quad (6-105d)$$

For the structure of Fig. 6.20(b), we have

$$\nabla \times \mathbf{H} = 0 \quad (6-106a)$$

$$\oint_C \mathbf{H} \cdot d\mathbf{l} = NI_0 \quad (6-106b)$$

$$\mathbf{B} = \mu \mathbf{H} \quad (6-106c)$$

$$\psi = \int_A \mathbf{B} \cdot d\mathbf{S} \quad (6-106d)$$

Equation (6-106a) results from the fact that there are no true currents in the magnetic material. In Eq. (6-106b), the factor  $N$  on the right side takes into account the fact that the filamentary wire penetrates a surface bounded by the path  $C$  as many times as there are number of turns in the entire

winding. Alternatively, if we pull the path  $C$  out of the toroid, it will be cut at as many points as there are number of turns in the entire winding, that is,  $N$  times. Equations (6-105a)–(6-105d) and (6-106a)–(6-106d) indicate an analogy between the electric and magnetic circuits of Figs. 6.20(a) and 6.20(b) as follows:

$$\mathbf{E} \leftrightarrow \mathbf{H} \quad (6-107\text{a})$$

$$V_0 \leftrightarrow NI_0 \quad (6-107\text{b})$$

$$\mathbf{J}_c \leftrightarrow \mathbf{B} \quad (6-107\text{c})$$

$$\sigma \leftrightarrow \mu \quad (6-107\text{d})$$

$$I_c \leftrightarrow \psi \quad (6-107\text{e})$$

This analogy permits the solution of magnetic circuit problems from a knowledge of the solution of electric circuit problems.

The ratio of  $V_0$  to  $I_c$  is the resistance  $R$  of the electric circuit of Fig. 6.20(a). The analogous quantity for the magnetic circuit of Fig. 6.20(b) is the ratio of  $NI_0$  to  $\psi$ . It is known as the reluctance and is denoted by the symbol  $\mathcal{R}$ . The resistance is purely a function of the dimensions of the conductor and the conductivity. For a magnetic core of the same dimensions as the conductor, the reluctance can therefore be obtained simply by replacing  $\sigma$  in  $R$  by  $\mu$ . We note, however, that, unlike  $\sigma$  for conductors,  $\mu$  for magnetic materials used for the cores is a function of the magnetic flux density in the material. This makes the reluctance analogous to a nonlinear resistor. Thus, to complete the analogy, we have

$$R = \frac{V_0}{I_c} \leftrightarrow \mathcal{R} = \frac{NI_0}{\psi} \quad (6-107\text{f})$$

For the structure of Fig. 6.20(a), an exact expression for the resistance can be obtained by taking into account the variation of  $\mathbf{E}$  over the cross section of the toroid. However, an approximate expression sufficient for practical purposes can be obtained by assuming that  $\mathbf{E}$  is uniform over the cross-sectional area and equal to its value at the mean radius of the toroid, especially if the radius of cross-section is small compared to the mean radius of the toroid. Thus

$$\begin{aligned} lE_\phi &= V_0 \\ J_c &= \sigma E_\phi = \frac{\sigma V_0}{l} \\ I_c &= J_c A = \frac{\sigma V_0 A}{l} \\ R &= \frac{V_0}{I_c} = \frac{l}{\sigma A} \end{aligned} \quad (6-108)$$

It follows from the analogy that the reluctance of the structure of Fig.

6.20(b) is

$$\mathcal{R} = \frac{NI_0}{\psi} = \frac{l}{\mu A} \quad (6-109)$$

In fact, if we assume that the magnetic field intensity  $\mathbf{H}$  is uniform over the cross-sectional area and equal to its value at the mean radius of the toroid, we have

$$\begin{aligned} lH_\phi &= NI_0 \\ B_\phi &= \mu H_\phi = \frac{\mu NI_0}{l} \\ \psi &= B_\phi A = \frac{\mu NI_0 A}{l} \\ \mathcal{R} &= \frac{NI_0}{\psi} = \frac{l}{\mu A} \end{aligned}$$

which agrees with (6-109). The equivalent circuit representations of (6-108) and (6-109) are shown in Figs. 6.22(a) and (b).

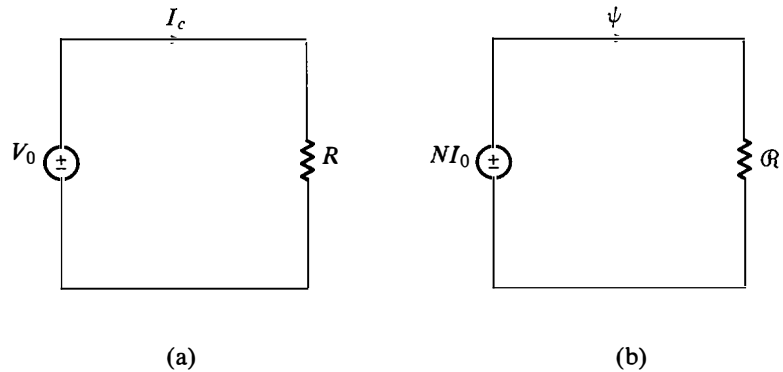


**Fig. 6.22.** Equivalent circuit representations for the structures of Figs. 6.20(a) and (b).

**EXAMPLE 6-15.** The structure shown in Fig. 6.23(a) is that of a magnetic circuit containing three legs with an air gap in the center leg. A filamentary wire of  $N$  turns carrying current  $I$  is wound around the center leg. The core material is annealed sheet steel, for which the  $B$  versus  $H$  curve is shown in Fig. 6.23(b). The dimensions of the magnetic circuit are

$$\begin{aligned} A_2 &= 5 \text{ cm}^2 & A_1 &= A_3 = 3 \text{ cm}^2 \\ l_2 &= 10 \text{ cm} & l_1 &= l_3 = 20 \text{ cm}, \quad l_g = 0.1 \text{ cm} \end{aligned}$$

We wish to obtain the equivalent circuit and find  $NI$  required to establish a magnetic flux of  $8 \times 10^{-4}$  Wb in the air gap.

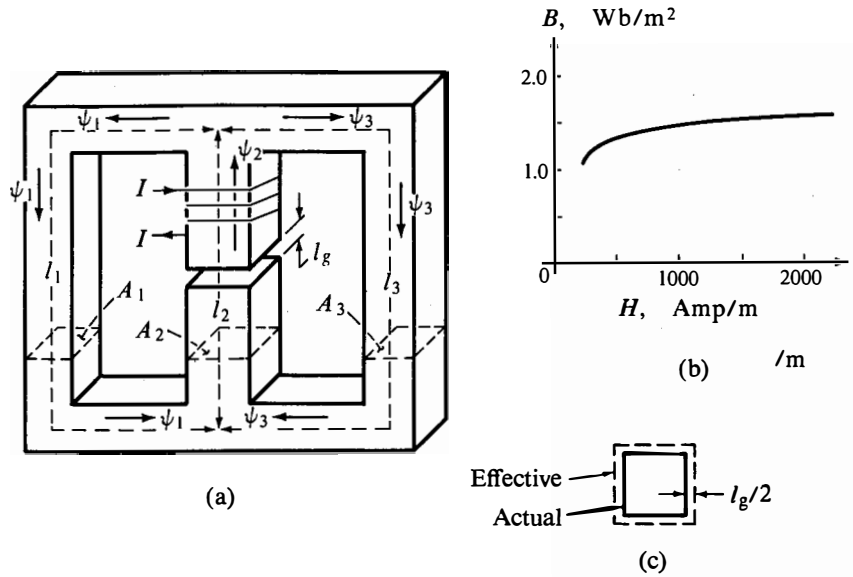


Fig. 6.23. (a) A magnetic circuit. (b)  $B$ - $H$  curve for annealed sheet steel. (c) Effective and actual cross sections for the air gap of the magnetic circuit of (a).

The current in the winding establishes a magnetic flux in leg 2 which divides between legs 1 and 3. In the air gap, fringing of the flux occurs. This is taken into account by using an effective cross section which is greater than the actual cross section, as shown in Fig. 6.23(c). Using subscripts 1, 2, 3, and  $g$  for the fields and permeabilities associated with the three legs and the air gap, respectively, we can write the following equations:

$$\begin{aligned}
 NI &= H_2 l_2 + H_g l_g + H_1 l_1 \\
 &= \psi_2 \frac{l_2}{\mu_2 A_2} + \psi_g \frac{l_g}{\mu_g A_g} + \psi_1 \frac{l_1}{\mu_1 A_1} \\
 &= \psi_2 \mathcal{R}_2 + \psi_g \mathcal{R}_g + \psi_1 \mathcal{R}_1
 \end{aligned} \tag{6-110}$$

$$\begin{aligned}
 0 &= H_3 l_3 - H_1 l_1 \\
 &= \psi_3 \frac{l_3}{\mu_3 A_3} - \psi_1 \frac{l_1}{\mu_1 A_1} \\
 &= \psi_3 \mathcal{R}_3 - \psi_1 \mathcal{R}_1
 \end{aligned} \tag{6-111}$$

The equivalent circuit corresponding to Eqs. (6-110) and (6-111) can be drawn as shown in Fig. 6.24, taking into account the fact that  $\psi_g = \psi_2$ . To determine the required  $NI$ , we note that

$$B_2 = \frac{\psi_2}{A_2} = \frac{8 \times 10^{-4}}{5 \times 10^{-4}} = 1.6 \text{ Wb/m}^2$$

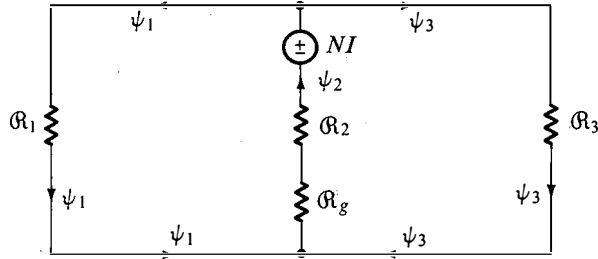


Fig. 6.24. Equivalent circuit for analyzing the magnetic circuit of Fig. 6.23(a).

From Fig. 6.23(b), the value of  $H_2$  is 2200 amp/m. Since legs 1 and 3 are identical, their reluctances are equal so that the flux  $\psi_2$  divides equally between the two legs. Thus  $\psi_1 = \psi_3 = \psi_2/2 = 4 \times 10^{-4}$  Wb/m<sup>2</sup>. Then

$$B_1 = \frac{\psi_1}{A_1} = \frac{4 \times 10^{-4}}{3 \times 10^{-4}} = 1.333 \text{ Wb/m}^2$$

From Fig. 6.23(b), the value of  $H_1$  is 475 amp/m. The effective cross section of the air gap is  $(\sqrt{5} + l_g)^2 = 2.34 \text{ cm}^2$ . The flux density in the air gap is

$$B_g = \frac{\psi_g}{A_g} = \frac{8 \times 10^{-4}}{2.34^2 \times 10^{-4}} = 1.46 \text{ Wb/m}^2$$

The magnetic field intensity in the air gap is

$$H_g = \frac{B_g}{\mu_g} = \frac{B_g}{\mu_0} = \frac{1.46}{4\pi \times 10^{-7}} = 0.1162 \times 10^7 \text{ Wb/m}^2$$

From (6-110), we then have

$$\begin{aligned} NI &= H_2 l_2 + H_g l_g + H_1 l_1 \\ &= 2200 \times 0.10 + 0.1162 \times 10^7 \times 10^{-3} + 475 \times 0.20 \\ &= 1477 \text{ amp-turns} \end{aligned}$$

We note that a large part of the ampere-turns is due to high reluctance of the air gap. ■

## 6.6 Quasistatics; The Field Basis of Low-Frequency Circuit Theory

In Section 6.4 we considered three structures, shown in Figs. 6.13(a), (b), and (c), from the point of view of static fields. Let us now consider the three structures driven by time-varying sources. The resulting fields are then time varying. From Maxwell's equations for time-varying fields, we know that a time-varying electric field is accompanied by a time-varying magnetic field and vice versa. Thus, for example, a time-varying voltage source applied to the structure of Fig. 6.13(b) results in a time-varying electric field which has associated with it a time-varying magnetic field as shown in Fig. 6.25(a).

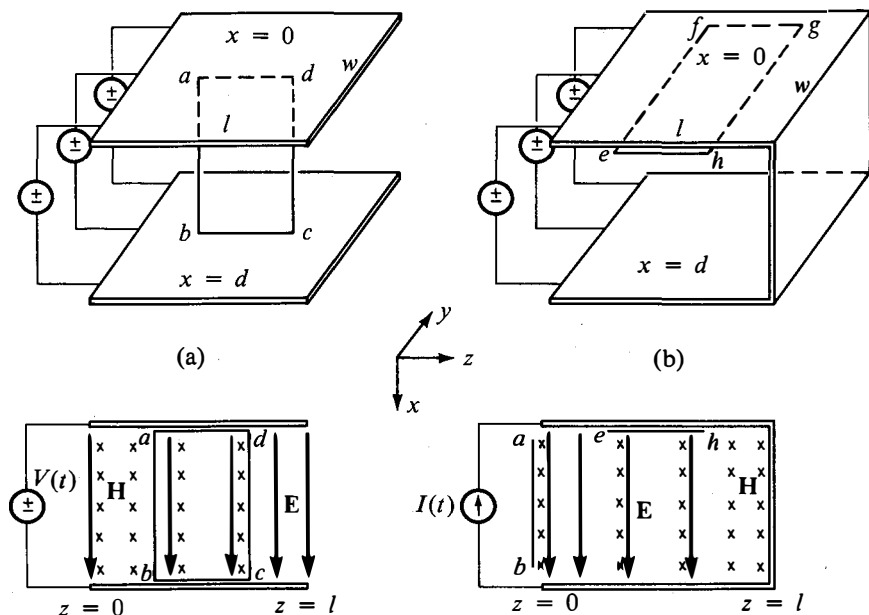


Fig. 6.25. For illustrating the behavior of the structures of Figs. 6.13(b) and (c) for time-varying sources.

A certain amount of magnetic energy is then associated with the structure in addition to the electric energy. We can no longer say that the structure behaves like a single capacitor as in the case of static fields. Furthermore, applying Faraday's law to a rectangular path  $abcd$  as shown in Fig. 6.25(a), we have

$$\int_a^b \mathbf{E} \cdot d\mathbf{l} - \int_d^c \mathbf{E} \cdot d\mathbf{l} = \frac{d}{dt} \int_{\text{area } abcd} \mu H_y dS \tag{6-112}$$

It follows from (6-112) that the voltage between  $a$  and  $b$  is not necessarily equal to the voltage between  $d$  and  $c$  because of the time-varying magnetic field. The voltage along the structure is dependent on  $z$ . However, under certain conditions, the time-varying magnetic field is negligible so that the electric field distribution at any time can be approximated by the static field distribution resulting from a constant voltage source between the plates having a value equal to that of the source voltage at that time. Such approximations are known as quasistatic approximations and the corresponding fields are known as quasistatic fields. Thus, for the structure of Fig. 6.13(b) under the quasistatic approximation,  $\partial \mathbf{B} / \partial t$  is negligible so that

$$\nabla \times \mathbf{E} \approx 0 \tag{6-113}$$

$$E_x(t) \approx \frac{V(t)}{d} \tag{6-114}$$



The magnitude of the resulting time-varying charge on either plate is

$$Q(t) = (lw)\epsilon E_x(t) = \frac{\epsilon w l}{d} V(t) = CV(t) \tag{6-115}$$

where  $C = \epsilon w l/d$  is the same as the capacitance obtained for the direct voltage source. Differentiating both sides of (6-115) with respect to time, we have

$$\frac{dQ}{dt} = \frac{d}{dt}(CV) \tag{6-116}$$

But, according to the law of conservation of charge,  $dQ/dt$  must be equal to the current  $I$  flowing into the plate from the voltage source. Thus Eq. (6-116) becomes

$$I = \frac{d}{dt}(CV) \tag{6-117}$$

which is the familiar voltage-to-current relationship used in circuit theory for a capacitor. For the sinusoidally time-varying case, Eq. (6-117) reduces to

$$\bar{I} = j\omega C\bar{V} \tag{6-118}$$

where  $\bar{I}$  and  $\bar{V}$  are the phasor current and phasor voltage, respectively, and  $\omega$  is the radian frequency of the voltage source.

Similarly, a time-varying current source applied to the structure of Fig. 6.13(c) results in a time-varying magnetic field which has associated with it a time-varying electric field as shown in Fig. 6.25(b). A certain amount of electric energy is then associated with the structure in addition to the magnetic energy. We can no longer say that the structure behaves like a single inductor as in the case of static fields. Furthermore, applying the integral form of Maxwell's curl equation for  $\mathbf{H}$  to a rectangular path  $efghe$  as shown in Fig. 6.25(b), we have

$$\int_e^f \mathbf{H} \cdot d\mathbf{l} - \int_h^g \mathbf{H} \cdot d\mathbf{l} = \frac{d}{dt} \int_{\substack{\text{area} \\ efghe}} \epsilon E_x dS \tag{6-119}$$

Since  $H$  is zero outside the structure, it follows from (6-119) that the current crossing the line  $ef$  is not necessarily equal to the current crossing the line  $hg$  because of the time-varying electric field. The current flowing along the structure is dependent on  $z$ . However, under the quasistatic approximation,  $\partial\mathbf{D}/\partial t$  is negligible so that the magnetic field distribution at any time can be approximated by the static magnetic field distribution resulting from the flow of a direct current having a value equal to that of the source current at that time. Thus

$$\nabla \times \mathbf{H} \approx 0 \tag{6-120}$$

$$H_y(t) \approx \frac{I(t)}{w} \tag{6-121}$$

The resulting time-varying magnetic flux linking the current is

$$\psi(t) = (dl)\mu H_y(t) = \frac{\mu dl}{w} I(t) = LI(t) \quad (6-122)$$

where  $L = \mu dl/w$  is the same as the inductance obtained for the direct current source. Differentiating both sides of (6-122) with respect to time, we have

$$\frac{d\psi}{dt} = \frac{d}{dt}(LI) \quad (6-123)$$

However, applying Faraday's law to the rectangular contour bounding the magnetic flux linking the current and noting that the contribution to  $\oint \mathbf{E} \cdot d\mathbf{l}$  is entirely from the path  $ab$  shown in Fig. 6.25(b), we have

$$\int_a^b \mathbf{E} \cdot d\mathbf{l} = \frac{d\psi}{dt} \quad (6-124)$$

The left side of (6-124) is the voltage  $V(t)$  across the current source. Thus Eq. (6-123) becomes

$$V = \frac{d}{dt}(LI) \quad (6-125)$$

which is the familiar voltage-to-current relationship used in circuit theory for an inductor. For the sinusoidally time-varying case, Eq. (6-125) reduces to

$$\bar{V} = j\omega L\bar{I} \quad (6-126)$$

where  $\bar{V}$  and  $\bar{I}$  are the phasor voltage and phasor current, respectively, and  $\omega$  is the radian frequency of the current source.

Finally, for the structure of Fig. 6.13(a) under the quasistatic approximation, both  $\partial\mathbf{B}/\partial t$  and  $\partial\mathbf{D}/\partial t$  are negligible so that

$$\nabla \times \mathbf{E} \approx 0 \quad (6-127a)$$

$$\nabla \times \mathbf{H} \approx \mathbf{J}_c \quad (6-127b)$$

In view of (6-127a), we have

$$E_x(t) = \frac{V(t)}{d} \quad (6-128)$$

The conduction current flowing from the upper plate to the lower plate is

$$I_c(t) = (lw)\sigma E_x(t) = \frac{\sigma wl}{d} V(t) \quad (6-129)$$

In view of (6-127b),  $\oint \mathbf{H} \cdot d\mathbf{l}$  around a rectangular path surrounding the conductor in the cross-sectional plane is equal to the conduction current  $I_c$ . But the same quantity is also equal to the current  $I$  drawn from the voltage source. Thus

$$I(t) = \frac{\sigma wl}{d} V(t) = GV(t) \quad (6-130a)$$

or

$$V(t) = \frac{d}{\sigma wl} I(t) = RI(t) \quad (6-130b)$$

where  $G = \sigma w l / d$  and  $R = d / \sigma w l$  are the same as the conductance and resistance, respectively, obtained for the direct voltage source. Equations (6-130a) and (6-130b) are the familiar voltage-to-current relationships used in circuit theory for conductance and resistance, respectively. For the sinusoidally time-varying case, we have

$$\bar{I} = G\bar{V} \quad (6-131a)$$

and

$$\bar{V} = R\bar{I} \quad (6-131b)$$

where  $\bar{I}$  and  $\bar{V}$  are the phasor current and phasor voltage, respectively.

To summarize what we have learned thus far in this section, the voltage-to-current relationships used in circuit theory for a capacitor, inductor, and resistor given by (6-117), (6-125), and (6-130b), respectively, are valid only under the quasistatic approximation. For the quasistatic approximation to hold,  $\partial\mathbf{B}/\partial t$  must be negligible for the case of the capacitor,  $\partial\mathbf{D}/\partial t$  must be negligible for the case of the inductor, and both  $\partial\mathbf{B}/\partial t$  and  $\partial\mathbf{D}/\partial t$  must be negligible for the case of the resistor. To illustrate a method for determining the quantitative condition for the quasistatic approximation to hold in a particular case, we consider the structure of Fig. 6.25(b) in detail for the sinusoidally time-varying case in the following example.

**EXAMPLE 6-16.** The parallel plate structure of Fig. 6.25(b) is driven by a sinusoidally time-varying current source. It is desired to show that the quasistatic approximation holds, that is, that the structure behaves like a single inductor as viewed by the current source for the condition

$$f \ll \frac{1}{2\pi l \sqrt{\mu\epsilon}}$$

where  $f$  is the frequency of the current source and  $\mu$  and  $\epsilon$  are the permeability and permittivity, respectively, of the medium between the plates.

Under the quasistatic approximation, the time-varying magnetic field distribution at any particular time must be approximately the same as that of the static magnetic field resulting from a direct current equal to the value of the source current at that time. Thus, denoting the phasor corresponding to this magnetic field by  $\bar{H}_y^q$ , we have

$$\bar{H}_y^q = \frac{\bar{I}_0}{w} \quad (6-132)$$

where  $\bar{I}_0 = [\bar{I}]_{z=0}$  is the phasor corresponding to the source current. This time-varying magnetic field induces a time-varying electric field in the  $x$  direction in accordance with Maxwell's curl equation for  $\mathbf{E}$ , given in phasor form by

$$\nabla \times \bar{\mathbf{E}} = -j\omega\bar{\mathbf{B}}$$

Denoting the phasor corresponding to this electric field by  $\bar{E}'_x$ , we have

$$\frac{\partial \bar{E}'_x}{\partial z} = -j\omega \bar{B}'_y = -j\omega \mu \bar{H}'_y = -j\omega \mu \frac{\bar{I}_0}{w} \quad (6-133)$$

Integrating (6-133) with respect to  $z$ , we obtain

$$\bar{E}'_x = -j\omega \mu \frac{\bar{I}_0}{w} (z - l) \quad (6-134)$$

where we have evaluated the arbitrary constant of integration by using the boundary condition that  $[\bar{E}'_x]_{z=l} = 0$ . If  $\partial \mathbf{D} / \partial t$  is not negligible, the time-varying electric field corresponding to the phasor  $\bar{E}'_x$  produces a time-varying magnetic field in the  $y$  direction in accordance with Maxwell's curl equation for  $\mathbf{H}$ , given in phasor form by

$$\nabla \times \bar{\mathbf{H}} = j\omega \bar{\mathbf{D}}$$

Denoting the phasor corresponding to this induced magnetic field by  $\bar{H}'_y$ , we have

$$-\frac{\partial \bar{H}'_y}{\partial z} = j\omega \bar{D}'_x = j\omega \epsilon \bar{E}'_x = \omega^2 \mu \epsilon \frac{\bar{I}_0}{w} (z - l) \quad (6-135)$$

Integrating (6-135) with respect to  $z$ , we obtain

$$\bar{H}'_y = -\omega^2 \mu \epsilon \frac{\bar{I}_0}{w} \left[ \frac{(z - l)^2}{2} - \frac{l^2}{2} \right] \quad (6-136)$$

where we have evaluated the arbitrary constant of integration by using the boundary condition that  $[\bar{H}'_y]_{z=0} = 0$  since the condition that the current at  $z = 0$ , as determined by the tangential magnetic field intensity at  $z = 0$  must be equal to the source current is satisfied by (6-132) alone.

Now, the time-varying magnetic field corresponding to the phasor given by (6-136) induces a time-varying electric field. Denoting the phasor corresponding to this induced electric field by  $\bar{E}''_x$ , we have

$$\frac{\partial \bar{E}''_x}{\partial z} = -j\omega \mu \bar{H}'_y = j\omega^3 \mu^2 \epsilon \frac{\bar{I}_0}{w} \left[ \frac{(z - l)^2}{2} - \frac{l^2}{2} \right] \quad (6-137)$$

Integrating (6-137) with respect to  $z$ , we obtain

$$\bar{E}''_x = j\omega^3 \mu^2 \epsilon \frac{\bar{I}_0}{w} \left[ \frac{(z - l)^3}{6} - \frac{l^2(z - l)}{2} \right] \quad (6-138)$$

where we have again evaluated the arbitrary constant of integration by using the boundary condition that  $[\bar{E}''_x]_{z=l} = 0$ . Continuing in this manner, we obtain the successively induced magnetic and electric fields as

$$\bar{H}''_y = \omega^4 \mu^2 \epsilon^2 \frac{\bar{I}_0}{w} \left[ \frac{(z - l)^4}{24} - \frac{l^2(z - l)^2}{4} + \frac{5l^4}{24} \right] \quad (6-139)$$

$$\bar{E}'''_x = -j\omega^5 \mu^3 \epsilon^2 \frac{\bar{I}_0}{w} \left[ \frac{(z - l)^5}{120} - \frac{l^2(z - l)^3}{12} + \frac{5l^4(z - l)}{24} \right] \quad (6-140)$$

$$\begin{aligned}\bar{H}_y'''' &= -\omega^6 \mu^3 \epsilon^3 \frac{\bar{I}_0}{w} \left[ \frac{(z-l)^6}{720} - \frac{l^2(z-l)^4}{48} + \frac{5l^4(z-l)^2}{48} - \frac{61l}{720} \right] \\ \bar{E}_x'''' &= \dots \\ \bar{H}_y'''' &= \dots\end{aligned}\quad (6-141)$$

The total electric field is given by

$$\begin{aligned}\bar{E}_x &= \bar{E}_x' + \bar{E}_x'' + \bar{E}_x''' + \dots \\ &= -j\omega\mu \frac{\bar{I}_0}{w}(z-l) + j\omega^3 \mu^2 \epsilon \frac{\bar{I}_0}{w} \left[ \frac{(z-l)^3}{6} - \frac{l^2(z-l)}{2} \right] \\ &\quad - j\omega^5 \mu^3 \epsilon^2 \frac{\bar{I}_0}{w} \left[ \frac{(z-l)^5}{120} - \frac{l^2(z-l)^3}{12} + \frac{5l^4(z-l)}{24} \right] + \dots \\ &= -j\sqrt{\frac{\mu}{\epsilon}} \frac{\bar{I}_0}{w} \left( 1 + \frac{\omega^2 \mu \epsilon l^2}{2} + \frac{5\omega^4 \mu^2 \epsilon^2 l^4}{24} + \dots \right) \\ &\quad \times \left[ \omega\sqrt{\mu\epsilon}(z-l) - (\omega\sqrt{\mu\epsilon})^3 \frac{(z-l)^3}{3!} + (\omega\sqrt{\mu\epsilon})^5 \frac{(z-l)^5}{5!} - \dots \right] \\ &= -j\sqrt{\frac{\mu}{\epsilon}} \frac{\bar{I}_0}{w} \frac{\sin \omega\sqrt{\mu\epsilon}(z-l)}{\cos \omega\sqrt{\mu\epsilon}l}\end{aligned}\quad (6-142)$$

The total electric field at  $z = 0$  is given by

$$[\bar{E}_x]_{z=0} = j\sqrt{\frac{\mu}{\epsilon}} \frac{\bar{I}_0}{w} \tan \omega\sqrt{\mu\epsilon}l \quad (6-143)$$

This result could have been obtained simply by adding  $[\bar{E}_x']_{z=0}$ ,  $[\bar{E}_x'']_{z=0}$ ,  $[\bar{E}_x''']_{z=0}$ , and so on. However, Eq. (6-142) was derived to point out that the electric field and hence the voltage along the structure varies sinusoidally with distance. Similarly, if we add  $\bar{H}_y^0$ ,  $\bar{H}_y'$ ,  $\bar{H}_y''$ ,  $\bar{H}_y'''$ , and so on, we obtain the total magnetic field as

$$\bar{H}_y = \frac{\bar{I}_0 \cos \omega\sqrt{\mu\epsilon}(z-l)}{w \cos \omega\sqrt{\mu\epsilon}l} \quad (6-144)$$

indicating that the magnetic field and hence the current along the structure varies cosinusoidally with distance.

The phasor voltage across the current source is given by

$$\begin{aligned}\bar{V}_0 &= [\bar{V}]_{z=0} = \int_a^b [\bar{E}_x]_{z=0} dl \\ &= j\sqrt{\frac{\mu}{\epsilon}} \frac{\bar{I}_0 d}{w} \tan \omega\sqrt{\mu\epsilon}l \\ &= j\omega \frac{\mu dl}{w} \bar{I}_0 \frac{\tan \omega\sqrt{\mu\epsilon}l}{\omega\sqrt{\mu\epsilon}l} \\ &= j\omega L \bar{I}_0 \frac{\tan \omega\sqrt{\mu\epsilon}l}{\omega\sqrt{\mu\epsilon}l}\end{aligned}\quad (6-145)$$

where  $L = \mu dl/w$  is the inductance of the structure computed from static field considerations. Equation (6-145) represents the voltage-to-current rela-

tionship at the source end of the structure under the condition for which  $\partial \mathbf{D} / \partial t$  is not negligible. For  $\omega \sqrt{\mu \epsilon} l \ll 1$ ,  $\tan \omega \sqrt{\mu \epsilon} l \approx \omega \sqrt{\mu \epsilon} l$  and Eq. (6-145) reduces to

$$\bar{V}_0 = j\omega L \bar{I}_0$$

which is the voltage-to-current relationship for a single inductor. Thus, for the quasistatic approximation to hold, the condition to be satisfied is

$$f \ll \frac{1}{2\pi l \sqrt{\mu \epsilon}} \quad (6-146)$$

As a numerical example, for  $l = 0.1$  m,  $\mu = \mu_0$ , and  $\epsilon = \epsilon_0$ , the value of  $1/2\pi l \sqrt{\mu \epsilon}$  is  $(1500/\pi) \times 10^6$ . For a value of  $1/10$  for  $\omega \sqrt{\mu \epsilon} l$ , the frequency must be less than  $150/\pi$  MHz for the structure to behave essentially like a single inductor. ■

**EXAMPLE 6-17.** In Example 6-16 we showed that the quasistatic approximation holds for the structure of Fig. 6.25(b) for the condition  $f \ll 1/2\pi l \sqrt{\mu \epsilon}$ . The structure then behaves like a single inductor as shown in Fig. 6.26(a). It is desired to examine the behavior of the structure as viewed from the source end for frequencies beyond the value for which the quasistatic approximation holds.

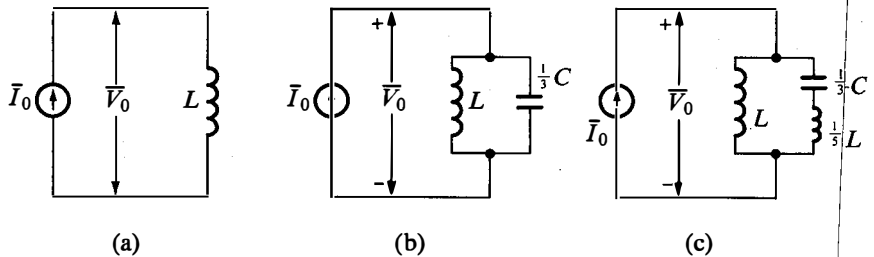


**Fig. 6.26.** (a) Equivalent circuit for the input behavior of the structure of Fig. 6.25(b) under quasistatic approximation. (b) and (c) Same as (a) except for frequencies higher and higher than those for which the quasistatic approximation is valid. The values of  $L$  and  $C$  are  $\mu dl/w$  and  $\epsilon wl/d$ , respectively.

Expressing  $\tan \omega \sqrt{\mu \epsilon} l$  as a sum of infinite series in powers of  $\omega \sqrt{\mu \epsilon} l$ , Eq. (6-145) can be written as

$$\bar{V}_0 = j\omega L \bar{I}_0 \left( 1 + \frac{1}{3} \omega^2 \mu \epsilon l^2 + \frac{2}{15} \omega^4 \mu^2 \epsilon^2 l^4 + \dots \right) \quad (6-147)$$

For the quasistatic approximation, we neglect all the terms involving powers of  $\omega \sqrt{\mu \epsilon} l$  in comparison with 1 in the series on the right side of (6-147). For a frequency slightly higher than the value for which condition (6-146) is

acceptable, we have to include the second term in the series. Thus we have

$$\begin{aligned}\bar{V}_0 &\approx j\omega L \bar{I}_0 \left(1 + \frac{1}{3}\omega^2 \mu \epsilon l^2\right) \\ &= j\omega L \bar{I}_0 \left(1 + \frac{1}{3}\omega^2 LC\right)\end{aligned}\quad (6-148)$$

where  $C = \epsilon w l / d$  is the capacitance computed from static field considerations if the structure were open circuited at  $z = l$ . Rearranging (6-148), we get

$$\begin{aligned}\bar{I}_0 &= \frac{\bar{V}_0}{j\omega L(1 + \frac{1}{3}\omega^2 LC)} \approx \frac{\bar{V}_0}{j\omega L} \left(1 - \frac{1}{3}\omega^2 LC\right) \\ &= \bar{V}_0 \left(\frac{1}{j\omega L} + j\omega \frac{C}{3}\right)\end{aligned}\quad (6-149)$$

The voltage-to-current relationship given by (6-149) corresponds to that of an inductor of value  $L$  in parallel with a capacitor of value  $\frac{1}{3}C$  as shown in Fig. 6.26(b). Thus the same structure which behaves almost like a single inductor at low frequencies governed by (6-146) acts like an inductor in parallel with a capacitor as the frequency is increased. For still higher frequencies, we have to include one more term in the series on the right side of (6-147), giving us

$$\begin{aligned}\bar{V}_0 &\approx j\omega L \bar{I}_0 \left(1 + \frac{1}{3}\omega^2 \mu \epsilon l^2 + \frac{2}{15}\omega^4 \mu^2 \epsilon^2 l^4\right) \\ &= j\omega L \bar{I}_0 \left(1 + \frac{1}{3}\omega^2 LC + \frac{2}{15}\omega^4 L^2 C^2\right)\end{aligned}$$

or

$$\begin{aligned}\bar{I}_0 &= \frac{\bar{V}_0}{j\omega L} \left(1 + \frac{1}{3}\omega^2 LC + \frac{2}{15}\omega^4 L^2 C^2\right)^{-1} \\ &= \frac{\bar{V}_0}{j\omega L} \left(1 - \frac{1}{3}\omega^2 LC - \frac{1}{45}\omega^4 L^2 C^2 + \text{higher-order terms}\right) \\ &\approx \frac{\bar{V}_0}{j\omega L} \left(1 - \frac{1}{3}\omega^2 LC - \frac{1}{45}\omega^4 L^2 C^2\right) \\ &= \frac{\bar{V}_0}{j\omega L} + \bar{V}_0 \left(j\frac{\omega C}{3} + j\frac{\omega^3 L C^2}{45}\right) \\ &= \frac{\bar{V}_0}{j\omega L} + \frac{\bar{V}_0}{1/[(j\omega C/3)(1 + \omega^2 LC/15)]} \\ &\approx \frac{\bar{V}_0}{j\omega L} + \frac{\bar{V}_0}{(3/j\omega C)(1 - \omega^2 LC/15)} \\ &= \frac{\bar{V}_0}{j\omega L} + \frac{\bar{V}_0}{(3/j\omega C) + (j\omega L/5)}\end{aligned}\quad (6-150)$$

The equivalent circuit corresponding to (6-150) is shown in Fig. 6.26(c). It is now evident that as the frequency is increased, more and more elements are added to the equivalent circuit. For an arbitrarily high frequency, we must

include all terms in the series. We then have, from (6-145),

$$\begin{aligned}\frac{\bar{V}_0}{\bar{I}_0} &= j\omega L \frac{\tan \omega\sqrt{\mu\epsilon}l}{\omega\sqrt{\mu\epsilon}l} \\ &= j\sqrt{\frac{L}{C}} \tan \omega\sqrt{LC}\end{aligned}\quad (6-151)$$

Since  $\tan \omega\sqrt{LC}$  can be negative if  $\omega\sqrt{LC}$  falls in the second or third quadrant, the reactance viewed by the current source can even be capacitive!

## 6.7 Transmission-Line Equations; The Distributed Circuit Concept

In Example 6-16 we obtained the fields between the parallel plates of the structure shown in Fig. 6.25(b) by starting with the quasistatic magnetic field and using successively the two curl equations

$$\nabla \times \bar{\mathbf{E}} = -j\omega\bar{\mathbf{B}} = -j\omega\mu\bar{\mathbf{H}} \quad (6-152a)$$

$$\nabla \times \bar{\mathbf{H}} = j\omega\bar{\mathbf{D}} = j\omega\epsilon\bar{\mathbf{E}} \quad (6-152b)$$

to find the successively induced electric and magnetic fields. The total electric field is the sum of all the electric fields found successively and the total magnetic field is the sum of all the magnetic fields found successively. These two total fields must satisfy the two curl equations simultaneously. Thus, denoting the total electric field by  $\bar{\mathbf{E}}(z) = \bar{E}_x(z)\mathbf{i}_x$  and the total magnetic field by  $\bar{\mathbf{H}}(z) = \bar{H}_y(z)\mathbf{i}_y$ , we have, from (6-152a) and (6-152b), respectively,

$$\frac{\partial \bar{E}_x}{\partial z} = -j\omega\mu\bar{H}_y \quad (6-153a)$$

$$-\frac{\partial \bar{H}_y}{\partial z} = j\omega\epsilon\bar{E}_x \quad (6-153b)$$

However, the voltage between the two conductors in any plane normal to the  $z$  direction is given by

$$\bar{V}(z) = \int_{x=0}^d \bar{E}_x(z) dx = \bar{E}_x d \quad (6-154a)$$

The current along the conductors crossing any plane normal to the  $z$  direction is given by

$$\bar{I}(z) = \int_{y=0}^w \bar{H}_y(z) dy = \bar{H}_y w \quad (6-154b)$$

Substituting for  $\bar{E}_x$  and  $\bar{H}_y$  in (6-153a) and (6-153b) from (6-154a) and (6-154b), respectively, we get

$$\frac{\partial \bar{V}}{\partial z} = -j\omega\frac{\mu d}{w}\bar{I} = -j\omega\mathcal{L}\bar{I} \quad (6-155)$$

$$\frac{\partial \bar{I}}{\partial z} = -j\omega\frac{\epsilon w}{d}\bar{V} = -j\omega\mathcal{C}\bar{V} \quad (6-156)$$



where  $\mathcal{L} = \mu d/w$  and  $\mathcal{C} = \epsilon w/d$  are the inductance and capacitance, respectively, per unit length of the structure computed from static fields.

Equations (6-155) and (6-156) relate the time-varying voltage distribution along the  $z$  direction to the time-varying current distribution along the  $z$  direction. While we have obtained these equations for the particular case of a structure consisting of two parallel plane conductors, they are general and hold for any structure consisting of two parallel, infinitely long, perfect conductors having arbitrary but uniform cross sections. To prove this, let us consider such a structure having the cross section shown in Fig. 6.27.

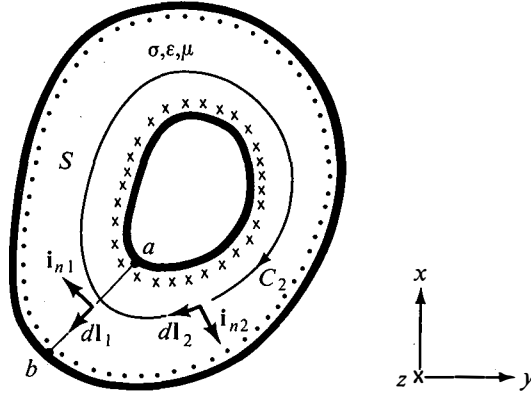


Fig. 6.27. For deriving the transmission-line equations.

For the sake of generality, we consider the dielectric to be imperfect with uniform conductivity  $\sigma$  and also work with arbitrarily time-varying fields instead of sinusoidally time-varying fields. Thus the electric and magnetic fields between the conductors are given by

$$\begin{aligned} \mathbf{E}(x, y, z, t) &= E_x(x, y, z, t)\mathbf{i}_x + E_y(x, y, z, t)\mathbf{i}_y \\ &= \mathbf{E}_{xy}(x, y, z, t) \end{aligned} \tag{6-157a}$$

$$\begin{aligned} \mathbf{H}(x, y, z, t) &= H_x(x, y, z, t)\mathbf{i}_x + H_y(x, y, z, t)\mathbf{i}_y \\ &= \mathbf{H}_{xy}(x, y, z, t) \end{aligned} \tag{6-157b}$$

Substituting (6-157a) and (6-157b) in

$$\nabla \times \mathbf{E} = -\frac{\partial \mathbf{B}}{\partial t}$$

we have

$$-\frac{\partial E_y}{\partial z}\mathbf{i}_x + \frac{\partial E_x}{\partial z}\mathbf{i}_y = -\frac{\partial B_x}{\partial t}\mathbf{i}_x - \frac{\partial B_y}{\partial t}\mathbf{i}_y \tag{6-158}$$

Taking the cross product of both sides of (6-158) with the unit vector  $\mathbf{i}_z$ ,

we get

$$-\frac{\partial E_y}{\partial z} \mathbf{i}_y - \frac{\partial E_x}{\partial z} \mathbf{i}_x = -\frac{\partial}{\partial t} (\mathbf{i}_z \times \mathbf{B}_{xy})$$

or

$$\frac{\partial \mathbf{E}_{xy}}{\partial z} = \frac{\partial}{\partial t} (\mathbf{i}_z \times \mathbf{B}_{xy}) \quad (6-159)$$

Performing line integration of both sides of (6-159) from point  $a$  on the inner conductor to point  $b$  on the outer conductor, we have

$$\int_a^b \frac{\partial \mathbf{E}_{xy}}{\partial z} \cdot d\mathbf{l}_1 = \int_a^b \frac{\partial}{\partial t} (\mathbf{i}_z \times \mathbf{B}_{xy}) \cdot d\mathbf{l}_1$$

or

$$\begin{aligned} \frac{\partial}{\partial z} \int_a^b \mathbf{E}_{xy} \cdot d\mathbf{l}_1 &= -\frac{\partial}{\partial t} \int_a^b \mathbf{B}_{xy} \cdot (\mathbf{i}_z \times d\mathbf{l}_1) \\ &= -\frac{\partial}{\partial t} \int_a^b \mathbf{B}_{xy} \cdot \mathbf{i}_{n1} dl_1 \end{aligned} \quad (6-160)$$

where  $\mathbf{i}_{n1}$  is the unit vector normal to  $d\mathbf{l}_1$  as shown in Fig. 6.27. The integral on the left side of (6-160) is simply the voltage  $V$  between the conductors in the plane in which the line integral is evaluated since the magnetic field has no  $z$  component. The integral on the right side of (6-160) is the magnetic flux per unit length in the  $z$  direction, linking the inner conductor if the conductors are carrying a direct current equal to the current  $I$  crossing the plane containing the path  $ab$ . It is therefore equal to  $\mathcal{L}I$ , where  $\mathcal{L}$  is the inductance per unit length of the structure computed from static field considerations. Thus we have

$$\frac{\partial V(z, t)}{\partial z} = -\frac{\partial}{\partial t} [\mathcal{L}I(z, t)] = -\mathcal{L} \frac{\partial I(z, t)}{\partial t} \quad (6-161)$$

Similarly, substituting (6-157a) and (6-157b) in

$$\nabla \times \mathbf{H} = \mathbf{J}_c + \frac{\partial \mathbf{D}}{\partial t} = \sigma \mathbf{E} + \frac{\partial \mathbf{D}}{\partial t}$$

we have

$$-\frac{\partial H_y}{\partial z} \mathbf{i}_x + \frac{\partial H_x}{\partial z} \mathbf{i}_y = \sigma E_x \mathbf{i}_x + \sigma E_y \mathbf{i}_y + \frac{\partial D_x}{\partial t} \mathbf{i}_x + \frac{\partial D_y}{\partial t} \mathbf{i}_y \quad (6-162)$$

Taking the cross product of both sides of (6-162) with the unit vector  $\mathbf{i}_z$ , we get

$$-\frac{\partial H_y}{\partial z} \mathbf{i}_y - \frac{\partial H_x}{\partial z} \mathbf{i}_x = \sigma (\mathbf{i}_z \times \mathbf{E}_{xy}) + \frac{\partial}{\partial t} (\mathbf{i}_z \times \mathbf{D}_{xy})$$

or

$$\frac{\partial \mathbf{H}_{xy}}{\partial z} = -\sigma (\mathbf{i}_z \times \mathbf{E}_{xy}) - \frac{\partial}{\partial t} (\mathbf{i}_z \times \mathbf{D}_{xy}) \quad (6-163)$$

Performing line integration of both sides of (6-163) around the closed path  $C_2$  surrounding the inner conductor, we have

$$\oint_{C_2} \frac{\partial \mathbf{H}_{xy}}{\partial z} \cdot d\mathbf{l}_2 = - \oint_{C_2} \sigma (\mathbf{i}_z \times \mathbf{E}_{xy}) \cdot d\mathbf{l}_2 - \oint_{C_2} \frac{\partial}{\partial t} (\mathbf{i}_z \times \mathbf{D}_{xy}) \cdot d\mathbf{l}_2$$

or

$$\begin{aligned} \frac{\partial}{\partial z} \oint_{C_2} \mathbf{H}_{xy} \cdot d\mathbf{l}_2 &= - \oint_{C_2} \sigma \mathbf{E}_{xy} \cdot (d\mathbf{l}_2 \times \mathbf{i}_z) - \frac{\partial}{\partial t} \oint_{C_2} \mathbf{D}_{xy} \cdot (d\mathbf{l}_2 \times \mathbf{i}_z) \\ &= - \oint_{C_2} \sigma \mathbf{E}_{xy} \cdot \mathbf{i}_{n2} dl_2 - \frac{\partial}{\partial t} \oint_{C_2} \mathbf{D}_{xy} \cdot \mathbf{i}_{n2} dl_2 \end{aligned} \quad (6-164)$$

where  $\mathbf{i}_{n2}$  is the unit vector normal to  $d\mathbf{l}_2$  on  $C_2$  as shown in Fig. 6.27. The integral on the left side of (6-164) is the current  $I$  in the positive  $z$  direction on the inner conductor (or the current in the negative  $z$  direction on the outer conductor) crossing the plane in which the closed path  $C_2$  lies since the electric field has no  $z$  component. The first integral on the right side of (6-164) is the conduction current per unit length in the  $z$  direction, flowing from the inner to the outer conductor if the voltage between the two conductors is a direct voltage equal to the voltage  $V$  in the plane containing the path  $C_2$ . This current is equal to  $\mathcal{G}V$ , where  $\mathcal{G}$  is the conductance per unit length computed from static field considerations. The second integral on the right side of (6-164) is the displacement flux, per unit length in the  $z$  direction, from the inner to the outer conductor if the voltage between the two conductors is a direct voltage equal to the voltage  $V$  in the plane containing the path  $C_2$ . This flux is equal to the magnitude of the charge per unit length on either conductor, which in turn is equal to  $\mathcal{C}V$ , where  $\mathcal{C}$  is the capacitance per unit length computed from static field considerations. Thus we have

$$\begin{aligned} \frac{\partial I(z, t)}{\partial z} &= -\mathcal{G}V(z, t) - \frac{\partial}{\partial t} [\mathcal{C}V(z, t)] \\ &= -\mathcal{G}V(z, t) - \mathcal{C} \frac{\partial V(z, t)}{\partial t} \end{aligned} \quad (6-165)$$

Equations (6-161) and (6-165) describe the behavior of the voltage and current as functions of distance along the structure and of time. The structure itself is known as a transmission line since electromagnetic energy transmission occurs along the structure due to the time-varying fields, as we will learn later. Equations (6-161) and (6-165) are therefore known as the transmission-line equations. To obtain the circuit equivalent of the transmission-line equations, let us consider a section of infinitesimal length  $\Delta z$  along the line between  $z$  and  $z + \Delta z$ . From (6-161) and (6-165), we then have

$$\begin{aligned} \lim_{\Delta z \rightarrow 0} \frac{V(z + \Delta z, t) - V(z, t)}{\Delta z} &= -\mathcal{G} \frac{\partial V(z, t)}{\partial t} \\ \lim_{\Delta z \rightarrow 0} \frac{I(z + \Delta z, t) - I(z, t)}{\Delta z} &= \lim_{\Delta z \rightarrow 0} \left[ -\mathcal{G}V(z + \Delta z, t) - \mathcal{C} \frac{\partial V(z + \Delta z, t)}{\partial t} \right] \end{aligned}$$

or, for  $\Delta z \rightarrow 0$ ,

$$V(z + \Delta z, t) - V(z, t) = -\mathcal{L} \Delta z \frac{\partial I(z, t)}{\partial t} \tag{6-166a}$$

$$I(z + \Delta z, t) - I(z, t) = -\mathcal{G} \Delta z V(z + \Delta z, t) - \mathcal{C} \Delta z \frac{\partial V(z + \Delta z, t)}{\partial t} \tag{6-166b}$$

The circuit theory equivalent of Eqs. (6-166a) and (6-166b) can be drawn as shown in Fig. 6.28 by recognizing that Eq. (6-166a) is Kirchhoff's voltage

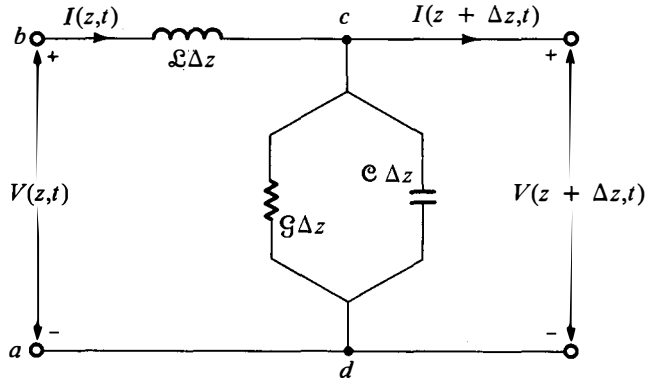


Fig. 6.28. Circuit equivalent for an infinitesimal length  $\Delta z$  of a transmission line.

law written for the loop  $abcd$  and that Eq. (6-166b) is Kirchhoff's current law written for node  $c$ . Thus an infinitesimal length  $\Delta z$  of the structure is equivalent to the circuit shown in Fig. 6.28 as  $\Delta z \rightarrow 0$ . It follows that the circuit representation for a portion of length  $l$  of the structure consists of infinite number of such sections in cascade as shown in Fig. 6.29. In other

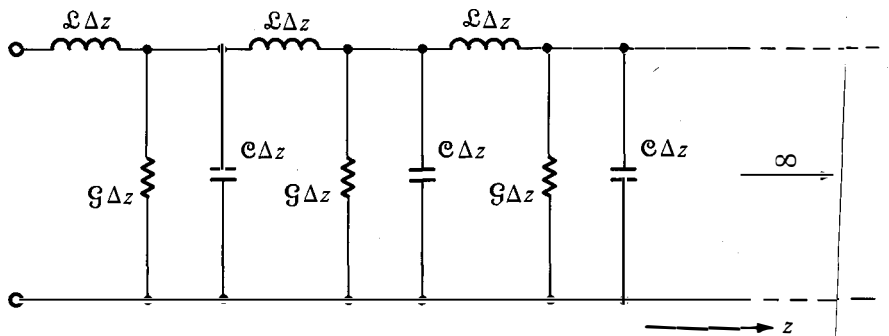


Fig. 6.29. Distributed circuit representation of a transmission line.

words, the structure can no longer be represented by a collection of lumped circuit elements. The conductance, capacitance, and inductance are “distributed” uniformly and overlappingly along the structure, giving rise to the concept of a “distributed circuit.” Physically, the electric stored energy, the magnetic stored energy, and the power dissipation due to conduction current flow are distributed uniformly and overlappingly along the line.

Before we conclude this section, we wish to show that the power flow across any cross-sectional plane of the transmission line as computed from surface integration of the Poynting vector is equal to the product of the voltage and current in that plane. To do this, let us again consider the structure of Fig. 6.27. Considering an infinite plane surface (which is a spherical surface of infinite radius and hence a closed surface) in the cross-sectional plane and noting that the fields outside the conductors are zero, the power flow  $P$  across any cross-sectional plane is simply the surface integral of the Poynting vector over the cross-sectional surface  $S$  between the conductors. Thus

$$\begin{aligned} P(z, t) &= \int_S \mathbf{E}_{xy}(z, t) \times \mathbf{H}_{xy}(z, t) \cdot \mathbf{i}_z dS \\ &= \int_a^b \oint_{C_2} (\mathbf{E}_{xy} \times \mathbf{H}_{xy}) \cdot (d\mathbf{l}_1 \times d\mathbf{l}_2) \\ &= \int_a^b \oint_{C_2} (\mathbf{E}_{xy} \cdot d\mathbf{l}_1)(\mathbf{H}_{xy} \cdot d\mathbf{l}_2) \\ &\quad - \int_a^b \oint_{C_2} (\mathbf{E}_{xy} \cdot d\mathbf{l}_2)(\mathbf{H}_{xy} \cdot d\mathbf{l}_1) \end{aligned} \quad (6-167)$$

Since we can always choose  $C_2$  such that  $d\mathbf{l}_2$  is everywhere normal to  $\mathbf{E}_{xy}$  or, alternatively, since we can always choose the path  $ab$  such that  $d\mathbf{l}_1$  is everywhere normal to  $\mathbf{H}_{xy}$ , the second integral on the right side of (6-167) is equal to zero. Since  $\int_a^b \mathbf{E}_{xy} \cdot d\mathbf{l}_1$  is independent of the path on  $S$  chosen from  $a$  to  $b$  or, alternatively, since  $\oint_{C_2} \mathbf{H}_{xy} \cdot d\mathbf{l}_2$  is independent of the contour  $C_2$  on  $S$ , Eq. (6-167) simplifies to

$$\begin{aligned} P(z, t) &= \left( \int_a^b \mathbf{E}_{xy} \cdot d\mathbf{l}_1 \right) \left( \oint_{C_2} \mathbf{H}_{xy} \cdot d\mathbf{l}_2 \right) \\ &= V(z, t) I(z, t) \end{aligned} \quad (6-168)$$

which is the desired result.

## PART II. Electromagnetic Waves

### 6.8 The Wave Equation ; Uniform Plane Waves and Transmission-Line Waves

In Section 4.11 we stated that time-varying electric and magnetic fields give rise to the phenomenon of electromagnetic wave propagation. In this section we introduce the topic of wave propagation. Let us consider a perfect dielectric region free of charges and for which  $\mu$  and  $\epsilon$  are constants. Maxwell's equations for such a medium are

$$\nabla \cdot \mathbf{D} = 0 \quad (6-169a)$$

$$\nabla \cdot \mathbf{B} = 0 \quad (6-169b)$$

$$\nabla \times \mathbf{E} = -\frac{\partial \mathbf{B}}{\partial t} \quad (6-169c)$$

$$\nabla \times \mathbf{H} = \frac{\partial \mathbf{D}}{\partial t} \quad (6-169d)$$

Taking the curl of both sides of (6-169c), we have

$$\nabla \times \nabla \times \mathbf{E} = -\nabla \times \frac{\partial \mathbf{B}}{\partial t} \quad (6-170)$$

Using the vector identity

$$\nabla \times \nabla \times \mathbf{A} \equiv \nabla(\nabla \cdot \mathbf{A}) - \nabla^2 \mathbf{A}$$

for the left side of (6-170) and interchanging  $\partial/\partial t$  and the curl operation on the right side since the curl operation has to do with differentiation with respect to space coordinates, we obtain

$$\nabla(\nabla \cdot \mathbf{E}) - \nabla^2 \mathbf{E} = -\frac{\partial}{\partial t}(\nabla \times \mathbf{B}) \quad (6-171)$$

However, from (6-169a),  $\nabla \cdot \mathbf{E} = 0$  and from (6-169d),  $\nabla \times \mathbf{B} = \mu\epsilon \partial \mathbf{E}/\partial t$ . Thus (6-171) reduces to

$$\nabla^2 \mathbf{E} = \mu\epsilon \frac{\partial^2 \mathbf{E}}{\partial t^2} \quad (6-172)$$

For sinusoidally time-varying fields, we have the phasor form of (6-172) as

$$\nabla^2 \bar{\mathbf{E}} = -\omega^2 \mu\epsilon \bar{\mathbf{E}} \quad (6-173)$$

Note that the left side of (6-172) is the Laplacian of a vector and not of a scalar. Equation (6-172) is known as the vector wave equation. Equating the like components on either side of (6-172), we obtain three scalar wave

equations. Thus, in cartesian coordinates, we have

$$\nabla^2 E_x = \mu\epsilon \frac{\partial^2 E_x}{\partial t^2}$$

$$\nabla^2 E_y = \mu\epsilon \frac{\partial^2 E_y}{\partial t^2}$$

$$\nabla^2 E_z = \mu\epsilon \frac{\partial^2 E_z}{\partial t^2}$$

In the most general case, we can have all three components of  $\mathbf{E}$  and each one of these can be dependent on all three space coordinates  $x$ ,  $y$ , and  $z$  and on time. But let us assume for simplicity that  $E_y = E_z = 0$ . Then we have

$$\nabla^2 E_x = \frac{\partial^2 E_x}{\partial x^2} + \frac{\partial^2 E_x}{\partial y^2} + \frac{\partial^2 E_x}{\partial z^2} = \mu\epsilon \frac{\partial^2 E_x}{\partial t^2} \quad (6-174)$$

We are still faced with a three-dimensional second-order partial differential equation. Our aim at present is to illustrate that time-varying electric and magnetic fields give rise to electromagnetic wave propagation. Hence let us simplify the problem further by assuming that  $E_x$  is independent of  $x$  and  $y$ . Thus

$$\mathbf{E} = E_x(z, t)\mathbf{i}_x \quad (6-175)$$

and Eq. (6-174) simplifies to

$$\frac{\partial^2 E_x}{\partial z^2} = \mu\epsilon \frac{\partial^2 E_x}{\partial t^2} \quad (6-176)$$

Equation (6-176) is the one-dimensional scalar wave equation. Its solution can be found by using the Laplace transform technique or the separation of variables technique. However, we will here write down the solution and show that it indeed satisfies the equation. Thus let us consider

$$E_x(z, t) = A f(t - \sqrt{\mu\epsilon}z) + B g(t + \sqrt{\mu\epsilon}z) \quad (6-177)$$

where  $f$  and  $g$  are any functions of the respective arguments and  $A$  and  $B$  are arbitrary constants. Then

$$\frac{\partial E_x}{\partial z} = -A\sqrt{\mu\epsilon} f'(t - \sqrt{\mu\epsilon}z) + B g'(t + \sqrt{\mu\epsilon}z)$$

$$\frac{\partial^2 E_x}{\partial z^2} = A\mu\epsilon f''(t - \sqrt{\mu\epsilon}z) + B\mu\epsilon g''(t + \sqrt{\mu\epsilon}z) \quad (6-178a)$$

$$\frac{\partial E_x}{\partial t} = A f'(t - \sqrt{\mu\epsilon}z) + B g'(t + \sqrt{\mu\epsilon}z)$$

$$\frac{\partial^2 E_x}{\partial t^2} = A f''(t - \sqrt{\mu\epsilon}z) + B g''(t + \sqrt{\mu\epsilon}z) \quad (6-178b)$$

where the primes denote differentiation with respect to the respective arguments. From (6-178a) and (6-178b), we note that (6-177) satisfies (6-176)

and hence is the solution for (6-176). The forms of the functions  $f$  and  $g$  depend upon the particular problem under consideration. Some examples are  $\cos \omega(t - \sqrt{\mu\epsilon}z)$ ,  $e^{-(t - \sqrt{\mu\epsilon}z)^2}$ , and  $(t + \sqrt{\mu\epsilon}z) \sin(t + \sqrt{\mu\epsilon}z)$ . In the general case, the solution can be a superposition of several different functions of  $(t - \sqrt{\mu\epsilon}z)$  and  $(t + \sqrt{\mu\epsilon}z)$ .

To discuss the meaning of the functions  $f$  and  $g$  in the solution for  $E_x$ , let us consider a specific example

$$f(t - \sqrt{\mu\epsilon}z) = e^{-(t - \sqrt{\mu\epsilon}z)} u(t - \sqrt{\mu\epsilon}z)$$

Assigning one value for  $t$  at a time, we can obtain a series of functions of  $z$ . The time history of these functions can be illustrated conveniently by a three-dimensional plot in which the three axes represent time  $t$ , distance  $z$ , and the value of the function  $f$ . Such a plot for the function under consideration is shown in Fig. 6.30. We note from Fig. 6.30 that the function of  $z$  at

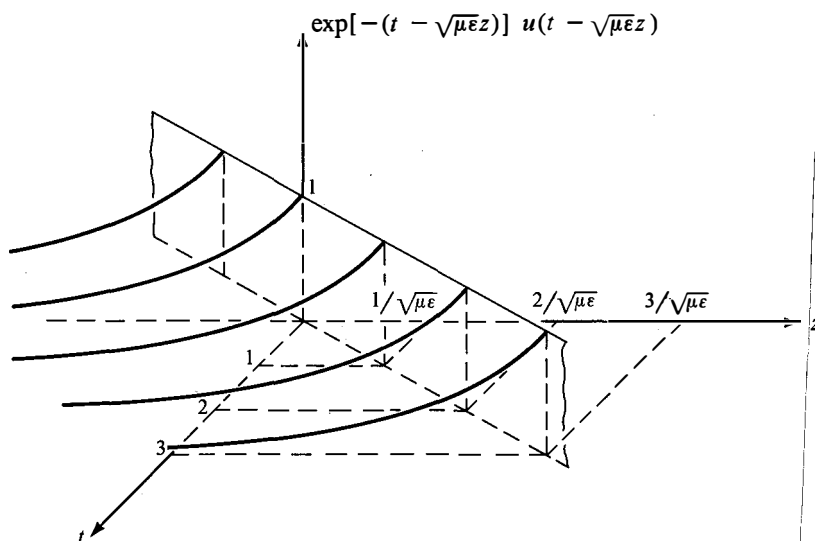


**Fig. 6.30.** Three-dimensional representation of the function  $e^{-(t - \sqrt{\mu\epsilon}z)} u(t - \sqrt{\mu\epsilon}z)$  for illustrating the concept of a traveling wave.

any value of time is exactly the same as the function of  $z$  at a preceding value of time but shifted towards the direction of increasing  $z$ . For example, by following the peak in the function, we note that from time  $t = 0$  to time  $t = 1$ , the peak shifts from  $z = 0$  to  $z = 1/\sqrt{\mu\epsilon}$ . Thus the function  $f(t - \sqrt{\mu\epsilon}z)$  represents a waveform traveling in the positive  $z$  direction with a velocity  $1/\sqrt{\mu\epsilon}$ . The solution is said to correspond to a traveling wave in the positive  $z$  direction, or a (+) wave. The word “wave” is used here in the sense that it represents any arbitrary function of  $z$  and not necessarily a sinusoidally



varying function of  $z$ . The fact that the velocity of propagation is  $1/\sqrt{\mu\epsilon}$  can be proved in general by following any particular point of the function and noting down its positions  $z_1$  and  $z_2$  for two times  $t_1$  and  $t_2$ . Obviously then,

$$t_1 - \sqrt{\mu\epsilon}z_1 = t_2 - \sqrt{\mu\epsilon}z_2$$

or the velocity of propagation is

$$v = \frac{z_2 - z_1}{t_2 - t_1} = \frac{1}{\sqrt{\mu\epsilon}}$$

Note that the units of  $1/\sqrt{\mu\epsilon}$  are

$$\left[ \frac{\text{newtons}}{(\text{ampere})^2} \times \frac{(\text{coulomb})^2}{(\text{newton})(\text{meter})^2} \right]^{-1/2} = \frac{\text{ampere-meters}}{\text{coulomb}} = \frac{\text{meters}}{\text{second}}$$

For free space,  $1/\sqrt{\mu\epsilon} = 1/\sqrt{\mu_0\epsilon_0} = 3 \times 10^8$  m/sec, which is the velocity of light.

We now suspect that the function  $g(t + \sqrt{\mu\epsilon}z)$  represents wave motion in the direction of decreasing values of  $z$ , that is, in the negative  $z$  direction. To check if this is true, we note that, to follow a particular point associated with the function, an observer has to move in space and time such that

$$t + \sqrt{\mu\epsilon}z = \text{constant}$$

or

$$dt + \sqrt{\mu\epsilon} dz = 0$$

or the velocity with which the observer has to move in the positive  $z$  direction is

$$v = \frac{dz}{dt} = -\frac{1}{\sqrt{\mu\epsilon}}$$

The negative sign for the velocity signifies that the observer must actually move in the negative  $z$  direction with a velocity of  $1/\sqrt{\mu\epsilon}$ . Thus the function  $g(t + \sqrt{\mu\epsilon}z)$  does indeed represent a traveling wave in the negative  $z$  direction, or a  $(-)$  wave.

Now, the solution for the magnetic field associated with the electric field can be obtained by substituting (6-177) into (6-169c). Thus we obtain

$$-\frac{\partial \mathbf{B}}{\partial t} = \frac{\partial E_x}{\partial z} \mathbf{i}_y = [-A\sqrt{\mu\epsilon} f'(t - \sqrt{\mu\epsilon}z) + B\sqrt{\mu\epsilon} g'(t + \sqrt{\mu\epsilon}z)] \mathbf{i}_y,$$

or

$$\mathbf{H} = H_y(z, t) \mathbf{i}_y = \left[ A\sqrt{\frac{\epsilon}{\mu}} f(t - \sqrt{\mu\epsilon}z) - B\sqrt{\frac{\epsilon}{\mu}} g(t + \sqrt{\mu\epsilon}z) \right] \mathbf{i}_y$$

Defining

$$\eta = \sqrt{\frac{\mu}{\epsilon}} \quad (6-179)$$

we have

$$H_y(z, t) = \frac{1}{\eta} [A f(t - \sqrt{\mu\epsilon}z) - B g(t + \sqrt{\mu\epsilon}z)] \quad (6-180)$$

The quantity  $\eta$  is known as the intrinsic or characteristic impedance of the medium. Note that the units of  $\eta$  are

$$\left[ \frac{\text{newtons}}{(\text{ampere})^2} \cdot \frac{(\text{coulomb})^2}{(\text{newton})(\text{meter})^2} \right]^{1/2} = \frac{\text{newton-meters}}{\text{coulomb-ampere}} = \frac{\text{volts}}{\text{ampere}} = \text{ohms}$$

For free space,  $\eta = \eta_0 = \sqrt{\mu_0/\epsilon_0} = 120\pi$  or 377 ohms.

Denoting the electric fields in the (+) and (-) waves as  $E_x^+$  and  $E_x^-$ , respectively, and the magnetic fields in the (+) and (-) waves as  $H_y^+$  and  $H_y^-$ , respectively, we have

$$E_x = E_x^+ + E_x^- \quad (6-181a)$$

$$H_y = H_y^+ + H_y^- \quad (6-181b)$$

Comparing (6-181a) and (6-181b) with (6-177) and (6-180), respectively, we note that

$$H_y^+ = \frac{E_x^+}{\eta} \quad \text{and} \quad H_y^- = -\frac{E_x^-}{\eta} \quad (6-182)$$

The Poynting vectors associated with the (+) and (-) waves are

$$\mathbf{P}^+ = E_x^+ \mathbf{i}_x \times H_y^+ \mathbf{i}_y = E_x^+ \mathbf{i}_x \times \frac{E_x^+}{\eta} \mathbf{i}_x = \frac{(E_x^+)^2}{\eta} \mathbf{i}_z \quad (6-183a)$$

$$\mathbf{P}^- = E_x^- \mathbf{i}_x \times H_y^- \mathbf{i}_y = (E_x^- \mathbf{i}_x) \times \left( -\frac{E_x^-}{\eta} \mathbf{i}_y \right) = -\frac{(E_x^-)^2}{\eta} \mathbf{i}_z \quad (6-183b)$$

Equations (6-183a) and (6-183b) indicate that the power flow associated with the (+) wave is indeed in the positive  $z$  direction and the power flow associated with the (-) wave is indeed in the negative  $z$  direction.

Summarizing what we have learned thus far in this section, time-varying electric and magnetic fields give rise to electromagnetic wave propagation. A simple solution consists of waves traveling in the positive and negative  $z$  directions and having electric fields entirely in the  $x$  direction and magnetic fields entirely in the  $y$  direction. Furthermore, the fields are uniform in the planes transverse to the direction of propagation, that is, in the planes  $z = \text{constant}$ . For this reason they are known as uniform plane waves. In reality, uniform plane waves do not exist. However, at distances far from a radiating antenna and the ground, the radiated waves are approximately uniform plane waves. The uniform plane waves are a very important building block in the study of electromagnetic waves.

**EXAMPLE 6-18.** A uniform plane wave traveling in the positive  $z$  direction in free space has its electric field entirely along the  $x$  direction. The time variation of the electric field intensity in the  $z = 0$  plane is shown in Fig. 6.31(a). Find and sketch the variation with  $z$  of the magnetic field intensity at  $t = 2 \mu\text{sec}$ .

The magnetic field intensity is entirely in the  $y$  direction and its value for any  $(z, t)$  is equal to the value of the corresponding electric field intensity

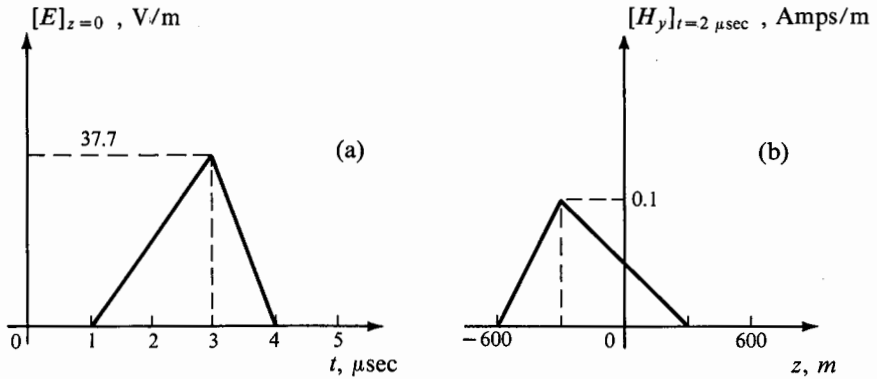


Fig. 6.31. (a) Electric field intensity in the  $z = 0$  plane versus time. (b) Magnetic field intensity at  $t = 2 \mu\text{sec}$  versus  $z$  for the uniform plane wave of Example 6.18.

divided by 377 ohms. The velocity of propagation of the wave in free space is  $3 \times 10^8$  m/sec. Since the wave is propagating in the positive  $z$  direction, an amplitude which exists in the  $z = 0$  plane at any time  $t$  must exist in the plane  $z = (2 \times 10^{-6} - t) \times 3 \times 10^8$  m at  $t = 2 \mu\text{sec}$ . Hence the variation with  $z$  of the magnetic field intensity at  $t = 2 \mu\text{sec}$  is as shown in Fig. 6.31(b). ■

We now direct our attention to the (+) wave to define certain important parameters for the sinusoidally time-varying case and to develop expressions for the fields in a uniform plane wave traveling in an arbitrary direction with reference to a coordinate system. Let us consider a uniform plane wave characterized by sinusoidally time-varying electric and magnetic fields given by

$$\mathbf{E}(z, t) = E_0 \cos [\omega(t - \sqrt{\mu\epsilon}z) + \phi_0] \mathbf{i}_x \quad (6-184a)$$

$$\mathbf{H}(z, t) = \frac{E_0}{\sqrt{\mu/\epsilon}} \cos [\omega(t - \sqrt{\mu\epsilon}z) + \phi_0] \mathbf{i}_y \quad (6-184b)$$

where  $E_0$  and  $\phi_0$  are constants. At any particular value of  $z$ , say  $z_0$ , the fields vary with time in the manner shown in Fig. 6.32(a). Any particular value of the field repeats in time at intervals of  $2\pi/\omega$ . The number of times the value repeats in 1 sec is equal to  $\omega/2\pi$  or  $f$ , which is the well-known parameter frequency. At any particular value of time, say  $t = t_0$ , the fields vary with distance  $z$  in the manner shown in Fig. 6.32(b). Any particular value of the field repeats in distance at intervals of  $2\pi/\omega\sqrt{\mu\epsilon}$ . This interval is known as the wavelength,  $\lambda$ . Thus

$$\lambda = \frac{2\pi}{\omega\sqrt{\mu\epsilon}} = \frac{1}{f\sqrt{\mu\epsilon}} \quad (6-185)$$

But  $1/\sqrt{\mu\epsilon}$  is the velocity of propagation of the wave. In this case, it is known

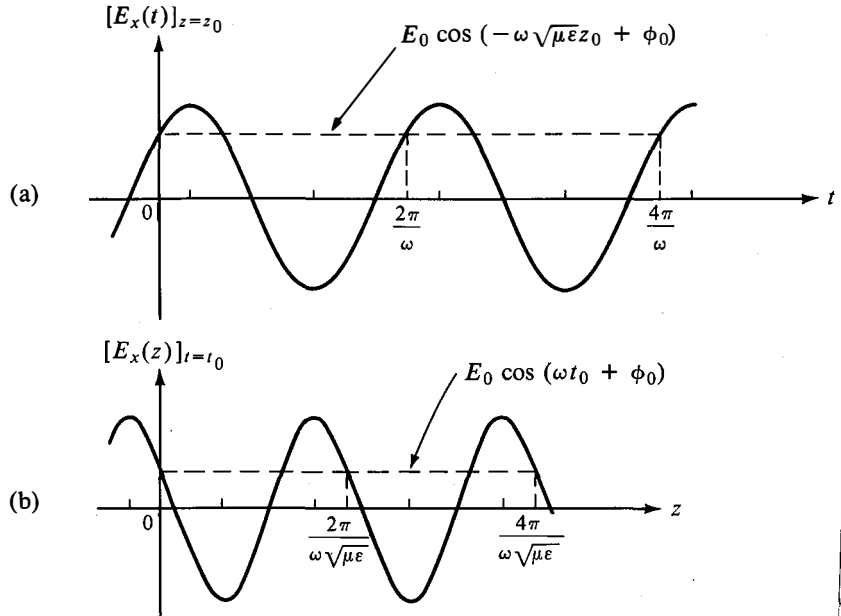


**Fig. 6.32.** (a) Electric field intensity in a  $z = \text{constant}$  plane versus time. (b) Electric field intensity at a fixed time versus  $z$ , for a uniform plane wave in the sinusoidal steady state and traveling in the  $z$  direction.

as the phase velocity since the argument of the cosine function is known as the phase and an observer has to travel with a velocity  $1/\sqrt{\mu\epsilon}$  in the  $z$  direction to follow a constant phase of the field, that is, to stay on a particular constant phase surface. The constant phase surfaces are the planes  $z = \text{constant}$ . Denoting the phase velocity by  $v_p$ , we have

$$v_p = \frac{1}{\sqrt{\mu\epsilon}} \quad (6-186)$$

Substituting (6-186) into (6-185), we get

$$v_p = \lambda f \quad (6-187)$$

Equation (6-187) is an important relationship which relates the space and time variations of the fields in an electromagnetic wave. For free space, Eq. (6-187) gives a simple formula

$$(\text{wavelength in meters}) \times (\text{frequency in megahertz}) = 300$$

The quantity  $\omega\sqrt{\mu\epsilon}$  is the rate at which the phase changes with distance  $z$  at any particular time. It is known as the phase constant and is denoted by  $\beta$ . Thus

$$\beta = \omega\sqrt{\mu\epsilon} \quad (6-188)$$

and

$$\lambda = \frac{2\pi}{\beta} \quad (6-189)$$

$$v_p = \frac{\omega}{\beta} \quad (6-190)$$

The units of  $\beta$  are (radians/second)(seconds/meter) or radians per meter.

For a wave traveling in the  $z$  direction, the phase changes most rapidly in the  $z$  direction since, looking in any other direction, the distance between any two particular constant phase surfaces is longer than the distance between the same two constant phase surfaces as seen looking in the  $z$  direction, as shown in Fig. 6.33. Thus, if we choose the coordinate system such

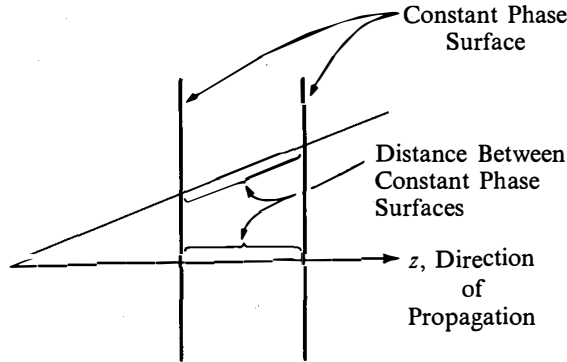


Fig. 6.33. Distances between two constant phase surfaces for a uniform plane wave as seen along different directions.

that the wave is traveling in an arbitrary direction with reference to the coordinate system, the rates at which the phase changes along the coordinate axes are all less than the rate at which the phase changes along the direction of propagation which is normal to the constant phase surfaces. Denoting the phase constants along the  $x$ ,  $y$ , and  $z$  directions by  $\beta_x$ ,  $\beta_y$ , and  $\beta_z$ , respectively, and the phase at the origin at  $t = 0$  by  $\phi_0$ , we note that the phase at any point  $(x, y, z)$  is  $\omega t - (\beta_x x + \beta_y y + \beta_z z) + \phi_0$ . The constant phase surfaces are the planes given by

$$\beta_x x + \beta_y y + \beta_z z = \text{constant} \quad (6-191)$$

The direction of the gradient of the scalar function  $\beta_x x + \beta_y y + \beta_z z$  is the direction of the normal to the constant phase surfaces and hence is the direction of propagation whereas the magnitude of the gradient gives the rate of change of phase with distance or the phase constant  $\beta$  along the normal and hence along the direction of propagation. Thus, noting that

$$\nabla(\beta_x x + \beta_y y + \beta_z z) = \beta_x \mathbf{i}_x + \beta_y \mathbf{i}_y + \beta_z \mathbf{i}_z$$

the direction of propagation is along the vector  $\beta_x \mathbf{i}_x + \beta_y \mathbf{i}_y + \beta_z \mathbf{i}_z$  and the phase constant along the direction of propagation is

$$\beta = (\beta_x^2 + \beta_y^2 + \beta_z^2)^{1/2} \quad (6-192)$$

We can combine these two facts by defining vector  $\boldsymbol{\beta}$  as

$$\boldsymbol{\beta} = \beta_x \mathbf{i}_x + \beta_y \mathbf{i}_y + \beta_z \mathbf{i}_z \quad (6-193)$$

so that the direction of  $\boldsymbol{\beta}$  is the direction of propagation and the magnitude of  $\boldsymbol{\beta}$  is the phase constant. Hence  $\boldsymbol{\beta}$  is known as the propagation vector. The phase at any point  $(x, y, z)$  can then be written as  $\omega t - \boldsymbol{\beta} \cdot \mathbf{r} + \phi_0$ , where  $\mathbf{r}$  is the position vector  $x\mathbf{i}_x + y\mathbf{i}_y + z\mathbf{i}_z$ .

Denoting the electric field intensity in the plane of zero phase as  $\mathbf{E}_0$ , we can now write the expression for the electric field intensity vector associated with a uniform plane wave propagating along the direction of  $\boldsymbol{\beta}$  as

$$\mathbf{E} = \mathbf{E}_0 \cos(\omega t - \boldsymbol{\beta} \cdot \mathbf{r} + \phi_0) \quad (6-194a)$$

or the complex vector as

$$\bar{\mathbf{E}} = \mathbf{E}_0 e^{j\phi_0} e^{-j\boldsymbol{\beta} \cdot \mathbf{r}} = \bar{\mathbf{E}}_0 e^{-j\boldsymbol{\beta} \cdot \mathbf{r}} \quad (6-194b)$$

where  $\bar{\mathbf{E}}_0 = \mathbf{E}_0 e^{j\phi_0}$ . Since  $\mathbf{E}_0$  must be entirely transverse to the direction of propagation, it follows that

$$\boldsymbol{\beta} \cdot \mathbf{E}_0 = 0 \quad \text{or} \quad \boldsymbol{\beta} \cdot \bar{\mathbf{E}}_0 = 0 \quad (6-195)$$

Similarly, the magnetic field intensity vector associated with the wave which is in phase with  $\mathbf{E}$  can be written as

$$\mathbf{H} = \mathbf{H}_0 \cos(\omega t - \boldsymbol{\beta} \cdot \mathbf{r} + \phi_0) \quad (6-196a)$$

or the complex vector as

$$\bar{\mathbf{H}} = \mathbf{H}_0 e^{j\phi_0} e^{-j\boldsymbol{\beta} \cdot \mathbf{r}} = \bar{\mathbf{H}}_0 e^{-j\boldsymbol{\beta} \cdot \mathbf{r}} \quad (6-196b)$$

where  $\bar{\mathbf{H}}_0 = \mathbf{H}_0 e^{j\phi_0}$ . Since  $\mathbf{H}_0$  must be entirely transverse to the direction of propagation, it follows that

$$\boldsymbol{\beta} \cdot \mathbf{H}_0 = 0 \quad \text{or} \quad \boldsymbol{\beta} \cdot \bar{\mathbf{H}}_0 = 0 \quad (6-197)$$

Furthermore  $\mathbf{E}_0$  and  $\mathbf{H}_0$  must be normal to each other with their cross product (Poynting vector) pointing in the direction of propagation and with the ratio of their magnitudes given by

$$\frac{E_0}{H_0} = \sqrt{\frac{\mu}{\epsilon}} = \frac{\omega \mu}{\omega \sqrt{\mu \epsilon}} = \frac{\omega \mu}{\beta} \quad (6-198)$$

In vector notation, we express the preceding statement as

$$\mathbf{H}_0 = \frac{1}{\omega \mu} \boldsymbol{\beta} \times \mathbf{E}_0 \quad (6-199)$$

and hence

$$\bar{\mathbf{H}} = \frac{1}{\omega \mu} \boldsymbol{\beta} \times \bar{\mathbf{E}} \quad (6-200)$$

These properties associated with a uniform plane wave are illustrated in Fig. 6.34.

The wavelength  $\lambda$  along the direction of propagation is given by

$$\lambda = \frac{2\pi}{\beta} \quad (6-201)$$

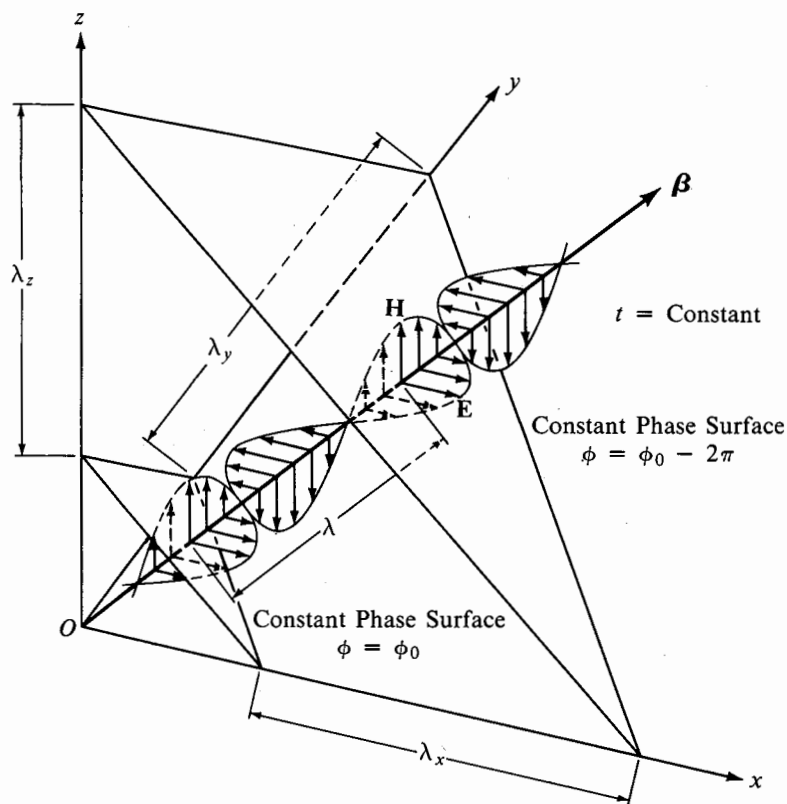


Fig. 6.34. For illustrating the various concepts associated with a uniform plane wave traveling in an arbitrary direction.

The apparent wavelengths  $\lambda_x$ ,  $\lambda_y$ , and  $\lambda_z$  along the coordinate axes  $x$ ,  $y$ , and  $z$ , respectively, as shown in Fig. 6.34 are given by

$$\lambda_x = \frac{2\pi}{\beta_x} \quad \lambda_y = \frac{2\pi}{\beta_y} \quad \lambda_z = \frac{2\pi}{\beta_z} \quad (6-202)$$

Substituting (6-201) and (6-202) into (6-192), we have

$$\frac{1}{\lambda^2} = \frac{1}{\lambda_x^2} + \frac{1}{\lambda_y^2} + \frac{1}{\lambda_z^2} \quad (6-203)$$

The phase velocity along the direction of propagation is given by

$$v_p = \frac{\omega}{\beta} \quad (6-204)$$

For an observer moving along the  $x$  axis,  $y$  and  $z$  are constants. Hence the observer has to travel with a velocity equal to  $\omega/\beta_x$  to remain on a particular constant phase surface. This velocity is known as the apparent phase velocity in the  $x$  direction. Thus the apparent phase velocities  $v_{px}$ ,  $v_{py}$ , and  $v_{pz}$  in the  $x$ ,  $y$ , and  $z$  directions are

$$v_{px} = \frac{\omega}{\beta_x} \quad v_{py} = \frac{\omega}{\beta_y} \quad v_{pz} = \frac{\omega}{\beta_z} \quad (6-205)$$

Substituting (6-204) and (6-205) into (6-192), we have

$$\frac{1}{v_p^2} = \frac{1}{v_{px}^2} + \frac{1}{v_{py}^2} + \frac{1}{v_{pz}^2} \quad (6-206)$$

Note that the apparent wavelengths and phase velocities along the coordinate axes are greater than the wavelength and the phase velocity, respectively, along the direction of propagation, since the phase changes less rapidly with distance along the coordinate axes than along the direction of propagation. We will now consider an example to consolidate our understanding of the uniform plane wave propagating in an arbitrary direction with reference to a set of coordinate axes.

**EXAMPLE 6-19.** The orientation of the propagation vector  $\beta$  for a uniform plane wave of 12 MHz propagating in free space is as shown in Fig. 6.35. It makes

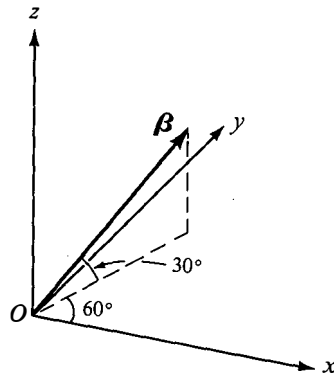


**Fig. 6.35.** Orientation of the propagation vector  $\beta$  for the uniform plane wave of Example 6-19.

an angle of 30° upwards with the horizontal ( $xy$ ) plane and its projection on the  $xy$  plane makes an angle of 60° with the  $x$  axis. The electric field intensity has no upward ( $z$ ) component and its magnitude as a function of time at  $x = 0$ ,  $y = 0$  and  $z = 0$  is  $10 \cos(\omega t - 30^\circ)$  volts/m, where  $\omega$  is the angular frequency. It is desired to find the expressions for the complex field vectors  $\bar{\mathbf{E}}$  and  $\bar{\mathbf{H}}$ .



Since the medium is free space, the phase velocity along the propagation vector is  $1/\sqrt{\mu_0\epsilon_0} = 3 \times 10^8$  m/sec. From (6-204), we have

$$\beta = \frac{\omega}{v_p} = \frac{2\pi f}{v_p} = \frac{2\pi \times 12 \times 10^6}{3 \times 10^8} = 0.08\pi$$

From the given orientation of the propagation vector, we have

$$\begin{aligned}\boldsymbol{\beta} &= 0.08\pi(\cos 30^\circ \cos 60^\circ \mathbf{i}_x + \cos 30^\circ \sin 60^\circ \mathbf{i}_y + \sin 30^\circ \mathbf{i}_z) \\ &= 0.02\pi(\sqrt{3}\mathbf{i}_x + 3\mathbf{i}_y + 2\mathbf{i}_z)\end{aligned}$$

The solution for  $\bar{\mathbf{E}}$  is of the form  $\bar{\mathbf{E}}_0 e^{-j\boldsymbol{\beta}\cdot\mathbf{r}}$ . Since  $\mathbf{E}$  has no  $z$  component, we can write

$$\bar{\mathbf{E}}_0 = \bar{E}_{x0}\mathbf{i}_x + \bar{E}_{y0}\mathbf{i}_y$$

From (6-195), we have

$$\boldsymbol{\beta} \cdot \bar{\mathbf{E}}_0 = \beta_x \bar{E}_{x0} + \beta_y \bar{E}_{y0} = 0$$

Since  $\beta_x$  and  $\beta_y$  are both real,  $\bar{E}_{x0}$  and  $\bar{E}_{y0}$  must be either in phase or in phase opposition for the above equation to be true. Hence let

$$\bar{E}_{x0} = E_{x0}e^{j\alpha} \quad \text{and} \quad \bar{E}_{y0} = E_{y0}e^{j\alpha}$$

so that

$$\bar{\mathbf{E}}_0 = (E_{x0}\mathbf{i}_x + E_{y0}\mathbf{i}_y)e^{j\alpha}$$

and

$$\beta_x E_{x0} + \beta_y E_{y0} = 0.02\pi(\sqrt{3}E_{x0} + 3E_{y0}) = 0$$

or

$$E_{x0} = -\sqrt{3}E_{y0}$$

From the given function of time for the electric field intensity magnitude at  $x = 0$ ,  $y = 0$  and  $z = 0$ , that is,  $\mathbf{r} = 0$ , we have

$$|E_{x0}\mathbf{i}_x + E_{y0}\mathbf{i}_y| e^{j\alpha} = 10e^{-j30^\circ}$$

or

$$|E_{x0}\mathbf{i}_x + E_{y0}\mathbf{i}_y| = [E_{x0}^2 + E_{y0}^2]^{1/2} = 10 \quad \text{and} \quad \alpha = -\frac{\pi}{6}$$

Substituting  $E_{x0} = -\sqrt{3}E_{y0}$  in the above equation, we obtain  $4E_{y0}^2 = 100$  or  $E_{y0} = 5$  and  $E_{x0} = -5\sqrt{3}$ . Thus

$$\bar{\mathbf{E}}_0 = (-5\sqrt{3}e^{-j\pi/6}\mathbf{i}_x + 5e^{-j\pi/6}\mathbf{i}_y)$$

The required expression for  $\mathbf{E}$  is then given by

$$\bar{\mathbf{E}} = 5(-\sqrt{3}\mathbf{i}_x + \mathbf{i}_y)e^{-j\pi/6}e^{-j0.02\pi(\sqrt{3}x+3y+2z)}$$

The corresponding expression for  $\bar{\mathbf{H}}$  can be obtained by using (6-200) as

follows:

$$\begin{aligned}\bar{\mathbf{H}} &= \frac{1}{\omega\mu} \boldsymbol{\beta} \times \bar{\mathbf{E}} \\ &= \frac{1}{96\pi} \begin{vmatrix} \mathbf{i}_x & \mathbf{i}_y & \mathbf{i}_z \\ \sqrt{3} & 3 & 2 \\ -\sqrt{3} & 1 & 0 \end{vmatrix} e^{-j\pi/6} e^{-j0.02\pi(\sqrt{3}x+3y+2z)} \\ &= \frac{1}{48\pi} (-\mathbf{i}_x - \sqrt{3}\mathbf{i}_y + 2\sqrt{3}\mathbf{i}_z) e^{-j\pi/6} e^{-j0.02\pi(\sqrt{3}x+3y+2z)}\end{aligned}$$

We can also find the wavelength along the direction of propagation and the apparent wavelengths and velocities of propagation along the  $x$ ,  $y$ , and  $z$  axes. Thus

$$\begin{aligned}\lambda &= \frac{2\pi}{\beta} = \frac{2\pi}{0.08\pi} = 25 \text{ m} \\ \lambda_x &= \frac{2\pi}{\beta_x} = \frac{2\pi}{0.02\sqrt{3}\pi} = 57.7 \text{ m} \\ \lambda_y &= \frac{2\pi}{\beta_y} = \frac{2\pi}{0.06\pi} = 33.3 \text{ m} \\ \lambda_z &= \frac{2\pi}{\beta_z} = \frac{2\pi}{0.04\pi} = 50 \text{ m} \\ v_{px} &= \frac{\omega}{\beta_x} = \frac{24\pi \times 10^6}{0.02\sqrt{3}\pi} = 6.928 \times 10^8 \text{ m/sec} \\ v_{py} &= \frac{\omega}{\beta_y} = \frac{24\pi \times 10^6}{0.06\pi} = 4 \times 10^8 \text{ m/sec} \\ v_{pz} &= \frac{\omega}{\beta_z} = \frac{24\pi \times 10^6}{0.04\pi} = 6 \times 10^8 \text{ m/sec}\end{aligned}$$

Note that

$$\frac{1}{57.7^2} + \frac{1}{33.3^2} + \frac{1}{50^2} = \frac{1}{25^2}$$

and

$$\frac{1}{6.928^2} + \frac{1}{4^2} + \frac{1}{6^2} = \frac{1}{3^2}$$

in agreement with (6-203) and (6-206), respectively. ■

In Section 4.9 we discussed polarization of vector fields. The fields we found in the preceding example are linearly polarized. We then say that the wave is linearly polarized. If we combine two linearly polarized uniform plane waves propagating in the same direction and having electric field vectors equal in magnitude but oriented perpendicular to each other and differing in phase by  $\pi/2$ , we obtain a circularly polarized uniform plane

wave. For example, a uniform plane wave characterized by the electric field intensity vector

$$\bar{\mathbf{E}} = 2.5(-\mathbf{i}_x - \sqrt{3}\mathbf{i}_y + 2\sqrt{3}\mathbf{i}_z)e^{j\pi/3}e^{-j0.02\pi(\sqrt{3}x+3y+2z)}$$

when superimposed with the uniform plane wave of Example 6-19, would result in a circularly polarized uniform plane wave. In general, two linearly polarized uniform plane waves propagating in the same direction result in an elliptically polarized uniform plane wave.

We have introduced the topic of electromagnetic wave propagation by considering uniform plane waves. The uniform plane waves are a special class of waves known as transverse electromagnetic waves, abbreviated TEM waves, so named because the electric and magnetic fields are entirely transverse to the direction of propagation, that is, components of  $\mathbf{E}$  and  $\mathbf{H}$  along the direction of propagation are zero. For a general TEM wave, the fields are not uniform but are functions of position in the transverse plane. The electromagnetic field between the conductors of a transmission line made up of perfect conductors is entirely transverse to the line axis and is in general nonuniform in the cross-sectional plane. In fact, we considered such a field [Eqs. (6-157a) and (6-157b)] in Section 6.7 and, by substituting into Maxwell's curl equations, we obtained the transmission-line equations given by (6-161) and (6-165). For a perfect dielectric medium between the conductors, that is, for  $\sigma = 0$ , these equations are

$$\frac{\partial V(z, t)}{\partial z} = -\mathcal{E} \frac{\partial I(z, t)}{\partial t} \quad (6-207)$$

and

$$\frac{\partial I(z, t)}{\partial z} = \mathcal{C} \frac{\partial V(z, t)}{\partial t} \quad (6-208)$$

where, with reference to Fig. 6.27,

$$V(z, t) = \int_a^b \mathbf{E}(x, y, z, t) \cdot d\mathbf{l}_1 \quad (6-209a)$$

and

$$I(z, t) = \oint_{C_2} \mathbf{H}(x, y, z, t) \cdot d\mathbf{l}_2 \quad (6-209b)$$

are, respectively, the voltage between the conductors and the current along the conductors for any  $(z, t)$ .

Eliminating  $I$  from (6-207) and (6-208), we obtain a differential equation for  $V$  alone as

$$\frac{\partial^2 V(z, t)}{\partial z^2} = \mathcal{L}\mathcal{C} \frac{\partial^2 V(z, t)}{\partial t^2} \quad (6-210)$$

This equation is completely analogous to Eq. (6-176). It is the wave equation for the TEM wave propagation guided by the conductors of the transmission line except that it is written in terms of the voltage between the conductors instead of the electric field in the medium between the conductors. We can

write the solution for (6-210) from our experience with the solution of (6-176). The solution is

$$V(z, t) = V^+(t - \sqrt{\mathcal{L}\mathcal{C}}z) + V^-(t + \sqrt{\mathcal{L}\mathcal{C}}z) \quad (6-211)$$

where the subscripts + and - indicate (+) and (-) waves. The corresponding solution for the line current  $I$  can be obtained by substituting (6-211) into (6-207) or (6-208). This gives

$$I(z, t) = \sqrt{\frac{\mathcal{C}}{\mathcal{L}}} [V^+(t - \sqrt{\mathcal{L}\mathcal{C}}z) - V^-(t + \sqrt{\mathcal{L}\mathcal{C}}z)]$$

Defining

$$Z_0 = \sqrt{\frac{\mathcal{L}}{\mathcal{C}}} \quad (6-212)$$

we have

$$I(z, t) = \frac{1}{Z_0} [V^+(t - \sqrt{\mathcal{L}\mathcal{C}}z) - V^-(t + \sqrt{\mathcal{L}\mathcal{C}}z)] \quad (6-213)$$

The quantity  $Z_0$  is the characteristic impedance of the transmission line analogous to the intrinsic impedance of the dielectric medium.

Thus the general solutions for the voltage and current along a transmission line are superpositions of (+) and (-) traveling waves along the line with velocities equal to  $1/\sqrt{\mathcal{L}\mathcal{C}}$  in the respective directions. We will refer to these voltage and current waves as "transmission-line waves." They are completely analogous to the uniform plane waves with the analogy as follows:

$$\begin{aligned} V &\longleftrightarrow E_x \\ I &\longleftrightarrow H_y \\ \mathcal{L} &\longleftrightarrow \mu \\ \mathcal{C} &\longleftrightarrow \epsilon \\ \frac{1}{\sqrt{\mathcal{L}\mathcal{C}}} &\longleftrightarrow \frac{1}{\sqrt{\mu\epsilon}} \\ \sqrt{\frac{\mathcal{L}}{\mathcal{C}}} &\longleftrightarrow \sqrt{\frac{\mu}{\epsilon}} \end{aligned} \quad (6-214)$$

We should, however, keep in mind that the phenomenon is one of transverse *electromagnetic* waves guided by the conductors of the transmission line. It is not necessary to work with the fields since, because of the transverse electromagnetic nature of the fields, we are able to define uniquely the voltage and current for any transverse plane. In other words, if we consider two points  $a$  and  $b$  in the same transverse plane on the two conductors, the voltage between these two points is uniquely defined by the electric field in that plane since a closed path lying in that plane and passing through  $a$  and  $b$  does not enclose any magnetic flux. Similarly, the current flowing across a transverse plane in one direction along the inner conductor and returning in the opposite direction along the outer conductor is uniquely defined by the

magnetic field in that plane since a closed path surrounding the inner conductor and lying in that plane does not enclose any electric flux. One or both of these properties are not satisfied if one or both of the fields have axial (or longitudinal) components. This is the case for TE or transverse electric waves which contain a magnetic field component along the guide axis and for TM or transverse magnetic waves which contain an electric field component along the guide axis. We will discuss such waves in Section 6.12.

Returning to the solutions for the voltage and current for the transmission-line waves given by (6-211) and (6-213), we write them concisely as

$$V = V^+ + V^- \quad (6-215a)$$

$$I = I^+ + I^- \quad (6-215b)$$

In writing (6-215a) and (6-215b), we follow the notation that both  $I^+$  and  $I^-$  flow in the positive  $z$  direction along one conductor (say,  $a$ ) and return in the negative  $z$ -direction along the other conductor (say,  $b$ ) and that both  $V^+$  and  $V^-$  have the same polarities with conductor  $a$  positive with respect to conductor  $b$ , as shown in Fig. 6.36. These notations are consistent with

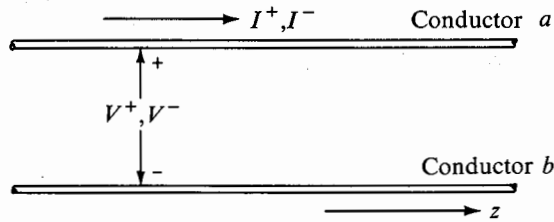


Fig. 6.36. Polarities for voltages and currents associated with (+) and (-) transmission-line waves.

the corresponding notations for the  $z$ -directed uniform plane waves which consider the electric fields for both (+) and (-) waves to be in the  $x$  direction and the magnetic fields for both (+) and (-) waves to be in the  $y$  direction. Comparing (6-215a) and (6-215b) with (6-211) and (6-213), respectively, we have

$$I^+ = \frac{V^+}{Z_0} \quad (6-216a)$$

and

$$I^- = -\frac{V^-}{Z_0} \quad (6-216b)$$

The power flow in the  $z$  direction associated with the (+) wave is

$$P^+ = V^+ I^+ = V^+ \left( \frac{V^+}{Z_0} \right) = \frac{(V^+)^2}{Z_0} \quad (6-217a)$$

The power flow in the  $z$  direction associated with the  $(-)$  wave is

$$P^- = V^- I^- = V^- \left( -\frac{V^-}{Z_0} \right) = -\frac{(V^-)^2}{Z_0} \quad (6-217b)$$

where the minus sign on the right side signifies that the power flow is indeed in the negative  $z$  direction. Thus, if the notation of Fig. 6.36 is followed, together with Eqs. (6-216a) and (6-216b), the different directions of power flow for the  $(+)$  and  $(-)$  waves are taken care of automatically.

### 6.9 Traveling Waves in Time Domain

In the previous section we introduced uniform plane waves and transmission-line waves and discussed the analogy between them. We are now ready to consider simultaneously uniform plane waves incident normally on plane boundaries between different dielectric media and transmission-line waves. In this section we will discuss transient waves. To do this, let us consider the case of two semiinfinite perfect dielectric media characterized by  $\epsilon_1, \mu_1$  and  $\epsilon_2, \mu_2$ , respectively, and separated by the plane  $z = 0$  as shown in Fig. 6.37(a). A uniform plane wave with electric field  $E_x^+$  and magnetic field  $H_y^+$  is incident normally on the boundary. The transmission-line analogy of this problem consists of two transmission lines of different characteristic

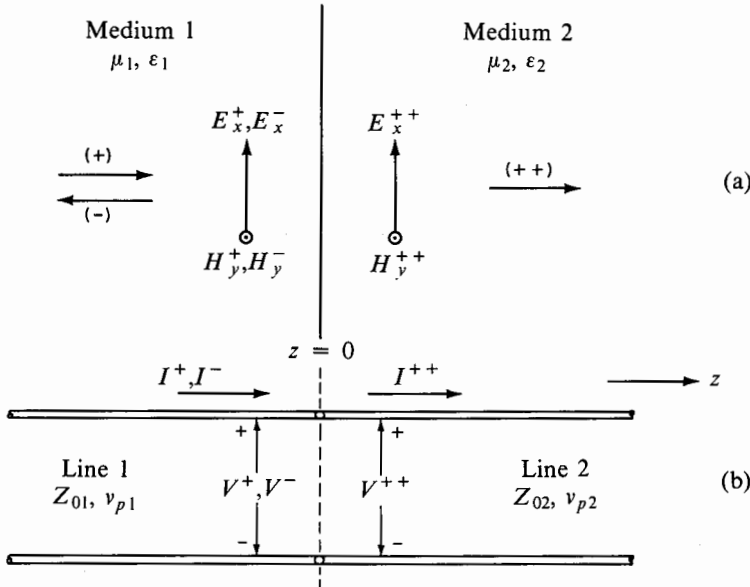


**Fig. 6.37.** (a) Normal incidence of a uniform plane wave on a plane boundary between two semiinfinite dielectric media. (b) Transmission-line analog of (a).

impedances  $Z_{01}$  and  $Z_{02}$  and velocities of propagation  $v_{p1}$  and  $v_{p2}$ , respectively, connected in cascade as shown in Fig. 6.37(b). The specification of  $Z_0$  and  $v_p$  for a transmission line is equivalent to the specification of  $\mathcal{L}$  and  $\mathcal{C}$  since  $Z_0 = \sqrt{\mathcal{L}/\mathcal{C}}$  and  $v_p = 1/\sqrt{\mathcal{L}\mathcal{C}}$ . A (+) wave characterized by voltage  $V^+$  and current  $I^+$  is incident on the junction  $z = 0$ . We are not interested in the time variation of the incident waves at present. We merely wish to determine the transmission and reflection properties at the boundary. Obviously, there is no need to write equations for both the plane wave and transmission line cases because of the analogy. Hence we will simply write the equations in terms of the transmission-line parameters  $V$ ,  $I$ , and  $Z_0$  with the understanding that they can be replaced by  $E_x$ ,  $H_y$ , and  $\eta$ , respectively.

The relationship between  $V^+$  and  $I^+$  is given by

$$I^+ = \frac{V^+}{Z_{01}} \quad (6-218)$$

The incident wave cannot be transmitted into line 2 as it is, since the voltage-to-current ratio in line 2 must be equal to  $Z_{02}$ . Thus, let the transmitted wave voltage and current be  $V^{++}$  and  $I^{++}$ , respectively. The incident and transmitted waves alone cannot satisfy the boundary conditions at the junction, which require that the voltages on either side of the junction be equal and the currents on either side of the junction be equal. These conditions are analogous to the boundary conditions for the fields, which state that the tangential electric fields ( $E_x$ ) must be continuous and that the tangential magnetic fields ( $H_y$ ) must be continuous (in the absence of a surface current) at the boundary between the dielectrics. To satisfy the boundary conditions, there is only one possibility. This is setting up a (-) wave in line 1 which reflects part of the incident power into line 1. Let the voltage and current in this reflected wave be  $V^-$  and  $I^-$ , respectively. The voltage-to-current relationships for the transmitted and reflected waves are

$$I^{++} = \frac{V^{++}}{Z_{02}} \quad (6-219)$$

and

$$I^- = -\frac{V^-}{Z_{01}} \quad (6-220)$$

The boundary conditions at  $z = 0$  are

$$V^+ + V^- = V^{++} \quad (6-221a)$$

$$I^+ + I^- = I^{++} \quad (6-221b)$$

Substituting (6-218), (6-219), and (6-220) into (6-221b), we have

$$\frac{V^+}{Z_{01}} - \frac{V^-}{Z_{01}} = \frac{V^{++}}{Z_{02}} \quad (6-222)$$

Solving (6-221a) and (6-222) for  $V^-$ , we get

$$V^- = V^+ \frac{Z_{02} - Z_{01}}{Z_{02} + Z_{01}} \quad (6-223)$$

We now define a quantity  $\Gamma$ , known as the voltage reflection coefficient, as the ratio of the (-) wave or reflected wave voltage to the (+) wave or incident wave voltage. From (6-223), the voltage reflection coefficient is given by

$$\Gamma = \frac{V^-}{V^+} = \frac{Z_{02} - Z_{01}}{Z_{02} + Z_{01}} \quad (6-224)$$

We then note that the current reflection coefficient is

$$\frac{I^-}{I^+} = \frac{-V^-/Z_{01}}{V^+/Z_{01}} = -\frac{V^-}{V^+} = -\Gamma \quad (6-225)$$

We also define a quantity  $\tau_v$ , known as the voltage transmission coefficient, as the ratio of the (++) wave or transmitted wave voltage to the (+) wave or incident wave voltage. Thus

$$\begin{aligned} \tau_v &= \frac{V^{++}}{V^+} = \frac{V^+ + V^-}{V^+} = 1 + \frac{V^-}{V^+} \\ &= 1 + \Gamma = \frac{2Z_{02}}{Z_{02} + Z_{01}} \end{aligned} \quad (6-226)$$

The current transmission coefficient  $\tau_I$  is given by

$$\begin{aligned} \tau_I &= \frac{I^{++}}{I^+} = \frac{I^+ + I^-}{I^+} = 1 + \frac{I^-}{I^+} \\ &= 1 - \Gamma = \frac{2Z_{01}}{Z_{02} + Z_{01}} \end{aligned} \quad (6-227)$$

At this point, we may be surprised to note that the transmitted voltage, or the transmitted current can be greater than the incident voltage or the incident current, respectively, depending upon whether  $\Gamma$  is positive or negative, that is,  $Z_{02} > Z_{01}$  or  $Z_{02} < Z_{01}$ . However, this is not of concern since it is the power balance that must be satisfied. To check this, we note that

$$\begin{aligned} P^+, \text{ incident power} &= V^+ I^+ \\ P^-, \text{ reflected power} &= V^- I^- = (\Gamma V^+) (-\Gamma I^+) \\ &= -\Gamma^2 V^+ I^+ = -\Gamma^2 P^+ \end{aligned}$$

where the minus sign signifies that the actual power flow is in the negative  $z$  direction, and

$$\begin{aligned} P^{++}, \text{ transmitted power} &= V^{++} I^{++} = [(1 + \Gamma)V^+][(1 - \Gamma)I^+] \\ &= (1 - \Gamma^2)V^+ I^+ = (1 - \Gamma^2)P^+ \end{aligned}$$

Thus  $P^{++} = P^+ + P^-$ , which verifies the power balance at the junction. The fact is that if the transmitted voltage is greater than the incident voltage, the transmitted current is less than the incident current and vice versa so that the transmitted power is less than the incident power. We will now consider an example to illustrate the application of the formulas for the reflection and transmission coefficients.



**EXAMPLE 6-20.** In Fig. 6.38, the region  $z < 0$  is free space, the region  $0 < z < 1.5$  m is a perfect dielectric of permittivity  $4\epsilon_0$ , and the region  $z > 1.5$  m is a perfect dielectric of permittivity  $9\epsilon_0$ . The leading edge of a uniform plane wave of  $0.01 \mu\text{sec}$  duration and having  $E_x$  equal to 1 volt/m is incident on the  $z = -3$  m plane at  $t = 0$ . It is desired to find and sketch  $E_x$  in the planes  $z = -3$  m and  $z = 2.5$  m as functions of time for  $t \geq 0$ .

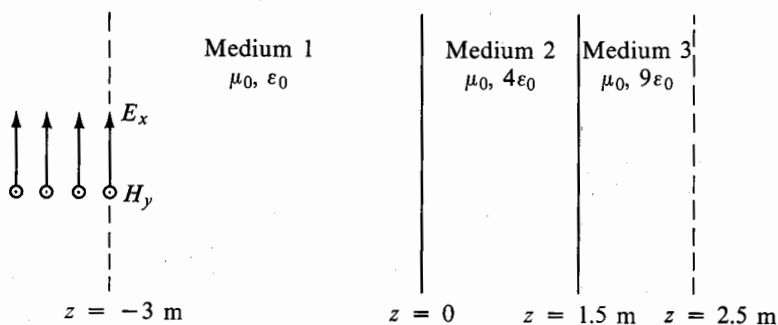


**Fig. 6.38.** Three dielectric media for Example 6-20.

The intrinsic impedances for the three media are  $\eta_0$ ,  $\eta_0/2$ , and  $\eta_0/3$ , respectively, where  $\eta_0 (= \sqrt{\mu_0/\epsilon_0})$  is 377 ohms. The velocities of propagation in the three media are  $c$ ,  $c/2$ , and  $c/3$ , respectively, where  $c (= 1/\sqrt{\mu_0\epsilon_0})$  is  $3 \times 10^8$  m/sec. The leading edge of the uniform plane wave strikes the interface  $z = 0$  at  $t = 3/(3 \times 10^8)$  sec =  $0.01 \mu\text{sec}$ . The reflection coefficient for this wave at  $z = 0$  is  $(\eta_0/2 - \eta_0)/(\eta_0/2 + \eta_0) = -\frac{1}{3}$  and the transmission coefficient is  $1 + (-\frac{1}{3}) = \frac{2}{3}$ . Hence the reflected wave  $E_x$  has a value  $-\frac{1}{3}$  that of the incident wave  $E_x$  and its leading edge reaches the  $z = -3$  m plane at  $t = 0.02 \mu\text{sec}$ . The transmitted wave  $E_x$  has a value  $\frac{2}{3}$  that of the incident wave  $E_x$  and its leading edge strikes the interface  $z = 1.5$  m at  $t = [10^{-8} + 1.5/(1.5 \times 10^8)]$  sec =  $0.02 \mu\text{sec}$ . The reflection coefficient for this wave at  $z = 1.5$  m is  $(\eta_0/3 - \eta_0/2)/(\eta_0/3 + \eta_0/2) = -\frac{1}{5}$  and the transmission coefficient is  $1 + (-\frac{1}{5}) = \frac{4}{5}$ . Thus the transmitted wave  $E_x$  in medium 3 has a value of  $(\frac{4}{5} \times \frac{2}{3})$  or  $\frac{8}{15}$  that of the incident wave  $E_x$  in medium 1. Its leading edge reaches the  $z = 2.5$  m plane at  $t = (2 \times 10^{-8} + 1/10^8) = 0.03 \mu\text{sec}$ . Now, the reflected wave at the interface  $z = 1.5$  m travels towards the interface  $z = 0$  and strikes it at  $t = 0.03 \mu\text{sec}$ . It then violates the boundary conditions at  $z = 0$ , which have thus far been satisfied by the incident and reflected waves in medium 1 and the transmitted wave in medium 2 if they still exist at the interface. In any case, to satisfy the boundary conditions, it sets up a reflected wave into medium 2 and a transmitted wave into medium 1. By superposition, the reflection and transmission coefficients are the same as if this wave alone were incident on the interface. Hence the reflection coefficient for this wave at  $z = 0$  is  $(\eta_0 - \eta_0/2)/(\eta_0 + \eta_0/2) = \frac{1}{3}$  and the

transmission coefficient is  $1 + \frac{1}{3} = \frac{4}{3}$ . The transmitted wave travels towards the interface  $z = -3$  m. The reflected wave travels towards the interface  $z = 1.5$  m and sets up reflected and transmitted waves. This process continues indefinitely.

To keep track of the bouncing back and forth of the transient waves between the interfaces, we resort to a "bounce diagram" as shown in Fig. 6.39. The bounce diagram is essentially a two-dimensional representation

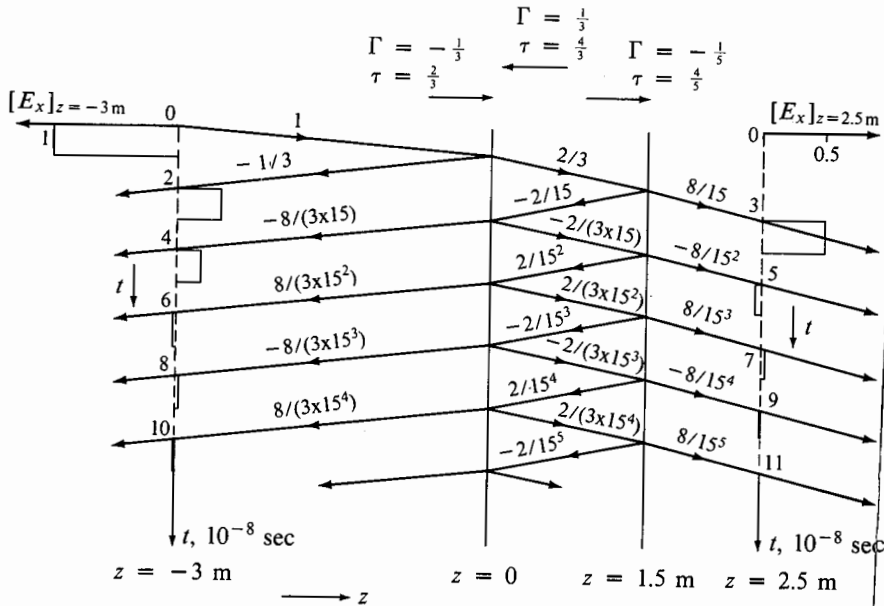


Fig. 6.39. Bounce diagram for keeping track of transient waves in the dielectric media of Fig. 6.38.

of transient waves bouncing back and forth. Distance along the direction of propagation is represented horizontally and time is represented vertically. Reflection and transmission coefficient values at the interfaces are written at the top of the diagram for quick reference, with appropriate arrows indicating directions of incidence. Criss-cross lines are drawn as shown on the diagram to indicate the progress of the waves as functions of  $z$  and  $t$ , with the numerical value of  $E_x$  for each leg of travel shown beside the line corresponding to that leg. The time functions of  $E_x$  representing the waves for each leg are drawn along the time axes in the planes of interest as shown on the bounce diagram. The bounce diagram of Fig. 6.39 is for  $E_x$  (or  $V$ ). Similar bounce diagrams can be drawn for  $H_y$  (or  $I$ ), taking note that the reflection coefficient for  $H_y$  (or  $I$ ) is the negative of the reflection coefficient for  $E_x$  (or  $V$ ). From Fig. 6.39, we can now draw the required sketches of  $E_x$  versus  $t$  in the planes

$z = -3$  m and  $z = 2.5$  m. These are shown in Figs. 6.40(a) and (b), respectively. ■

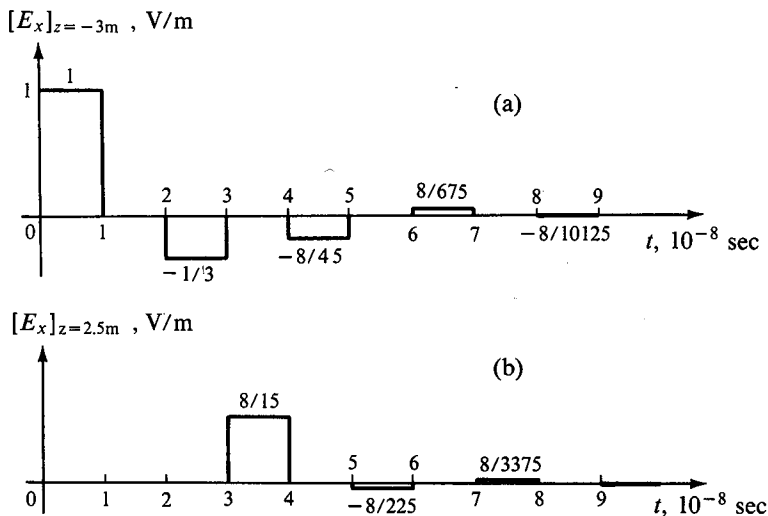


Fig. 6.40.  $E_x$  in the planes  $z = -3$  m and  $z = 2.5$  m versus time from the bounce diagram of Fig. 6.39.

### 6.10 Traveling Waves in Sinusoidal Steady State; Standing Waves

In the preceding section we discussed transient traveling waves. In this section we consider traveling waves in sinusoidal steady state. Once again, we deal simultaneously with uniform plane waves at normal incidence and transmission-line waves, keeping in mind the analogy between the two. From (6-211) and (6-213), the general solutions for the line voltage and line current in the sinusoidal steady state are

$$V(z, t) = V^+ \cos[\omega(t - \sqrt{\mathcal{L}\mathcal{C}}z) + \phi^+] + V^- \cos[\omega(t + \sqrt{\mathcal{L}\mathcal{C}}z) + \phi^-]$$

$$I(z, t) = \frac{1}{Z_0} \{ V^+ \cos[\omega(t - \sqrt{\mathcal{L}\mathcal{C}}z) + \phi^+] - V^- \cos[\omega(t + \sqrt{\mathcal{L}\mathcal{C}}z) + \phi^-] \}$$

The corresponding expressions for the phasor line voltage and phasor line current are

$$\bar{V}(z) = \bar{V}^+ e^{-j\beta z} + \bar{V}^- e^{j\beta z} \tag{6-228a}$$

$$\bar{I}(z) = \frac{1}{Z_0} (\bar{V}^+ e^{-j\beta z} - \bar{V}^- e^{j\beta z}) \tag{6-228b}$$

where we have substituted  $\beta$  for  $\omega\sqrt{\mathcal{L}\mathcal{C}}$ . For sinusoidal steady-state problems, it is convenient to use a distance variable  $d$  which is in opposition to  $z$ , that

is, a variable which increases as we go away from the load and towards the generator as shown in Fig. 6.41. The wave which progresses away from the generator is still denoted as the (+) wave and the wave which progresses

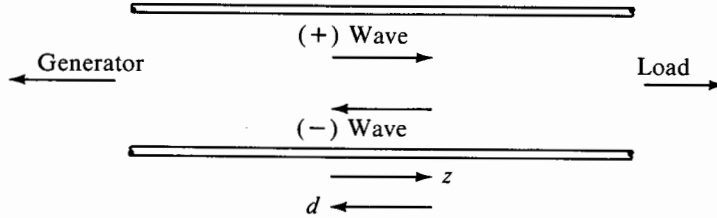


Fig. 6.41. For illustrating the distance variable  $d$  used for sinusoidal steady-state analysis of traveling waves.

towards the generator is still denoted as the (-) wave. In terms of  $d$ , the solutions for  $\vec{V}$  and  $\vec{I}$  are then given by

$$\vec{V}(d) = \vec{V}^+ e^{j\beta d} + \vec{V}^- e^{-j\beta d} \tag{6-229a}$$

$$\vec{I}(d) = \frac{1}{Z_0} (\vec{V}^+ e^{j\beta d} - \vec{V}^- e^{-j\beta d}) \tag{6-229b}$$

We will be working with these equations for the remainder of this section.

Let us now consider a semiinfinite perfect dielectric medium characterized by  $\epsilon$  and  $\mu$  and bounded by a perfect conductor in the plane  $d = 0$  as shown in Fig. 6.42(a). The corresponding transmission-line equivalent is a

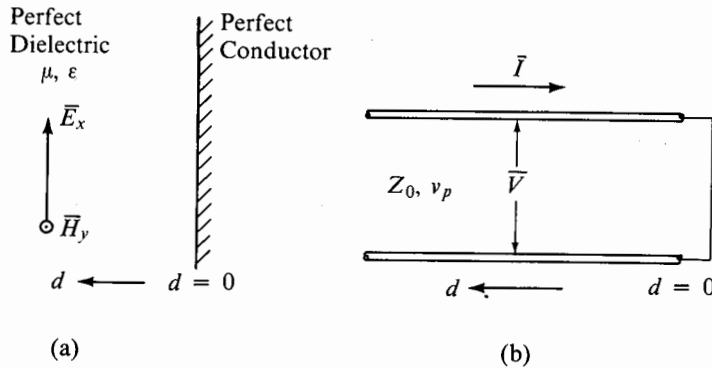


Fig. 6.42. (a) Normal incidence of a uniform plane wave on a plane perfect conductor. (b) Transmission-line analog of (a).

line short circuited at  $d = 0$  as shown in Fig. 6.42(b). Let us assume that sinusoidally time-varying traveling waves exist in the medium due to a source which is not shown in the figure and that conditions have reached steady state. We wish to determine the characteristics of the waves satisfying the boundary condition at the perfect conductor (or short circuit). This boun-

dary condition is

$$[\bar{E}_x]_{d=0} = 0 \quad \text{or} \quad [\bar{V}]_{d=0} = 0$$

Applying this boundary condition to the general solution for  $\bar{V}(d)$  given by (6-229a), we obtain

$$0 = \bar{V}^+ + \bar{V}^- \quad \text{or} \quad \bar{V}^- = -\bar{V}^+$$

The particular solutions for the voltage and current are then given by

$$\bar{V}(d) = \bar{V}^+ e^{j\beta d} - \bar{V}^+ e^{-j\beta d} = 2j\bar{V}^+ \sin \beta d \quad (6-230a)$$

$$\bar{I}(d) = \frac{1}{Z_0} (\bar{V}^+ e^{j\beta d} + \bar{V}^+ e^{-j\beta d}) = 2 \frac{\bar{V}^+}{Z_0} \cos \beta d \quad (6-230b)$$

The instantaneous voltage and current are given by

$$\begin{aligned} V(d, t) &= \Re \{ \bar{V}(d) e^{j\omega t} \} \\ &= \Re \{ 2e^{j\pi/2} |\bar{V}^+| e^{j\theta} \sin \beta d e^{j\omega t} \} \\ &= -2 |\bar{V}^+| \sin \beta d \sin (\omega t + \theta) \end{aligned} \quad (6-231a)$$

$$\begin{aligned} I(d, t) &= \Re \{ \bar{I}(d) e^{j\omega t} \} \\ &= \Re \left\{ 2 \frac{|\bar{V}^+|}{Z_0} e^{j\theta} \cos \beta d e^{j\omega t} \right\} \\ &= 2 \frac{|\bar{V}^+|}{Z_0} \cos \beta d \cos (\omega t + \theta) \end{aligned} \quad (6-231b)$$

where  $\theta$  is the phase angle of  $\bar{V}^+$ . The instantaneous line voltage and line current given by (6-231a) and (6-231b), respectively, are sketched in Fig. 6.43 as functions of  $d$  for various values of  $t$ . The following characteristics can be inferred from these sketches:

- The line voltage is zero at  $d = 0, \pi/\beta, 2\pi/\beta, \dots = 0, \lambda/2, \lambda, \dots$  for all values of time. Hence there is no power flow across these planes for all values of time. If we short circuit the line (or place perfect conductors) at these values of  $d$ , there will be no effect on the voltage and current (fields) at any other value of  $d$ .
- The line current is zero at  $d = \pi/2\beta, 3\pi/2\beta, \dots = \lambda/4, 3\lambda/4, \dots$  for all values of time. Hence there is no power flow across these planes for all values of time. If we open circuit the line (or place imaginary magnetic conductors) at these values of  $d$ , there will be no change in the voltage and current (fields) at any other value of  $d$ .
- Whenever the line voltage has maximum amplitude, the line current has zero amplitude and vice versa. Thus the line voltage and line current are out of phase in distance by  $\pi/2\beta$  or  $\lambda/4$ .
- Whenever the line voltage is maximum at all values of  $d$ , the line current is zero at all values of  $d$  and vice versa. Thus the line voltage and line current are out of phase in time by  $\pi/2\omega$  or  $T/4$ , where  $T$  is the period corresponding to  $\omega$ .

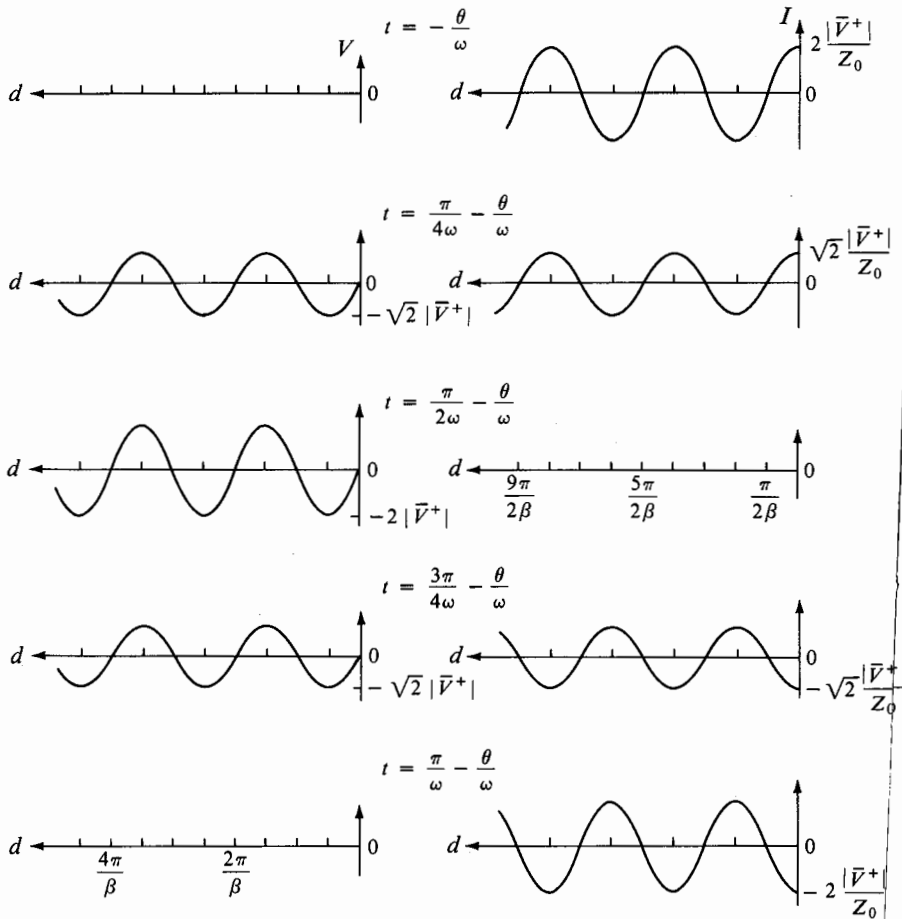


**Fig. 6.43.** Voltage and current versus distance for various values of time for the short-circuited line of Fig. 6.42(b).

We conclude from these characteristics that the situation for a short-circuited line consists of voltage and current waves which stand still and only increase and decrease in amplitude in each section of  $\lambda/2$  in length between the voltage nodes (zeros) and between the current nodes (zeros), respectively, similar to the oscillations executed by a string tied down at one end and vibrated at a point half a wavelength from the tie-down point. These waves are therefore known as “complete standing waves.” Complete standing waves are the result of (+) and (-) traveling waves of equal magnitude. Whatever power is incident on the short circuit by the (+) wave is reflected entirely in the form of the (-) wave since the short circuit cannot absorb any power. While there is instantaneous power flow at values of  $d$  between the voltage and current nodes, there is no time-average power flow for any value of  $d$ , as

can be seen from

$$\begin{aligned}\langle P \rangle &= \frac{1}{2} \operatorname{Re}[\bar{V}(d)\bar{I}^*(d)] \\ &= \frac{1}{2} \operatorname{Re}\left[(2j\bar{V}^+ \sin \beta d)\left(2\frac{\bar{V}^{+*}}{Z_0} \cos \beta d\right)\right] \\ &= \frac{1}{2} \operatorname{Re}\left(2j\frac{|\bar{V}^+|^2}{Z_0} \sin 2\beta d\right) = 0\end{aligned}$$

The amplitudes of the sinusoidally time-varying line voltage and line current as functions of  $d$  are

$$|\bar{V}(d)| = 2|j||\bar{V}^+||\sin \beta d| = 2|\bar{V}^+||\sin \beta d| \quad (6-232a)$$

$$|\bar{I}(d)| = 2\left|\frac{\bar{V}^+}{Z_0}\right||\cos \beta d| \quad (6-232b)$$

These amplitudes are sketched in Fig. 6.44. The patterns of Fig. 6.44 are known as “standing wave patterns.” Standing wave patterns are easily measured in the laboratory with the aid of moving probes which sample the electric field.

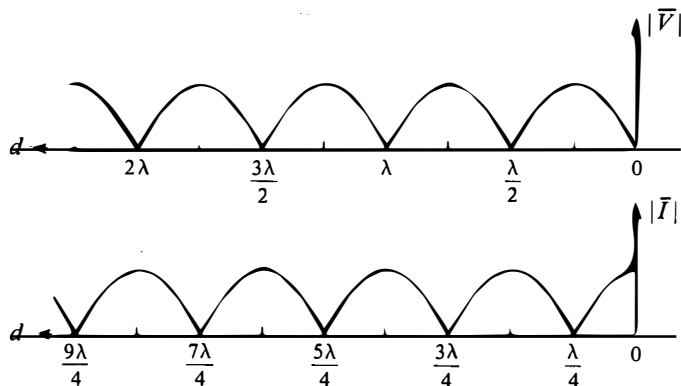


**Fig. 6.44.** Standing wave patterns for voltage and current along a short-circuited line.

**EXAMPLE 6-21.** A transmission line of length  $l$  and short circuited at both ends has certain energy stored in it. From the preceding discussion, this energy must exist in the form of complete standing waves on the line. What are the possible standing wave patterns and the corresponding frequencies?

The voltage must be zero at both ends of the line since it is short circuited at both ends. It follows from the standing wave patterns of Fig. 6.44 that the current must be maximum at both ends. Thus the possible voltage and current standing wave patterns are as shown in Fig. 6.45. They must consist of integral numbers of half-sinusoidal variations over the length

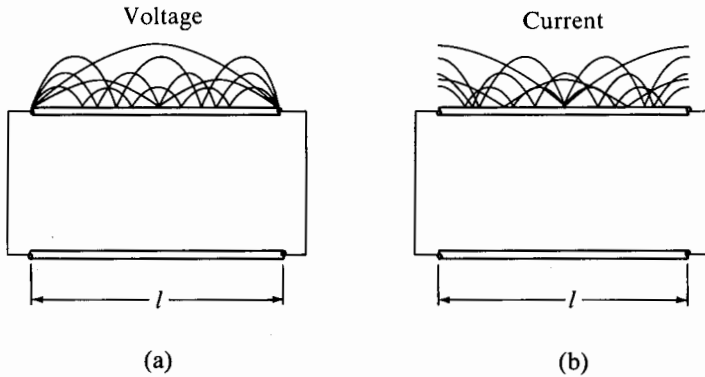


Fig. 6.45. Standing wave patterns for (a) voltage and (b) current along a line short circuited at both ends.

of the line; that is, the wavelengths  $\lambda_n$  corresponding to these standing wave patterns must be such that

$$l = n \frac{\lambda_n}{2} \quad n = 1, 2, 3, \dots$$

or

$$\lambda_n = \frac{2l}{n} \quad n = 1, 2, 3, \dots$$

The corresponding frequencies are

$$f_n = \frac{v_p}{\lambda_n} = \frac{nv_p}{2l} \quad n = 1, 2, 3, \dots$$

where  $v_p$  is the phase velocity. These frequencies are known as the “natural frequencies of oscillation.” The standing wave patterns are said to correspond to the different “natural modes of oscillation.” The lowest frequency (corresponding to the longest wavelength) is known as the “fundamental” frequency of oscillation and the corresponding mode is known as the fundamental mode. The quantity  $n$  is called the mode number. ■

Returning now to the expressions for the phasor line voltage and the phasor line current given by (6-230a) and (6-230b), respectively, we define the ratio of these two quantities as the line (or wave) impedance  $\bar{Z}(d)$  at that point seen looking towards the short circuit. Thus

$$\bar{Z}(d) = \frac{\bar{V}(d)}{\bar{I}(d)} = \frac{2j\bar{V}^+ \sin \beta d}{2(\bar{V}^+/Z_0) \cos \beta d} = jZ_0 \tan \beta d \quad (6-233)$$

In particular, the input impedance  $\bar{Z}_{in}$  of a short-circuited line of length  $l$  is given by

$$\bar{Z}_{in} = jZ_0 \tan \beta l = jZ_0 \tan \frac{2\pi f l}{v_p} \quad (6-234)$$



This expression is the same as the expression (6-151) derived by the step-by-step solution of Maxwell's curl equations for the fields in the parallel-plate structure of Fig. 6.25(b). We now note that the condition for quasistatic approximation given by (6-146) can be stated alternatively as

$$\beta l \ll 1 \quad \text{or} \quad l \ll \lambda$$

For a fixed  $l$ ,  $\tan(2\pi f/v_p)l$  becomes alternatively positive and negative as  $f$  increases and hence the input reactance alternates between inductive and capacitive as illustrated in Fig. 6.46. It can be seen that frequencies at which

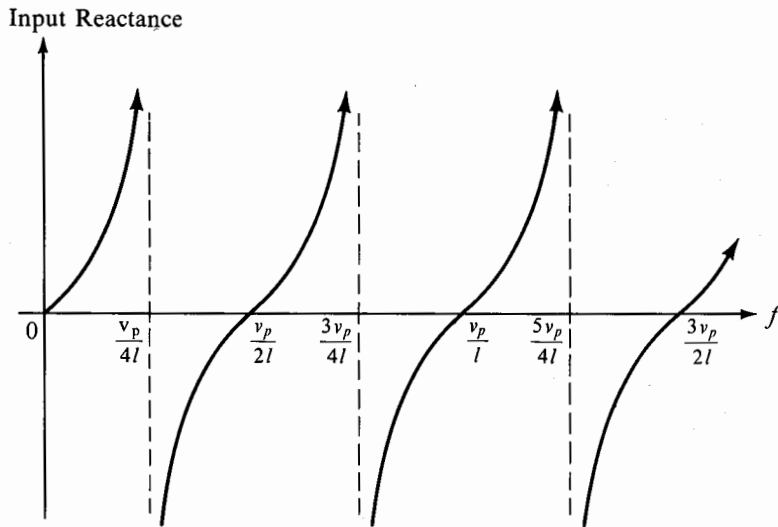


**Fig. 6.46.** Variation of the input reactance of a short-circuited line of length  $l$  with frequency.

the input reactance is zero are the same as the natural frequencies of oscillation if the input were short circuited. Likewise, the frequencies at which the input reactance is infinity are the same as the natural frequencies of oscillation if the input were open circuited. These properties of short-circuited line sections permit them to be used as inductive and capacitive elements and resonant circuits at high frequencies. We will illustrate an application by means of the following example.

**EXAMPLE 6-22.** To determine the location of a short circuit in an air-insulated parallel wire line, a voltage generator of variable frequency is connected at its input. The generator frequency is varied continuously from a value of 100 MHz upwards and the current drawn from the generator is monitored. It is found that the current reaches a minimum at 100.02 MHz and then a maximum at 100.05 MHz. How far is the location of the short circuit from the generator?

The current minimum occurs at a frequency for which the input impedance is infinity. The current maximum occurs at a frequency for which the input impedance is zero. From Fig. 6.46, the difference between adjacent frequencies for which the input reactances of a short-circuited line are infinity and zero is equal to  $v_p/4l$ . Hence, for this problem,  $v_p/4l$  is  $(100.05 - 100.02)$  or 0.03 MHz. Since the line is air insulated, the velocity of propagation is  $3 \times 10^8$  m/sec. Hence  $l = (3 \times 10^8)/(4 \times 0.03 \times 10^6) = 2500$  m. Thus the location of the short circuit is 2.5 km away from the generator. ■

We have thus far discussed complete standing waves which result from the superposition of (+) and (-) waves of equal magnitudes. Let us now consider the general case of the superposition of (+) and (-) waves of unequal magnitudes, thereby giving rise to "partial standing waves." Such a situation can arise when uniform plane waves are incident normally on a plane interface between two different dielectrics or interfaces between several dielectrics in cascade. We first define the generalized reflection coefficient  $\bar{\Gamma}(d)$  as the ratio of the phasor voltage associated with the (-) wave to the phasor voltage associated with the (+) wave at a given  $d$ . Thus, from (6-229a), we have

$$\bar{\Gamma}(d) = \frac{\bar{V}^- e^{-j\beta d}}{\bar{V}^+ e^{j\beta d}} = \frac{\bar{V}^-}{\bar{V}^+} e^{-j2\beta d} = \bar{\Gamma}(0) e^{-j2\beta d} \quad (6-235)$$

where  $\bar{\Gamma}(0) = \bar{V}^-/\bar{V}^+$  is the reflection coefficient at  $d = 0$ . We note that the magnitude of  $\bar{\Gamma}(d)$  is constant whereas the phase angle changes linearly with  $d$ . Using (6-235), we can write the general solutions for  $\bar{V}(d)$  and  $\bar{I}(d)$  as

$$\bar{V}(d) = \bar{V}^+ e^{j\beta d} [1 + \bar{\Gamma}(d)] \quad (6-236a)$$

$$\bar{I}(d) = \frac{\bar{V}^+}{Z_0} e^{j\beta d} [1 - \bar{\Gamma}(d)] \quad (6-236b)$$

The line (or wave) impedance  $\bar{Z}(d)$  is given by

$$\bar{Z}(d) = \frac{\bar{V}(d)}{\bar{I}(d)} = Z_0 \frac{1 + \bar{\Gamma}(d)}{1 - \bar{\Gamma}(d)} \quad (6-237)$$

Conversely,

$$\bar{\Gamma}(d) = \frac{\bar{Z}(d) - Z_0}{\bar{Z}(d) + Z_0} \quad (6-238)$$

To study the standing wave patterns corresponding to (6-236a) and (6-236b), we look at the magnitudes of  $\bar{V}(d)$  and  $\bar{I}(d)$ . These are given by

$$\begin{aligned} |\bar{V}(d)| &= |\bar{V}^+| |e^{j\beta d}| |1 + \bar{\Gamma}(d)| \\ &= |\bar{V}^+| |1 + \bar{\Gamma}(0) e^{-j2\beta d}| \end{aligned} \quad (6-239a)$$

$$\begin{aligned} |\bar{I}(d)| &= \frac{|\bar{V}^+|}{Z_0} |e^{j\beta d}| |1 - \bar{\Gamma}(d)| \\ &= \frac{|\bar{V}^+|}{Z_0} |1 - \bar{\Gamma}(0) e^{-j2\beta d}| \end{aligned} \quad (6-239b)$$

To sketch  $|\bar{V}(d)|$  and  $|\bar{I}(d)|$ , it is sufficient if we consider the quantities  $|1 + \bar{\Gamma}(0)e^{-j2\beta d}|$  and  $|1 - \bar{\Gamma}(0)e^{-j2\beta d}|$  since  $|\bar{V}^+|$  is simply a constant, dependent upon the source of the waves. Each of these quantities consists of two complex numbers one of which is a constant equal to  $(1 + j0)$  and the other of which has a constant magnitude  $|\bar{\Gamma}(0)|$  but a variable phase angle  $\theta - 2\beta d$ , where  $\theta$  is the phase angle of  $\bar{\Gamma}(0)$ . To evaluate  $|1 + \bar{\Gamma}(0)e^{-j2\beta d}|$  and  $|1 - \bar{\Gamma}(0)e^{-j2\beta d}|$ , we make use of the constructions in the complex  $\bar{\Gamma}$  plane as shown in Figs. 6.47(a) and (b), respectively. In both

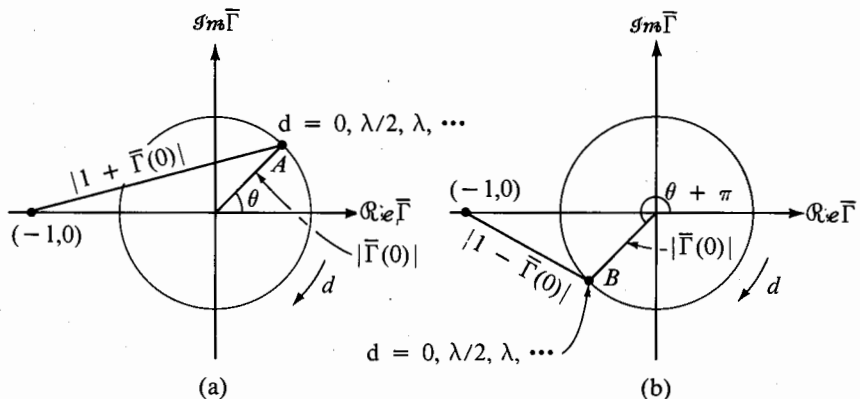


Fig. 6.47.  $\bar{\Gamma}$ -plane diagrams for sketching the voltage and current standing wave patterns for a partial standing wave.

diagrams, we draw circles with centers at the origin and having radii equal to  $|\bar{\Gamma}(0)|$ . For  $d = 0$ , the complex number  $\bar{\Gamma}(0)e^{-j2\beta d}$  is equal to  $\bar{\Gamma}(0)$  or  $|\bar{\Gamma}(0)|e^{j\theta}$ , which is represented by point  $A$  in Fig. 6.47(a). To add  $(1 + j0)$  and  $\bar{\Gamma}(0)$ , we simply draw a line from the point  $(-1, 0)$  to the point  $A$ . The length of this line gives  $|1 + \bar{\Gamma}(0)|$ , which is proportional to the amplitude of the voltage standing wave at  $d = 0$ . As  $d$  increases, point  $A$ , representing  $\bar{\Gamma}(0)e^{-j2\beta d}$ , moves around the circle in the clockwise direction. The line joining  $(-1, 0)$  to the point  $A$  whose length is  $|1 + \bar{\Gamma}(0)e^{-j2\beta d}|$  executes the motion of a "crank." To subtract  $\bar{\Gamma}(0)$  from  $(1 + j0)$  we locate point  $B$  in Fig. 6.47(b), which is diametrically opposite to point  $A$  in Fig. 6.47(a), and draw a line from  $(-1, 0)$  to point  $B$ . The length of this line gives  $|1 - \bar{\Gamma}(0)|$ , which is proportional to the amplitude of the current standing wave at  $d = 0$ . As  $d$  increases,  $B$  moves around the circle in the clockwise direction following the movement of  $A$  in Fig. 6.47(a). The line joining  $(-1, 0)$  to the point  $B$  whose length is  $|1 - \bar{\Gamma}(0)e^{-j2\beta d}|$  executes the motion of a "crank." From these constructions, we note the following facts:

- (a) Point  $A$  lies along the positive real axis and point  $B$  lies along the negative real axis for  $\theta - 2\beta d = 0, -2\pi, -4\pi, -6\pi, \dots$  or  $d = (\lambda/4\pi)(\theta + 2n\pi)$ , where  $n = 0, 1, 2, 3, \dots$ . Hence, at these

values of  $d$ , the voltage magnitude is maximum and equal to  $|\bar{V}^+|[1 + |\bar{\Gamma}(0)|]$  whereas the current magnitude is minimum and equal to  $(|\bar{V}^+|/Z_0)[1 - |\bar{\Gamma}(0)|]$ . The voltage and current are in phase. Thus their ratio, that is, the line impedance, is real and maximum.

- (b) Point  $A$  lies along the negative real axis and point  $B$  lies along the positive real axis for  $\theta - 2\beta d = -\pi, -3\pi, -5\pi, -7\pi, \dots$  or  $d = (\lambda/4\pi)[\theta + (2n - 1)\pi]$ , where  $n = 1, 2, 3, 4, \dots$ . Hence, at these values of  $d$ , the voltage magnitude is minimum and equal to  $|\bar{V}^+|[1 - |\bar{\Gamma}(0)|]$  whereas the current magnitude is maximum and equal to  $(|\bar{V}^+|/Z_0)[1 + |\bar{\Gamma}(0)|]$ . The voltage and current are in phase. Thus their ratio, that is, the line impedance, is real and minimum.
- (c) Between maxima and minima, the voltage and current magnitudes vary in accordance with the lengths of the lines joining  $(-1, 0)$  to the points  $A$  and  $B$ , respectively, as they move around the circles. These variations are not sinusoidal with distance. The variations near the minima are sharper than those near the maxima. Also, the voltage and current are not in phase. Hence their ratio, that is, the line impedance, is complex.

With the aid of the preceding discussion, we now sketch the standing wave patterns for the line voltage and line current as shown in Fig. 6.48. The standing wave patterns should not be misinterpreted as the voltage and current remaining constant with time at a given point. On the other hand, at every point on the line, the voltage and current vary sinusoidally with time as shown in the insets of Fig. 6.48, with the amplitudes of these sinusoidal variations equal to the magnitudes indicated by the standing wave patterns. We now define a quantity known as the voltage standing wave ratio, abbreviated as VSWR, as the ratio of the maximum voltage  $V_{\max}$  to the minimum voltage  $V_{\min}$  in the standing wave patterns. Thus

$$\text{VSWR} = \frac{V_{\max}}{V_{\min}} = \frac{|\bar{V}^+|[1 + |\bar{\Gamma}(0)|]}{|\bar{V}^+|[1 - |\bar{\Gamma}(0)|]} = \frac{1 + |\bar{\Gamma}(0)|}{1 - |\bar{\Gamma}(0)|} \quad (6-240)$$

The VSWR is a measure of the standing waves on the line. It is an easily measurable parameter. We note the following special cases:

- (a) For a pure traveling wave, that is, for a (+) wave alone,  $\bar{V}^- = 0$ ,  $\bar{\Gamma} = 0$ , and hence  $\text{VSWR} = 1$ ; that is, the standing wave pattern is simply a line representing constant magnitude. This is the case if the line is infinitely long or if it is terminated by its characteristic impedance.
- (b) For a complete standing wave,  $\bar{V}^-$  and  $\bar{V}^+$  have equal magnitudes;  $|\bar{\Gamma}| = 1$  and hence  $\text{VSWR} = \infty$ . This is indeed the case with the standing wave pattern of Fig. 6.44.

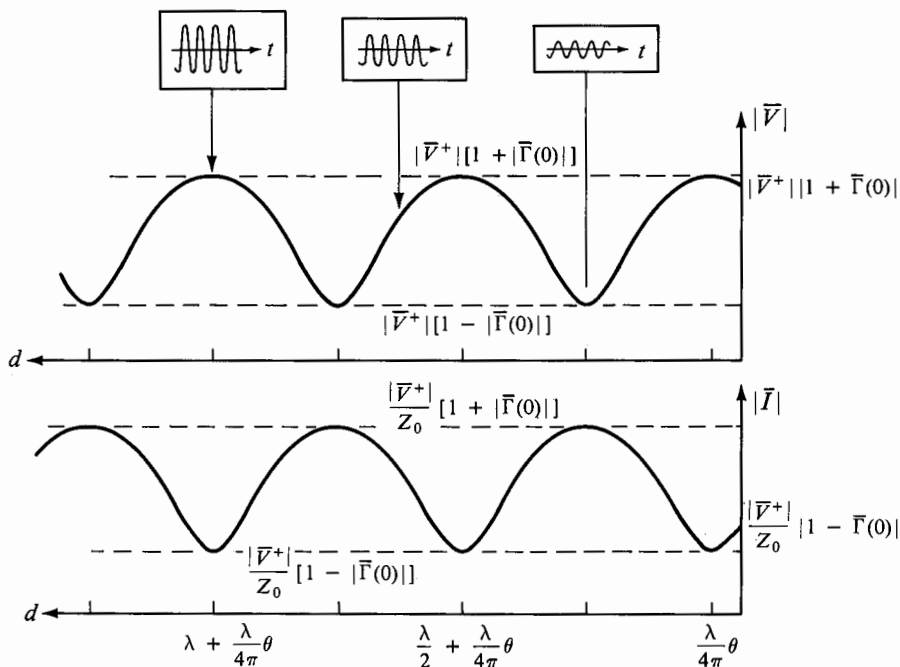


Fig. 6.48. Voltage and current standing wave patterns for a partial standing wave. The insets show time variations of voltage at points along the line.

**EXAMPLE 6-23.** In Fig. 6.49(a), a plane dielectric slab of thickness 3.75 cm and permittivity  $4\epsilon_0$  is sandwiched between two semiinfinite media 1 and 3. Medium 1 is free space and medium 3 is a perfect dielectric of permittivity  $9\epsilon_0$ . A uniform plane wave of frequency 3000 MHz is incident normally on the slab from medium 1 and sinusoidal steady-state conditions are established in all media. It is desired to find and sketch the standing wave patterns for the fields in all media.

The intrinsic impedances of the three media are  $\eta_0$ ,  $\eta_0/2$ , and  $\eta_0/3$ , respectively. The velocities of propagation in the three media are  $c$ ,  $c/2$ , and  $c/3$ , respectively, where  $c = 3 \times 10^8$  m/sec. The wavelength in medium 2 for 3000 MHz is 5 cm. Hence the electrical length of medium 2 is  $3\lambda/4$ . The transmission-line analog of the problem is shown in Fig. 6.49(b). We solve this problem in a step-by-step manner as follows:

(a) Line 3 has only a (+) wave since it extends to infinity. Hence VSWR for that line is equal to 1. The line impedance is independent of distance and equal to the characteristic impedance  $\eta_0/3$ .

(b) At the junction between two lines, the boundary conditions dictate that  $\bar{V}$  and  $\bar{I}$  be continuous (analogous to  $\bar{E}_x$  and  $\bar{H}_y$  being continuous at

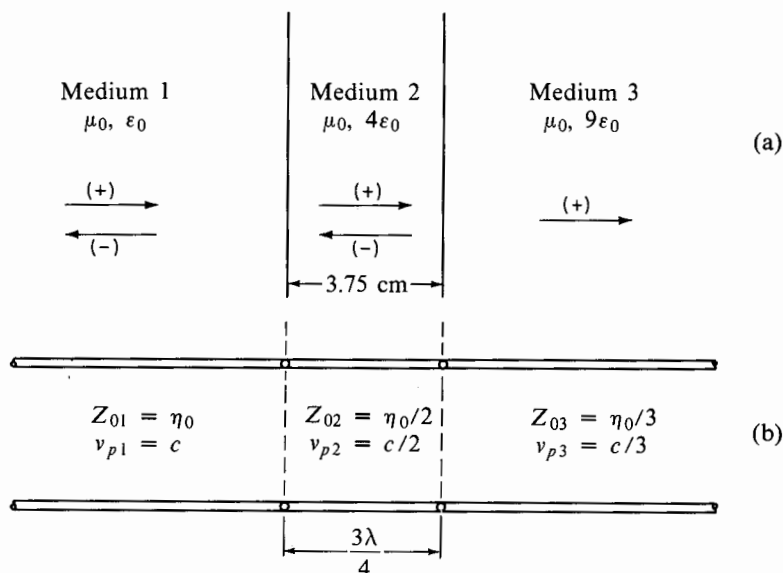


Fig. 6.49. (a) A plane dielectric slab sandwiched between two semiinfinite dielectric media. (b) Transmission-line analog of (a) for uniform plane waves at normal incidence.

the interface between the two dielectric media). Hence the ratio of these two quantities must be continuous. The line impedance at the right end of line 2 is therefore equal to the line impedance at the left end of line 3, which is equal to  $\eta_0/3$ .

(c) From (6-238), the reflection coefficient at the right end of line 2 is

$$\bar{\Gamma}_1 = \frac{\eta_0/3 - Z_{02}}{\eta_0/3 + Z_{02}} = \frac{\eta_0/3 - \eta_0/2}{\eta_0/3 + \eta_0/2} = -\frac{1}{5}$$

(d) From (6-240), VSWR for line 2 is

$$\frac{1 + |\bar{\Gamma}_1|}{1 - |\bar{\Gamma}_1|} = \frac{1 + \frac{1}{5}}{1 - \frac{1}{5}} = 1.5$$

Also, since  $\bar{\Gamma}_1$  is purely real and negative, the voltage magnitude is minimum at the right end of line 2, as can be seen from the construction of Fig. 6.47(a).

(e) From (6-235), the reflection coefficient at the left end of line 2 is

$$\bar{\Gamma}_2 = \bar{\Gamma}_1 e^{-j2\beta_2(3\lambda_2/4)} = -\frac{1}{5} e^{-j3\pi} = \frac{1}{5}$$

(f) From (6-237), the line impedance at the left end of line 2 is

$$Z_{02} \frac{1 + \bar{\Gamma}_2}{1 - \bar{\Gamma}_2} = \frac{\eta_0}{2} \frac{1 + \frac{1}{5}}{1 - \frac{1}{5}} = \frac{3}{4} \eta_0$$

(g) Since the line impedance at a junction between two lines has to be continuous from the discussion in (b) above, the line impedance at the right end of line 1 is  $\frac{3}{4}\eta_0$ . From (6-238), the reflection coefficient at the right end of line 1 is

$$\bar{\Gamma}_3 = \frac{3\eta_0/4 - Z_{01}}{3\eta_0/4 + Z_{01}} = \frac{3\eta_0/4 - \eta_0}{3\eta_0/4 + \eta_0} = -\frac{1}{7}$$

(h) From (6-240), VSWR for line 1 is

$$\frac{1 + |\bar{\Gamma}_3|}{1 - |\bar{\Gamma}_3|} = \frac{1 + \frac{1}{7}}{1 - \frac{1}{7}} = \frac{4}{3}$$

Also, since  $\bar{\Gamma}_3$  is purely real and negative, the line voltage is a minimum at the right end of line 1.

From the above results and noting that the wavelength in medium 1 for 3000 MHz is 10 cm, we now sketch the standing wave pattern for the electric field intensity (based on a magnitude of unity in medium 3) as shown by the solid curves in Fig. 6.50. The standing wave pattern for the magnetic

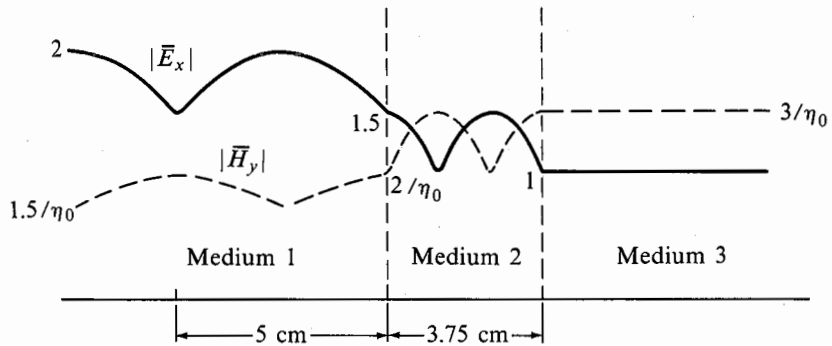


Fig. 6.50. Standing wave patterns for the fields in the three media of Fig. 6.49.

field intensity follows from the fact that  $|\bar{E}_x|/|\bar{H}_y| = \eta_0/3$  in medium 3 and by noting that wherever  $|\bar{E}_x|$  is maximum,  $|\bar{H}_y|$  is minimum and vice versa. It is shown by the dashed curves in Fig. 6.50. ■

**EXAMPLE 6-24.** One important type of problem is that of matching between two dielectric media of different permittivities. For example, in Fig. 6.49(a), we can choose the thickness and permittivity of medium 2 so that reflected wave is eliminated in medium 1. Then all the power incident on the interface between media 1 and 2 is transmitted into medium 3 (although standing waves exist in medium 2). Let us determine the minimum thickness and permittivity of medium 2 required to achieve such a match.

To determine the required quantities, we note that, for a particular line

of characteristic impedance  $Z_0$ , the product of the line impedances at two values of  $d$  separated by an odd multiple of  $\lambda/4$  is given by

$$\begin{aligned}
 \{\bar{Z}[d]\} \left\{ \bar{Z} \left[ d + (2n - 1) \frac{\lambda}{4} \right] \right\} \\
 &= \left\{ Z_0 \frac{1 + \bar{\Gamma}(d)}{1 - \bar{\Gamma}(d)} \right\} \left\{ Z_0 \frac{1 + \bar{\Gamma}[d + (2n - 1)\lambda/4]}{1 - \bar{\Gamma}[d + (2n - 1)\lambda/4]} \right\} \\
 &= Z_0^2 \left[ \frac{1 + \bar{\Gamma}(d)}{1 - \bar{\Gamma}(d)} \right] \left[ \frac{1 + \bar{\Gamma}(d)e^{-j2\beta(2n-1)\lambda/4}}{1 - \bar{\Gamma}(d)e^{-j2\beta(2n-1)\lambda/4}} \right] \quad (6-241) \\
 &= Z_0^2 \left[ \frac{1 + \bar{\Gamma}(d)}{1 - \bar{\Gamma}(d)} \right] \left[ \frac{1 + \bar{\Gamma}(d)e^{-j(2n-1)\pi}}{1 - \bar{\Gamma}(d)e^{-j(2n-1)\pi}} \right] \\
 &= Z_0^2 \left[ \frac{1 + \bar{\Gamma}(d)}{1 - \bar{\Gamma}(d)} \right] \left[ \frac{1 - \bar{\Gamma}(d)}{1 + \bar{\Gamma}(d)} \right] = Z_0^2
 \end{aligned}$$

where  $n$  can take any integer value. For eliminating standing waves in line 1, the impedance seen at the right end of line 1 must be equal to  $Z_{01} = \eta_0$ . Hence the line impedance at the left end of line 2 must be  $\eta_0$ . However, the impedance seen at the right end of line 2 is equal to  $Z_{03} = \eta_0/3$ . Hence, according to (6-241), we must have a minimum length of  $\lambda/4$  and a characteristic impedance equal to  $\sqrt{\eta_0(\eta_0/3)}$  or  $\eta_0/\sqrt{3}$  for line 2 to achieve the required match. For the intrinsic impedance of medium 2 to be  $\eta_0/\sqrt{3}$ , its permittivity must be  $3\epsilon_0$ . Since the wavelength for 3000 MHz in medium 2 is then  $10/\sqrt{3}$  cm, the minimum required thickness is  $2.5/\sqrt{3}$  or 1.4434 cm. This technique of matching is known as matching by "quarter-wave transformer." ■

## 6.11 Transmission-Line Matching; the Smith Chart

In the previous section we discussed complete standing waves resulting from (+) and (-) waves of equal magnitudes, and then partial standing waves resulting from (+) and (-) waves of unequal magnitudes. While standing waves are useful from the point of view of energy storage, they are unwanted from the point of view of energy transmission. To elaborate upon this, we note that the time-average power flow down the line is given by

$$\begin{aligned}
 \langle P \rangle &= \frac{1}{2} \operatorname{Re}(\bar{V}\bar{I}^*) \\
 &= \frac{1}{2} \operatorname{Re} \left\{ \bar{V}^+ e^{j\beta d} [1 + \bar{\Gamma}(d)] \frac{\bar{V}^{+*}}{Z_0} e^{-j\beta d} [1 - \bar{\Gamma}^*(d)] \right\} \\
 &= \frac{1}{2} \operatorname{Re} \left\{ \frac{|\bar{V}^+|^2}{Z_0} [1 - |\bar{\Gamma}(d)|^2 + \bar{\Gamma}(d) - \bar{\Gamma}^*(d)] \right\} \\
 &= \frac{|\bar{V}^+|^2}{2Z_0} [1 - |\bar{\Gamma}(d)|^2] = \frac{|\bar{V}^+|^2}{2Z_0} [1 - |\bar{\Gamma}(0)|^2] \quad (6-242) \\
 &= \left\{ \frac{|\bar{V}^+|}{2} [1 + |\bar{\Gamma}(0)|] \right\} \left\{ \frac{|\bar{V}^+|}{Z_0} [1 - |\bar{\Gamma}(0)|] \right\} \\
 &= \frac{V_{\max} V_{\min}}{2Z_0} = \frac{I_{\max} I_{\min} Z_0}{2} \\
 &= \frac{V_{\max}^2}{2(\text{VSWR})Z_0} = \frac{I_{\max}^2}{2(\text{VSWR})} Z_0
 \end{aligned}$$



where  $V_{\max}$ ,  $V_{\min}$ ,  $I_{\max}$ , and  $I_{\min}$  are the maximum and minimum magnitudes of voltage and current, respectively, in the standing wave patterns. From (6-242), the limitations imposed by standing waves on power transfer down a line are evident. For a particular line, there is an upper limit for the electric field which the dielectric can withstand and hence there is a breakdown voltage. For a particular value of the breakdown voltage, the power that can be transmitted down the line is inversely proportional to the VSWR, according to (6-242). Similarly, there can be an upper limit for the current that can be carried by the conductors of the line without overheating them. Again, (6-242) states that, for a particular value of this current, the power that can be transmitted down the line is inversely proportional to the VSWR.

Another and perhaps more serious limitation imposed by standing waves concerns the input impedance of the line. In the presence of standing waves, that is, when the load impedance is not equal to the characteristic impedance, it follows from (6-237) that the input impedance of the line will vary with frequency since the electrical length of the line and hence  $\bar{\Gamma}(d) = \bar{\Gamma}(0)e^{-j2\beta d}$  changes. This sensitivity to frequency increases with the electrical length of the line. To show this, let the length of the line be  $l = n\lambda$ . If the frequency is changed by an amount  $\Delta f$ , then the change in  $n$  is given by

$$\Delta n = \Delta\left(\frac{l}{\lambda}\right) = \Delta\left(\frac{lf}{v_p}\right) = \frac{l}{v_p} \Delta f = \frac{n\lambda}{v_p} \Delta f = n \frac{\Delta f}{f}$$

Thus  $\Delta n$ , the change in the number of wavelengths corresponding to the line length, is proportional to  $n$ .

For these reasons, it is necessary to eliminate standing waves on the line by connecting a "matching" device near the load such that the line views an effective impedance equal to its own characteristic impedance on the generator side of the matching device. The matching device should not at the same time absorb any power. Small sections of short-circuited lines known as stubs connected in parallel with the line at appropriate distances from the load are used for this purpose since their input impedance is purely reactive and hence they do not absorb any power. Indeed we are making use of standing waves (on the stub) to eliminate standing waves (on the line between the generator and the stub)! This technique of matching is known as stub matching. We now illustrate the principle behind the stub matching technique by means of an example.

**EXAMPLE 6-25.** A lossless transmission line having a characteristic impedance of 50 ohms is terminated by a load impedance  $\bar{Z}_R$  equal to  $(30 - j40)$  ohms. It is desired to find the location and the length of a lossless, short-circuited stub connected in parallel with the line so that a match is obtained between the generator driving this line and the load, assuming that the characteristic impedance of the stub is 50 ohms.

The principle behind the stub matching technique consists of finding the location nearest to the load at which the real part of the line admittance (reciprocal of the line impedance) is equal to the line characteristic admittance

$Y_0$  (reciprocal of the line characteristic impedance  $Z_0$ ). The imaginary part of the line admittance is then cancelled by placing in parallel with the line a short-circuited stub of appropriate length so that its input susceptance is equal to the negative of the imaginary part of the line admittance to the right of the stub as shown in Fig. 6.51. The line admittance seen from the left of the stub is

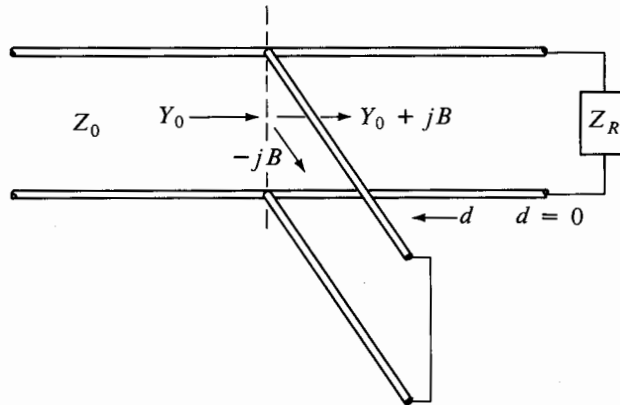


Fig. 6.51. Transmission-line matching by means of a stub.

the stub is then equal to  $(Y_0 + jB) + (-jB) = Y_0$ . The line impedance seen from the left of the stub into the junction of the line and the stub is therefore equal to  $Z_0$  and a match is achieved. To find the required parameters, we proceed in a step-by-step manner as follows:

- (a) Find the reflection coefficient at the load.

$$\bar{\Gamma}(0) = \frac{\bar{Z}_R - Z_0}{\bar{Z}_R + Z_0} = \frac{(30 - j40) - 50}{(30 - j40) + 50} = 0.5e^{-j\pi/2}$$

- (b) Find the reflection coefficient as a function of  $d$ .

$$\bar{\Gamma}(d) = \bar{\Gamma}(0)e^{-j2\beta d} = 0.5e^{-j(2\beta d + \pi/2)}$$

- (c) Find the line admittance as a function of  $d$ .

$$\begin{aligned} \bar{Y}(d) &= \frac{1}{\bar{Z}(d)} = \frac{1}{Z_0} \left[ \frac{1 - \bar{\Gamma}(d)}{1 + \bar{\Gamma}(d)} \right] \\ &= \frac{1}{50} \left[ \frac{1 - 0.5e^{-j(2\beta d + \pi/2)}}{1 + 0.5e^{-j(2\beta d + \pi/2)}} \right] \\ &= 0.02 \frac{0.75 + j \cos 2\beta d}{1.25 - \sin 2\beta d} \end{aligned}$$

- (d) Set the real part of  $\bar{Y}(d)$  equal to  $Y_0$  and solve for  $d$ .

$$0.02 \frac{0.75}{1.25 - \sin 2\beta d} = 0.02$$

or

$$\sin 2\beta d = 0.5$$

$$2\beta d = \frac{\pi}{6} \quad \text{or} \quad \frac{5\pi}{6}$$

$$d = \frac{\lambda}{24} \quad \text{or} \quad \frac{5\lambda}{24}$$

Thus the stub must be located at a distance  $\lambda/24$  or  $5\lambda/24$  from the load.

(e) To find the length of the stub, we note that the imaginary part of  $\bar{Y}(d)$  is  $(0.02 \cos 2\beta d)/(1.25 - \sin 2\beta d)$ . Its value at the stub location is

$$B = \begin{cases} 0.02 \times 1.15 & \text{for } d = \frac{\lambda}{24} \\ 0.02 \times (-1.15) & \text{for } d = \frac{5\lambda}{24} \end{cases}$$

(f) The input impedance of a short-circuited line of length  $l$  is given by (6-234). The input admittance is

$$\bar{Y}_{in} = \frac{1}{\bar{Z}_{in}} = \frac{1}{jZ_0 \tan \beta l} = -jY_0 \cot \beta l$$

Thus the stub length  $l$  must be such that

$$-jY_0 \cot \beta l = \begin{cases} -j0.02 \times 1.15 & \text{for } d = \frac{\lambda}{24} \\ j0.02 \times 1.15 & \text{for } d = \frac{5\lambda}{24} \end{cases}$$

or

$$l = \begin{cases} 0.113\lambda & \text{for } d = \frac{\lambda}{24} \\ 0.387\lambda & \text{for } d = \frac{5\lambda}{24} \quad \blacksquare \end{cases}$$

The steps involved in the analytical solution of the stub matching problem in the preceding example consist of conversion from line impedance to reflection coefficient, then going along the constant  $|\bar{\Gamma}|$  circle in the complex-plane diagram of Fig. 6.47 to find  $\bar{\Gamma}(d)$  and then converting back to impedance. This process of conversion and reconversion from one quantity to the other can be eliminated by constructing a chart which associates with each point in the complex  $\bar{\Gamma}$  plane the corresponding impedance or admittance. One such chart is known as the Smith chart. To discuss the basis of Smith chart construction, we define the normalized line impedance,  $\bar{z}(d)$ , as the ratio of the line impedance  $\bar{Z}(d)$  to the characteristic impedance  $Z_0$ . Thus

$$\bar{z}(d) = \frac{\bar{Z}(d)}{Z_0} = \frac{1 + \bar{\Gamma}(d)}{1 - \bar{\Gamma}(d)} \quad (6-243)$$

Conversely,

$$\bar{\Gamma}(d) = \frac{\bar{z}(d) - 1}{\bar{z}(d) + 1} \quad (6-244)$$

Letting  $\bar{z}(d) = r + jx$ , we have

$$\bar{\Gamma}(d) = \frac{r + jx - 1}{r + jx + 1} = \frac{(r - 1) + jx}{(r + 1) + jx}$$

and

$$|\bar{\Gamma}(d)| = \left[ \frac{(r - 1)^2 + x^2}{(r + 1)^2 + x^2} \right]^{1/2} \leq 1$$

for positive values of  $r$ . Thus, for passive line impedances, the reflection coefficient lies inside or on the circle of unit radius in the  $\bar{\Gamma}$  plane. We will hereafter call this circle the unit circle. Conversely, each point inside or on the unit circle represents a possible value of reflection coefficient corresponding to a unique value of passive normalized line impedance in view of (6-243). Hence all possible values of passive normalized line impedances can be mapped onto the region bounded by the unit circle.

To determine how the normalized line impedance values are mapped onto the region bounded by the unit circle, we note that

$$\bar{\Gamma} = \frac{r + jx - 1}{r + jx + 1} = \frac{r^2 - 1 + x^2}{(r + 1)^2 + x^2} + j \frac{2x}{(r + 1)^2 + x^2}$$

so that

$$\Re e(\bar{\Gamma}) = \frac{r^2 - 1 + x^2}{(r + 1)^2 + x^2}$$

$$\Im m(\bar{\Gamma}) = \frac{2x}{(r + 1)^2 + x^2}$$

Let us now discuss different cases:

- (a)  $\bar{z}$  is purely real; that is,  $x = 0$ . Then

$$\Re e(\bar{\Gamma}) = \frac{r - 1}{r + 1} \quad \text{and} \quad \Im m(\bar{\Gamma}) = 0$$

Purely real values of  $\bar{z}$  are represented by points on the real axis. For example,  $r = 0, \frac{1}{3}, 1, 3,$  and  $\infty$  are represented by  $\bar{\Gamma} = -1, -\frac{1}{2}, 0, \frac{1}{2},$  and  $1$ , respectively, as shown in Fig. 6.52(a).

- (b)  $\bar{z}$  is purely imaginary; that is,  $r = 0$ . Thus

$$|\bar{\Gamma}| = \left| \frac{x^2 - 1}{x^2 + 1} + j \frac{2x}{x^2 + 1} \right| = 1$$

and

$$\angle \bar{\Gamma} = \tan^{-1} \frac{2x}{x^2 - 1}$$

Purely imaginary values of  $\bar{z}$  are represented by points on the unit circle. For example,  $x = 0, 1, \infty, -1,$  and  $-\infty$  are represented by

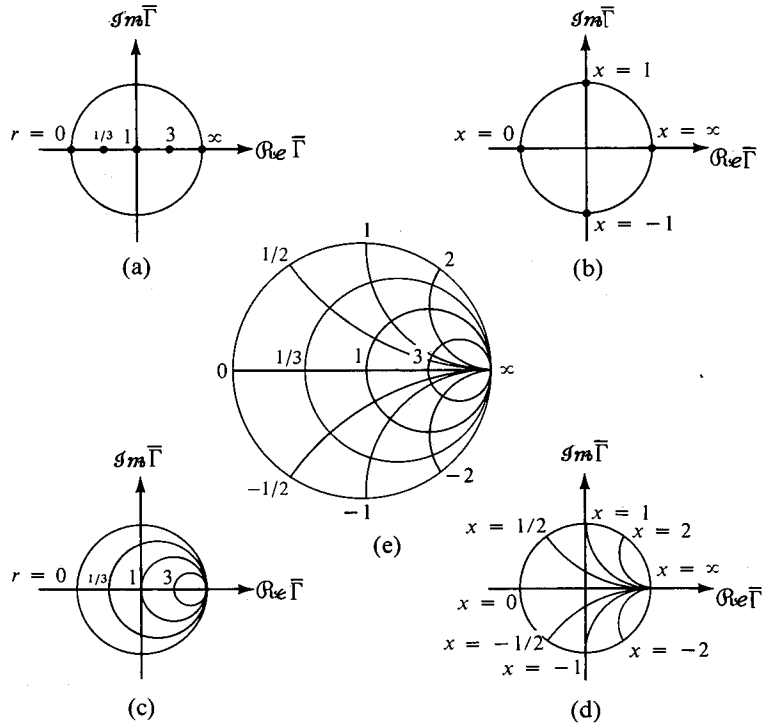


Fig. 6.52. Development of the Smith chart by transformation from  $\bar{z}$  to  $\bar{\Gamma}$ .

$\bar{\Gamma} = 1/\pi, 1/\pi/2, 1/0^\circ, 1/-\pi/2$  and  $1/2\pi$ , respectively, as shown in Fig. 6.52(b).

(c)  $\bar{z}$  is complex but its real part is constant. Then

$$\begin{aligned} & \left[ \text{Re}(\bar{\Gamma}) - \frac{r}{r+1} \right]^2 + [\text{Im}(\bar{\Gamma})]^2 \\ &= \left[ \frac{r^2 - 1 + x^2}{(r+1)^2 + x^2} - \frac{r}{r+1} \right]^2 + \left[ \frac{2x}{(r+1)^2 + x^2} \right]^2 = \left( \frac{1}{r+1} \right)^2 \end{aligned}$$

This is the equation of a circle with center at  $\text{Re}(\bar{\Gamma}) = r/(r+1)$  and  $\text{Im}(\bar{\Gamma}) = 0$  and radius equal to  $1/(r+1)$ . Thus loci of constant  $r$  are circles in the  $\bar{\Gamma}$  plane with centers at  $[r/(r+1), 0]$  and radii  $1/(r+1)$ . For example, for  $r = 0, 1/3, 1, 3$ , and  $\infty$ , the centers of the circles are  $(0, 0), (1/4, 0), (1/2, 0), (3/4, 0)$ , and  $(1, 0)$ , respectively, and the radii are  $1, 3/4, 1/2, 1/4$ , and  $0$ , respectively. These circles are shown in Fig. 6.52(c).

(d)  $\bar{z}$  is complex but its imaginary part is constant. Then

$$\begin{aligned} & [\Re\{\bar{\Gamma}\} - 1]^2 + \left[ \Im\{\bar{\Gamma}\} - \frac{1}{x} \right]^2 \\ &= \left[ \frac{r^2 - 1 + x^2}{(r+1)^2 + x^2} - 1 \right]^2 + \left[ \frac{2x}{(r+1)^2 + x^2} - \frac{1}{x} \right]^2 = \left( \frac{1}{x} \right)^2 \end{aligned}$$

This is the equation of a circle with center at  $\Re\{\bar{\Gamma}\} = 1$  and  $\Im\{\bar{\Gamma}\} = 1/x$  and radius equal to  $1/|x|$ . Thus locii of constant  $x$  are circles in the  $\bar{\Gamma}$  plane with centers at  $(1, 1/x)$  and radii equal to  $1/|x|$ . For example, for  $x = 0, \pm\frac{1}{2}, \pm 1, \pm 2,$  and  $\pm\infty$ , the centers of the circles are  $(1, \infty), (1, \pm 2), (1, \pm 1), (1, \pm\frac{1}{2}),$  and  $(1, 0)$ , respectively, and the radii are  $\infty, 2, 1, \frac{1}{2},$  and  $0$ , respectively. Portions of these circles which fall inside the unit circle are shown in Fig. 6.52(d). Portions which fall outside the unit circle represent active impedances.

Combining (c) and (d), we obtain the chart of Fig. 6.52(e). In a commercially available form shown in Fig. 6.53, the Smith chart contains circles of constant  $r$  and constant  $x$  for very small increments of  $r$  and  $x$ , respectively, so that interpolation between the contours can be carried out accurately. We now illustrate the application of the Smith chart by means of some examples.

**EXAMPLE 6-26.** A transmission line of characteristic impedance 50 ohms is terminated by a load impedance  $\bar{Z}_R = (15 - j20)$  ohms. It is desired to find the following quantities by using the Smith chart.

- (1) Reflection coefficient at the load.
- (2) VSWR on the line.
- (3) Distance of the first voltage minimum of the standing wave pattern from the load.
- (4) Line impedance at  $d = 0.05\lambda$ .
- (5) Line admittance at  $d = 0.05\lambda$ .
- (6) Location nearest to the load at which the real part of the line admittance is equal to the line characteristic admittance.

We proceed with the solution of the problem in the following step-by-step manner with reference to Fig. 6.54.

- (a) Find the normalized load impedance.

$$\bar{z}_R = \frac{\bar{Z}_R}{Z_0} = \frac{15 - j20}{50} = 0.3 - j0.4$$

- (b) Locate the normalized load impedance on the Smith chart at the intersection of the 0.3 constant normalized resistance circle and  $-0.4$  constant normalized reactance circle (point *A*).

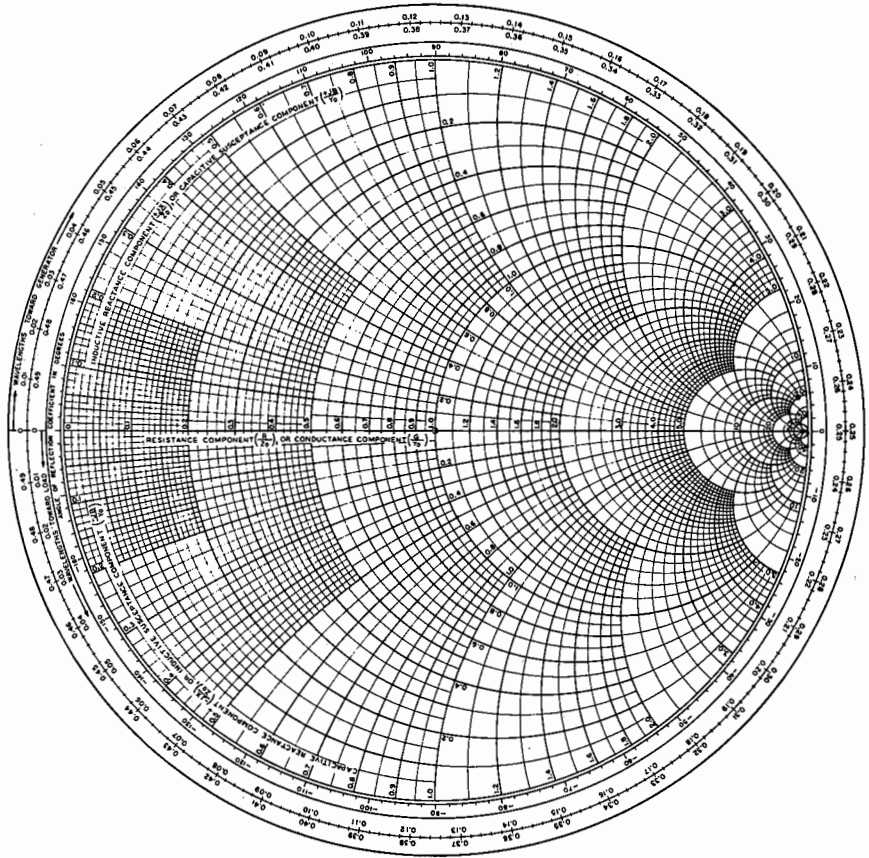


Fig. 6.53. The Smith chart (Copyrighted by and reproduced with the permission of Kay Elemetrics Corp., Pine Brook, N.J.).

(c) Locating point *A* actually amounts to computing the reflection coefficient at the load since the Smith chart is a transformation in the  $\bar{\Gamma}$  plane. The magnitude of the reflection coefficient is the distance from the center (*O*) of the Smith chart (origin of the  $\bar{\Gamma}$  plane) to the point *A* based on a radius of unity for the outermost circle. For this example,  $|\bar{\Gamma}(0)| = 0.6$ . The phase angle of  $\bar{\Gamma}(0)$  is the angle measured from the horizontal axis to the right of *O* (positive real axis in the  $\bar{\Gamma}$  plane) to the line *OA* in the counter-clockwise direction. This angle is indicated on the chart along its circumference. For this example,  $\angle \bar{\Gamma}(0) = 227^\circ$ . Thus

$$\bar{\Gamma}(0) = 0.6e^{j227^\circ}$$

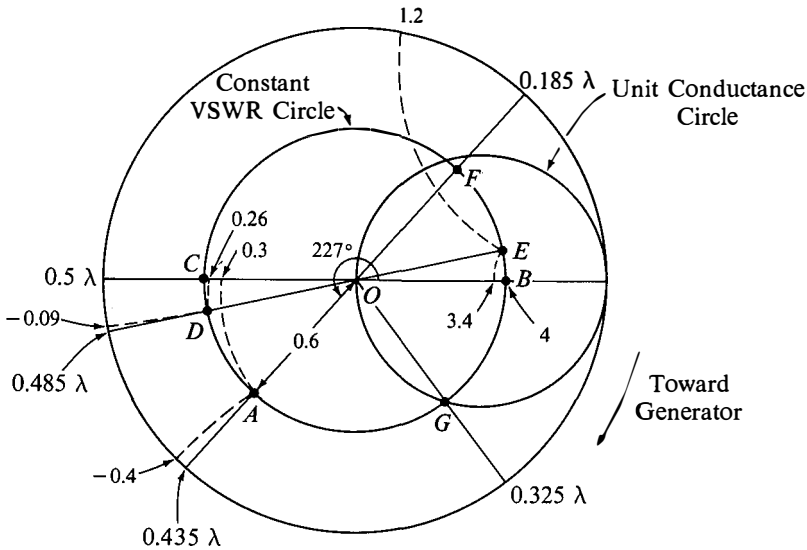


Fig. 6.54. For illustrating the various procedures to be followed in using the Smith chart.

(d) To find the VSWR, we recall that at the location of a voltage maximum, the line impedance is purely real and maximum. Denoting this impedance as  $R_{max}$ , we have

$$R_{max} = \frac{V_{max}}{I_{min}} = \frac{|\bar{V}^+|(1 + |\bar{\Gamma}|)}{(|\bar{V}^+|/Z_0)(1 - |\bar{\Gamma}|)} = Z_0(\text{VSWR}) \quad (6-245)$$

Thus the normalized value of  $R_{max}$  is equal to the VSWR. We therefore move along the line to the location of the voltage maximum, which involves going around the constant  $|\bar{\Gamma}|$  circle to the point on the positive real axis. To do this on the Smith chart, we draw a circle passing through  $A$  and with center at  $O$ . This circle is known as the “constant VSWR circle” since for points on this circle,  $|\bar{\Gamma}|$  and hence  $\text{VSWR} = (1 + |\bar{\Gamma}|)/(1 - |\bar{\Gamma}|)$  is a constant. Impedance values along this circle are normalized line impedances as seen moving along the line. In particular, since point  $B$  (the intersection of the constant VSWR circle with the horizontal axis to the right of  $O$ ) corresponds to voltage maximum, the normalized impedance value at point  $B$  which is purely real and maximum, is equal to the VSWR. Thus, for this example,  $\text{VSWR} = 4$ .

(e) Just as point  $B$  represents the position of a voltage maximum on the line, point  $C$  (intersection of the constant VSWR circle with the horizontal axis to the left of  $O$ , i.e., the negative real axis of the  $\bar{\Gamma}$  plane) represents the location of a voltage minimum. Hence, to find the distance of the first voltage minimum from the load, we move along the constant VSWR circle starting at point  $A$  (load impedance) towards the generator (clockwise



direction on the chart) to reach point  $C$ . Distance moved along the constant VSWR circle in this process can be determined by recognizing that one complete revolution around the chart ( $\Gamma$ -plane diagram) constitutes movement on the line by  $0.5\lambda$ . However, it is not necessary to compute in this manner since distance scales in terms of  $\lambda$  are provided along the periphery of the chart for movement in both directions. For this example, the distance from the load to the first voltage minimum =  $(0.5 - 0.435)\lambda = 0.065\lambda$ . Conversely, if the VSWR and the location of the voltage minimum are specified, we can find the load impedance following the above procedures in reverse.

(f) To find the line impedance at  $d = 0.05\lambda$ , we start at point  $A$  and move along the constant VSWR circle towards the generator (in the clockwise direction) by a distance of  $0.05\lambda$  to reach point  $D$ . This step is equivalent to finding the reflection coefficient at  $d = 0.05\lambda$  knowing the reflection coefficient at  $d = 0$  and then computing the normalized line impedance by using (6-243). Thus, from the coordinates corresponding to point  $D$ , the normalized line impedance at  $d = 0.05\lambda$  is  $(0.26 - j0.09)$  and hence the line impedance at  $d = 0.05\lambda$  is  $50(0.26 - j0.09)$  or  $(13 - j4.5)$  ohms.

(g) To find the line admittance at  $d = 0.05\lambda$ , we recall that

$$[\bar{z}(d)] \left[ \bar{z} \left( d + \frac{\lambda}{4} \right) \right] = Z_0^2$$

so that

$$[\bar{z}(d)] \left[ \bar{z} \left( d + \frac{\lambda}{4} \right) \right] = 1$$

or

$$\bar{y}(d) = \bar{z} \left( d + \frac{\lambda}{4} \right) \quad (6-246)$$

Thus the normalized line admittance at a point  $D$  is the same as the normalized line impedance at a distance  $\lambda/4$  from it. Hence, to find  $\bar{y}(0.05\lambda)$ , we start at point  $D$  and move along the constant VSWR circle by a distance  $\lambda/4$  to reach point  $E$  (we note that this point is diametrically opposite to point  $D$ ) and read its coordinates. This gives  $\bar{y}(0.05\lambda) = (3.4 + j1.2)$ . We then have  $\bar{Y}(0.05\lambda) = \bar{y}(0.05\lambda) \times Y_0 = (3.4 + j1.2) \times 1/50 = (0.068 + j0.024)$  mhos.

(h) Relationship (6-246) permits us to use the Smith chart as an admittance chart instead of an impedance chart. In other words, if we want to find the normalized line admittance  $\bar{y}(Q)$  at a point  $Q$  on the line, knowing the normalized line admittance  $\bar{y}(P)$  at another point  $P$  on the line, we can simply locate  $\bar{y}(P)$  by entering the chart at coordinates equal to its real and imaginary parts and then moving along the constant VSWR circle by the amount of the distance from  $P$  to  $Q$  in the proper direction to obtain the coordinates equal to the real and imaginary parts of  $\bar{y}(Q)$ . Thus it is not necessary first to locate  $\bar{z}(P)$  diametrically opposite to  $\bar{y}(P)$  on the constant VSWR circle, then move along the constant VSWR circle to locate  $\bar{z}(Q)$ ,

and then find  $\bar{y}(Q)$  diametrically opposite to  $\bar{z}(Q)$ . To find the location nearest to the load at which the real part of the line admittance is equal to the line characteristic admittance, we first locate  $\bar{y}(0)$  at point  $F$  diametrically opposite to point  $A$  which corresponds to  $\bar{z}(0)$ . We then move along the constant VSWR circle towards the generator to reach point  $G$  on the circle corresponding to constant real part equal to unity (we call this circle the "unit conductance circle"). Distance moved from  $F$  to  $G$  is read off the chart as  $(0.325 - 0.185)\lambda = 0.14\lambda$ . This is the distance closest to the load at which the real part of the normalized line admittance is equal to unity and hence the real part of the line admittance is equal to the line characteristic admittance. ■

**EXAMPLE 6-27.** It is desired to solve the stub matching problem of Example 6-25 by using the Smith chart.

We make use of the principle of stub matching illustrated in Example 6-25 and the procedures learned in Example 6-26 to solve this problem in the following step-by-step manner with reference to Fig. 6.55.

(a) Find the normalized load impedance.

$$\bar{z}_R = \frac{\bar{Z}_R}{Z_0} = \frac{30 - j40}{50} = 0.6 - j0.8$$

Locate the normalized load impedance on the Smith chart at point  $A$ .

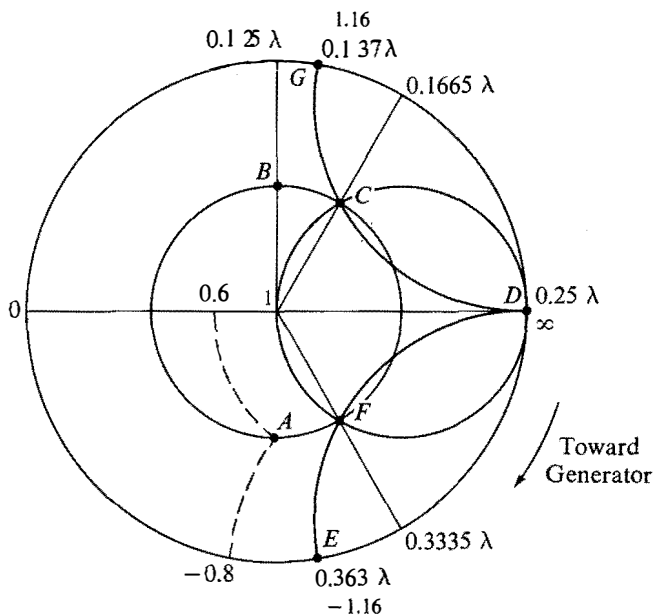


**Fig. 6.55.** Solution of transmission-line matching problem by using the Smith chart.

(b) Draw the constant VSWR circle passing through point *A*. This is the locus of the normalized line impedance as well as the normalized line admittance. Starting at point *A*, go around the constant VSWR circle by half a revolution to reach point *B* diametrically opposite to point *A*. Point *B* corresponds to the normalized load admittance.

(c) Starting at point *B*, go around the constant VSWR circle towards the generator until point *C* on the unit conductance circle is reached. This point corresponds to the normalized line admittance having the real part equal to unity and hence it corresponds to the location of the stub. The distance moved from point *B* to point *C* (not from point *A* to point *C*) is equal to the distance from the load at which the stub must be located. Thus the location of the stub from the load =  $(0.1665 - 0.125)\lambda = 0.0415\lambda$ .

(d) Read off the Smith chart the normalized susceptance value corresponding to point *C*. This value is 1.16 and it is the imaginary part of the normalized line admittance at the location of the stub. The imaginary part of the line admittance is equal to  $1.16 \times Y_0 = (1.16/50)$  mhos. The input susceptance of the stub must therefore be equal to  $-(1.16/50)$  mhos.

(e) This step consists of finding the length of a short-circuited stub having an input susceptance equal to  $-(1.16/50)$  mhos. We can use the Smith chart for this purpose since this simply consists of finding the distance between two points on a line (the stub in this case) at which the admittances (purely imaginary in this case) are known. Thus, since the short circuit corresponds to a susceptance of infinity, we start at point *D* and move towards the generator along the constant VSWR circle through *D* (the outermost circle) to reach point *E* corresponding to  $-j1.16$ , which is the input admittance of the stub normalized with respect to its own characteristic admittance. The distance moved from *D* to *E* is the required length of the stub. Thus length of the short-circuited stub =  $(0.363 - 0.25)\lambda = 0.113\lambda$ .

(f) The results obtained for the location and the length of the stub agree with one of the solutions found analytically in Example 6-25. The second solution can be obtained by noting that in step (c) above, we can go around the constant VSWR circle from point *B* until point *F* on the unit conductance circle is reached instead of stopping at point *C*. The stub location for this solution is  $(0.3335 - 0.125)\lambda = 0.2085\lambda$ . The required input susceptance of the stub is  $(1.16/50)$  mhos. The length of the stub is the distance from point *D* to point *G* in the clockwise direction. This is  $(0.137 + 0.25)\lambda = 0.387\lambda$ . These values are the same as the second solution obtained in Example 6-25. ■

We have illustrated the use of the Smith chart by considering the transmission-line matching problem. However, from the procedures learned in Example 6.26, it can be seen that the Smith chart can be used for all transmission-line and analogous plane-wave problems involving reflection, transmission, and matching. As a further illustration of the applications of

the Smith chart, we will learn in the following section that waveguide problems can be treated by using transmission-line equivalents. Thus the Smith chart can be used for solving these and many other problems.

## 6.12 Waveguides; Dispersion and Group Velocity

In Section 6.8 we obtained the solution for the one-dimensional wave equation as (+) and (-) uniform plane waves traveling along that dimension and then deduced the expressions for the fields in a uniform plane wave traveling in an arbitrary direction with reference to a coordinate system. We now make use of these expressions to discuss uniform plane waves incident obliquely on a perfect conductor and then introduce the concept of waveguides. Since an arbitrarily polarized uniform plane wave can be decomposed into linearly polarized uniform plane waves, we consider linearly polarized uniform plane waves only for this discussion. Let us consider a perfect conductor occupying the  $x = 0$  plane and upon which is incident a uniform plane wave having the electric field vector

$$\begin{aligned}\bar{\mathbf{E}}_i &= \bar{E}_0 e^{-j\beta_i \cdot \mathbf{r}_i} \\ &= \bar{E}_0 e^{-j(\beta \cos \theta_i i_x + \beta \sin \theta_i i_z) \cdot \mathbf{r}_i} \\ &= \bar{E}_0 e^{-j(\beta x \cos \theta_i + \beta z \sin \theta_i)} i_y\end{aligned}\quad (6-247a)$$

where  $\bar{E}_0$  is a constant,  $\beta = \omega\sqrt{\mu\epsilon}$ , and  $\theta_i$  is the angle between the propagation vector  $\beta_i$  and the normal to the conductor as shown in Fig. 6.56. The expression for the corresponding magnetic field vector can be obtained by using (6-200) as follows:

$$\begin{aligned}\bar{\mathbf{H}}_i &= \frac{1}{\omega\mu} \beta_i \times \bar{\mathbf{E}}_i \\ &= \sqrt{\frac{\epsilon}{\mu}} (-\bar{E}_0 \sin \theta_i i_x + \bar{E}_0 \cos \theta_i i_z) e^{-j(\beta x \cos \theta_i + \beta z \sin \theta_i)}\end{aligned}\quad (6-247b)$$

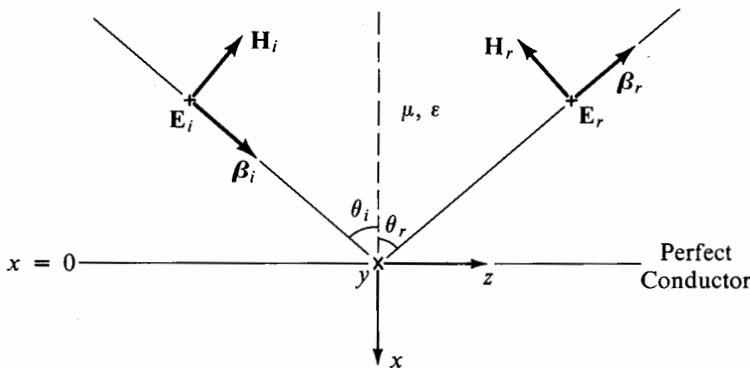


Fig. 6.56. Oblique incidence of a uniform plane wave on a perfect conductor.

Since the boundary condition at a perfect conductor surface dictates that the tangential component of the electric field be zero, a reflected wave must exist which cancels completely the tangential component (which is the only component in this case) of the electric field vector of the incident wave at the surface of the conductor. Such cancellation is possible only if the tangential component of the electric field in the reflected wave at the surface of the conductor is entirely in the  $y$  direction, that is, the same as the direction of the tangential component of the electric field vector of the incident wave. Furthermore, since we are dealing with linearly polarized uniform plane waves, the electric field in the reflected wave must everywhere be in the same direction. Hence it must have a  $y$  component only everywhere. Thus the electric and magnetic fields of the reflected wave can be written as

$$\begin{aligned}\bar{\mathbf{E}}_r &= \bar{E}'_0 e^{-j\beta_r \cdot \mathbf{r}} \mathbf{i}_y \\ &= \bar{E}'_0 e^{-j(-\beta \cos \theta_r \mathbf{i}_x + \beta \sin \theta_r \mathbf{i}_z) \cdot \mathbf{r}} \mathbf{i}_y \\ &= \bar{E}'_0 e^{j(\beta x \cos \theta_r - \beta z \sin \theta_r)} \mathbf{i}_y\end{aligned}\quad (6-248a)$$

$$\begin{aligned}\bar{\mathbf{H}}_r &= \frac{1}{\omega \mu} \boldsymbol{\beta}_r \times \bar{\mathbf{E}}_r \\ &= \sqrt{\frac{\epsilon}{\mu}} (-\bar{E}'_0 \sin \theta_r \mathbf{i}_x - \bar{E}'_0 \cos \theta_r \mathbf{i}_z) e^{j(\beta x \cos \theta_r - \beta z \sin \theta_r)}\end{aligned}\quad (6-248b)$$

where  $\bar{E}'_0$  is a constant,  $\beta = \omega \sqrt{\mu \epsilon}$ , and  $\theta_r$  is the angle between the propagation vector  $\boldsymbol{\beta}_r$  and the normal to the conductor as shown in Fig. 6.56.

Adding the incident and reflected fields, we obtain the components of the total electric and magnetic fields as

$$\bar{E}_y = \bar{E}_0 e^{-j(\beta x \cos \theta_i + \beta z \sin \theta_i)} + \bar{E}'_0 e^{j(\beta x \cos \theta_r - \beta z \sin \theta_r)} \quad (6-249a)$$

$$\begin{aligned}\bar{H}_x &= \sqrt{\frac{\epsilon}{\mu}} [-\bar{E}_0 \sin \theta_i e^{-j(\beta x \cos \theta_i + \beta z \sin \theta_i)} \\ &\quad - \bar{E}'_0 \sin \theta_r e^{j(\beta x \cos \theta_r - \beta z \sin \theta_r)}]\end{aligned}\quad (6-249b)$$

$$\begin{aligned}\bar{H}_z &= \sqrt{\frac{\epsilon}{\mu}} [\bar{E}_0 \cos \theta_i e^{-j(\beta x \cos \theta_i + \beta z \sin \theta_i)} \\ &\quad - \bar{E}'_0 \cos \theta_r e^{j(\beta x \cos \theta_r - \beta z \sin \theta_r)}]\end{aligned}\quad (6-249c)$$

Applying the boundary condition at the surface of the conductor, we have

$$[\bar{E}_y]_{z=0} = \bar{E}_0 e^{-j\beta x \sin \theta_i} + \bar{E}'_0 e^{-j\beta x \sin \theta_r} = 0 \quad \text{for all } z \quad (6-250)$$

Equation (6-250) can be satisfied only if the exponential factors are equal for all  $z$ . Thus we obtain the result

$$\theta_r = \theta_i \quad (6-251)$$

that is, the angle of reflection is equal to the angle of incidence, which is the familiar law of reflection in optics. Substituting (6-251) into (6-250), we have

$$\bar{E}'_0 = -\bar{E}_0 \quad (6-252)$$

Substituting (6-251) and (6-252) into (6-249a)–(6-249c), we obtain the follow-

ing expressions for the components of the total fields:

$$\bar{E}_y = -2j\bar{E}_0 \sin(\beta x \cos \theta_i) e^{-j\beta z \sin \theta_i} \quad (6-253a)$$

$$\bar{H}_x = \sqrt{\frac{\epsilon}{\mu}} 2j\bar{E}_0 \sin \theta_i \sin(\beta x \cos \theta_i) e^{-j\beta z \sin \theta_i} \quad (6-253b)$$

$$\bar{H}_z = \sqrt{\frac{\epsilon}{\mu}} 2\bar{E}_0 \cos \theta_i \cos(\beta x \cos \theta_i) e^{-j\beta z \sin \theta_i} \quad (6-253c)$$

The exponential factor in (6-253a)–(6-253c) lends a pure traveling wave character in the  $z$  direction to the fields whereas the sine and cosine factors involving  $x$  lend a complete standing wave character in the  $x$  direction. In fact, the complex Poynting vector is given by

$$\begin{aligned} \bar{\mathbf{P}} &= \frac{1}{2} \bar{\mathbf{E}} \times \bar{\mathbf{H}}^* = \frac{1}{2} [\bar{E}_y \bar{H}_z^* \mathbf{i}_x + (-\bar{E}_x)(\bar{H}_z^*) \mathbf{i}_z] \\ &= \frac{1}{2} \sqrt{\frac{\epsilon}{\mu}} [-2j |\bar{E}_0|^2 \cos \theta_i \sin(2\beta x \cos \theta_i) \mathbf{i}_x \\ &\quad + 4 |\bar{E}_0|^2 \sin \theta_i \sin^2(\beta x \cos \theta_i) \mathbf{i}_z] \end{aligned} \quad (6-254)$$

Thus the time-average power flow is entirely in the  $z$  direction whereas the reactive power flow is associated entirely with the  $x$  direction. The situation can therefore be described as one of complete standing waves in the  $x$  direction traveling as a whole in the  $z$  direction.

We note from (6-253a) that  $\bar{E}_y$  is equal to zero not only at the surface of the conductor ( $x = 0$ ), but also in other planes given by

$$\sin(\beta x \cos \theta_i) = 0$$

or

$$\beta x \cos \theta_i = -m\pi \quad m = 1, 2, 3, \dots$$

or

$$x = -\frac{m\pi}{\beta \cos \theta_i} = -\frac{m\lambda}{2 \cos \theta_i} \quad m = 1, 2, 3, \dots \quad (6-255)$$

where  $\lambda = 2\pi/\beta$  is the wavelength along the direction of incidence (or reflection). Introduction of perfect conductors in planes parallel to the conductor surface and at distances of integral multiples of  $\lambda/(2 \cos \theta_i)$  from it does not alter in any way the total field, once it is established. Let us introduce a perfectly conducting plate in the plane  $x = -m\lambda/(2 \cos \theta_i)$  as shown in Fig. 6.57, where  $m$  can take any integer value. The two conductors support standing waves in the  $x$  direction while permitting traveling waves in the  $z$  direction. The phenomenon is actually one of uniform plane waves bouncing obliquely between the two plane conductors as shown in Fig. 6.57. The structure is known as a parallel-plate “waveguide.” The total magnetic field has a component in the  $z$  direction, which is the direction of time-average power flow whereas the electric field is entirely transverse to the  $z$  direction. For this reason, the waves are known as “transverse electric” or TE waves.

Let us now fix the spacing between the parallel plates as  $a$  and discuss the

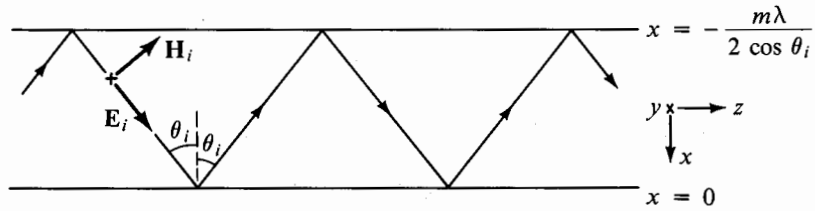


**Fig. 6.57.** Bouncing of a uniform plane wave obliquely along a parallel-plate waveguide.

behavior of the guided waves as the frequency of the source exciting these waves is varied. Setting  $m\lambda/(2 \cos \theta_i)$  equal to  $a$ , we have

$$\cos \theta_i = \frac{m\lambda}{2a} \tag{6-256}$$

From (6-256), we note that, for very high frequencies,  $\lambda \approx 0$ ,  $\cos \theta_i \approx 0$ ,  $\theta_i \approx 90^\circ$ , and the waves slide between the plates almost like a TEM wave. As the frequency is decreased,  $\lambda$  increases,  $\cos \theta_i$  increases,  $\theta_i$  decreases, and the waves bounce obliquely between the plates, progressing in the  $z$  direction until, for  $\lambda = 2a/m$ ,  $\cos \theta_i = 1$ ,  $\theta_i = 0^\circ$ , and the waves bounce back and forth between the plates and normal to them so that there is no progress in the  $z$  direction. These different cases are illustrated in Figs. 6.58(a)–(d).

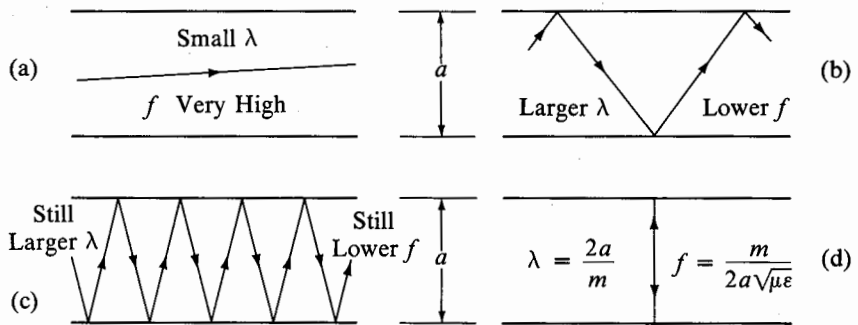


**Fig. 6.58.** Bouncing of uniform plane waves of different frequencies between parallel plane conductors of fixed spacing for illustrating the “cutoff” phenomenon.

For  $\lambda > 2a/m$ ,  $\cos \theta_i > 1$ ,  $\sin \theta_i = \sqrt{1 - \cos^2 \theta_i}$  becomes imaginary, the exponents in the expressions for the total fields become real, and the situation no longer corresponds to one of wave propagation; the fields diminish in magnitude along  $z$ . Thus there is a wavelength below which propagation occurs and above which there is no propagation. This is known as the cutoff

wavelength and is denoted by the symbol  $\lambda_c$ . Here,

$$\lambda_c = \frac{2a}{m} \quad m = 1, 2, 3, \dots \quad (6-257)$$

The corresponding cutoff frequency is given by

$$f_c = \frac{v_p}{\lambda_c} = \frac{m}{2a\sqrt{\mu\epsilon}} \quad m = 1, 2, 3, \dots \quad (6-258)$$

where  $v_p = 1/\sqrt{\mu\epsilon}$  is the phase velocity along the direction of incidence (or reflection). For  $f > f_c$ , propagation occurs and for  $f < f_c$ , there is no propagation.

Substituting  $\lambda_c$  for  $2a/m$  in (6-256), we have

$$\begin{aligned} \cos \theta_i &= \frac{\lambda}{\lambda_c}, \quad \sin \theta_i = \sqrt{1 - \left(\frac{\lambda}{\lambda_c}\right)^2} \\ \beta \cos \theta_i &= \frac{2\pi}{\lambda} \frac{\lambda}{\lambda_c} = \frac{2\pi}{\lambda_c} = \frac{m\pi}{a} \\ \beta \sin \theta_i &= \frac{2\pi}{\lambda} \sqrt{1 - \left(\frac{\lambda}{\lambda_c}\right)^2} \end{aligned}$$

But  $\beta \sin \theta_i$  is the component of the propagation vector  $\boldsymbol{\beta}$ , in the  $z$  direction, that is, along the guide axis. Hence the wavelength in the  $z$  direction, which we call the guide wavelength  $\lambda_g$ , is given by

$$\lambda_g = \frac{2\pi}{\beta \sin \theta_i} = \frac{\lambda}{\sqrt{1 - (\lambda/\lambda_c)^2}} = \frac{\lambda}{\sqrt{1 - (f_c/f)^2}} \quad (6-259)$$

Now, substituting for  $\beta \cos \theta_i$  and  $\beta \sin \theta_i$  in the expressions for the components of the total fields given by (6-253a)–(6-253c), we obtain expressions independent of  $\theta_i$  as

$$\bar{E}_y = -2j\bar{E}_0 \sin\left(\frac{m\pi x}{a}\right) e^{-j(2\pi/\lambda_g)z} \quad (6-260a)$$

$$\bar{H}_x = 2j\frac{\bar{E}_0}{\eta} \frac{\lambda}{\lambda_g} \sin\left(\frac{m\pi x}{a}\right) e^{-j(2\pi/\lambda_g)z} \quad (6-260b)$$

$$\bar{H}_z = 2\frac{\bar{E}_0}{\eta} \frac{\lambda}{\lambda_c} \cos\left(\frac{m\pi x}{a}\right) e^{-j(2\pi/\lambda_g)z} \quad (6-260c)$$

where  $\eta = \sqrt{\mu/\epsilon}$  and  $\lambda_g$  and  $\lambda_c$  are given by (6-259) and (6-257), respectively. The solution for the fields corresponding to each value of  $m$  is called a mode. The  $x$  dependence of the fields is sinusoidal with  $m$  half-sine variations between the plates. The fields are independent of the  $y$  coordinate; that is, they have zero half-sine variations along the  $y$  direction. The solutions are therefore said to correspond to  $TE_{m,0}$  modes, where the first and second subscripts represent the number of half-sine variations of the fields in the  $x$  and  $y$  directions, respectively. The cutoff wavelength is smaller and the cutoff frequency is higher, the larger the value of  $m$ . For any particular wave frequency, all modes for which the cutoff frequencies are less than the wave



frequency can propagate down the guide. The mode which has the lowest cutoff frequency is known as the dominant mode. Here, the  $TE_{1,0}$  mode is the dominant mode.

From the expressions for the fields, we note that the constant phase surfaces are the planes  $z = \text{constant}$ . The rate of change of phase with distance along  $z$ , that is, along the normal to the constant phase surfaces, is  $2\pi/\lambda_g$ . Hence the phase velocity in the  $z$  direction, which we denote as  $v_{pz}$ , is given by

$$v_{pz} = \frac{\omega}{(2\pi/\lambda_g)} = \frac{\omega}{\beta \sin \theta_i} = \frac{v_p}{\sqrt{1 - (\lambda/\lambda_c)^2}} = \frac{v_p}{\sqrt{1 - (f_c/f)^2}} \quad (6-261)$$

where  $v_p = 1/\sqrt{\mu\epsilon}$ . We note that  $v_{pz}$  is simply the apparent phase velocity of the obliquely bouncing waves along the  $z$  direction. We also note that  $v_{pz}$  is a function of frequency  $f$ , the consequence of which we will discuss later in this section. The constant amplitude surfaces are given by  $x = \text{constant}$ . Thus, for the total fields, the amplitude is not constant over the constant phase surfaces.

From the point of view of time-average power flow, the field components of interest are  $-\bar{E}_y$  and  $\bar{H}_x$ , as can be seen from (6-254). The wave impedance obtained by taking the ratio of these two components is known as the guide impedance and is denoted by the symbol  $\eta_g$ . Thus

$$\eta_g = \frac{-\bar{E}_y}{\bar{H}_x} = \eta \frac{\lambda_g}{\lambda} = \frac{\eta}{\sqrt{1 - (\lambda/\lambda_c)^2}} = \frac{\eta}{\sqrt{1 - (f_c/f)^2}} \quad (6-262)$$

Now, using the analogy

$$\begin{aligned} -\bar{E}_y &\leftrightarrow \bar{V} \\ \bar{H}_x &\leftrightarrow \bar{I} \\ \lambda_g &\leftrightarrow \lambda \\ v_{pz} &\leftrightarrow v_p \\ \eta_g &\leftrightarrow \eta \end{aligned} \quad (6-263)$$

we can develop a transmission-line equivalent as shown in Fig. 6.59 which is valid for power flow in the  $z$  direction. Employing the transmission-line techniques discussed in Sections 6.9, 6.10, and 6.11 in conjunction with this equivalent, we can solve reflection, transmission, and matching problems

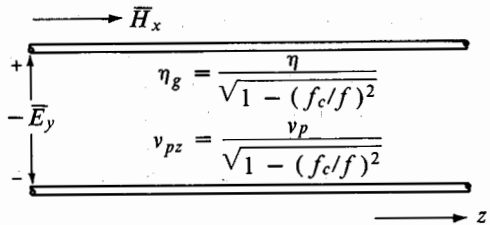


Fig. 6.59. Transmission-line equivalent for power flow along the guide for TE waves in a parallel-plate waveguide.

involving TE modes in waveguides. The proof is left as an exercise (Problem 6.68) for the student. We will now consider some examples, to consolidate what we have learned thus far in this section.

**EXAMPLE 6-28.** The dimension  $a$  of a parallel-plate waveguide is 5.0 cm. Determine the propagating  $TE_{m,0}$  modes for a wave frequency of 10,000 MHz, assuming free space between the plates. For each propagating mode, find (a) the cutoff frequency  $f_c$ , (b) the angle  $\theta_i$  at which the wave bounces obliquely between the conductors, (c) the guide wavelength  $\lambda_g$ , (d) the phase velocity  $v_{pz}$ , and (e) the guide impedance  $\eta_g$ .

From (6-257), the cutoff wavelengths are  $\lambda_c = 2a/m = 10/m$  cm. The wave frequency of 10,000 MHz corresponds to a wavelength  $\lambda$  of 3 cm in free space. Hence the propagating  $TE_{m,0}$  modes are  $TE_{1,0}$  ( $\lambda_c = 10$  cm),  $TE_{2,0}$  ( $\lambda_c = 5$  cm), and  $TE_{3,0}$  ( $\lambda_c = 10/3$  cm). For each propagating mode, the quantities  $f_c$ ,  $\theta_i$ ,  $\lambda_g$ ,  $v_{pz}$ , and  $\eta_g$  can be computed by using the following formulas:

$$f_c = \frac{v_p}{\lambda_c} = \frac{1}{\lambda_c \sqrt{\mu_0 \epsilon_0}}$$

$$\theta_i = \cos^{-1} \frac{\lambda}{\lambda_c}$$

$$\lambda_g = \frac{\lambda}{\sqrt{1 - (\lambda/\lambda_c)^2}}$$

$$v_{pz} = \frac{v_p}{\sqrt{1 - (\lambda/\lambda_c)^2}} \quad \text{where } v_p = \frac{1}{\sqrt{\mu_0 \epsilon_0}}$$

$$\eta_g = \frac{\eta}{\sqrt{1 - (\lambda/\lambda_c)^2}} \quad \text{where } \eta = \sqrt{\frac{\mu_0}{\epsilon_0}}$$

The computed values are as follows:

Mode	$TE_{1,0}$	$TE_{2,0}$	$TE_{3,0}$
$f_c$ , MHz	3000	6000	9000
$\theta_i$ , deg	72.55	53.13	25.15
$\lambda_g$ , cm	3.145	3.75	6.883
$v_{pz}$ , m/sec	$3.145 \times 10^8$	$3.75 \times 10^8$	$6.883 \times 10^8$
$\eta_g$ , ohms	395.2	471.2	864.9

**EXAMPLE 6-29.** A parallel-plate waveguide extending in the  $z$  direction and having  $a = 3$  cm has a dielectric discontinuity at  $z = 0$  as shown in Fig. 6.60(a). For  $TE_{1,0}$  waves of frequency 6,000 MHz incident from the free-space side, (a) find the fraction of the incident power transmitted into the region  $z > 0$ , and (b) find the length and permittivity of a quarter-wave section required to achieve a match between the two media.

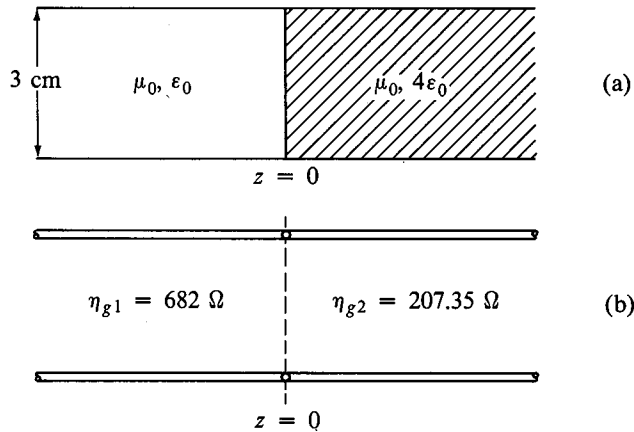


Fig. 6.60. (a) Dielectric discontinuity in a parallel-plate waveguide. (b) Transmission-line equivalent for power flow across the discontinuity for the  $TE_{1,0}$  mode.

Since the discontinuity exists over the entire transverse section of the waveguide, we can use the transmission-line equivalent of Fig. 6.59 for each section of the guide. For the  $TE_{1,0}$  mode,  $\lambda_c = 2a = 6$  cm. For  $f = 6000$  MHz, the wavelength in free space is  $\lambda_1 = 5$  cm and the wavelength in a dielectric of permittivity  $4\epsilon_0$  is  $\lambda_2 = 2.5$  cm. Since  $\lambda_1$  and  $\lambda_2$  are both less than  $\lambda_c$ , the  $TE_{1,0}$  mode can propagate in both sections. Denoting the guide parameters associated with sections 1 and 2 by subscripts 1 and 2, respectively, we have

$$\eta_{g1} = \frac{\eta_1}{\sqrt{1 - (\lambda_1/\lambda_c)^2}} = \frac{377}{\sqrt{1 - (5/6)^2}} = 682 \text{ ohms}$$

$$\eta_{g2} = \frac{\eta_2}{\sqrt{1 - (\lambda_2/\lambda_c)^2}} = \frac{188.5}{\sqrt{1 - (2.5/6)^2}} = 207.35 \text{ ohms}$$

The transmission-line equivalent for power flow in the  $z$  direction is shown in Fig. 6.60(b). The reflection coefficient at  $z = 0$  is then given by

$$\bar{\Gamma} = \frac{\eta_{g2} - \eta_{g1}}{\eta_{g2} + \eta_{g1}} = \frac{207.35 - 682}{207.35 + 682} = -0.5337$$

Thus the fraction of incident power transmitted into the region  $z > 0$  is  $1 - |\bar{\Gamma}|^2 = 1 - 0.5337^2 = 0.715$ . The characteristic impedance of a quarter-wave section required to achieve a match between line 1 and line 2 must be equal to  $\sqrt{\eta_{g1}\eta_{g2}}$ . Denoting the parameters associated with the quarter-wave section by subscript 3, we have

$$\eta_{g3} = \frac{\eta_3}{\sqrt{1 - (\lambda_3/\lambda_c)^2}} = \sqrt{\eta_{g1}\eta_{g2}}$$

or

$$\frac{\eta_1 \sqrt{\epsilon_1/\epsilon_3}}{\sqrt{1 - (\lambda_1/\lambda_c)^2 (\epsilon_1/\epsilon_3)}} = \sqrt{\eta_{g1} \eta_{g2}}$$

$$\frac{\epsilon_1/\epsilon_3}{1 - (5/6)^2 (\epsilon_1/\epsilon_3)} = \frac{\eta_{g1} \eta_{g2}}{\eta_1^2} = \frac{682 \times 207.35}{377^2} = 0.995$$

$$\epsilon_3 = 1.6995 \epsilon_0$$

Hence the permittivity of the quarter-wave matching section must be equal to  $1.6995 \epsilon_0$ . To determine the required length of the matching section, we compute the guide wavelength in the section as

$$\lambda_{g3} = \frac{\lambda_3}{\sqrt{1 - (\lambda_3/\lambda_c)^2}} = \frac{\lambda_1/\sqrt{1.6995}}{\sqrt{1 - (\lambda_1/\lambda_c)^2 (1/1.6995)}}$$

$$= \frac{3.8355}{\sqrt{1 - 0.4086}} = 4.9874 \text{ cm}$$

Hence the required length =  $\lambda_g/4 = 1.24685 \text{ cm}$ . ■

We have merely introduced the concept of a waveguide by considering  $TE_{m,0}$  modes in a parallel-plate guide. Since the electric field is entirely along the  $y$  direction, that is, tangential to the plates, introduction of two more conductors in two  $y = \text{constant}$  planes, say  $y = 0$  and  $y = b$ , does not in any way alter the field configuration of the  $TE_{m,0}$  mode. We then have a metallic pipe with rectangular cross section in the  $xy$  plane as shown in Fig. 6.61. Such a structure is known as a “rectangular waveguide.” The fields

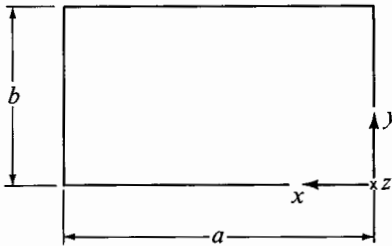


Fig. 6.61. Cross section of a rectangular waveguide.

in the  $TE_{m,0}$  modes have  $m$  half-sinusoidal variations in the  $x$  direction and no variations in the  $y$  direction. They are due to uniform plane waves having electric field in the  $y$  direction only and bouncing obliquely between the walls  $x = 0$  and  $x = a$ . In a similar manner, we can have uniform plane waves having electric field in the  $x$  direction only and bouncing obliquely between the walls  $y = 0$  and  $y = b$ , resulting in  $TE_{0,n}$  modes. The cutoff wavelengths and frequencies for these modes can be obtained by substituting  $b$  for  $a$  and  $n$  for  $m$  in (6-257) and (6-258), respectively. We can even have  $TE_{m,n}$  modes due to uniform plane waves having both  $x$  and  $y$  components of electric field and bouncing between all four walls, satisfying the boundary condition

that the tangential electric fields at the walls are zero. We can repeat the entire discussion by starting with uniform plane waves incident obliquely on a perfect conductor with their magnetic field entirely parallel to the plane of the conductor, leading to transverse magnetic or TM modes. We should, however, note that  $TM_{m,0}$  and  $TM_{0,n}$  modes are not possible in rectangular waveguides. To see why this is so, we note, for example, that  $TM_{m,0}$  modes in parallel-plate waveguides contain  $x$  components of electric fields and it is not possible to place conductors in  $y = \text{constant}$  planes without creating half-sine variations of  $E_x$  in the  $y$  direction. For a particular frequency, all modes for which the cutoff frequencies are less than that frequency can propagate along the guide. However, in practice, waveguides are designed to transmit only the dominant mode, that is, the  $TE_{10}$  mode by a suitable choice of the dimensions  $a$  and  $b$ .

We will now discuss the consequence of  $v_{pz}$ , the phase velocity along the guide axis, being a function of frequency. Let us consider a wave which is made up of a group of waves of different frequencies. If the phase velocity is independent of frequency, the different frequency components maintain the same phase relationships at each and every point along the direction of propagation, thereby preserving the waveshape as it travels. We can then say that the group as a whole travels with the phase velocity. If, on the other hand, the phase velocity is dependent on frequency, the different frequency components do not maintain the same phase relationships at points along the direction of propagation, thereby changing the waveshape. This phenomenon is known as "dispersion," so termed after the phenomenon of dispersion of colors by a prism. In the presence of dispersion, we cannot say that the group as a whole travels with any one of the phase velocities of its components. However, we can attribute a velocity known as the "group velocity," denoted by  $v_g$  for the group travel under certain conditions.

To discuss the concept of group velocity, let us consider a group of two waves of frequencies  $\omega_1$  and  $\omega_2$  ( $> \omega_1$ ). Let the associated phase constants be  $\beta_1$  and  $\beta_2$ . Then the phase velocities associated with  $\omega_1$  and  $\omega_2$  are  $v_{p1} = \omega_1/\beta_1$  and  $v_{p2} = \omega_2/\beta_2$ , respectively. Let us consider an instant of time, say  $t = 0$ , at which the variations of the two waveforms with distance are as shown in Fig. 6.62(a), in which there is a coincidence of the two waveforms at the point designated  $A_1, A_2$ . For the parallel-plate waveguide, Eq. (6-261) indicates that the phase velocity decreases as frequency is increased. Hence, as the two waves travel along  $z$ , the waveform for  $\omega_2$  slides backwards relative to the waveform for  $\omega_1$ . Thus, while the points  $B_1$  and  $B_2$  of Fig. 6.62(a) both move in the positive  $z$  direction as time progresses, the spacing between them decreases continuously until, at a time  $\Delta t$ , the two points coincide as shown in Fig. 6.62(b). The variation with distance of one waveform relative to the other is then exactly the same as in Fig. 6.62(a). For an observer, the group as a whole appears to be shifted in

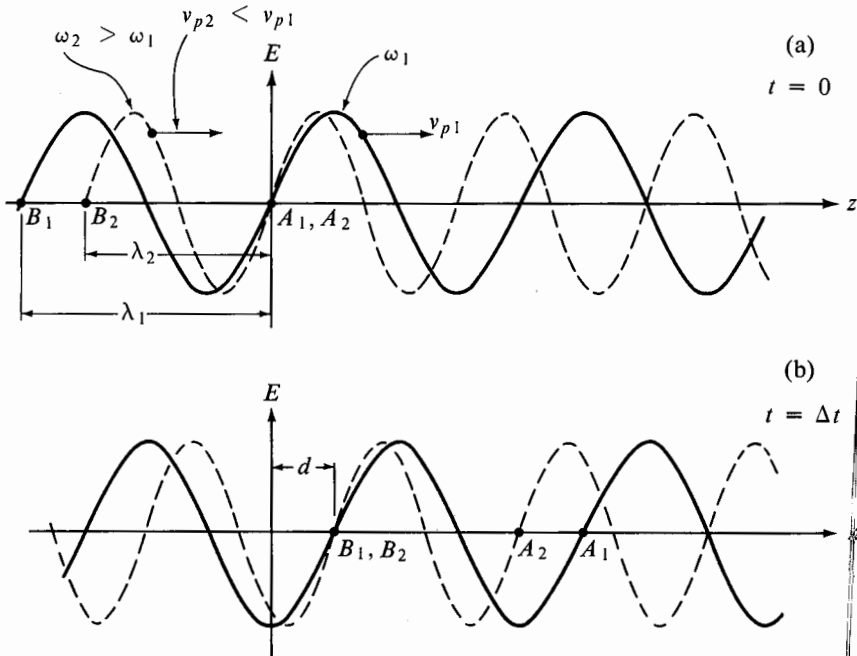


**Fig. 6.62.** For illustrating the concept of group velocity and for deriving an expression for the group velocity.

distance by  $d$  in time  $\Delta t$ . Hence the group velocity is

$$v_g = \frac{d}{\Delta t}$$

But

the distance moved by  $B_1$  in time  $\Delta t = \lambda_1 + d$

the distance moved by  $B_2$  in time  $\Delta t = \lambda_2 + d$

where  $\lambda_1$  and  $\lambda_2$  are the wavelengths corresponding to  $\omega_1$  and  $\omega_2$ . From the phase velocities associated with  $\omega_1$  and  $\omega_2$ , we then have

$$\lambda_1 + d = \frac{\omega_1}{\beta_1} \Delta t$$

$$\lambda_2 + d = \frac{\omega_2}{\beta_2} \Delta t$$

These two equations can be solved to obtain  $\Delta t$  and  $d$  as

$$\Delta t = \frac{\lambda_1 - \lambda_2}{(\omega_1/\beta_1) - (\omega_2/\beta_2)} = 2\pi \frac{\beta_2 - \beta_1}{\omega_1\beta_2 - \omega_2\beta_1}$$

$$d = \frac{(\omega_2/\beta_2)\lambda_1 - (\omega_1/\beta_1)\lambda_2}{(\omega_1/\beta_1) - (\omega_2/\beta_2)} = 2\pi \frac{\omega_2 - \omega_1}{\omega_1\beta_2 - \omega_2\beta_1}$$

so that

$$v_g = \frac{\omega_2 - \omega_1}{\beta_1 - \beta_1} \quad (6-264)$$

Between times zero and  $\Delta t$ , the distance variation of one waveform relative to the other is obviously such that the group is not identical to a displaced version of the group at  $t = 0$ . However, let us look at the waveform obtained by adding the two signals. This is given by

$$\begin{aligned} E &= E_0 \cos(\omega_1 t - \beta_1 z) + E_0 \cos(\omega_2 t - \beta_2 z) \\ &= E_0 \cos \left[ \left( \frac{\omega_1 + \omega_2}{2} t - \frac{\beta_1 + \beta_2}{2} z \right) - \left( \frac{\omega_2 - \omega_1}{2} t - \frac{\beta_2 - \beta_1}{2} z \right) \right] \\ &\quad + E_0 \cos \left[ \left( \frac{\omega_1 + \omega_2}{2} t - \frac{\beta_1 + \beta_2}{2} z \right) + \left( \frac{\omega_2 - \omega_1}{2} t - \frac{\beta_2 - \beta_1}{2} z \right) \right] \\ &= 2E_0 \cos \left( \frac{\omega_2 - \omega_1}{2} t - \frac{\beta_2 - \beta_1}{2} z \right) \cos \left( \frac{\omega_1 + \omega_2}{2} t - \frac{\beta_1 + \beta_2}{2} z \right) \end{aligned} \quad (6-265)$$

The right side of (6-265) represents a wave of frequency  $(\omega_1 + \omega_2)/2$  traveling with a phase velocity  $(\omega_1 + \omega_2)/(\beta_1 + \beta_2)$  and with its amplitude modulated in accordance with another wave of frequency  $(\omega_2 - \omega_1)/2$  traveling with a phase velocity  $(\omega_2 - \omega_1)/(\beta_2 - \beta_1)$ , as shown in Fig. 6.63. Thus,

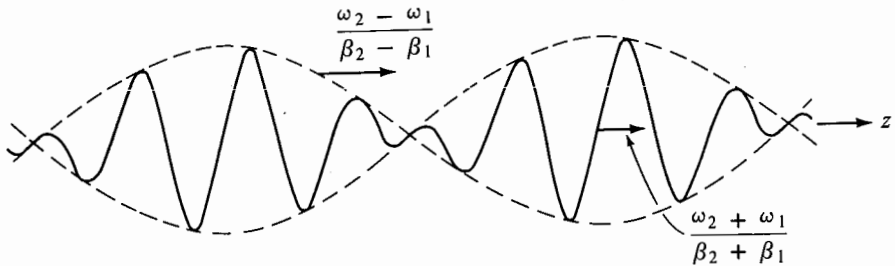


**Fig. 6.63.** For illustrating that the envelope of the superposition of two waves of frequencies  $\omega_1$  and  $\omega_2$  and phase constants  $\beta_1$  and  $\beta_2$ , respectively, moves with the group velocity  $(\omega_2 - \omega_1)/(\beta_2 - \beta_1)$ .

although the waveform for  $(\omega_1 + \omega_2)/2$  is changing in phase in accordance with the phase velocity  $(\omega_1 + \omega_2)/(\beta_1 + \beta_2)$ , its envelope is moving with the velocity  $(\omega_2 - \omega_1)/(\beta_2 - \beta_1)$ . As far as the amplitude is concerned, the entire group appears to be moving with the velocity  $(\omega_2 - \omega_1)/(\beta_2 - \beta_1)$ .

For the parallel-plate waveguide, the phase constant corresponding to  $v_{pz}$  is

$$\beta_z = \frac{\omega}{v_{pz}} = \frac{\omega}{v_p} \sqrt{1 - \left( \frac{f_c}{f} \right)^2} = \beta \sqrt{1 - \left( \frac{\omega_c}{\omega} \right)^2} \quad (6-266)$$

The variation of  $\beta_z$  with  $\omega$  is shown in Fig. 6.64. A diagram of this kind is known as the  $\omega - \beta_z$  diagram or the dispersion diagram. The phase velocity corresponding to any particular frequency is given by the slope of the line

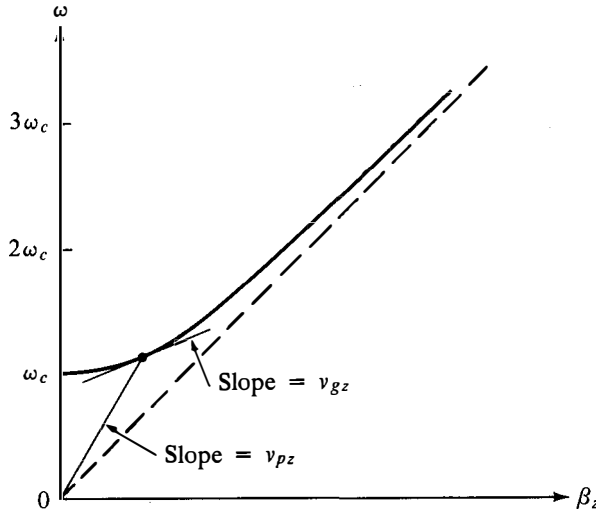


Fig. 6.64.  $\beta_z$  versus  $\omega$  for the parallel-plate waveguide.

drawn from the origin to the point on the curve corresponding to that frequency. The group velocity corresponding to any two frequencies  $\omega_1$  and  $\omega_2$  is given by the slope of the line joining the two points on the curve corresponding to those two frequencies. If we have a band of frequencies, we can find group velocities for each pair of these frequencies in this manner. We can attribute a group velocity to the entire group only if all these group velocities are equal. From Fig. 6.64, we see that this is not possible for a wide band of frequencies because of the nonlinear dependence of  $\beta_z$  upon  $\omega$ . Hence it is not meaningful to talk of a group velocity for a group of waves comprising a wide band of frequencies. If, on the other hand, the frequencies are contained in a narrow band about a predominant frequency  $\omega$ , then we can approximate the nonlinear  $\omega - \beta_z$  curve in that narrow band by a straight line having the slope equal to that of the actual curve at  $\omega$  so that it is meaningful to attribute a velocity to that group. This group velocity is given by

$$v_{gz} = \frac{d\omega}{d\beta_z} \quad (6-267)$$



For  $\beta_z$  given by (6-266),

$$\begin{aligned} \frac{d\beta_z}{d\omega} &= \beta \left[ 1 - \left( \frac{\omega_c}{\omega} \right)^2 \right]^{-1/2} \frac{\omega_c^2}{\omega^3} + \frac{d\beta}{d\omega} \left[ 1 - \left( \frac{\omega_c}{\omega} \right)^2 \right]^{1/2} \\ &= \frac{\omega_c^2}{v_p \omega^2} \left[ 1 - \left( \frac{\omega_c}{\omega} \right)^2 \right]^{-1/2} + \frac{1}{v_p} \left[ 1 - \left( \frac{\omega_c}{\omega} \right)^2 \right]^{1/2} \\ &= \frac{1}{v_p} \left[ 1 - \left( \frac{\omega_c}{\omega} \right)^2 \right]^{-1/2} \end{aligned}$$

and

$$\begin{aligned} v_{gz} &= \frac{d\omega}{d\beta_z} = v_p \sqrt{1 - \left( \frac{\omega_c}{\omega} \right)^2} \\ &= v_p \sqrt{1 - \left( \frac{f_c}{f} \right)^2} = v_p \sqrt{1 - \left( \frac{\lambda}{\lambda_c} \right)^2} < v_p \end{aligned} \tag{6-268}$$

Substituting for  $\sqrt{1 - (\lambda/\lambda_c)^2}$  in terms of  $\theta_i$ , we have

$$v_{gz} = v_p \sin \theta_i$$

Thus the group velocity is the component of  $v_p$  along the  $z$  axis. It is the distance between two constant  $z$  planes divided by the time taken by a point on the obliquely bouncing wavefront to pass from one plane to the other as shown in Fig. 6.65. This gives the physical interpretation for the group

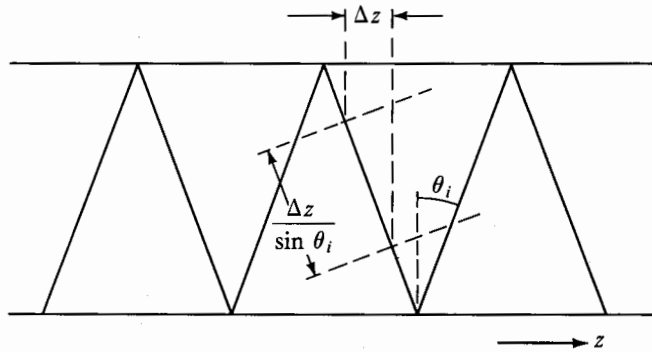


Fig. 6.65. For illustrating that the group velocity is the velocity with which energy propagates along the guide axis.

velocity as the velocity with which energy propagates along the guide axis. In fact, this physical interpretation is valid not only in this case but, in general, whenever a meaningful velocity can be attributed to the group.

Finally, we note a simple relationship between  $v_{pz}$ ,  $v_{gz}$ , and  $v_p$  as

$$v_{pz} v_{gz} = v_p^2 \tag{6-269}$$

Because the dispersion which we have discussed here is caused by the geome-

try associated with the bouncing of the waves between the walls, it is known as “geometric dispersion.” There are other types of dispersion as we will learn in later sections. The relationship (6-267) also holds for these other types of dispersion since its derivation is independent of the mechanism causing the dispersion.

### 6.13 Waves in Imperfect Dielectrics and Conductors; Attenuation and the Skin Effect

Thus far we have been concerned with wave propagation in perfect dielectric media ( $\sigma = 0$ ). In this section we will discuss wave propagation in lossy media, especially in good conductors. We restrict our discussion to sinusoidal steady state. For a medium characterized by conductivity  $\sigma$ , permittivity  $\epsilon$ , and permeability  $\mu$ , we recall that Maxwell’s curl equations are given by

$$\nabla \times \mathbf{E} = -\frac{\partial \mathbf{B}}{\partial t} = -\mu \frac{\partial \mathbf{H}}{\partial t}$$

$$\nabla \times \mathbf{H} = \mathbf{J} + \frac{\partial \mathbf{D}}{\partial t} = \sigma \mathbf{E} + \epsilon \frac{\partial \mathbf{E}}{\partial t}$$

For sinusoidally time-varying fields, we have

$$\nabla \times \bar{\mathbf{E}} = -j\omega\mu\bar{\mathbf{H}} \quad (6-270a)$$

$$\nabla \times \bar{\mathbf{H}} = \sigma\bar{\mathbf{E}} + j\omega\epsilon\bar{\mathbf{E}} = (\sigma + j\omega\epsilon)\bar{\mathbf{E}} \quad (6-270b)$$

Taking the curl of (6-270a) on both sides and using the vector identity for  $\nabla \times \nabla \times \bar{\mathbf{E}}$ , we obtain

$$\nabla(\nabla \cdot \bar{\mathbf{E}}) - \nabla^2 \bar{\mathbf{E}} = -j\omega\mu\nabla \times \bar{\mathbf{H}} \quad (6-271)$$

But from (6-270b), we have

$$\nabla \cdot \bar{\mathbf{E}} = \frac{1}{\sigma + j\omega\epsilon} \nabla \cdot \nabla \times \bar{\mathbf{H}} = 0 \quad (6-272)$$

Substituting (6-272) and (6-270b) into (6-271), we obtain the vector wave equation for the electric field as

$$\nabla^2 \bar{\mathbf{E}} = j\omega\mu(\sigma + j\omega\epsilon)\bar{\mathbf{E}} \quad (6-273)$$

Defining a complex quantity  $\bar{\gamma}$  as

$$\bar{\gamma}^2 = j\omega\mu(\sigma + j\omega\epsilon) \quad (6-274)$$

we write (6-273) as

$$\nabla^2 \bar{\mathbf{E}} = \bar{\gamma}^2 \bar{\mathbf{E}} \quad (6-275)$$

Assuming that the electric field has only an  $x$  component, which is dependent on the  $z$  coordinate only, that is,

$$\bar{\mathbf{E}} = \bar{E}_x(z)\mathbf{i}_x$$

Eq. (6-275) reduces to

$$\frac{\partial^2 \bar{E}_x}{\partial z^2} = \bar{\gamma}^2 \bar{E}_x \quad (6-276)$$

The solution for (6-276) is given by

$$\bar{E}_x(z) = \bar{A}e^{-\bar{\gamma}z} + \bar{B}e^{\bar{\gamma}z} \quad (6-277)$$

where  $\bar{A}$  and  $\bar{B}$  are arbitrary constants. Since  $\bar{\gamma}$  is a complex number, we can write

$$\bar{\gamma} = \alpha + j\beta \quad (6-278)$$

where  $\alpha$  and  $\beta$  are the real and imaginary parts of  $\bar{\gamma}$ , respectively. Substituting (6-278) into (6-277) and also writing  $\bar{A} = Ae^{j\theta}$  and  $\bar{B} = Be^{j\phi}$ , we have

$$\bar{E}_x(z) = Ae^{-\alpha z} e^{-j\beta z} e^{j\theta} + Be^{\alpha z} e^{j\beta z} e^{j\phi} \quad (6-279)$$

and

$$\begin{aligned} E_x(z, t) &= \Re e[\bar{E}_x(z)e^{j\omega t}] \\ &= Ae^{-\alpha z} \cos(\omega t - \beta z + \theta) + Be^{\alpha z} \cos(\omega t + \beta z + \phi) \end{aligned} \quad (6-280)$$

Ignoring the factors  $e^{-\alpha z}$  and  $e^{\alpha z}$  on the right side of (6-280) for a moment, we note that the first and second terms represent the (+) and (-) waves, respectively. The factor  $e^{-\alpha z}$  decreases in value as  $z$  increases, thereby resulting in attenuation of the (+) wave as it progresses in the positive  $z$  direction. Similarly, the factor  $e^{\alpha z}$  decreases in value as  $z$  decreases, thereby resulting in the attenuation of the (-) wave as it progresses in the negative  $z$  direction. The factor  $\alpha$  is therefore known as the "attenuation constant." The units of  $\alpha$  are nepers per meter. The word "neper" is a variation of the spelling of the name Napier. The factor  $\beta$  is, of course, the "phase constant" associated with the traveling waves. Since  $\alpha$  and  $\beta$  together characterize the propagation of the wave, the factor  $\bar{\gamma}$  is known as the "propagation constant." Since we have identified the two terms on the right side of (6-277) as representing (+) and (-) waves, respectively, we can replace  $\bar{A}$  and  $\bar{B}$  by  $\bar{E}_x^+$  and  $\bar{E}_x^-$ , respectively, and write

$$\bar{E}_x(z) = \bar{E}_x^+ e^{-\bar{\gamma}z} + \bar{E}_x^- e^{\bar{\gamma}z} \quad (6-281a)$$

The corresponding solution for  $\bar{\mathbf{H}}$  contains a  $y$  component only which can be obtained by substituting (6-281a) into (6-270a). Thus

$$\bar{H}_y(z) = \frac{1}{\bar{\eta}} (\bar{E}_x^+ e^{-\bar{\gamma}z} - \bar{E}_x^- e^{\bar{\gamma}z}) \quad (6-281b)$$

where

$$\bar{\eta} = \frac{j\omega\mu}{\bar{\gamma}} = \sqrt{\frac{j\omega\mu}{\sigma + j\omega\epsilon}} \quad (6-282)$$

is the intrinsic impedance of the medium, which is now complex. Equations (6-281a) and (6-281b) together represent uniform plane-wave solution for the lossy medium since, in the planes of constant phase, the amplitudes of the fields are uniform although there is attenuation from one plane to another.

To obtain the expressions for  $\alpha$  and  $\beta$ , we substitute (6-278) into (6-274) and equate the real and imaginary parts on both sides of the resulting equation. Thus we have

$$\alpha^2 - \beta^2 = -\omega^2 \mu \epsilon \quad \text{and} \quad 2\alpha\beta = \omega \mu \sigma$$

Solving these two equations for  $\alpha$ , we get

$$\alpha^2 = \frac{\omega^2 \mu \epsilon}{2} \left( \pm \sqrt{1 + \frac{\sigma^2}{\omega^2 \epsilon^2}} - 1 \right)$$

The minus sign associated with the square root in the above equation makes  $\alpha$  imaginary. Hence we ignore it to obtain

$$\alpha = \omega \left[ \frac{\mu \epsilon}{2} \left( \sqrt{1 + \frac{\sigma^2}{\omega^2 \epsilon^2}} - 1 \right) \right]^{1/2} \quad (6-283)$$

and

$$\beta = \sqrt{\alpha^2 + \omega^2 \mu \epsilon} = \omega \left[ \frac{\mu \epsilon}{2} \left( \sqrt{1 + \frac{\sigma^2}{\omega^2 \epsilon^2}} + 1 \right) \right]^{1/2} \quad (6-284)$$

Note that if  $\sigma = 0$ , Eqs. (6-283), (6-284), and (6-282) give  $\alpha = 0$ ,  $\beta = \omega \sqrt{\mu \epsilon}$ , and  $\bar{\eta} = \sqrt{\mu/\epsilon}$ , which correspond to a perfect dielectric medium. Since  $\beta$  given by (6-284) is not a linear function of  $\omega$ , the wave propagation in the lossy medium is characterized by dispersion. This type of dispersion is known as “conductive” dispersion since it is due to the conductivity of the medium.

The expressions for  $\alpha$  and  $\beta$  given by (6-283) and (6-284), respectively, are very complicated. They can, however, be reduced to simple expressions for two special cases. We now consider these two special cases:

(a) *Good dielectrics:*  $\sigma \ll \omega \epsilon$ ; that is, conduction current is very small compared to displacement current. We can then write

$$\sqrt{1 + \left( \frac{\sigma}{\omega \epsilon} \right)^2} \approx 1 + \frac{\sigma^2}{2\omega^2 \epsilon^2} - \frac{\sigma^4}{8\omega^4 \epsilon^4}$$

The simplified expressions for  $\alpha$ ,  $\beta$ , and  $\bar{\eta}$  are

$$\alpha \approx \omega \sqrt{\frac{\mu \epsilon}{2} \left( \frac{\sigma^2}{2\omega^2 \epsilon^2} - \frac{\sigma^4}{8\omega^4 \epsilon^4} \right)} \approx \frac{1}{2} \sigma \sqrt{\frac{\mu}{\epsilon}} \left( 1 - \frac{\sigma^2}{8\omega^2 \epsilon^2} \right) \quad (6-285a)$$

$$\beta \approx \omega \sqrt{\frac{\mu \epsilon}{2} \left( 2 + \frac{\sigma^2}{2\omega^2 \epsilon^2} \right)} \approx \omega \sqrt{\mu \epsilon} \left( 1 + \frac{\sigma^2}{8\omega^2 \epsilon^2} \right) \quad (6-285b)$$

$$\begin{aligned} \bar{\eta} &= \sqrt{\frac{j\omega \mu}{j\omega \epsilon (1 + \sigma/j\omega \epsilon)}} = \sqrt{\frac{\mu}{\epsilon}} \left( 1 - j \frac{\sigma}{\omega \epsilon} \right)^{-1/2} \\ &\approx \sqrt{\frac{\mu}{\epsilon}} \left[ \left( 1 - \frac{3}{8} \frac{\sigma^2}{\omega^2 \epsilon^2} \right) + j \frac{\sigma}{2\omega \epsilon} \right] \end{aligned} \quad (6-285c)$$

where we have retained all terms up to and including the second power in  $\sigma/\omega \epsilon$ . Although the first-term approximation of the attenuation constant given by (6-285a) seems to be independent of frequency,  $\sigma$  and  $\epsilon$  are, in general, functions of frequency as stated in Section 5.10. In fact, the quantity  $\sigma/\omega \epsilon$  is very nearly constant for several dielectrics over wide frequency ranges.

(b) *Good conductors:*  $\sigma \gg \omega\epsilon$ ; that is, conduction current is very large compared to displacement current. We can then write

$$\sqrt{1 + \left(\frac{\sigma}{\omega\epsilon}\right)^2} \approx \frac{\sigma}{\omega\epsilon}$$

The simplified expressions for  $\alpha$ ,  $\beta$ , and  $\bar{\eta}$  are

$$\alpha \approx \omega \sqrt{\frac{\mu\epsilon}{2} \left(\frac{\sigma}{\omega\epsilon} - 1\right)} \approx \omega \sqrt{\frac{\mu\sigma}{2\omega}} = \sqrt{\frac{\omega\mu\sigma}{2}} = \sqrt{\pi f \mu \sigma} \quad (6-286a)$$

$$\beta \approx \omega \sqrt{\frac{\mu\epsilon}{2} \left(\frac{\sigma}{\omega\epsilon} + 1\right)} \approx \omega \sqrt{\frac{\mu\sigma}{2\omega}} = \sqrt{\frac{\omega\mu\sigma}{2}} = \sqrt{\pi f \mu \sigma} \quad (6-286b)$$

$$\bar{\eta} \approx \sqrt{\frac{j\omega\mu}{\sigma}} = (1 + j) \sqrt{\frac{\omega\mu}{2\sigma}} = (1 + j) \sqrt{\frac{\pi f \mu}{\sigma}} \quad (6-286c)$$

**EXAMPLE 6-30.** For uniform plane waves in sea water ( $\sigma = 4$  mhos/m,  $\epsilon = 80\epsilon_0$ ,  $\mu = \mu_0$ ), find  $\alpha$ ,  $\beta$ ,  $\bar{\eta}$ , and  $\lambda$  for two frequencies: (a) 10,000 MHz and (b) 25 kHz.

The frequency at which  $\sigma = \omega\epsilon$  is equal to  $4/(2\pi \times 80 \times 10^{-9}/36\pi)$  or 900 MHz. Hence, for 10,000 MHz,  $\sigma \ll \omega\epsilon$ , sea water is a good dielectric and for 25 kHz,  $\sigma \gg \omega\epsilon$ , sea water is a good conductor.

Thus, for 10,000 MHz, we have

$$\begin{aligned} \alpha &\approx \frac{1}{2} \sigma \sqrt{\frac{\mu}{\epsilon}} \left(1 - \frac{\sigma^2}{8\omega^2\epsilon^2}\right) \approx \frac{1}{2} \sigma \sqrt{\frac{\mu}{\epsilon}} = \frac{1}{2} \times 4 \times \sqrt{\frac{\mu_0}{80\epsilon_0}} = 2 \times \frac{377}{\sqrt{80}} \\ &= 84.3 \text{ nepers/m} \end{aligned}$$

$$\begin{aligned} \beta &\approx \omega \sqrt{\mu\epsilon} \left(1 + \frac{\sigma^2}{8\omega^2\epsilon^2}\right) \approx \omega \sqrt{\mu\epsilon} = \frac{2\pi \times 10 \times 10^9 \times \sqrt{80}}{3 \times 10^8} \\ &= 1873 \text{ rad/m} \end{aligned}$$

$$\bar{\eta} \approx \sqrt{\frac{\mu}{\epsilon}} \left[ \left(1 - \frac{3}{8} \frac{\sigma^2}{\omega^2\epsilon^2}\right) + j \frac{\sigma}{2\omega\epsilon} \right] \approx \sqrt{\frac{\mu}{\epsilon}} = \frac{377}{\sqrt{80}} = 42.15 \text{ ohms}$$

$$\lambda = \frac{2\pi}{\beta} = \frac{2\pi}{1873} = 3.353 \times 10^{-3} \text{ m} = 3.353 \text{ mm}$$

as compared to 30 mm in free space.

For 25 kHz, we have

$$\alpha \approx \sqrt{\pi f \mu \sigma} = \sqrt{\pi \times 25 \times 10^3 \times 4\pi \times 10^{-7} \times 4} = 0.2\pi \text{ nepers/m}$$

$$\beta \approx \sqrt{\pi f \mu \sigma} = \alpha = 0.2\pi \text{ rad/m}$$

$$\begin{aligned} \bar{\eta} &\approx (1 + j) \sqrt{\frac{\pi f \mu}{\sigma}} = (1 + j) \sqrt{\frac{\pi \times 25 \times 10^3 \times 4\pi \times 10^{-7}}{4}} \\ &= 0.05\pi(1 + j) \text{ ohms} \end{aligned}$$

$$\lambda = \frac{2\pi}{\beta} = \frac{2\pi}{0.2\pi} = 10 \text{ m}$$

as compared to 12 km in free space.



the conductivity is  $5.8 \times 10^7$  mhos/m so that the skin depth is given by

$$\delta_{\text{copper}} = \frac{1}{\sqrt{\pi f \times 4\pi \times 10^{-7} \times 5.8 \times 10^7}} = \frac{0.066}{\sqrt{f}} \text{ m} \quad (6-289)$$

For a frequency of  $10^6$  Hz, the skin depth of copper is 0.066 mm. Thus the fields are attenuated to  $e^{-1}$  times their values at the surface in a distance of 0.066 mm even at the low frequency of 1 MHz. In a distance of one wavelength in the conductor, the attenuation is equal to  $e^{\alpha\lambda} = e^{\alpha(2\pi/\beta)} = e^{2\pi}$  nepers/m since  $\beta$  is equal to  $\alpha$ . In terms of decibels, this attenuation is  $20 \log_{10} e^{2\pi} = 20 \log_e e^{2\pi}/\log_e 10 = 40\pi/2.3026 = 54.5$ . In view of the rapid attenuation of the fields inside the conductor, the fields and the current given by density  $\mathbf{J} = \sigma\mathbf{E}$  are concentrated close to the surface of the conductor. This phenomenon is known as the "skin effect."

Because of the skin effect, a conductor of finite thickness equal to a few skin depths can for all practical purposes be considered as a conductor of infinite depth. Hence, if a wave is incident upon it from one side, its effect is not felt on the other side, thereby "shielding" one side of the conductor from the other. Furthermore, since there is no reflected wave inside the conductor, we can compute the power flow into the conductor by surface integration of the Poynting vector corresponding to  $\bar{E}_x$  and  $\bar{H}_y$  given by (6-287a) and (6-287b). Thus, noting that

$$\bar{E}_x(0) = \bar{E}_{x_0} \quad \text{and} \quad \bar{H}_y(0) = \frac{\bar{E}_{x_0}}{\bar{\eta}}$$

we obtain the complex Poynting vector at the conductor surface as

$$\begin{aligned} \bar{\mathbf{P}} &= \frac{1}{2} [\bar{E}_x(0)\mathbf{i}_x \times \bar{H}_y^*(0)\mathbf{i}_y] = \frac{1}{2} \bar{E}_{x_0} \frac{\bar{E}_{x_0}^*}{\bar{\eta}^*} \mathbf{i}_z \\ &= \frac{1}{2} \frac{|\bar{E}_{x_0}|^2}{\bar{\eta}^*} \mathbf{i}_z = \frac{1}{2} \frac{|\bar{H}_y(0)|^2 |\bar{\eta}|^2}{\bar{\eta}^*} \mathbf{i}_z \\ &= \frac{1}{2} \bar{\eta} |\bar{H}_y(0)|^2 \mathbf{i}_z \end{aligned}$$

For a surface  $S$  of length  $l$  in the  $x$  direction and width  $w$  in the  $y$  direction, the complex power flow into the conductor is

$$\bar{P}_{\text{in}} = \int_S \bar{\mathbf{P}} \cdot d\mathbf{S} = \bar{P}_z(lw) = \frac{1}{2} lw \bar{\eta} |\bar{H}_y(0)|^2 \quad (6-290)$$

However, applying Maxwell's curl equation for  $\bar{\mathbf{H}}$  in integral form to the closed path  $abcd$  shown in Fig. 6.66, we have

$$\oint_{abcd} \bar{\mathbf{H}} \cdot d\mathbf{l} = \int_{\text{area } abcd} (\sigma \bar{\mathbf{E}} + j\omega\epsilon \bar{\mathbf{E}}) \cdot d\mathbf{S} \quad (6-291)$$

The left side of (6-291) has a contribution from  $ab$  only, since along  $bc$  and  $da$ ,  $\bar{\mathbf{H}}$  is perpendicular to the path and along  $cd$ ,  $\bar{\mathbf{H}}$  is zero. Along  $ab$ ,  $\bar{\mathbf{H}} = \bar{H}_y(0)\mathbf{i}_y$ , so that the integral is  $w\bar{H}_y(0)$ . On the right side of (6-291), the

second term in the integrand can be ignored since  $\sigma \gg \omega\epsilon$ . Hence the integral is simply the conduction current flowing in the conductor. Denoting this by  $\bar{I}_x$ , we have

$$w\bar{H}_y(0) = \bar{I}_x \quad \text{or} \quad \bar{H}_y(0) = \frac{\bar{I}_x}{w} \quad (6-292)$$

Substituting (6-292) into (6-290), we get

$$\bar{P}_{in} = \frac{1}{2}\bar{\eta}\frac{l}{w}|\bar{I}_x|^2 \quad (6-293)$$

Substituting for  $\bar{\eta}$  in (6-293) from (6-286c), we have

$$\begin{aligned} \bar{P}_{in} &= \frac{1}{2}(1+j)\sqrt{\frac{\pi f\mu}{\sigma}}\frac{l}{w}|\bar{I}_x|^2 \\ &= \frac{1}{2}(1+j)\frac{l}{\sigma\delta w}|\bar{I}_x|^2 \\ &= \frac{1}{2}\frac{l}{\sigma\delta w}|\bar{I}_x|^2 + j\frac{1}{2}\frac{l}{\sigma\delta w}|\bar{I}_x|^2 \end{aligned} \quad (6-294)$$

From (5-206), the real part on the right side of (6-294) is the time-average power dissipated in the conductor. It is also exactly the result that would be obtained by computing the time-average power dissipated under quasistatic conditions in a conductor of length  $l$ , width  $w$ , thickness  $\delta$ , and conductivity  $\sigma$  if the current  $\bar{I}_x$  were distributed uniformly over the cross section of the conductor. This gives an alternative significance for the skin depth  $\delta$ . We will denote the resistance  $l/\sigma\delta w$  by the symbol  $R_s$ . From (5-206), the imaginary part on the right side of (6-294) is  $2\omega$  times the time-average magnetic stored energy in the conductor since the time-average electric stored energy is negligible in view of  $\sigma \gg \omega\epsilon$ . In fact, a volume integration of  $\frac{1}{4}\mu|\bar{H}_y|^2$  gives exactly the imaginary part of the right side of (6-294) divided by  $2\omega$ , that is,

$$\frac{1}{4}\frac{l}{\omega\sigma\delta w}|\bar{I}_x|^2$$

This energy is the same as the time-average magnetic energy stored under quasistatic conditions in an inductor of value  $l/\omega\sigma\delta w$  if the current  $|\bar{I}_x|$  were flowing in it. This inductance is the internal inductance of the conductor which we denote as  $L_i$ . Thus the impedance offered by a portion of the conductor of length  $l$  and width  $w$  to the current flowing in it is given by

$$\bar{Z}_i = R_s + j\omega L_i = \frac{l}{\sigma\delta w} + j\frac{l}{\sigma\delta w} \quad (6-295)$$

This impedance is known as the "internal impedance." We may emphasize that the formulas for skin depth and internal impedance developed here are strictly valid for plane conductors only. However, if the radius of a cylindrical conductor is very large compared to the skin depth for the material of the conductor, these formulas can be used with negligible error.



**EXAMPLE 6-31.** Figure 6.67 shows the cross section of a hollow cylindrical conductor of radius  $a$  and thickness  $d \ll a$ , in which current flows axially. It is desired to find the approximate expression for the internal impedance of the conductor per unit length in the axial direction if the skin depth  $\delta$  for the material is  $\ll d$ .

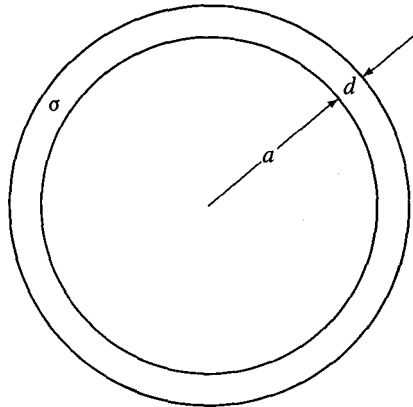


**Fig. 6.67.** Cross section of a hollow cylindrical conductor of thickness small compared to its radius.

Since  $d$  is  $\ll a$ , we can assume that the required internal impedance is approximately equal to the internal impedance of a plane conductor of appropriate width. If  $d$  is not  $\ll a$ , we cannot use this approximation and the problem must be solved in cylindrical coordinates. If  $\delta$  is  $\ll d$ , it is actually immaterial whether the conductor is hollow or not since the current does not penetrate much below the surface and hence the depth can be assumed to be infinity for the purpose of computing the internal impedance. Thus the required internal impedance is approximately the same as the internal impedance of a plane conductor of infinite depth and width equal to  $2\pi a$ . From (6-295), this is equal to  $(1 + j)/2\pi a \sigma \delta$  per unit length in the axial direction. ■

In Sections 6.8, 6.9, and 6.10, we considered transmission-line waves between perfect conductors with the medium between them as a perfect dielectric. These waves are exactly TEM since the perfect conductors ( $\sigma = \infty$ ) do not require any axial electric field to maintain a current flow along them. If the dielectric is now made imperfect, the waves are still exactly TEM except that attenuation takes place as they propagate down the line. In fact, the transmission-line equivalent circuit in Section 6.7 was derived by considering the dielectric to be imperfect. On the other hand, if the conductors are imperfect, the finite conductivity requires an axial electric field for the current to flow along the conductors. This axial electric field in the conductors is accompanied by an axial electric field in the dielectric since the boundary condition at the interface between the dielectric and the conductor requires that the tangential electric field be continuous. Thus the electric field between

the conductors is no longer entirely transverse and hence the waves are no longer exactly TEM waves. However, if the conductors are good conductors, as is the case in practice, the axial electric field is very small compared to the transverse electric field and the waves between the conductors are almost TEM waves. In the conductors, the axial component of the electric field dominates so that power flow is almost normal to the dielectric-conductor interface. The situation as compared to the perfect conductor case is illustrated in Fig. 6.68. Thus, as the wave propagates, it gets attenuated

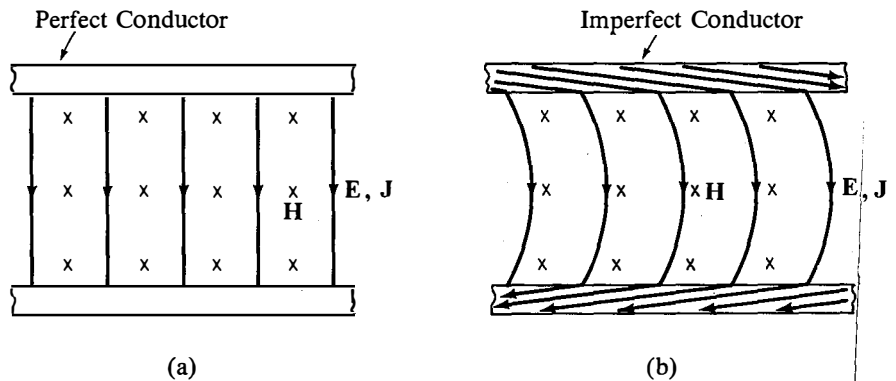


Fig. 6.68. Fields for a transmission line employing (a) perfect conductors, and (b) imperfect conductors.

partly due to power dissipation in the lossy dielectric and partly due to energy leakage into the conductors which is dissipated in the conductors. The power dissipation in the lossy dielectric is accounted for in the distributed equivalent circuit by the conductance in parallel with the capacitor. The power dissipation in the conductors can be accounted for by introducing into the series branch an impedance which is offered by the conductors to the current flow. Since the current flow is almost parallel to the conductor surface, this impedance is approximately the same as the internal impedance given by (6-295) per unit length. Thus we obtain the distributed equivalent circuit for a lossy transmission line as shown in Fig. 6.69, where the factor 2 takes into account the two conductors and

$\mathcal{R}_s$  = resistance per unit length of the conductor due to skin effect,  
 $\mathcal{L}_i$  = internal inductance per unit length of the conductor due to skin effect,

$\mathcal{G}$ ,  $\mathcal{L}$ ,  $\mathcal{C}$  = conductance, inductance, and capacitance per unit length if the conductors were perfect.

The circuit of Fig. 6.69 forms the basis for lossy transmission-line theory which follows along lines similar to lossless transmission-line theory but is characterized by attenuation and dispersion.

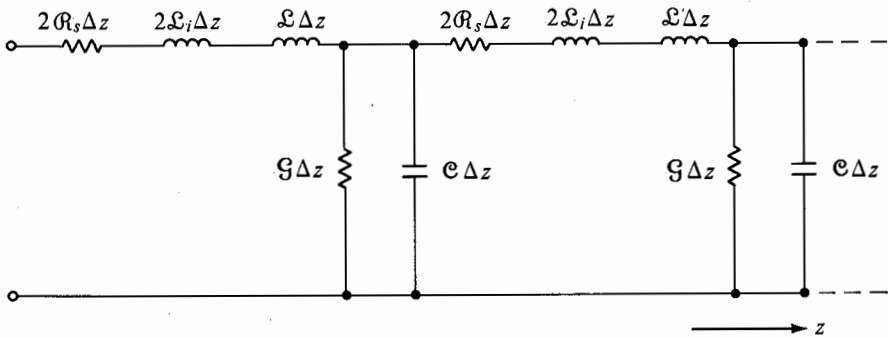


Fig. 6.69. Distributed equivalent circuit for a lossy transmission line.

The concept of internal impedance is useful not only for a lossy transmission line but for any system involving waves between imperfect but good conductors, since it permits the estimation of the power loss in the conductors from the solutions for the fields in the corresponding lossless case. This is because, for good conductors, it is reasonable to assume that the fields between the conductors differ very little from the lossless case so that the current flowing in the conductors can be obtained from the tangential magnetic fields. Then, since these currents flow very nearly parallel to the conductor surface, power loss can be computed by using  $\frac{1}{2} |\vec{I}|^2 R_s$ . We will use this technique in the following section for deriving the  $Q$  factor for a parallel-plate resonator employing imperfect but good conductors.

#### 6.14 Resonators; Laser Oscillation

In Section 6.10 we discussed complete standing waves resulting from the superposition of (+) and (-) waves of equal magnitudes. For a short-circuited line (or a semiinfinite dielectric medium terminated by a perfect conductor), we found that the line voltage (or the electric field) is zero at distances of integral multiples of  $\lambda/2$  from the short circuit (or the perfect conductor). Hence, if we short circuit the line (or place a perfect conductor) at these points, there will be no effect on the voltage and current (or fields) at any other point. Alternatively, if we have a line of length  $l$  which is short circuited at both ends (or a dielectric medium between two parallel, perfectly conducting plates) and containing some stored energy, this energy must exist in the form of complete standing waves having wavelengths such that  $l = n\lambda_n/2$ , that is,  $\lambda_n = 2l/n$ , or  $\beta_n = 2\pi/\lambda_n = n\pi/l$ , where  $n = 1, 2, 3, \dots$  as discussed in Example 6-21. The corresponding frequencies are given by  $\omega_n = n\pi v_p/l$ .

Thus let us consider a system of two infinite, parallel, perfectly conducting plates as shown in Fig. 6.70, between which the medium is a perfect

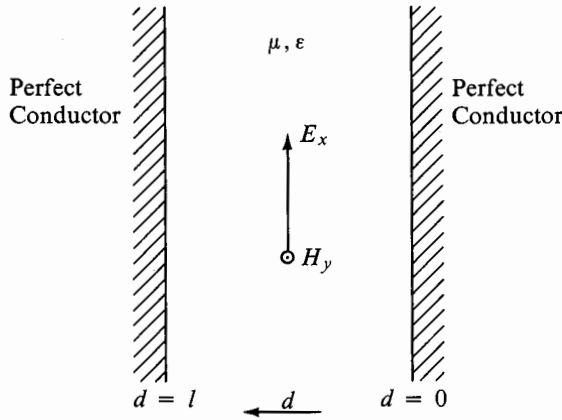


Fig. 6.70. Parallel-plate resonator consisting of two infinite-plane, perfectly conducting plates.

dielectric and energy is stored in the form of standing waves having field components  $E_x$  and  $H_y$ . From (6-231a) and (6-231b), the expressions for these fields that satisfy the boundary condition at  $d = 0$  can be written as

$$E_x(d, t) = -2E_0 \sin \beta d \sin \omega t \quad (6-296a)$$

$$H_y(d, t) = 2 \frac{E_0}{\eta} \cos \beta d \cos \omega t \quad (6-296b)$$

where  $E_0$  is a constant, the value of which we need not know, and  $\eta = \sqrt{\mu/\epsilon}$ . Substituting  $\beta = n\pi/l$  and  $\omega = n\pi v_p/l = n\pi/l\sqrt{\mu\epsilon}$  in (6-296a) and (6-296b), we obtain

$$E_x(d, t) = -2E_0 \sin \frac{n\pi d}{l} \sin \frac{n\pi t}{l\sqrt{\mu\epsilon}} \quad (6-297a)$$

$$H_y(d, t) = 2\sqrt{\frac{\epsilon}{\mu}} E_0 \cos \frac{n\pi d}{l} \cos \frac{n\pi t}{l\sqrt{\mu\epsilon}} \quad (6-297b)$$

which satisfy the boundary condition at  $d = l$  for all  $t$ . The instantaneous electric and magnetic stored energy densities associated with these fields are

$$w_e(d, t) = \frac{1}{2} \epsilon E_x^2 = 2\epsilon E_0^2 \sin^2 \frac{n\pi d}{l} \sin^2 \frac{n\pi t}{l\sqrt{\mu\epsilon}} \quad (6-298a)$$

$$w_m(d, t) = \frac{1}{2} \mu H_y^2 = 2\epsilon E_0^2 \cos^2 \frac{n\pi d}{l} \cos^2 \frac{n\pi t}{l\sqrt{\mu\epsilon}} \quad (6-298b)$$

Let us for simplicity consider the case  $n = 1$ , that is, for which the standing waves have one-half wavelength between the plates, and sketch the energy densities as functions of  $d$  for different values of  $t$ , as shown in Fig. 6.71. We note from Fig. 6.71 and from Eqs. (6-298a) and (6-298b) that the

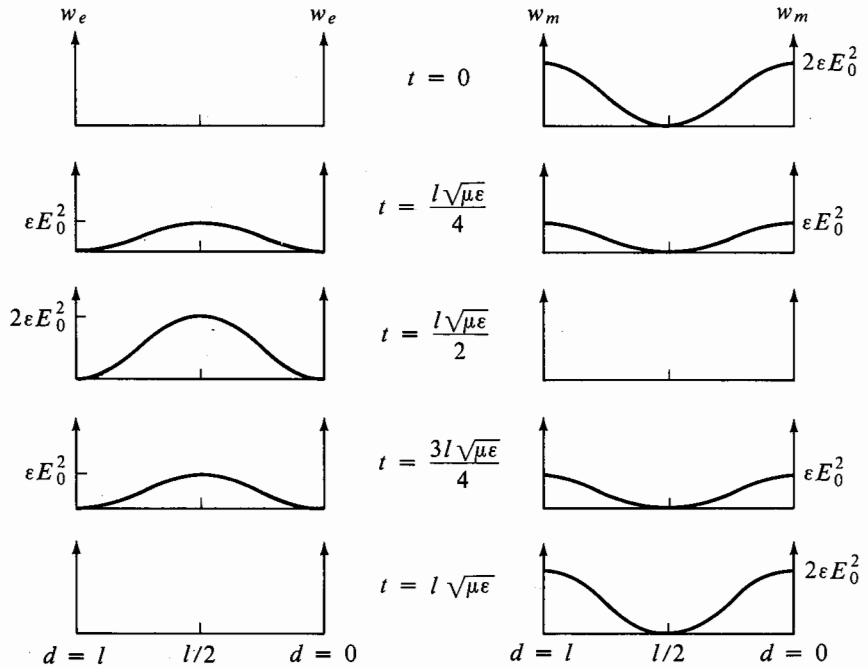


Fig. 6.71. Electric and magnetic energy densities versus  $d$  for various values of  $t$  for the parallel-plate resonator of Fig. 6.70.

stored energy density at all points is entirely magnetic at certain times ( $t = 0, l\sqrt{\mu\epsilon}, \dots$ ) and entirely electric at certain other times ( $t = l\sqrt{\mu\epsilon}/2, 3l\sqrt{\mu\epsilon}/2, \dots$ ) with the bulk of the magnetic energy stored close to the conducting plates and the bulk of the electric energy stored close to half way between the plates for all times. The total energy density in the two fields from  $d = 0$  to  $d = l$  must be constant with respect to time. To show that this is indeed true, we write

$$\begin{aligned}
 w(t) &= \int_{d=0}^l w_e(d, t) dd + \int_{d=0}^l w_m(d, t) dd \\
 &= \int_{d=0}^l 2\epsilon E_0^2 \sin^2 \frac{\pi d}{l} \sin^2 \frac{\pi t}{l\sqrt{\mu\epsilon}} dd \\
 &\quad + \int_{d=0}^l 2\epsilon E_0^2 \cos^2 \frac{\pi d}{l} \cos^2 \frac{\pi t}{l\sqrt{\mu\epsilon}} dd \\
 &= 2\epsilon E_0^2 \frac{l}{2} \left( \sin^2 \frac{\pi t}{l\sqrt{\mu\epsilon}} + \cos^2 \frac{\pi t}{l\sqrt{\mu\epsilon}} \right) = \epsilon_0 E_0^2 l
 \end{aligned}
 \tag{6-299}$$

The same result holds for any value of  $n$ . This process of exchange of energy stored between the plates from one field to the other is the phenomenon of resonance. The parallel-plate structure itself is known as a resonator, the

distributed counterpart of a lumped parameter resonant circuit. The frequencies  $f_n = n/2l\sqrt{\mu\epsilon}$  are the resonant frequencies or the natural frequencies of oscillation of the parallel-plate resonator.

The same concept can be extended to waveguides, discussed in Section 6.12. For example, by superimposing two  $TE_{m,0}$  waves of equal amplitudes propagating in positive and negative  $z$  directions in a parallel-plate waveguide, we can obtain complete standing  $TE_{m,0}$  waves in the guide, having nodes (zeros) of  $E_y$  at intervals of integer multiples of  $\lambda_g/2$  in  $z$ . By placing perfect conductors in these planes, we do not alter the fields in any other plane. Conversely, by placing perfect conductors in two transverse planes of a parallel-plate waveguide, separated by a distance  $d$ , we create a resonator which supports standing waves of guide wavelengths  $\lambda_{gn} = 2d/l$ , where  $l = 1, 2, 3, \dots$ . The corresponding modes are designated as  $TE_{m,0,l}$  modes where  $l$  stands for the number of half-wavelengths in the  $z$  direction. Proceeding in this manner to rectangular waveguides leads to resonators which are enclosed by perfect conductors on all sides. These are known as cavity resonators although the term "cavity" is also used for partially enclosed resonators. We will, however, not pursue these ideas any further, but consider the effect of conductor losses.

If the conductors of a resonator are imperfect, some of the energy is dissipated in them as it oscillates from one field to the other. We then associate a  $Q$  or "quality factor" to the resonator. The quality factor is defined as

$$\begin{aligned} Q &= 2\pi \frac{\text{energy stored}}{\text{energy dissipated per cycle}} \\ &= 2\pi \frac{\text{energy stored}}{\text{energy dissipated per second/number of cycles per second}} \quad (6-300) \\ &= 2\pi f \frac{\text{energy stored}}{\text{time-average power dissipated}} \end{aligned}$$

If the conductors are good conductors, the losses are small. The stored energy and power dissipated are then computed by assuming that the fields in the resonator are the same as in the lossless case, that is, perfect conductor case. We will use this technique to find the  $Q$  of a parallel-plate resonator in the following example.

**EXAMPLE 6-32.** For the parallel-plate resonator of Fig. 6.70, it is desired to find the  $Q$ , assuming that the plates are made up of imperfect conductors of conductivity  $\sigma$  and having thickness of several skin depths for the frequencies of interest.

From (6-299), the energy stored in the resonator per unit area of the plates is given by

$$w \approx \epsilon E_0^2 l \quad (6-301)$$

To find the time-average power dissipated, we note that the current flowing in the conductor per unit width in the  $y$  direction is equal to the tangential magnetic field at the surface of the conductor in accordance with (6-292), since the thickness of the conductor is several skin depths. Thus, for the conductor at  $d = 0$ ,

$$I_x = H_y(0) = 2\sqrt{\frac{\epsilon}{\mu}} E_0 \cos \frac{n\pi}{l\sqrt{\mu\epsilon}} t$$

or

$$\bar{I}_x = 2\sqrt{\frac{\epsilon}{\mu}} E_0$$

From (6-295), the resistance offered by the conductor per unit length in the  $x$  direction and unit width in the  $y$  direction is

$$R_s = \frac{1}{\sigma\delta} = \sqrt{\frac{\pi f \mu}{\sigma}}$$

where  $\delta$  is the skin depth for the frequency of interest. Thus the time-average power dissipated in the conductor per unit surface area is

$$P_d = \frac{1}{2} |\bar{I}_x|^2 R_s = 2\frac{\epsilon}{\mu} E_0^2 \sqrt{\frac{\pi f \mu}{\sigma}} = 2\epsilon E_0^2 \sqrt{\frac{\pi f}{\mu\sigma}} \quad (6-302)$$

Similarly, the time-average power dissipated in the conductor at  $d = l$  can be found to be the same as given by (6-302). Thus, from (6-300), (6-301), and (6-302), we have

$$Q = 2\pi f \frac{\epsilon E_0^2 l}{4\epsilon E_0^2 \sqrt{\pi f / \mu\sigma}} = \frac{l}{2} \sqrt{\pi f \mu\sigma} = \frac{l}{2\delta} \quad (6-303)$$

As a numerical example, we note that, for  $l = 1$  cm and free space between the plates, the wavelength corresponding to the fundamental frequency of oscillation, that is, for  $n = 1$ , is 2 cm and hence the frequency is 15,000 MHz. For plates made of copper, the skin depth at 15,000 MHz is  $0.066/(\sqrt{15 \times 10^9})$  m or  $5.38 \times 10^{-5}$  cm. Hence, from (6-303), the value of  $Q$  is  $1/(2 \times 5.38 \times 10^{-5})$  or 9280, which is very large compared to values encountered in circuit theory. It is left as an exercise (Problem 6.82) for the student to show that for a particular mode of operation, that is, for a fixed value of  $n$ ,  $Q$  is inversely proportional to  $\sqrt{f}$ . The above formula for  $Q$  takes into account only the losses in the conductors. In practice, there are other losses, for example, losses in the dielectric and losses due to radiation. ■

The bouncing of (+) and (−) waves between two parallel plates which results in resonance as we discussed for the parallel-plate resonator is employed at optical frequencies in the Fabry-Perot resonator for laser

amplification and oscillation. The Fabry-Perot resonator consists of two plane reflecting surfaces between which is an optically active medium characterized by a propagation constant  $\bar{\gamma} = \alpha + j\beta$ , where  $\alpha$  is negative. To determine the condition for oscillation, let us consider a normally incident uniform plane wave passing through the surface  $z = 0$  and setting up incident and reflected waves in the active medium as shown in Fig. 6.72. The steady-state situation in the medium can be thought of as a superposition of an

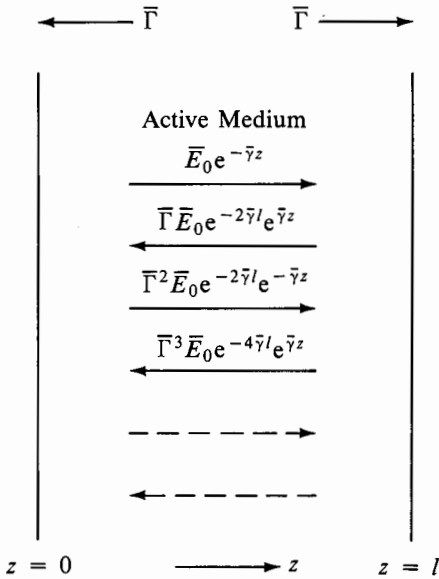


Fig. 6.72. Bouncing of (+) and (-) waves in an active medium between two parallel plates.

infinite number of (+) and (-) waves due to reflections and rereflections at the plates  $z = 0$  and  $z = l$ . Thus, denoting the electric field in the initial (+) wave in the medium (i.e., the wave which would exist if the medium extended to  $z = \infty$ ) to be  $\bar{E}_0 e^{-\bar{\gamma}z}$ , we obtain the field at  $z = l$  in the reflected or (-) wave due to it as  $\bar{\Gamma} \bar{E}_0 e^{-\bar{\gamma}l}$ , where  $\bar{\Gamma}$  is the reflection coefficient at  $z = l$ . Since this (-) wave is propagating towards  $z = 0$ , its field at any value of  $z$  is  $\bar{\Gamma} \bar{E}_0 e^{-\bar{\gamma}l} e^{-\bar{\gamma}(l-z)}$  or  $\bar{\Gamma} \bar{E}_0 e^{-2\bar{\gamma}l} e^{\bar{\gamma}z}$ . Thus the (-) wave field at  $z = 0$  is  $\bar{\Gamma} \bar{E}_0 e^{-2\bar{\gamma}l}$ . Then the field at  $z = 0$  in the rereflected or (- +) wave due to the reflection of the (-) wave at  $z = 0$  is  $(\bar{\Gamma})(\bar{\Gamma} \bar{E}_0 e^{-2\bar{\gamma}l})$ , where we assume that the reflecting surfaces are identical and hence the reflection coefficient for the (-) wave at  $z = 0$  is the same as the reflection coefficient for the (+) wave at  $z = l$ . Since the (- +) wave is propagating towards  $z = l$ , its field at any value of  $z$  is  $\bar{\Gamma}^2 \bar{E}_0 e^{-2\bar{\gamma}l} e^{-\bar{\gamma}z}$ . We can continue in this manner to obtain an infinite number of (+) and (-) waves in the active medium as shown in Fig. 6.72. The total field in the medium is the superposition of the



fields in all these waves. Thus it is given by

$$\begin{aligned}
 \bar{E}(z) &= \bar{E}_0 e^{-\bar{\gamma}z} + \bar{\Gamma} \bar{E}_0 e^{-2\bar{\gamma}l} e^{\bar{\gamma}z} \\
 &\quad + \bar{\Gamma}^2 \bar{E}_0 e^{-2\bar{\gamma}l} e^{-\bar{\gamma}z} + \bar{\Gamma}^3 \bar{E}_0 e^{-4\bar{\gamma}l} e^{\bar{\gamma}z} \\
 &\quad + \bar{\Gamma}^4 \bar{E}_0 e^{-4\bar{\gamma}l} e^{-\bar{\gamma}z} + \dots \\
 &= \bar{E}_0 [e^{-\bar{\gamma}z} (1 + \bar{\Gamma}^2 e^{-2\bar{\gamma}l} + \bar{\Gamma}^4 e^{-4\bar{\gamma}l} + \dots) \\
 &\quad + \bar{\Gamma} e^{\bar{\gamma}z} e^{-2\bar{\gamma}l} (1 + \bar{\Gamma}^2 e^{-2\bar{\gamma}l} + \dots)] \\
 &= \bar{E}_0 \frac{e^{-\bar{\gamma}z} + \bar{\Gamma} e^{-2\bar{\gamma}l} e^{\bar{\gamma}z}}{1 - \bar{\Gamma}^2 e^{-2\bar{\gamma}l}}
 \end{aligned} \tag{6-304}$$

From (6-304), we note that the condition for oscillation, that is, for a field to be set up in the medium for zero  $\bar{E}_0$ , is

$$1 - \bar{\Gamma}^2 e^{-2\bar{\gamma}l} = 0$$

or

$$\bar{\Gamma} e^{-\bar{\gamma}l} = \pm 1 \tag{6-305}$$

Denoting  $\bar{\Gamma} = |\bar{\Gamma}| e^{j\theta}$  and substituting for  $\bar{\gamma}$  in terms of  $\alpha$  and  $\beta$ , we write (6-305) as

$$|\bar{\Gamma}| e^{j\theta} e^{-\alpha l} e^{-j\beta l} = 1 e^{\pm jn\pi} \quad n = 0, 1, 2, 3, \dots$$

or

$$\begin{aligned}
 |\bar{\Gamma}| e^{-\alpha l} &= 1 \quad \text{and} \quad \theta - \beta l = \pm n\pi \\
 \alpha &= \frac{1}{l} \ln |\bar{\Gamma}| \quad \text{and} \quad \beta l = \theta \pm n\pi, \quad n = 0, 1, 2, 3, \dots
 \end{aligned} \tag{6-306}$$

where we choose only those values of  $n$  for which  $\beta l$  is greater than zero. While the condition  $\beta l = \theta + n\pi$  can be satisfied for several frequencies for a given  $l$ , the condition  $\alpha = (1/l) \ln |\bar{\Gamma}|$  is satisfied by a particular active medium only for a narrow range of frequencies, so that oscillation occurs only in that narrow range of frequencies. Note that for  $\bar{\Gamma} = -1$  as is the case for perfectly conducting plates, the condition for oscillation is

$$\alpha = \frac{1}{l} \ln 1 = 0 \quad \text{and} \quad \beta l = n\pi, \quad n = 1, 2, 3, \dots$$

which agrees with the result for the parallel-plate resonator.

## 6.15 Waves in Plasma; Ionospheric Propagation

Thus far we have discussed wave propagation in free space and perfect dielectrics and then in lossy dielectrics and good conductors. In free space and perfect dielectrics, the conduction current is zero so that the current is entirely of the displacement type. In lossy dielectrics, we have both conduction and displacement currents but the conduction current is small compared to the displacement current. In good conductors, the displacement current

is negligible compared to the conduction current. In this section we will discuss wave propagation in plasma. Plasma is a gaseous medium in which the atoms are ionized to produce positive ions and electrons, which are free to move under the influence of the electric and magnetic fields of a wave incident upon the medium. The positive ions are, however, heavy compared to electrons so that they are relatively immobile. The electron motion produces a current which influences the wave propagation. This current is different from the conduction current in metallic conductors, which is due to electron drift with an average velocity owing to the frictional mechanism provided by their collisions with the atomic lattice. The electrons in the plasma, on the other hand, are accelerated by the electric field although losing some of the energy due to their collisions with the heavy particles and other electrons. We will, however, neglect the effect of these collisions as well as the influence on the motion of an electron by the neighboring electrons. In addition, since the magnetic field of the incident wave has negligible influence on the electron motion, its effect will be ignored.

Thus the equation of motion of an electron is given by

$$\frac{d}{dt}(mv) = eE \quad (6-307)$$

where  $e$  and  $m$  are the charge and mass of the electron,  $v$  is its velocity, and  $E$  is the electric field of the wave. If  $N$  is the number density of the electrons in the plasma, the current density resulting from their motion is given by

$$\mathbf{J} = Nev \quad (6-308)$$

Combining (6-307) and (6-308), we get

$$\frac{\partial \mathbf{J}}{\partial t} = Ne \frac{dv}{dt} = \frac{Ne^2}{m} \mathbf{E} \quad (6-309)$$

For sinusoidally time-varying fields of radian frequency  $\omega$ , we have

$$j\omega \bar{\mathbf{J}} = \frac{Ne^2}{m} \bar{\mathbf{E}}$$

or

$$\bar{\mathbf{J}} = -j \frac{Ne^2}{m\omega} \bar{\mathbf{E}} \quad (6-310)$$

Equation (6-310) gives the expression for the current density which we have to use for  $\bar{\mathbf{J}}$  in Maxwell's equation for  $\nabla \times \bar{\mathbf{H}}$  to discuss wave propagation in plasma. Thus we have

$$\nabla \times \bar{\mathbf{E}} = -j\omega\mu_0 \bar{\mathbf{H}} \quad (6-311a)$$

$$\begin{aligned} \nabla \times \bar{\mathbf{H}} &= \bar{\mathbf{J}} + j\omega\epsilon_0 \bar{\mathbf{E}} \\ &= -j \frac{Ne^2}{m\omega} \bar{\mathbf{E}} + j\omega\epsilon_0 \bar{\mathbf{E}} \\ &= j\omega\epsilon_0 \left( 1 - \frac{Ne^2}{m\omega^2\epsilon_0} \right) \bar{\mathbf{E}} \end{aligned} \quad (6-311b)$$

Since the free electrons and heavy positive particles are distributed with statistical uniformity in the ionized region, the net space charge is zero so that

$$\nabla \cdot \bar{\mathbf{E}} = \frac{\bar{\rho}}{\epsilon_0} = 0 \quad (6-312)$$

Taking the curl of both sides of (6-311a) and making use of (6-311b) and (6-312), we obtain

$$\nabla^2 \bar{\mathbf{E}} = -\omega^2 \mu_0 \epsilon_0 \left(1 - \frac{Ne^2}{m\omega^2 \epsilon_0}\right) \bar{\mathbf{E}} \quad (6-313)$$

Equation (6-313) is the wave equation for a plasma medium. Comparing it with (6-173), we note that it is similar to the wave equation for a perfect dielectric medium with the permittivity  $\epsilon$  replaced by  $\epsilon_0(1 - Ne^2/m\omega^2 \epsilon_0)$ . We may therefore call the quantity  $\epsilon_0(1 - Ne^2/m\omega^2 \epsilon_0)$  the effective permittivity of a plasma medium.

We now define a quantity known as the plasma frequency,  $f_N$ , as

$$f_N = \frac{1}{2\pi} \sqrt{\frac{Ne^2}{m\epsilon_0}} = \sqrt{80.6N} \quad (6-314)$$

where  $f_N$  is in hertz and  $N$  is in electrons per cubic meter. The plasma frequency is simply another way of specifying the electron density in the plasma. Substituting (6-314) into (6-313), we have

$$\nabla^2 \bar{\mathbf{E}} = -\omega^2 \mu_0 \epsilon_0 \left(1 - \frac{f_N^2}{f^2}\right) \bar{\mathbf{E}} = \bar{\gamma}^2 \bar{\mathbf{E}}$$

where the propagation constant  $\bar{\gamma}$  is given by

$$\bar{\gamma} = j\omega \sqrt{\mu_0 \epsilon_0 \left(1 - \frac{f_N^2}{f^2}\right)} \quad (6-315)$$

Thus wave propagation in plasma is characterized by the propagation constant given by (6-315). We note that for  $f > f_N$ ,  $(1 - f_N^2/f^2) > 0$ ,  $\bar{\gamma}$  is purely imaginary, and the wave is propagated. For  $f < f_N$ ,  $(1 - f_N^2/f^2) < 0$ ,  $\bar{\gamma}$  is purely real, and the fields are attenuated. For the propagating range of frequencies, the phase constant is

$$\beta = \omega \sqrt{\mu_0 \epsilon_0 \left(1 - \frac{f_N^2}{f^2}\right)} \quad (6-316)$$

and the phase velocity  $v_p$  is given by

$$v_p = \frac{\omega}{\beta} = \frac{1}{\sqrt{\mu_0 \epsilon_0} \sqrt{1 - f_N^2/f^2}} = \frac{c}{\sqrt{1 - f_N^2/f^2}} \quad (6-317)$$

where  $c$  is the velocity of light in free space. In view of the dependence of  $v_p$  on the wave frequency, wave propagation in plasma is characterized by dispersion. This dispersion is known as parametric dispersion from the point of view that it is a consequence of the frequency dependence of the

effective permittivity of the medium. The group velocity is given by

$$v_g = \frac{d\omega}{d\beta} = c\sqrt{1 - \frac{f_N^2}{f^2}}$$

Note that

$$v_p v_g = c^2$$

**EXAMPLE 6-33.** An important example of plasma is the ionosphere, which is a region of the upper atmosphere extending from about 50 km to more than 1000 km above the earth. In this region the constituent gases are ionized, mostly due to ultraviolet radiation from the sun. The electron density in the ionosphere exists in several layers known as *D*, *E*, and *F* layers in which the ionization changes with the hour of the day, the season, and the sunspot cycle. For the purpose of our discussion, we will assume that the electron density increases continuously from zero at the lower boundary, reaching a peak at some height, typically lying between 250 and 350 km, and then decreases continuously as shown in Fig. 6.73(a). We will assume that it is uniform geographically, which is not the case in reality, and that the geometry is plane instead of spherical. Furthermore, wave propagation in the ionosphere is complicated by the presence of the earth's magnetic field. We will here ignore the effect of the earth's magnetic field. Let us consider a uniform plane wave of frequency  $f$  incident obliquely at the lower boundary of such a plane ionosphere at an angle  $\theta_0$  with the normal to the boundary, as shown in Fig. 6.73(b).

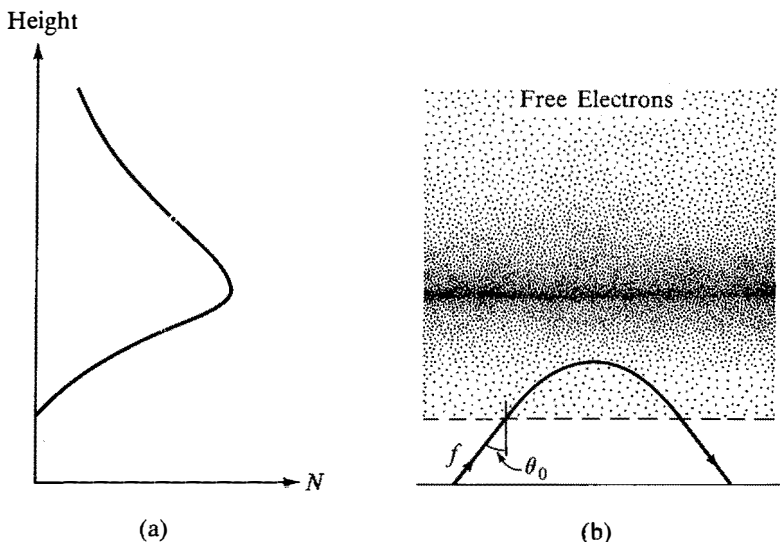


**Fig. 6.73.** (a) Variation of electron density versus height for a simplified ionosphere. (b) Path of a wave incident obliquely on the ionosphere.

We wish to investigate the path of the wave as it propagates in the ionized medium.

We divide the region into several infinitesimal slabs, in each of which the electron density can be considered to be uniform with height. Let us consider the boundary between the free space and the first slab, for which we will denote the plasma frequency as  $f_{N,1}$ . From (6-317), the phase velocity along the direction of propagation, that is, normal to the constant phase surfaces in this slab, is given by

$$v_{p,1} = \frac{c}{\sqrt{1 - f_{N,1}^2/f^2}}$$

For the waves in the free space and in the slab to be in step at the boundary, their apparent phase velocities along the boundary must be equal. This is the same as saying that the apparent wavelengths along the boundary must be equal. Since  $v_{p,1} > c$ , this is possible only if the direction of travel of the wave is bent away from the normal to the boundary as shown in Fig. 6.74.

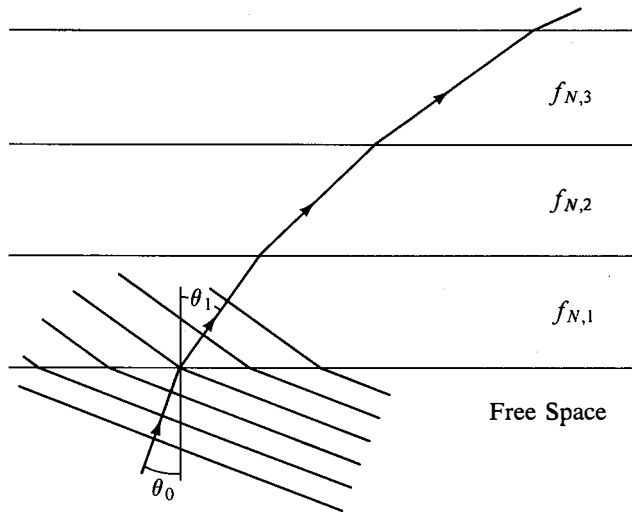


**Fig. 6.74.** For illustrating the bending of the path of a wave as it propagates in the ionosphere.

Thus, denoting the angle between the normal to the boundary and direction of travel in the slab by  $\theta_1$ , we have

$$\frac{c}{\sin \theta_0} = \frac{v_{p,1}}{\sin \theta_1}$$

or

$$\frac{c}{v_{p,1}} \sin \theta_1 = \sin \theta_0$$

Applying the same argument from one slab to the next, we obtain, for the  $i$ th and  $(i - 1)$ th slabs,

$$\frac{c}{v_{p,i}} \sin \theta_i = \frac{c}{v_{p,i-1}} \sin \theta_{i-1}$$

The quantity  $c/v_p$  is known as the phase refractive index. It is denoted by the symbol  $\mu$ , which is not to be confused with permittivity. Thus we have

$$\mu_i \sin \theta_i = \mu_{i-1} \sin \theta_{i-1}$$

which is known as Snell's law. For the series of slabs, we then have

$$\begin{aligned} \mu_i \sin \theta_i &= \mu_{i-1} \sin \theta_{i-1} = \mu_{i-2} \sin \theta_{i-2} = \cdots \\ &= \mu_2 \sin \theta_2 = \mu_1 \sin \theta_1 = \sin \theta_0 \end{aligned}$$

As the number of slabs is increased indefinitely, we approach the limiting case in which the path of the wave is no longer a series of straight lines but a continuous curve. As the wave penetrates into regions of higher and higher electron density, the phase velocity becomes larger and larger, the phase refractive index becomes smaller and smaller, the angle  $\theta$  becomes larger and larger, and the path bends gradually away from the normal to the boundary. Finally, a level may be reached at which the electron density is such that the phase refractive index is equal to  $\sin \theta_0$ , so that  $\sin \theta$  becomes equal to unity,  $\theta = 90^\circ$ , and the path is horizontal. Due to the curvature of the path, it is bent over and the wave is returned to the ground by a symmetrical path as shown in Fig. 6.73(b). For the level at which the path becomes horizontal, we have

$$\mu = \sin \theta_0$$

or

$$\begin{aligned} \sqrt{1 - \frac{f_N^2}{f^2}} &= \sin \theta_0 \\ f_N &= f \cos \theta_0 \end{aligned} \tag{6-318}$$

Thus a wave of frequency  $f$  which is incident obliquely at an angle  $\theta_0$  with the normal to the boundary is reflected from a level at which the plasma frequency is equal to  $f \cos \theta_0$ . For the special case of normal incidence on the ionosphere,  $\theta_0 = 0$  and the condition for reflection is

$$f_N = f$$

The wave is then reflected from a level at which the plasma frequency is equal to the wave frequency. Hence vertically incident waves of frequencies less than the maximum plasma frequency, typically about 10 MHz (but varying with time of the day, season, sunspot cycle, and geographic location) are reflected. Vertically incident waves of frequencies greater than the maximum plasma frequency are transmitted. The same is, of course, true if the transmitter is above the ionosphere. As the angle of incidence is made

oblique, waves of larger frequencies are reflected in accordance with (6-318). The earth's curvature, however, sets a limit for the highest frequency which can be reflected. ■

## 6.16 Radiation of Electromagnetic Waves

Thus far we have assumed that electromagnetic fields exist in a medium and then discussed their characteristics based on Maxwell's equations. In this section we will discuss how these fields are produced and are "radiated" away from the sources. To do this, we consider Maxwell's equations including the source terms and solve them simultaneously. The Maxwell's equations are

$$\nabla \cdot \mathbf{D} = \rho \quad (6-319a)$$

$$\nabla \cdot \mathbf{B} = 0 \quad (6-319b)$$

$$\nabla \times \mathbf{E} = -\frac{\partial \mathbf{B}}{\partial t} \quad (6-319c)$$

$$\nabla \times \mathbf{H} = \mathbf{J} + \frac{\partial \mathbf{D}}{\partial t} \quad (6-319d)$$

where  $\rho$  and  $\mathbf{J}$  are the source charge and current densities, respectively. To solve (6-319a)–(6-319d) simultaneously, we recall from Chapters 3 and 4 the following: In view of (6-319b), we can express  $\mathbf{B}$  as the curl of a vector potential  $\mathbf{A}$ ; that is,

$$\mathbf{B} = \nabla \times \mathbf{A} \quad (6-320)$$

Then, substituting (6-320) into (6-319c) and rearranging, we have

$$\nabla \times \left( \mathbf{E} + \frac{\partial \mathbf{A}}{\partial t} \right) = 0$$

so that  $\mathbf{E} + \partial \mathbf{A} / \partial t$  can be expressed as the gradient of a scalar potential. Thus  $\mathbf{E} + \partial \mathbf{A} / \partial t = -\nabla V$ , or

$$\mathbf{E} = -\nabla V - \frac{\partial \mathbf{A}}{\partial t} \quad (6-321)$$

We now substitute (6-320) and (6-321) into (6-319a) and (6-319d) to obtain a pair of coupled equations in  $V$  and  $\mathbf{A}$ . These are

$$\nabla \cdot \left( -\nabla V - \frac{\partial \mathbf{A}}{\partial t} \right) = \frac{\rho}{\epsilon}$$

$$\nabla \times \nabla \times \mathbf{A} - \mu\epsilon \frac{\partial}{\partial t} \left( -\nabla V - \frac{\partial \mathbf{A}}{\partial t} \right) = \mu \mathbf{J}$$

or

$$\nabla^2 V + \frac{\partial}{\partial t} (\nabla \cdot \mathbf{A}) = -\frac{\rho}{\epsilon} \quad (6-322a)$$

$$\nabla^2 \mathbf{A} - \nabla (\nabla \cdot \mathbf{A} + \mu\epsilon \frac{\partial V}{\partial t}) - \mu\epsilon \frac{\partial^2 \mathbf{A}}{\partial t^2} = -\mu \mathbf{J} \quad (6-322b)$$

Equations (6-322a) and (6-322b) seem to be very complicated. However, a vector is uniquely defined only if both its curl and divergence are specified. While the curl of  $\mathbf{A}$  is given by (6-320), we have not yet specified the divergence of  $\mathbf{A}$ . We now do this by setting

$$\nabla \cdot \mathbf{A} = -\mu\epsilon \frac{\partial V}{\partial t} \quad (6-323)$$

which is known as the Lorentz condition. This uncouples the equations (6-322a) and (6-322b) to give us

$$\nabla^2 V - \mu\epsilon \frac{\partial^2 V}{\partial t^2} = -\frac{\rho}{\epsilon} \quad (6-324)$$

$$\nabla^2 \mathbf{A} - \mu\epsilon \frac{\partial^2 \mathbf{A}}{\partial t^2} = -\mu\mathbf{J} \quad (6-325)$$

If we can solve these two equations for given charge and current distributions of densities  $\rho$  and  $\mathbf{J}$ , respectively, we can then find the fields by using (6-321) and (6-320).

Before we discuss the solution of (6-324) and (6-325), we will show that the continuity equation is implied by the Lorentz condition. To do this, we take the Laplacian of both sides of (6-323). We then have

$$\nabla^2(\nabla \cdot \mathbf{A}) = -\mu\epsilon \nabla^2 \frac{\partial V}{\partial t}$$

or

$$\nabla \cdot \nabla^2 \mathbf{A} = -\mu\epsilon \frac{\partial}{\partial t} \nabla^2 V \quad (6-326)$$

Substituting for  $\nabla^2 \mathbf{A}$  and  $\nabla^2 V$  in (6-326) from (6-325) and (6-324), respectively, we get

$$\nabla \cdot \left( \mu\epsilon \frac{\partial^2 \mathbf{A}}{\partial t^2} - \mu\mathbf{J} \right) = -\mu\epsilon \frac{\partial}{\partial t} \left( \mu\epsilon \frac{\partial^2 V}{\partial t^2} - \frac{\rho}{\epsilon} \right)$$

or

$$\mu\epsilon \frac{\partial^2}{\partial t^2} (\nabla \cdot \mathbf{A} + \mu\epsilon \frac{\partial V}{\partial t}) = \mu (\nabla \cdot \mathbf{J} + \frac{\partial \rho}{\partial t})$$

Thus, by assuming the Lorentz condition, we imply  $\nabla \cdot \mathbf{J} + \partial \rho / \partial t = 0$ , which is the continuity equation. Since the continuity equation must be satisfied by physical charge and current distributions, it is appropriate to use the Lorentz condition to uncouple (6-322a) and (6-322b).

Returning now to Eqs. (6-324) and (6-325), we note that their forms are familiar. They are wave equations with source terms on the right sides. Hence they are inhomogeneous wave equations. We will discuss the solutions to these equations from our knowledge of static fields and our experience with the homogeneous wave equations. It is sufficient if we discuss the solution for one of the two equations. The solution for the second equation follows from similarity. Let us therefore consider Eq. (6-324). For static fields, this



equation reduces to

$$\nabla^2 V = -\frac{\rho}{\epsilon}$$

which is Poisson's equation for the electrostatic potential. Let us consider a point charge  $Q_0$  at the origin. The electrostatic potential due to this point charge is given by

$$V(r) = \frac{Q_0}{4\pi\epsilon r}$$

For the time-varying case, we know that electromagnetic effects propagate with a finite velocity  $v$  which for the homogeneous wave equation corresponding to (6-324) is  $1/\sqrt{\mu\epsilon}$ . Hence, if the point charge at the origin is varying with time (due to current flowing into and/or away from the origin), its effect is felt at a distance  $r$  from the origin after a time delay of  $r/v$ . Conversely, the effect felt at a distance  $r$  from the origin at time  $t$  is due to the value of the charge which existed at the origin at an earlier time  $t - r/v$ . Thus, if the point charge at the origin is varying in the manner  $Q_0 \sin \omega t$ , we expect the time-varying electric potential due to it to be

$$V(r, t) = \frac{Q_0 \sin \omega(t - r/v)}{4\pi\epsilon r} \quad (6-327)$$

To verify if our reasoning is correct, we note that

$$\begin{aligned} \nabla^2 V &= \nabla^2 \left[ \frac{Q_0 \sin \omega(t - r/v)}{4\pi\epsilon r} \right] \\ &= \frac{Q_0}{4\pi\epsilon} \left\{ \left[ \sin \omega \left( t - \frac{r}{v} \right) \right] \nabla^2 \frac{1}{r} \right. \\ &\quad \left. + 2\nabla \sin \omega \left( t - \frac{r}{v} \right) \cdot \nabla \frac{1}{r} + \frac{1}{r} \nabla^2 \sin \omega \left( t - \frac{r}{v} \right) \right\} \\ &= -\frac{Q_0 \delta(\mathbf{r}) \sin \omega t}{\epsilon} - \frac{\omega^2 Q_0 \sin \omega(t - r/v)}{4\pi\epsilon r v^2} \end{aligned} \quad (6-328a)$$

where we have used the vector identity

$$\nabla^2(\phi\psi) = \phi \nabla^2\psi + 2 \nabla\phi \cdot \nabla\psi + \psi \nabla^2\phi$$

and the relation (see Problem 2-58)

$$\nabla^2 \frac{1}{r} = -4\pi\delta(\mathbf{r})$$

We also note that

$$\mu\epsilon \frac{\partial^2 V}{\partial t^2} = -\frac{\omega^2 Q_0 \sin \omega(t - r/v)}{4\pi\epsilon r v^2} \quad (6-328b)$$

From (6-328a) and (6-328b), we have

$$\nabla^2 V - \mu\epsilon \frac{\partial^2 V}{\partial t^2} = \frac{Q_0 \delta(\mathbf{r}) \sin \omega t}{\epsilon}$$

which agrees with (6-324) for a point charge  $Q_0 \sin \omega t$  at the origin.

It follows from (6-327) that, for a time-varying volume charge of density  $\rho(\mathbf{r}', t)$  in an infinitesimal volume  $dv'$  at a point  $P(\mathbf{r}')$ , the time-varying electric potential at a point  $Q(\mathbf{r})$  is given by

$$dV(\mathbf{r}, t) = \frac{\rho(\mathbf{r}', t - |\mathbf{r} - \mathbf{r}'|/v)}{4\pi\epsilon |\mathbf{r} - \mathbf{r}'|} dv' \quad (6-329a)$$

Similarly, from Eq. (6-325), the time-varying magnetic vector potential at a point  $Q(\mathbf{r})$  due to a time-varying volume current of density  $\mathbf{J}(\mathbf{r}', t)$  in an infinitesimal volume  $dv'$  at a point  $P(\mathbf{r}')$  is given by

$$d\mathbf{A}(\mathbf{r}, t) = \frac{\mu\mathbf{J}(\mathbf{r}', t - |\mathbf{r} - \mathbf{r}'|/v)}{4\pi |\mathbf{r} - \mathbf{r}'|} dv' \quad (6-329b)$$

Equations (6-329a) and (6-329b) tell us that, to find the time-varying electromagnetic potentials at a point  $Q(\mathbf{r})$  at a time  $t$  due to a volume charge  $\rho dv'$  and a volume current  $\mathbf{J} dv'$  at a point  $P(\mathbf{r}')$ , we can make use of the expressions for  $V$  and  $\mathbf{A}$  for the static case except that we have to use those values of  $\rho$  and  $\mathbf{J}$  which existed at  $P$  at a time  $t - |\mathbf{r} - \mathbf{r}'|/v$ . For this reason, these potentials are known as the "retarded potentials." The retarded potentials for volume charge and current distributions in an extended volume  $V'$  are given by the integrals of (6-329a) and (6-329b). These are

$$V(\mathbf{r}, t) = \int_{V'} \frac{\rho(\mathbf{r}', t - |\mathbf{r} - \mathbf{r}'|/v)}{4\pi\epsilon |\mathbf{r} - \mathbf{r}'|} dv' \quad (6-330)$$

$$\mathbf{A}(\mathbf{r}, t) = \int_{V'} \frac{\mu\mathbf{J}(\mathbf{r}', t - |\mathbf{r} - \mathbf{r}'|/v)}{4\pi |\mathbf{r} - \mathbf{r}'|} dv' \quad (6-331)$$

We will now evaluate the retarded potentials and then the fields for a simple but a very useful source known as the Hertzian dipole. We will find that the field expressions we will obtain are quite complicated even for this simplest case. The Hertzian dipole is an oscillating version of the static electric dipole. It consists of two equal and opposite time-varying charges  $Q_1(t) = Q_0 \sin \omega t$  and  $Q_2(t) = -Q_0 \sin \omega t$  separated by an infinitesimal distance  $dl$ . We will place the dipole at the origin and orient it along the  $z$  axis. The dipole moment is then given by  $d\mathbf{p} = Q_0 dl \sin \omega t \mathbf{i}_z$ . To satisfy the continuity equation, we connect the two charges by a filamentary wire so that the current flowing in the wire from  $Q_2$  to  $Q_1$  is

$$I(t) = \frac{dQ_1}{dt} = -\frac{dQ_2}{dt} = \omega Q_0 \cos \omega t = I_0 \cos \omega t$$

where  $I_0 = \omega Q_0$ . The Hertzian dipole and the time variations of  $Q_1$ ,  $Q_2$ , and  $I$  are shown in Fig. 6.75.

With reference to the notation of Fig. 6.75(a), the time-varying electric

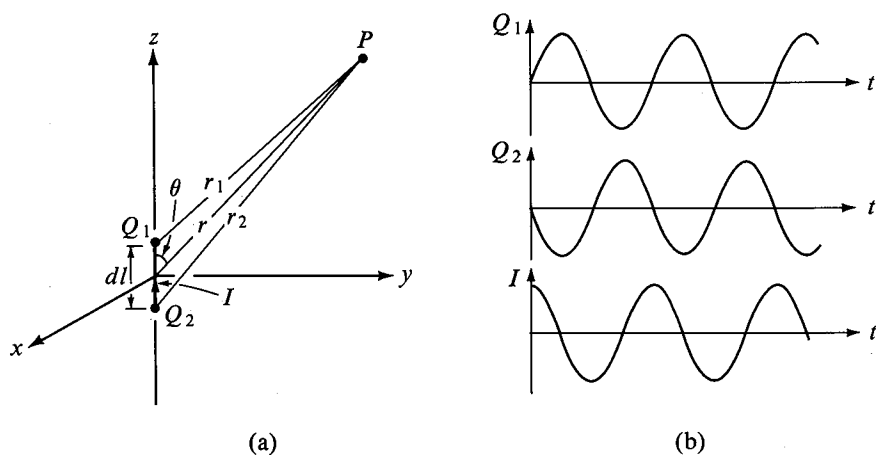


Fig. 6.75. (a) Hertzian dipole. (b) Time variations of  $Q_1$ ,  $Q_2$ , and  $I$  for the Hertzian dipole.

potential at point  $P$  is given by

$$\begin{aligned} V &= \frac{Q_1(t - r_1/v)}{4\pi\epsilon r_1} + \frac{Q_2(t - r_2/v)}{4\pi\epsilon r_2} \\ &= \frac{Q_0 \sin \omega(t - r_1/v)}{4\pi\epsilon r_1} - \frac{Q_0 \sin \omega(t - r_2/v)}{4\pi\epsilon r_2} \end{aligned}$$

We will let  $dl \rightarrow 0$ , keeping the product  $Q_0 dl$  constant and thereby obtaining a point dipole. We then have

$$\begin{aligned} V &\approx \frac{Q_0 \sin \omega\{t - [r - (dl/2) \cos \theta]/v\}}{4\pi\epsilon[r - (dl/2) \cos \theta]} - \frac{Q_0 \sin \omega\{t - [r + (dl/2) \cos \theta]/v\}}{4\pi\epsilon[r + (dl/2) \cos \theta]} \\ &= \frac{Q_0}{4\pi\epsilon r} \left[ \left(1 + \frac{dl}{2r} \cos \theta\right) \sin \omega\left(t - \frac{r}{v} + \frac{dl}{2v} \cos \theta\right) \right. \\ &\quad \left. - \left(1 - \frac{dl}{2r} \cos \theta\right) \sin \omega\left(t - \frac{r}{v} - \frac{dl}{2v} \cos \theta\right) \right] \\ &= \frac{Q_0}{4\pi\epsilon r} \left[ 2 \sin\left(\frac{\omega dl}{2v} \cos \theta\right) \cos \omega\left(t - \frac{r}{v}\right) \right. \\ &\quad \left. + \frac{dl \cos \theta}{r} \cos\left(\frac{\omega dl}{2v} \cos \theta\right) \sin \omega\left(t - \frac{r}{v}\right) \right] \\ &\rightarrow \frac{Q_0 dl \cos \theta}{4\pi\epsilon r} \left[ \frac{\omega \cos \omega(t - r/v)}{v} + \frac{\sin \omega(t - r/v)}{r} \right] \end{aligned} \tag{6-332}$$

We note from (6-332) that the time-varying electric potential due to the dipole is not simply equal to the electrostatic potential  $(Q_0 dl \cos \theta)/4\pi\epsilon r^2$  times the retardation factor  $\sin \omega(t - r/v)$ , but has an additional term. This arises because of the phase difference between the time-varying potentials associated with the individual point charges of the dipole.

To find the time-varying vector potential, we recall from Chapter 3 that the static vector potential due to a current element  $I_0 dl \mathbf{i}_z$  at the origin is  $(\mu I_0 dl / 4\pi r) \mathbf{i}_z$ . Hence the time-varying vector potential due to the time-varying current element of the Hertzian dipole is given by

$$\begin{aligned} \mathbf{A} &= \frac{\mu I_0 dl \cos \omega(t - r/v)}{4\pi r} \mathbf{i}_z \\ &= \frac{\mu I_0 dl \cos \omega(t - r/v)}{4\pi r} (\cos \theta \mathbf{i}_r - \sin \theta \mathbf{i}_\theta) \end{aligned} \quad (6-333)$$

We will now obtain the electromagnetic fields due to the Hertzian dipole by using (6-321) and (6-320). From (6-321), we have

$$\begin{aligned} \mathbf{E} &= -\nabla V - \frac{\partial \mathbf{A}}{\partial t} \\ &= \left( -\frac{\partial V}{\partial r} - \frac{\partial A_r}{\partial t} \right) \mathbf{i}_r + \left( -\frac{1}{r} \frac{\partial V}{\partial \theta} - \frac{\partial A_\theta}{\partial t} \right) \mathbf{i}_\theta \end{aligned} \quad (6-334a)$$

From (6-320), we have

$$\begin{aligned} \mathbf{H} &= \frac{\mathbf{B}}{\mu} = \frac{1}{\mu} \nabla \times \mathbf{A} \\ &= \frac{1}{\mu r} \left[ \frac{\partial}{\partial r} (r A_\theta) - \frac{\partial A_r}{\partial \theta} \right] \mathbf{i}_\phi \end{aligned} \quad (6-334b)$$

Thus the field components are given by

$$\begin{aligned} E_r &= -\frac{\partial V}{\partial r} - \frac{\partial A_r}{\partial t} \\ &= \frac{2\omega Q_0 dl \cos \theta}{4\pi \epsilon} \left[ \frac{\sin \omega(t - r/v)}{\omega r^3} + \frac{\cos \omega(t - r/v)}{v r^2} \right] \end{aligned} \quad (6-335a)$$

$$\begin{aligned} E_\theta &= -\frac{1}{r} \frac{\partial V}{\partial \theta} - \frac{\partial A_\theta}{\partial t} \\ &= \frac{\omega Q_0 dl \sin \theta}{4\pi \epsilon} \left[ \frac{\sin \omega(t - r/v)}{\omega r^3} + \frac{\cos \omega(t - r/v)}{v r^2} \right. \\ &\quad \left. - \frac{\omega \sin \omega(t - r/v)}{v^2 r} \right] \end{aligned} \quad (6-335b)$$

$$\begin{aligned} H_\phi &= \frac{1}{\mu r} \left[ \frac{\partial}{\partial r} (r A_\theta) - \frac{\partial A_r}{\partial \theta} \right] \\ &= \frac{I_0 dl \sin \theta}{4\pi} \left[ \frac{\cos \omega(t - r/v)}{r^2} - \frac{\omega \sin \omega(t - r/v)}{v r} \right] \end{aligned} \quad (6-335c)$$

Alternatively,  $E_r$  and  $E_\theta$  can be obtained from  $H_\phi$  by using Maxwell's curl equation for  $\mathbf{H}$  in which case it is not necessary to determine  $V$ . Writing the field expressions in phasor form, we have

$$\begin{aligned} \bar{E}_r &= \frac{2\bar{I}_0 dl \cos \theta}{4\pi \epsilon} \left( -\frac{j}{\omega r^3} + \frac{1}{v r^2} \right) e^{-j\omega r/v} \\ &= -\frac{2\beta^2 \eta \bar{I}_0 dl \cos \theta}{4\pi} \left[ \frac{1}{(j\beta r)^3} + \frac{1}{(j\beta r)^2} \right] e^{-j\beta r} \end{aligned} \quad (6-336)$$

$$\begin{aligned}\bar{E}_\theta &= \frac{\bar{I}_0 dl \sin \theta}{4\pi\epsilon} \left( -\frac{j}{\omega r^3} + \frac{1}{vr^2} + \frac{j\omega}{v^2 r} \right) e^{-j\omega r/v} \\ &= \frac{\beta^2 \eta \bar{I}_0 dl \sin \theta}{4\pi} \left[ \frac{1}{(j\beta r)^3} + \frac{1}{(j\beta r)^2} + \frac{1}{j\beta r} \right] e^{-j\beta r}\end{aligned}\quad (6-337)$$

$$\begin{aligned}\bar{H}_\phi &= \frac{\bar{I}_0 dl \sin \theta}{4\pi} \left( \frac{1}{r^2} + \frac{j\omega}{vr} \right) e^{-j\omega r/v} \\ &= -\frac{\beta^2 \bar{I}_0 dl \sin \theta}{4\pi} \left[ \frac{1}{(j\beta r)^2} + \frac{1}{j\beta r} \right] e^{-j\beta r}\end{aligned}\quad (6-338)$$

where  $\beta = \omega/v$ ,  $\eta = \sqrt{\mu/\epsilon} = 1/\epsilon v$ , and  $\bar{I}_0 = I_0 = \omega Q_0$ .

We note from (6-335a)–(6-335c) or (6-336)–(6-338) that the field expressions contain terms involving  $1/r^3$ ,  $1/r^2$ , and  $1/r$ . Very close to the dipole, the  $1/r^3$  and  $1/r^2$  terms dominate the  $1/r$  terms. Far from the dipole, the  $1/r^3$  and  $1/r^2$  terms are negligible and the fields are determined by the  $1/r$  terms. To see how far from the dipole, let us first consider the  $H_\phi$  component. The magnitudes of the two terms are equal for  $r = v/\omega = 1/\beta = \lambda/2\pi \approx 0.16\lambda$ . For the  $E_\theta$  component the combined magnitude of the  $1/r^3$  and  $1/r^2$  terms is equal to the  $1/r$  term for

$$\left( \frac{1}{\omega r^3} \right)^2 + \left( \frac{1}{vr^2} \right)^2 = \left( \frac{\omega}{v^2 r} \right)^2$$

or

$$\begin{aligned}r^4 - \left( \frac{\lambda}{2\pi} \right)^2 r^2 - \left( \frac{\lambda}{2\pi} \right)^4 &= 0 \\ r &= \sqrt{\frac{1 + \sqrt{5}}{2}} \frac{\lambda}{2\pi} \approx 0.2\lambda\end{aligned}$$

Thus, even in a distance of few wavelengths from the dipole, we can neglect the  $1/r^3$  and  $1/r^2$  terms in comparison with the  $1/r$  terms. The field expressions then reduce to

$$\begin{aligned}\bar{E}_r &= 0 \\ \bar{E}_\theta &= \frac{j\omega \bar{I}_0 dl \sin \theta}{4\pi\epsilon v^2 r} e^{-j\omega r/v} = \frac{j\beta \eta \bar{I}_0 dl \sin \theta}{4\pi r} e^{-j\beta r}\end{aligned}\quad (6-339)$$

$$\bar{H}_\phi = \frac{j\omega \bar{I}_0 dl \sin \theta}{4\pi v r} e^{-j\omega r/v} = \frac{j\beta \bar{I}_0 dl \sin \theta}{4\pi r} e^{-j\beta r}\quad (6-340)$$

These fields are known as the “radiation fields” because they are the components which contribute to radiation of electromagnetic waves away from the dipole. In fact, we will learn later that the  $1/r^3$  and  $1/r^2$  terms do not contribute to the time-average power flow even near the dipole. We note that the ratio of  $E_\theta$  to  $H_\phi$  given by (6-339) and (6-340) is equal to  $\eta = \sqrt{\mu/\epsilon}$  as for the case of the fields associated with a uniform plane wave, although the constant phase surfaces are  $r = \text{constant}$  and the constant amplitude surfaces are  $(\sin \theta)/r = \text{constant}$ . However, let us consider a spherical surface of large radius and centered at the dipole and divide it into small regions, in each of which  $\sin \theta$  may be considered to be constant. Then each small

region is approximately a plane surface on which the phase as well as magnitude are constants. Thus, over each small region, the fields are almost like uniform plane waves, with the amplitude differing from one region to the other. This is what we meant by the statement in Section 6.8 that, far from a radiating antenna, the radiated waves are approximately uniform plane waves.

Returning now to the field expressions given by (6-336)–(6-338), we obtain the complex Poynting vector as

$$\begin{aligned}
 \bar{\mathbf{P}} &= \frac{1}{2} \bar{\mathbf{E}} \times \bar{\mathbf{H}}^* \\
 &= \frac{1}{2} (\bar{E}_\theta \bar{H}_\phi^* \mathbf{i}_r - \bar{E}_r \bar{H}_\theta^* \mathbf{i}_\theta) \\
 &= \frac{|\bar{I}_0|^2 (dl)^2 \sin^2 \theta}{32\pi^2 \epsilon} \left( \frac{-j}{\omega r^3} + \frac{1}{vr^2} + \frac{j\omega}{v^2 r} \right) \left( \frac{1}{r^2} - \frac{j\omega}{vr} \right) \mathbf{i}_r \\
 &\quad - \frac{|\bar{I}_0|^2 (dl)^2 \sin 2\theta}{32\pi^2 \epsilon} \left( \frac{-j}{\omega r^3} + \frac{1}{vr^2} \right) \left( \frac{1}{r^2} - \frac{j\omega}{vr} \right) \mathbf{i}_\theta \\
 &= \frac{|\bar{I}_0|^2 (dl)^2 \sin^2 \theta}{32\pi^2 \epsilon} \left( \frac{\omega^2}{v^3 r^2} - j \frac{1}{\omega r^5} \right) \mathbf{i}_r \\
 &\quad + j \frac{|\bar{I}_0|^2 (dl)^2 \sin 2\theta}{32\pi^2 \epsilon} \left( \frac{\omega}{v^2 r^3} + \frac{1}{\omega r^5} \right) \mathbf{i}_\theta
 \end{aligned} \tag{6-341}$$

The time-average Poynting vector is given by

$$\begin{aligned}
 \langle \mathbf{P} \rangle &= \Re \{ \bar{\mathbf{P}} \} \\
 &= \frac{|\bar{I}_0|^2 (dl)^2 \sin^2 \theta}{32\pi^2 \epsilon} \frac{\omega^2}{v^3 r^2} \mathbf{i}_r
 \end{aligned} \tag{6-342}$$

which is exactly the same as the time-average Poynting vector due to the radiation fields given by (6-339) and (6-340). Thus the near fields, that is, the  $1/r^3$  and  $1/r^2$  terms, do not contribute to the time-average power flow even near the dipole. They contribute only to the reactive power, which is entirely due to them since the reactive power associated with the radiation fields is zero.

By integrating the time-average Poynting vector given by (6-342) over a surface of radius  $r$  centered at the dipole, we obtain the time-average power radiated by the dipole as

$$\begin{aligned}
 \langle P_{\text{rad}} \rangle &= \int_{\theta=0}^{\pi} \int_{\phi=0}^{2\pi} \langle \mathbf{P} \rangle \cdot r^2 \sin \theta \, d\theta \, d\phi \, \mathbf{i}_r \\
 &= \int_{\theta=0}^{\pi} \int_{\phi=0}^{2\pi} \frac{\omega^2 |\bar{I}_0|^2 (dl)^2}{32\pi^2 \epsilon v^3} \sin^3 \theta \, d\theta \, d\phi \\
 &= \frac{\omega^2 |\bar{I}_0|^2 (dl)^2}{32\pi^2 \epsilon v^3} \frac{8\pi}{3} = \frac{\omega^2 |\bar{I}_0|^2 (dl)^2}{12\pi \epsilon v^3} \\
 &= \frac{\eta \beta^2 |\bar{I}_0|^2 (dl)^2}{12\pi} = \frac{\pi \eta |\bar{I}_0|^2}{3} \left( \frac{dl}{\lambda} \right)^2
 \end{aligned} \tag{6-343}$$

We now see why the near fields cannot contribute to time-average power flow. The reason is that, from conservation of energy, the time-average power flow across a spherical surface of one radius must be equal to the time-average power flow across a spherical surface of a different radius, that is, it must be independent of  $r$  as indicated by (6-343). Since the surface area of the sphere varies as  $r^2$ , only those components of  $\mathbf{E}$  and  $\mathbf{H}$  which vary as  $1/r$  can satisfy this condition.

Rewriting (6-343) as

$$\langle P_{\text{rad}} \rangle = \frac{1}{2} |\bar{I}_0|^2 \left[ \frac{2\pi\eta}{3} \left( \frac{dl}{\lambda} \right)^2 \right]$$

we note that the power radiated by the dipole is the same as the time-average power dissipated in a resistance of value  $[(2\pi\eta/3)(dl/\lambda)^2]$  when a current  $I_0 \cos \omega t$  is passed through it. This is known as the "radiation resistance" and is denoted by the symbol  $R_{\text{rad}}$ . Thus, for the Hertzian dipole,

$$R_{\text{rad}} = \frac{2\pi\eta}{3} \left( \frac{dl}{\lambda} \right)^2 \text{ ohms}$$

For  $\eta = \eta_0 = 120\pi$ , that is, for the dipole in free space, we have

$$R_{\text{rad}} = 80\pi^2 \left( \frac{dl}{\lambda} \right)^2 \text{ ohms} \quad (6-344)$$

As a numerical example, for  $dl/\lambda$  equal to 0.01,  $R_{\text{rad}}$  is equal to 0.08 ohms. This value is too small to make a Hertzian dipole of  $dl/\lambda$  equal to 0.01 an effective radiator. This is why a practical dipole must be an appreciable fraction of a wavelength long. But then, Eq. (6-344) is no longer correct for the radiation resistance since the variation of current along the length of the dipole must be taken into account in obtaining the radiation fields and hence the radiated power. This can be done by considering the dipole as a series of Hertzian dipoles connected end to end and then using superposition. We will illustrate this by means of an example.

**EXAMPLE 6-34.** A practical short dipole is a center-fed straight wire antenna, having a length that is short compared to a wavelength. The current distribution along the wire can be approximated as shown in Fig. 6.76(a) in which the magnitude decreases uniformly from a maximum at the center to zero at the ends. It is desired to find the radiation resistance of the short dipole.

With reference to Fig. 6.76(a), the current distribution along the dipole can be written as

$$\bar{I}(z) = \begin{cases} \bar{I}_0 \left( 1 - \frac{2z}{L} \right) & \text{for } 0 < z < \frac{L}{2} \\ \bar{I}_0 \left( 1 + \frac{2z}{L} \right) & \text{for } -\frac{L}{2} < z < 0 \end{cases} \quad (6-345)$$

where  $\bar{I}_0$  is a constant. To determine the radiation fields, we can represent

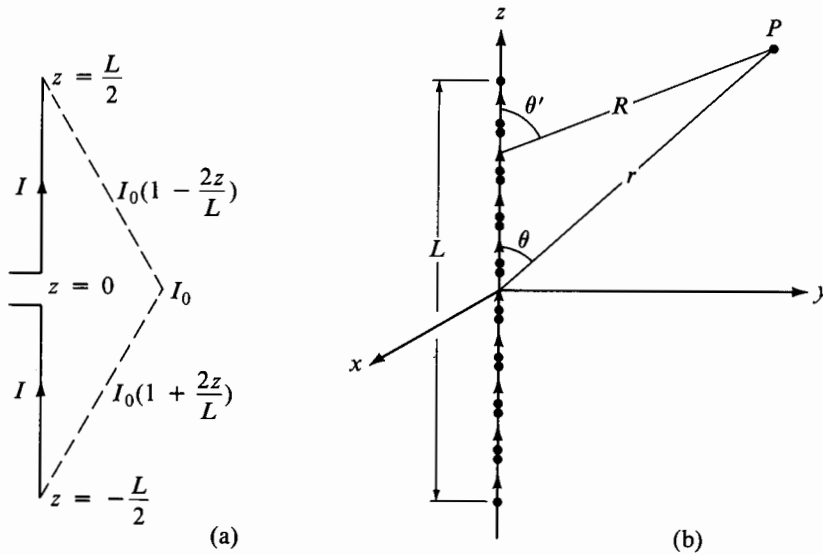


**Fig. 6.76.** (a) Current distribution along a short dipole. (b) Representation of the short dipole as a series of Hertzian dipoles for computing the radiation fields and the radiation resistance.

the short dipole as a series of Hertzian dipoles of infinitesimal lengths  $dz$  as shown in Fig. 6.76(b). From (6-339) and (6-340) and from superposition, the radiation fields for the short dipole are then given by

$$\bar{E}_\theta = \int_{z=-L/2}^{L/2} \frac{j\beta\eta\bar{I}(z)\sin\theta'}{4\pi R} e^{-j\beta R} dz \quad (6-346a)$$

$$\bar{H}_\phi = \int_{z=-L/2}^{L/2} \frac{j\beta\bar{I}(z)\sin\theta'}{4\pi R} e^{-j\beta R} dz \quad (6-346b)$$

where  $R$  and  $\theta'$  are as shown in Fig. 6.76(b). For  $R \gg L$ , as is the case for radiation fields, we can set  $\theta' \approx \theta$  and  $R \approx r$  in the numerators and denominators of the integrands on the right sides of (6-346a) and (6-346b). For the  $R$  in the exponential factors, however, we substitute  $(r - z \cos \theta)$  because, depending on the value of  $\beta$ ,  $e^{-j\beta R}$  can vary appreciably for  $-L/2 < z < L/2$ . Considering (6-346a), we then have

$$\begin{aligned} \bar{E}_\theta &= \int_{z=-L/2}^{L/2} \frac{j\beta\eta\bar{I}(z)\sin\theta}{4\pi r} e^{-j\beta r} e^{j\beta z \cos\theta} dz \\ &= \frac{j\beta\eta\sin\theta}{4\pi r} e^{-j\beta r} \int_{z=-L/2}^{L/2} \bar{I}(z) e^{j\beta z \cos\theta} dz \end{aligned} \quad (6-347)$$



Substituting (6-345) into (6-347), we obtain

$$\begin{aligned}\bar{E}_\theta &= \frac{j\beta\eta\bar{I}_0\sin\theta}{4\pi r} e^{-j\beta r} \left[ \int_{z=0}^{L/2} \left(1 - \frac{2z}{L}\right) e^{j\beta z \cos\theta} dz \right. \\ &\quad \left. + \int_{z=-L/2}^0 \left(1 + \frac{2z}{L}\right) e^{j\beta z \cos\theta} dz \right] \\ &= \frac{j\beta\eta\bar{I}_0\sin\theta}{4\pi r} e^{-j\beta r} \int_{z=0}^{L/2} \left(1 - \frac{2z}{L}\right) (e^{j\beta z \cos\theta} + e^{-j\beta z \cos\theta}) dz \\ &= \frac{j\beta\eta\bar{I}_0\sin\theta}{2\pi r} e^{-j\beta r} \int_{z=0}^{L/2} \left(1 - \frac{2z}{L}\right) \cos(\beta z \cos\theta) dz\end{aligned}\quad (6-348)$$

However, for  $L \ll \lambda$ ,  $\beta L = 2\pi L/\lambda \ll 1$ , and

$$\cos(\beta z \cos\theta) = 1 - \frac{(\beta z \cos\theta)^2}{2} + \dots \approx 1 \text{ for } -\frac{L}{2} < z < \frac{L}{2}$$

so that (6-348) simplifies to

$$\begin{aligned}\bar{E}_\theta &= \frac{j\beta\eta\bar{I}_0\sin\theta}{2\pi r} e^{-j\beta r} \int_{z=0}^{L/2} \left(1 - \frac{2z}{L}\right) dz \\ &= \frac{j\beta\eta L\bar{I}_0\sin\theta}{8\pi r} e^{-j\beta r}\end{aligned}$$

Likewise,

$$\bar{H}_\phi = \frac{j\beta L\bar{I}_0\sin\theta}{8\pi r} e^{-j\beta r}$$

The time-average radiated power is then given by

$$\begin{aligned}\langle P_{\text{rad}} \rangle &= \int_{\theta=0}^{\pi} \int_{\phi=0}^{2\pi} \frac{1}{2} (\bar{E}_\theta \bar{H}_\phi^*) r^2 \sin\theta \, d\theta \, d\phi \\ &= \int_{\theta=0}^{\pi} \int_{\phi=0}^{2\pi} \frac{\beta^2 \eta L^2 |\bar{I}_0|^2}{128\pi^2} \sin^3\theta \, d\theta \, d\phi \\ &= \frac{1}{2} |\bar{I}_0|^2 \left[ \frac{\pi\eta}{6} \left(\frac{L}{\lambda}\right)^2 \right]\end{aligned}$$

Thus, for  $\eta = \eta_0 = 120\pi$ , the radiation resistance of a short dipole of length  $L$  is given by

$$R_{\text{rad}} (\text{short dipole}) = 20\pi^2 \left(\frac{L}{\lambda}\right)^2 \quad (6-349)$$

As a numerical example, for  $L/\lambda = 0.1$ ,  $R_{\text{rad}} \approx 2$  ohms. ■

We will conclude this section with a brief discussion of the directional properties of the Hertzian and short dipoles. In this connection, we define the radiation intensity  $U$  of an antenna in a given direction as the power radiated per unit solid angle in that direction. Since the surface area of a

sphere of radius  $r$  is  $4\pi r^2$  and the solid angle subtended by it at its center is  $4\pi$ , the surface area per unit solid angle is  $r^2$ . Thus the radiation intensity is given by

$$U = \langle \mathbf{P} \rangle \cdot r^2 \mathbf{i}, \text{ watts/steradian}$$

From (6-342) the radiation intensity for the Hertzian dipole is

$$U = \frac{|\tilde{I}_0|^2 (dl)^2 \omega^2}{32\pi^2 \epsilon v^3} \sin^2 \theta$$

The quantity

$$\frac{|\tilde{I}_0|^2 (dl)^2 \omega^2}{32\pi^2 \epsilon v^3}$$

is a constant for a particular frequency and hence, by dividing  $U$  by this quantity, we obtain the normalized radiation intensity  $U_n$ , as

$$U_n = \sin^2 \theta \quad (6-350)$$

The same result holds for the short dipole of Example 6-34 since the power radiated by it is also proportional to  $\sin^2 \theta$ . A plot of  $U_n$  given by (6-350) versus  $\theta$  is shown in Fig. 6.77. This plot illustrates the directional properties

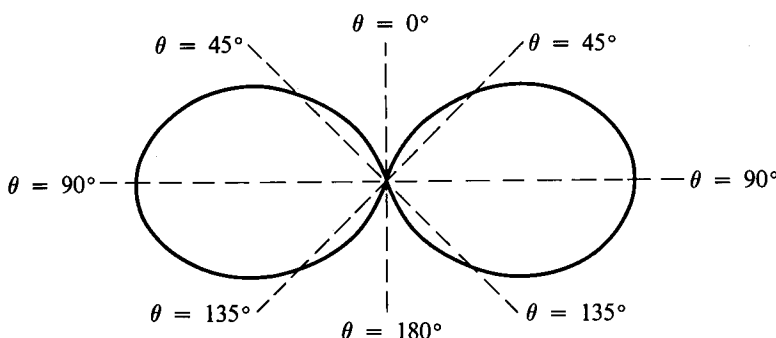


Fig. 6.77. Normalized radiation intensity versus  $\theta$  for Hertzian and short dipoles.

of the Hertzian and short dipoles. Their radiation intensities are maximum for  $\theta = 90^\circ$ , that is, broadside to the dipole and zero for  $\theta = 0$  and  $180^\circ$ , that is, along the dipole. The directivity  $D$  of an antenna is defined as the ratio of the maximum radiation intensity to the average radiation intensity. Thus

$$D = \frac{[U_n]_{\max}}{(1/4\pi) \int U_n d\Omega} = \frac{4\pi[U_n]_{\max}}{\int_{\theta=0}^{\pi} \int_{\phi=0}^{2\pi} U_n(\theta, \phi) \sin \theta d\theta d\phi}$$

where  $\Omega$  denotes the solid angle. For the Hertzian and short dipoles,

$$D = \frac{4\pi[\sin^2 \theta]_{\max}}{\int_{\theta=0}^{\pi} \int_{\phi=0}^{2\pi} \sin^3 \theta d\theta d\phi} = \frac{4\pi}{8\pi/3} = \frac{3}{2}$$

## PROBLEMS

- 6.1. For the following charge distributions, find the electrostatic potential everywhere using Poisson's and Laplace's equations.

$$(a) \rho = \begin{cases} z & \text{for } |z| < a \\ 0 & \text{for } |z| > a \end{cases} \text{cartesian coordinates}$$

$$(b) \rho = \begin{cases} \rho_0 & \text{for } r < a \\ 0 & \text{for } r > a \end{cases} \text{cylindrical coordinates}$$

$$(c) \rho = \begin{cases} 0 & \text{for } r < a \\ \rho_0 & \text{for } a < r < b \\ 0 & \text{for } r > b \end{cases} \text{spherical coordinates}$$

$$(d) \rho = \begin{cases} \rho_0 \left(1 - \frac{r^2}{a^2}\right) & \text{for } r < a \\ 0 & \text{for } r > a \end{cases} \text{spherical coordinates}$$

- 6.2. Show that the equation of motion of an electron in the space-charge limited vacuum diode of Example 6-2 is given by

$$\frac{d^3x}{dt^3} = \frac{eJ_0}{m\epsilon_0}$$

where  $e$  and  $m$  are the charge and mass of the electron, respectively, and  $J_0$  is the current density. For an electron leaving the cathode at  $t = 0$  and subject to the conditions stated in Example 6-2, obtain the solution for  $x(t)$  by solving the equation of motion. Then find the solution for  $V$ , which should agree with (6-22).

- 6.3. Verify the general solutions for the one-dimensional Laplace's equations and the particular solutions for the particular sets of boundary conditions listed in Table 6.1.

- 6.4. Two conductors occupying the surfaces  $r = a$  and  $r = b$  in cylindrical coordinates are kept at potentials  $V = V_0$  and  $V = 0$ , respectively. The region  $a < r < c (< b)$  is a perfect dielectric of permittivity  $\epsilon_1$  and the region  $c < r < b$  is a perfect dielectric of permittivity  $\epsilon_2$ . Find the solutions for the potentials in the two regions and the potential at the boundary  $r = c$ .

- 6.5. Two parallel conducting plates occupying the planes  $x = 0$  and  $x = d$  are kept at potentials  $V = 0$  and  $V = V_0$ , respectively. The medium between the two plates is a perfect dielectric of nonuniform permittivity given by

$$\epsilon = \epsilon_1 + (\epsilon_2 - \epsilon_1) \frac{x}{d}$$

where  $\epsilon_1$  and  $\epsilon_2$  are constants. Find the solutions for the potential and the electric field intensity between the plates.

- 6.6. The region  $0 < x < d$  is occupied by a medium characterized by the magnetization vector  $\mathbf{M} = M_0(d - x)\mathbf{i}_x$ , where  $M_0$  is a constant. By solving the analogous electrostatic problem, obtain  $\mathbf{H}$  and  $\mathbf{B}$  both inside and outside the region  $0 < x < d$ .

- 6.7. The region  $r < a$  in spherical coordinates is occupied by a medium characterized by the magnetization vector  $\mathbf{M} = M_0 \mathbf{i}_z$ , where  $M_0$  is a constant. (a) Set up the analogous electrostatic problem for obtaining  $\mathbf{H}$  and  $\mathbf{B}$  both inside and outside the region  $r < a$ . (b) Find the electric field intensity for this electrostatic problem from the answer to part (d) of Problem 5.11. (c) Find  $\mathbf{H}$  and  $\mathbf{B}$  both inside and outside the region  $r < a$ .
- 6.8. A conductor occupying the surfaces  $x > 0, y = 0$  and  $y > 0, x = 0$  is kept at zero potential. A second conductor occupying the surface  $xy = 2$  is kept at a potential of 100 volts, making sure that the edges where the two conductors touch are insulated. The medium between the conductors is charge free. Find the solutions for the potential and the electric field intensity between the conductors. Find the surface charge densities on the conductors.
- 6.9. The potential distribution at the mouth of the slot of Fig. 6.6 is given by

$$V = V_1 \sin \frac{\pi y}{b} + V_2 \sin \frac{3\pi y}{b} \quad \text{for } x = a, 0 < y < b$$

where  $V_1$  and  $V_2$  are constants. Find the solution for the potential distribution in the slot. Repeat the problem for

$$V = V_1 \sin^3 \frac{\pi y}{b} \quad \text{for } x = a, 0 < y < b$$

- 6.10. Two conductors occupying the planes  $x = 0$  and  $x = a$  are kept at zero potentials. A third conductor occupying the surface  $y = 0, 0 < x < a$  is kept at a constant potential  $V_0$ , making sure that the edges are insulated. Find the solutions for the potential in the region  $0 < x < a$  for both  $y > 0$  and  $y < 0$ . Show that the potential at large values of  $|y|$  varies with  $x$  approximately as  $\sin(\pi x/a)$ .
- 6.11. A thin rectangular slab of uniform conductivity  $\sigma_0$  mhos/m, shown in Fig. 6.78, has its edges coated with perfectly conducting material, making sure that the

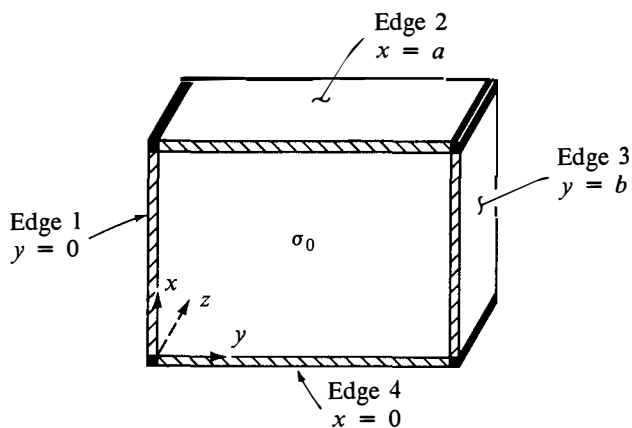


Fig. 6.78. For Problem 6.11.

corners are insulated. For each of the following cases, find the solution for the potential and hence for the current density in the conductor:

- (a) Edges 1 and 3 kept at zero potential; edge 2 kept at potential  $V_0$  and edge 4 kept at potential  $-V_0$ .
- (b) Edges 1 and 3 kept at zero potential; edges 2 and 4 kept at potential  $V_0$ .
- (c) Edges 1 and 4 kept at zero potential; edge 2 kept at potential  $V_1$  and edge 3 kept at potential  $V_2$ .

- 6.12. For the triangular box of Fig. 6.10, assume that the longer side is kept at zero potential and the shorter sides are kept at a potential of 100 volts. Find the potentials at points  $a$ ,  $b$ , and  $c$ .
- 6.13. An infinitely long line charge of uniform density  $\rho_{L0}$  C/m is situated parallel to and at a distance  $d$  from a grounded infinite plane conductor. Obtain the image charge and show that the induced surface charge on the conductor per unit length parallel to the line charge is equal to  $-\rho_{L0}$ .
- 6.14. For each of the arrangements shown in Fig. 6.79, find the image charges required to determine the electric field on the side of the actual charges. For case (a), find the electric field intensity everywhere on the conductor surface and show that the total induced charge is  $-Q$ .

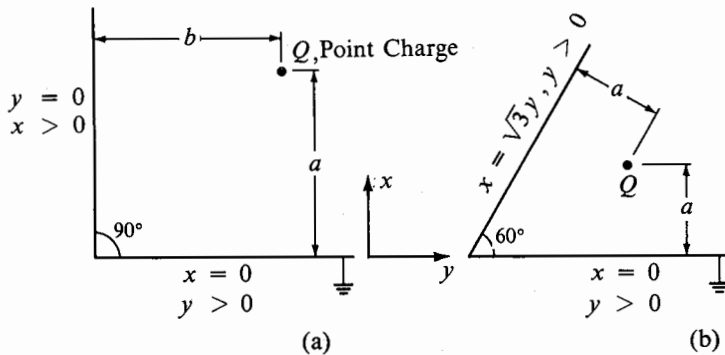


Fig. 6.79. For Problem 6.14.

- 6.15. For the infinitely long line charge of uniform density  $\rho_{L0}$  C/m parallel to an infinitely long grounded conducting cylinder in Example 6-11, show that the induced surface charge per unit length of the cylinder is  $-\rho_{L0}$ .
- 6.16. A point charge  $Q$  is situated at a distance  $d$  from the center of a grounded spherical conductor of radius  $a$  ( $< d$ ). Show that the image charge required for computing the field outside the spherical conductor is a point charge of value  $-Qa/d$ , lying at a distance  $a^2/d$  from the center of the conductor along the line joining the center to the charge  $Q$  and on the side of  $Q$ . What is the induced charge on the surface of the conductor?
- 6.17. For the problem of Example 6-4:
  - (a) Find the electric field intensities in the two regions  $0 < x < t$  and  $t < x < d$ .

- (b) Find the surface charge densities on the plates  $x = 0$  and  $x = d$ .  
 (c) Find the capacitance  $C$  per unit area of the plates and show that

$$\frac{1}{C} = \frac{1}{\epsilon_1/t} + \frac{1}{\epsilon_2/(d-t)}$$

- 6.18. For the parallel-plate arrangement of Problem 6.5, find the capacitance per unit area of the plates in three ways:  
 (a) From the definition  $C = Q/V_0$ , where  $Q$  is the magnitude of the charge per unit area on either plate.  
 (b) By evaluating the electric stored energy in the dielectric per unit area of the plates and using (6-81).  
 (c) By dividing the dielectric into several slabs, each having an infinitesimal thickness and using the result of Problem 6.17.
- 6.19. Derive the expressions for the conductance, capacitance, and inductance per unit length of the two-conductor configuration of Fig. 6.15(b).
- 6.20. For the two-conductor configuration of Fig. 6.15(d), find the locations of a pair of equal and opposite, infinitely long, uniform line charges parallel to the conductors such that two of the equipotential surfaces corresponding to the pair of line charges are the surfaces occupied by the conductors. Then find the expressions for conductance, capacitance, and inductance per unit length of the conductor system. Let  $d$  be equal to zero and show that these expressions reduce to those for the configuration of Fig. 6.15(b).
- 6.21. A current  $I$  amp flows with nonuniform volume density given by

$$\mathbf{J} = J_0 \frac{r}{a} \mathbf{i}_z$$

along an infinitely long cylindrical conductor of radius  $a$  having the  $z$  axis as its axis. The current returns with uniform surface density in the opposite direction along the surface of an infinitely long perfectly conducting cylinder of radius  $b$  ( $> a$ ) and coaxial with the inner conductor. Find the internal inductance per unit length of the inner conductor by using the method of flux linkages. Verify your answer by using the energy method.

- 6.22. A filamentary wire carrying a current  $I$  amp is closely wound around a toroidal magnetic core of rectangular cross section as shown in Fig. 6.80. The mean radius

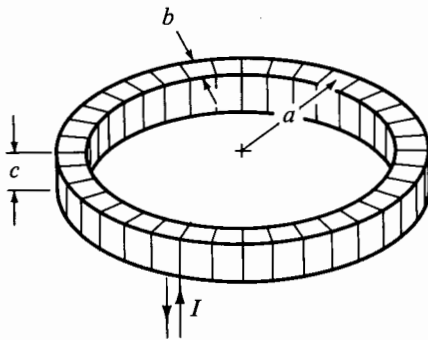


Fig. 6.80. For Problem 6.22.

of the toroidal core is  $a$  and the number of turns per unit length along the mean circumference of the toroid is  $N$ . Find the inductance of the toroid.

- 6.23. An infinitely long, uniformly wound solenoid of radius  $a$  and having  $N$  turns per unit length carries a current  $I$  amp. Find the inductance per unit length of the solenoid.
- 6.24. Show that  $L_{21} = L_{12}$ .
- 6.25. An infinitely long, uniformly wound solenoid of radius  $a$  and having  $N_1$  turns per unit length is coaxial with another infinitely long, uniformly wound solenoid of radius  $b$  ( $> a$ ) and having  $N_2$  turns per unit length. Find the mutual inductance per unit length of the solenoids.
- 6.26. A cylindrical slab of material lying between plane surfaces  $z = 0$  and  $z = d$  and having a cross-sectional area  $A = \pi a^2$  is characterized by nonuniform conductivity

$$\sigma = \frac{\sigma_0}{1 + z/d}$$

permittivity  $\epsilon = 4\epsilon_0$ , and permeability  $\mu = 2\mu_0$ , where  $\sigma_0$  is a constant. The surfaces  $z = 0$  and  $z = d$  are perfectly conducting. A current flows through perfectly conducting filamentary wires into the center of the plane surface  $z = d$  and out of the center of the plane surface  $z = 0$ . Assume that this current is established by appropriate connection of a battery of voltage  $V_0$  which is far away from the material so that the magnetic field outside the slab may be considered to be the same as that due to an infinitely long wire along the axis of the slab ( $z$  axis). Find the following quantities:

- The electric field intensity, the conduction current density, and the displacement flux density in the material.
- The surface charge densities on the perfectly conducting surfaces  $z = 0$  and  $z = d$ .
- The true charge density in the material.
- The polarization vector and the polarization charge distribution in the material.
- The magnetic field intensity and the magnetic flux density in the material.
- The current drawn from the battery and the magnetic field intensity outside the material.
- The surface current density on the perfectly conducting surfaces  $z = 0$  and  $z = d$ .
- The magnetization vector and the magnetization current distribution in the material.
- The power dissipation density and the power dissipated in the material and the conductance of the configuration.
- The electric stored energy density and the electric stored energy in the material and the capacitance of the configuration.
- The magnetic stored energy density and the magnetic stored energy in the material and the internal inductance of the configuration.
- The power flow into the material evaluated by surface integration of the Poynting vector.

- 6.27. A toroidal magnetic core of circular cross section and with an air gap has the following dimensions:

$$\text{area of cross section} = 2 \text{ cm}^2$$

$$\text{mean circumference} = 20 \text{ cm}$$

$$\text{air gap width} = 0.1 \text{ cm}$$

Find the ampere turns required to establish a magnetic flux of  $3 \times 10^{-4}$  Wb in the air gap if the core is made of annealed sheet steel. The effective area of the air gap is that of a circle whose radius exceeds the actual radius by half the width of the air gap.

- 6.28. For the magnetic circuit of Fig. 6.23, assume that there is no air gap. If  $NI$  is equal to 150 amp-turns, find the magnetic flux density in leg 2.
- 6.29. For the structure of Fig. 6.25(a), show that, under quasistatic conditions, the rate at which energy flows into the volume of the structure as obtained by surface integration of the Poynting vector over the surface bounding the volume is equal to

$$\frac{d}{dt} \left[ \frac{1}{2} CV^2(t) \right]$$

- 6.30. For the structure of Fig. 6.25(b), show that, under quasistatic conditions, the rate at which energy flows into the volume of the structure as obtained by surface integration of the Poynting vector over the surface bounding the volume is equal to

$$\frac{d}{dt} \left[ \frac{1}{2} LI^2(t) \right]$$

- 6.31. By proceeding in a manner similar to that in Example 6-16, show that the quasistatic approximation holds for the parallel-plate structure of Fig. 6.25(a), that is, the structure behaves like a single capacitor, for the condition

$$f \ll \frac{1}{2\pi l \sqrt{\mu\epsilon}}$$

Examine the input behavior of the structure for frequencies beyond the value for which the quasistatic approximation holds.

- 6.32. A time-varying voltage source drives the structure of Fig. 6.13(a). Assume that the conductor is a good conductor so that the displacement current can be neglected compared to the conduction current. Show that the quasistatic approximation holds, that is, the structure behaves essentially like a single resistor, for the condition

$$f \ll \frac{1}{\pi \mu \sigma l^2}$$

Investigate the approximation quantitatively for copper. Examine the input behavior of the structure for frequencies slightly beyond the value for which the quasistatic approximation holds and also for frequencies for which  $f \gg 1/\pi \mu \sigma l^2$ .

- 6.33. The structure shown in Fig. 6.81 is an arrangement of two parallel perfectly conducting plates connected at one end by a third perfectly conducting plate. A current source  $I(t) = 1 \cos 2\pi ft$  amp is connected between the plates at the other end so that it supplies a  $z$ -directed current uniformly distributed in the  $y$  direction to the structure. The medium between the plates is free space. For the purpose of this



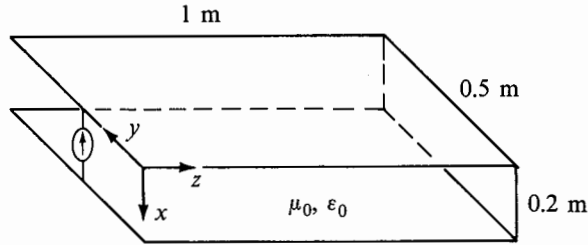


Fig. 6.81. For Problem 6.33.

problem, the arrangement can be assumed to be part of a structure infinite in extent in the  $y$  direction. The dimensions of the structure are indicated in the figure.

- (a) Find the voltage developed across the current source in the steady state if  $f = 150$  Hz.
- (b) Repeat part (a) if  $f = 150$  MHz.

6.34. Derive the transmission-line equations by considering the special case of two infinitely long, coaxial cylindrical conductors. Also show that the power flow along the conductor system is equal to the product of the voltage between the conductors and current along the conductors.

6.35. Show that two alternative representations of the circuit equivalent of the transmission-line equations (6-161) and (6-165) are as shown in Figs. 6.82(a) and (b).

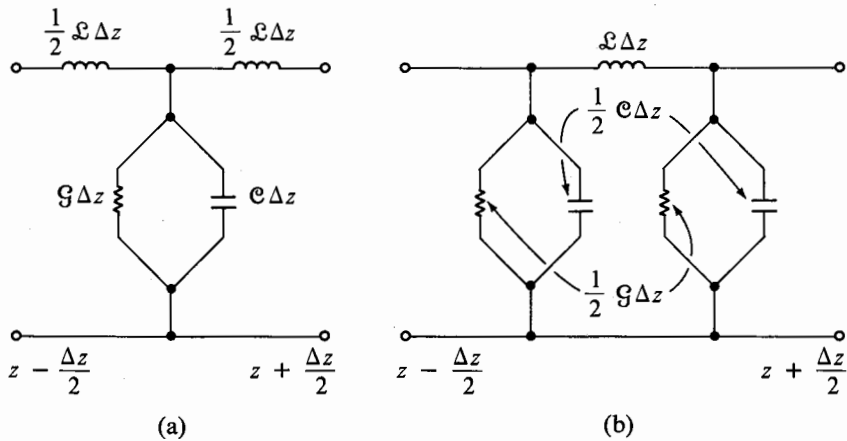


Fig. 6.82. For Problem 6.35.

6.36. Starting with the curl of both sides of (6-169d), derive the wave equation for  $\mathbf{H}$  given by

$$\nabla^2 \mathbf{H} = \mu \epsilon \frac{\partial^2 \mathbf{H}}{\partial t^2}$$

- 6.37. Solve Eq. (6-176) by using the separation of variables technique.
- 6.38. Draw three-dimensional sketches similar to that of Fig. 6.30 for the following functions:
- $e^{-|t-z|}$
  - $e^{-|t+z|}$
  - $(z-t)^2[u(z-t) - u(z-t-2)]$
- 6.39. A spherical balloon of uniform surface charge density and having its center at the origin possesses a constant total charge  $Q$ . Its radius  $c$  is made to vary sinusoidally between a minimum of  $(a-b)$  and a maximum of  $(a+b)$  in the manner
- $$c = a + b \cos 2\pi t.$$
- Describe and sketch how the electric field intensity vector  $\mathbf{E}$  varies with time in three regions  
 $0 < r < (a-b)$      $(a-b) < r < (a+b)$      $(a+b) < r < \infty$   
 Assume uniform surface charge density for all  $t$ .
  - From your answer to part (a) for the region  $(a+b) < r < \infty$ , what can you infer about wave propagation due to the fluctuating balloon? Explain.
- 6.40. A uniform plane wave traveling in the negative  $z$  direction in free space has its electric field entirely along the  $x$  direction. The space variation of the electric field intensity at time  $t = 0$  is shown in Fig. 6.83. Find and sketch the time variation of the magnetic field intensity in the  $z = 200$  m plane.

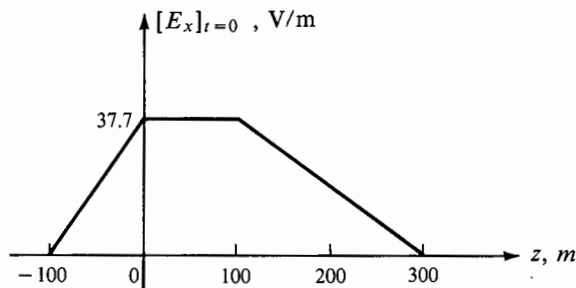


Fig. 6.83. For Problem 6.40.

- 6.41. The electric field intensity associated with a uniform plane wave traveling in a perfect dielectric medium is given by
- $$E_x(z, t) = 10 \cos(2\pi \times 10^7 t - 0.1\pi z) \text{ volts/m}$$
- Sketch  $E_x$  versus  $t$  for two values of  $z$ ,  $z = 0$  and  $z = 5$  m. What is the frequency of the wave?
  - Sketch  $E_x$  versus  $z$  for two values of  $t$ ,  $t = 0$  and  $t = \frac{1}{4} \times 10^{-7}$  sec. What is the wavelength?
  - What is the velocity of propagation?
  - Write the expression for the magnetic field intensity associated with the wave if  $\mu = \mu_0$ .
- 6.42. The complex electric field vector of a uniform plane wave propagating in free space is given by

$$\vec{\mathbf{E}} = (-\mathbf{i}_x - 2\sqrt{3}\mathbf{i}_y + \sqrt{3}\mathbf{i}_z)e^{-j0.04\pi(\sqrt{3}x - 2y - 3z)} \text{ volts/m}$$

- What is the direction of propagation of the wave?
- Find the wavelength along the direction of propagation.
- Find the frequency of the wave.
- Find the apparent wavelengths and the apparent phase velocities along the  $x$ ,  $y$ , and  $z$  axes.
- Discuss the polarization of the wave.
- Obtain the expression for the complex magnetic field vector of the wave.

6.43. A complex electric field vector is given by

$$\bar{\mathbf{E}} = \left[ \left( -\sqrt{3} - j\frac{1}{2} \right) \mathbf{i}_x + \left( 1 - j\frac{\sqrt{3}}{2} \right) \mathbf{i}_y + j\sqrt{3} \mathbf{i}_z \right] e^{-j0.02\pi(\sqrt{3}x+3y+2z)} \quad \text{volts/m}$$

- Perform the necessary tests and determine if the given  $\bar{\mathbf{E}}$  represents the electric field of a uniform plane wave.
- If your answer to part (a) is “yes,” repeat Problem 6.42 for the electric field vector of this problem.

6.44. The complex electric and magnetic field vectors in a perfect dielectric medium are given by

$$\bar{\mathbf{E}} = (-j\mathbf{i}_x - 2\mathbf{i}_y + j\sqrt{3}\mathbf{i}_z) e^{-j0.05\pi(\sqrt{3}x+z)} \quad \text{volts/m}$$

$$\bar{\mathbf{H}} = \frac{1}{60\pi} (\mathbf{i}_x - j2\mathbf{i}_y - \sqrt{3}\mathbf{i}_z) e^{-j0.05\pi(\sqrt{3}x+z)} \quad \text{amp/m}$$

- Perform the necessary tests and determine if these vectors represent the fields associated with a uniform plane wave.
- If your answer to part (a) is “yes,” find the direction of propagation, the wavelength along the direction of propagation, the velocity along the direction of propagation, and the frequency. Also, discuss the polarization of the wave.

6.45. Show that the units of  $1/\sqrt{\mathcal{L}\mathcal{C}}$  are meters per second and the units of  $\sqrt{\mathcal{L}/\mathcal{C}}$  are ohms.

6.46. The plane  $z = 0$  is occupied by a perfect conductor. The medium  $z < 0$  is free space. The leading edge of a uniform plane wave traveling in the positive  $z$  direction and having  $E_x(z)$  as shown in Fig. 6.84 is incident on the plane  $z = -150$  m at

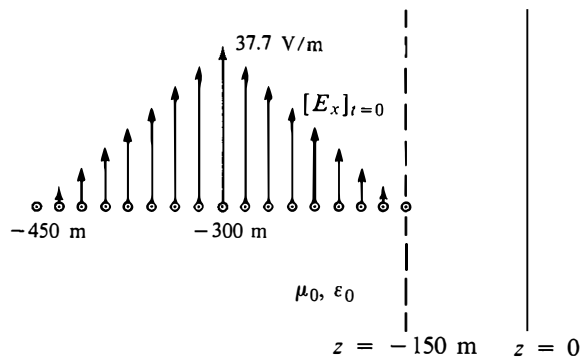


Fig. 6.84. For Problem 6.46.

$t = 0$ . Find and sketch  $E_x$  and  $H_y$  versus  $z$  for  $t$  equal to  $\frac{1}{4} \mu\text{sec}$ ,  $\frac{3}{4} \mu\text{sec}$ ,  $1 \mu\text{sec}$ ,  $1\frac{1}{4} \mu\text{sec}$ , and  $2 \mu\text{sec}$ . Also sketch  $E_x$  and  $H_y$  versus  $t$  in the plane  $z = -150 \text{ m}$ .

6.47. For the problem of Example 6-20:

- (a) Sketch  $E_x$  versus  $z$  for  $t = 0.015 \mu\text{sec}$  and  $0.035 \mu\text{sec}$ .
- (b) Draw the bounce diagram for  $H_y$  and sketch  $H_y$  in the planes  $z = -3 \text{ m}$  and  $z = 2.5 \text{ m}$  as functions of time for  $t \geq 0$ . Also sketch  $H_y$  versus  $z$  for values of  $t$  equal to  $0.015 \mu\text{sec}$  and  $0.035 \mu\text{sec}$ .

6.48. In the transmission-line system shown in Fig. 6.85, the switch  $S$  is closed at  $t = 0$ .

(a) Show that, for  $0 < t < l/v$ , a (+) wave of voltage

$$V^+(z, t) = \frac{Z_0}{R_g + Z_0} V_g \left( t - \frac{z}{v} \right)$$

exists on the line. What is the current associated with the (+) wave?

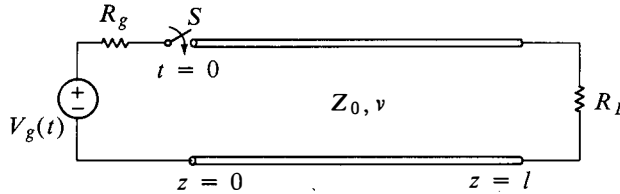


Fig. 6.85. For Problem 6.48.

(b) Show that for  $l/v < t < 2l/v$ , a (-) wave of voltage

$$V^-(z, t) = \frac{Z_0}{R_g + Z_0} \Gamma_R V_g \left( t - \frac{2l}{v} + \frac{z}{v} \right) \quad \text{where } \Gamma_R = \frac{R_L - Z_0}{R_L + Z_0}$$

exists on the line in addition to the (+) wave specified in part (a). What is the current associated with the (-) wave?

(c) Show that for  $2l/v < t < 3l/v$ , a (-+) wave of voltage

$$V^{-+}(z, t) = \frac{Z_0}{R_g + Z_0} \Gamma_R \Gamma_g V_g \left( t - \frac{2l}{v} - \frac{z}{v} \right) \quad \text{where } \Gamma_g = \frac{R_g - Z_0}{R_g + Z_0}$$

exists on the line in addition to the (+) and (-) waves specified in parts (a) and (b), respectively. What is the current associated with the (-+) wave?

(d) Show that the line voltage and line current at  $t = \infty$  are given by the expressions

$$V_{SS}(z, t) = \frac{Z_0}{R_g + Z_0} \left[ \sum_{n=0}^{\infty} (\Gamma_R \Gamma_g)^n V_g \left( t - \frac{2nl}{v} - \frac{z}{v} \right) + \Gamma_R \sum_{n=0}^{\infty} (\Gamma_R \Gamma_g)^n V_g \left( t - \frac{2nl}{v} + \frac{z}{v} - \frac{2l}{v} \right) \right]$$

$$I_{SS}(z, t) = \frac{1}{R_g + Z_0} \left[ \sum_{n=0}^{\infty} (\Gamma_R \Gamma_g)^n V_g \left( t - \frac{2nl}{v} - \frac{z}{v} \right) - \Gamma_R \sum_{n=0}^{\infty} (\Gamma_R \Gamma_g)^n V_g \left( t - \frac{2nl}{v} + \frac{z}{v} - \frac{2l}{v} \right) \right]$$

(e) Obtain closed-form expressions for  $V_{SS}(z, t)$  and  $I_{SS}(z, t)$  for two cases:

- (i)  $V_g(t) = V_0$ , a constant and (ii)  $V_g(t) = V_0 \cos \omega t$ .

- 6.49. A transmission-line of characteristic impedance  $Z_0$  is terminated by an inductor of value  $L$  henries. A (+) wave of constant voltage  $V_0$  is incident on the termination at  $t = 0$ . Show that the resulting (-) wave voltage at the termination is given by

$$V^-(t) = -V_0 + 2V_0e^{-(Z_0/L)t}$$

- 6.50. In Fig. 6.86, a transmission-line of characteristic impedance 50 ohms is terminated by a passive nonlinear element having the volt-ampere characteristic indicated in the figure. If a (+) wave of constant voltage 10 volts is incident on the termination, find the resulting (-) wave voltage.

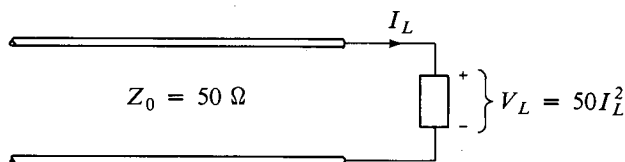


Fig. 6.86. For Problem 6.50.

- 6.51. Draw sketches of  $V$  and  $I$  given by Eqs. (6-231a) and (6-231b), respectively, versus  $t$  for values of  $d$  equal to 0,  $\lambda/8$ ,  $\lambda/4$ ,  $3\lambda/8$ , and  $\lambda/2$ . Consider  $\theta = 0$  for simplicity.
- 6.52. A transmission-line of length  $l$  is short circuited at one end and open circuited at the other end. What are the natural frequencies of oscillation? Sketch the voltage and current standing wave patterns for the first few modes. Repeat for a line of length  $l$  which is open circuited at both ends.
- 6.53. The transmission-line system shown in Fig. 6.87 is in sinusoidal steady state. The voltage source  $V_g(t)$  is equal to  $10 \cos 1000\pi t + 5 \cos 2000\pi t$  volts.

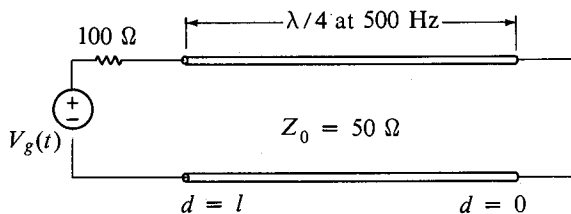


Fig. 6.87. For Problem 6.53.

- What is the impedance seen looking into the input terminals of the line for  $f = 500$  Hz? Sketch the voltage and current standing wave patterns for  $f = 500$  Hz.
- What is the impedance seen looking into the input terminals of the line for  $f = 1000$  Hz? Sketch the voltage and current standing wave patterns for  $f = 1000$  Hz.
- From the standing wave patterns of parts (a) and (b), compute the values of root-mean-square line voltages and line currents at  $d = 0$ ,  $d = l/2$ , and  $d = l$ .

- 6.54. Find the two lowest frequencies (zero excluded) for which a transmission-line of length  $l$  short circuited at its far end behaves at its input as an inductor of value equal to its inductance computed from static field considerations.
- 6.55. Show that the minima in the standing wave patterns of Fig. 6.48 are sharper than the maxima.
- 6.56. Show that the line impedance at a voltage maximum is  $Z_0(\text{VSWR})$  and the line impedance at a voltage minimum is  $Z_0/(\text{VSWR})$ .
- 6.57. Repeat Example 6-23 for frequency of the uniform plane wave equal to 6000 MHz. Find the fraction of the incident power transmitted into medium 3.
- 6.58. Repeat Example 6-23 for frequency of the uniform plane wave equal to 1500 MHz. Find the fraction of the incident power transmitted into medium 3. Also find the wave impedance in medium 1 at a distance of 4 cm from the interface between media 1 and 2.
- 6.59. Find the thickness and permittivity of a quarter-wave dielectric coating which will eliminate reflections of uniform plane waves of frequency 1500 MHz incident normally from free space onto a dielectric of permittivity  $16\epsilon_0$ . Assume all media to have  $\mu = \mu_0$ .
- 6.60. A transmission line of characteristic impedance 50 ohms is terminated by an unknown load impedance  $\bar{Z}_R$ . Standing wave measurements indicate VSWR equal to 3.0. Distance between successive voltage minima is 20 cm and distance between load and first voltage minimum is 15 cm.
- (a) Find  $\bar{Z}_R$ .
- (b) Find the location nearest to the load and the characteristic impedance of a quarter-wave section required to achieve a match between the line and the load.
- 6.61. A transmission line of characteristic impedance 50 ohms is terminated by a certain load impedance. It is found that the VSWR on the line is equal to 5.0. The first voltage minimum is located to be at  $0.1\lambda$  from the load. Determine analytically the location and the length of a short-circuited stub connected in parallel with the line so that a match is obtained between the line and the load. Assume the characteristic impedance of the stub to be 50 ohms. Repeat the problem for characteristic impedance of stub equal to 100 ohms.
- 6.62. A transmission line of characteristic impedance 50 ohms is terminated by a certain load impedance. It is found that the VSWR on the line is equal to 3.0. The first voltage minimum is located at 5.80 cm from the load and the next voltage minimum at 25.80 cm from the load. Find analytically the value of the minimum VSWR that can be achieved on the line by placing a stub in parallel with the line at the load.
- 6.63. A transmission line of characteristic impedance 100 ohms is terminated by a load impedance  $(80 + j200)$  ohms. Using the Smith chart, find the following quantities:
- (a) The reflection coefficient at the load.
- (b) VSWR on the line.
- (c) The distance of the first voltage minimum of the standing wave pattern from the load.
- (d) The line impedance at  $d = 0.1\lambda$ .

- (e) The line admittance at  $d = 0.1\lambda$ .
- (f) The location nearest to the load at which the real part of the line admittance is equal to the line characteristic admittance.
- 6.64. Solve Problem 6.58 using the Smith chart.
- 6.65. Solve Problem 6.61 using the Smith chart.
- 6.66. Solve Problem 6.62 using the Smith chart.
- 6.67. The dimension  $a$  of a parallel-plate waveguide filled with a dielectric of permittivity  $\epsilon = 4\epsilon_0$  is 4.0 cm. Determine the propagating  $TE_{m,0}$  modes for a wave frequency of 6000 MHz. For each propagating mode, find (a) the cutoff frequency, (b) the angle  $\theta_i$  at which the wave bounces obliquely between the conductors, (c) the guide wavelength  $\lambda_g$ , (d) the phase velocity  $v_{pz}$ , and (e) the guide impedance  $\eta_g$ .
- 6.68. Consider a parallel-plate waveguide extending in the  $z$  direction with a dielectric discontinuity at  $z = 0$ . A  $TE_{m,0}$  wave is incident on the discontinuity from the side  $z < 0$ . By making use of the boundary conditions at the discontinuity, show that each section of the guide can be replaced by the corresponding transmission-line equivalent shown in Fig. 6.59, for the purpose of solving reflection, transmission, and matching problems involving power flow in the  $z$  direction.
- 6.69. In Section 6.12 we introduced transverse electric or TE waves by considering oblique incidence of a linearly polarized uniform plane wave on a perfect conductor with its electric field entirely parallel to the plane of the conductor. To investigate transverse magnetic or TM waves, consider a linearly polarized, uniform plane wave having its magnetic field entirely along the  $y$  direction and incident obliquely upon a perfect conductor occupying the  $x = 0$  plane as shown in Fig. 6.88.

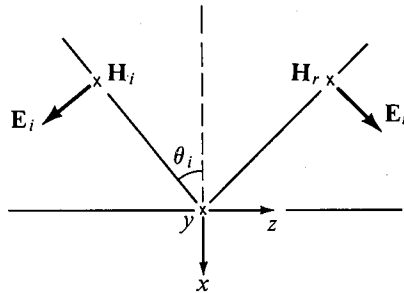


Fig. 6.88. For Problem 6.69.

- (a) Obtain the expressions for the total fields.
- (b) Show that  $\bar{E}_z = 0$  at the surface of the conductor as well as in planes  $x = -m\lambda/(2 \cos \theta_i)$ ,  $m = 1, 2, 3, \dots$
- (c) For a parallel-plate guide of spacing  $a$  between the plates, find the expressions for the cutoff wavelengths, cutoff frequencies, guide wavelengths, and the phase velocities in the  $z$  direction for the  $TM_{m,0}$  modes.
- (d) Write expressions for the total fields in the guide independent of  $\theta_i$ .
- (e) Define guide impedance and obtain the transmission-line equivalent for power flow along the guide.

- 6.70. Using the transmission-line equivalent determined in Problem 6.69, repeat Example 6-29 for  $TM_{1,0}$  waves of frequency 6000 MHz.
- 6.71. Show that

$$v_{gz} = \frac{v_{pz}}{1 - (\omega/v_{pz})(dv_{pz}/d\omega)}$$

- 6.72. For the parallel-plate waveguide of Problem 6.67, obtain the group velocities for the propagating modes for a wave of frequency 6000 MHz.
- 6.73. For a tapered transmission line, the inductance and capacitance per unit length are functions of position  $z$  along the line.
- (a) Show that the line voltage and line current in the sinusoidal steady state satisfy the equations

$$\frac{\partial^2 \bar{V}}{\partial z^2} - \frac{1}{\mathcal{L}} \left( \frac{\partial \mathcal{L}}{\partial z} \right) \left( \frac{\partial \bar{V}}{\partial z} \right) + \omega^2 \mathcal{L} \mathcal{C} \bar{V} = 0$$

$$\frac{\partial^2 \bar{I}}{\partial z^2} - \frac{1}{\mathcal{C}} \left( \frac{\partial \mathcal{C}}{\partial z} \right) \left( \frac{\partial \bar{I}}{\partial z} \right) + \omega^2 \mathcal{L} \mathcal{C} \bar{I} = 0$$

- (b) If  $\mathcal{L}(z)$  and  $\mathcal{C}(z)$  for a particular tapered transmission line are given by

$$\mathcal{L}(z) = \mathcal{L}_0 e^{-az} \quad \text{and} \quad \mathcal{C} = \mathcal{C}_0 e^{az}$$

where  $\mathcal{L}_0$ ,  $\mathcal{C}_0$ , and  $a$  are constants, find the solutions for  $\bar{V}$  and  $\bar{I}$  and show that there exists a cutoff frequency below which wave propagation does not occur.

- 6.74. Obtain the expression for the attenuation constant per wavelength in a lossy medium characterized by  $\sigma$ ,  $\mu$ , and  $\epsilon$ . Plot the attenuation constant per wavelength versus  $\sigma/\omega\epsilon$ .
- 6.75. For uniform plane waves in fresh lake water ( $\sigma = 10^{-3}$  mho/m,  $\epsilon = 80\epsilon_0$ ,  $\mu = \mu_0$ ), find  $\alpha$ ,  $\beta$ ,  $\bar{\eta}$ , and  $\lambda$  for two frequencies: (a) 100 MHz and (b) 10 kHz.
- 6.76. A uniform plane wave of frequency  $f$  is incident normally from free space onto a plane slab of good conductor of infinite depth and conductivity  $\sigma$ . Obtain the expression for the fraction of the incident power reflected and the fraction of the incident power transmitted into the conductor. Compute numerical values for incidence from free space to copper at 30 MHz.
- 6.77. (a) Express Eqs. (6-281a) and (6-281b) in terms of the distance variable  $d$ .  
 (b) Show that the wave impedance  $\bar{Z}(d)$  is given by

$$\bar{Z}(d) = \bar{\eta} \frac{1 + \bar{\Gamma}(d)}{1 - \bar{\Gamma}(d)}$$

where  $\bar{\Gamma}(d) = \bar{\Gamma}(0)e^{-2\gamma d} = \bar{\Gamma}(0)e^{-2\alpha d}e^{-j2\beta d}$ .

- (c) In Fig. 6.89, a thin slab of good conductor having a thickness  $t$  is backed by a perfect dielectric of thickness  $\lambda/4$  at the frequency of operation, which in turn is backed by a perfect conductor. Show that, for uniform plane waves incident normally on the good conductor, reflections are eliminated if  $\alpha_c t \ll 1$



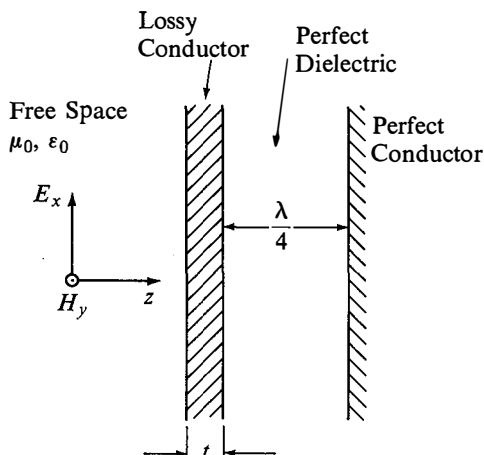


Fig. 6.89. For Problem 6.77.

and  $\sigma = 1/\eta_0 t$ , where  $\alpha_c$  and  $\sigma$  are the attenuation constant and conductivity, respectively, of the good conductor.

- 6.78. For the semiinfinite plane slab conductor of Fig. 6.66, show that (a) the real part on the right side of (6-294) is the same as the result that would be obtained by a volume integration of the time-average power dissipation density  $\frac{1}{2}\sigma |\bar{E}_x|^2$  and (b) the imaginary part on the right side of (6-294) divided by  $2\omega$  is the same as the result that would be obtained by a volume integration of the time-average magnetic stored energy density  $\frac{1}{4}\mu |\bar{H}_y|^2$ .
- 6.79. For the lossy transmission line of Fig. 6.69,
- Write the transmission-line equations.
  - Find  $\bar{\gamma}$  and  $\bar{Z}_0$ .
  - Show that for  $2\mathcal{R}_i/(2\mathcal{L}_i + \mathcal{L}) = \mathcal{G}/\mathcal{C}$ ,  $\beta = \omega\sqrt{(2\mathcal{L}_i + \mathcal{L})\mathcal{C}}$ . What is the attenuation constant for this condition?
- 6.80. For the parallel-plate resonator of Fig. 6.71, show that the total energy density in the two fields from  $d = 0$  to  $d = l$  computed by considering the energy density in the electric field at a time at which the magnetic field is zero everywhere between the plates is the same as that given by (6-299).
- 6.81. The arrangement shown in Fig. 6.90 is that of a parallel-plate resonator made up of two dielectric slabs of thicknesses  $t$  and  $(l - t)$  and backed by perfect conductors.

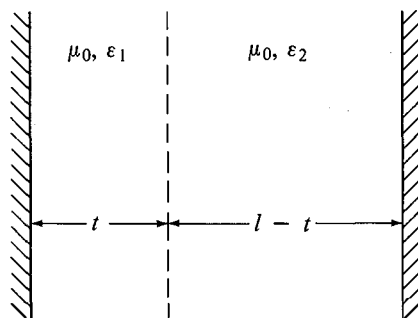
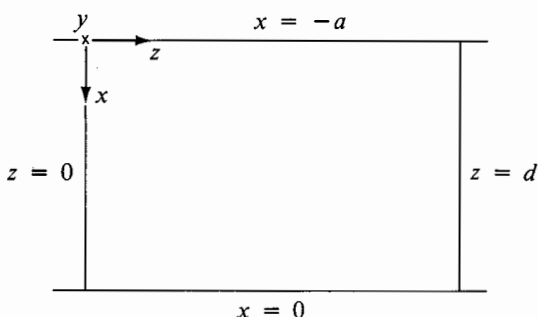


Fig. 6.90. For Problem 6.81.

- (a) Show that the resonant frequencies of the system are given by the roots of the equation

$$\tan \omega \sqrt{\mu_0 \epsilon_1} t + \sqrt{\frac{\epsilon_1}{\epsilon_2}} \tan \omega \sqrt{\mu_0 \epsilon_2} (l - t) = 0$$

- (b) Find the three lowest resonant frequencies if  $t = l/2$ ,  $l = 5.0$  cm,  $\epsilon_1 = \epsilon_0$ , and  $\epsilon_2 = 4\epsilon_0$ .
- 6.82.** For the parallel-plate resonator of Example 6-32, show that, for a particular mode of operation,  $Q$  is inversely proportional to  $\sqrt{f}$ .
- 6.83.** A resonator is formed by placing perfect conductors in two transverse planes  $z = 0$  and  $z = d$  of a parallel-plate waveguide of spacing  $a$ , as shown in Fig. 6.91.



**Fig. 6.91.** For Problem 6.83.

- (a) Show that the resonant frequencies corresponding to the  $TE_{m,0,l}$  modes are given by

$$f_{m,0,l} = \frac{1}{2\sqrt{\mu\epsilon}} \sqrt{\left(\frac{m}{a}\right)^2 + \left(\frac{l}{d}\right)^2}$$

Compute the lowest three resonant frequencies if  $a = d = 4$  cm. Identify the corresponding mode numbers. Assume free space for the medium between the plates.

- (b) Write the expressions for the fields corresponding to the  $TE_{1,0,1}$  mode. Derive the expression for the  $Q$  of the resonator for the  $TE_{1,0,1}$  mode, assuming that the plates are made up of imperfect conductors of conductivity  $\sigma$  and having thicknesses of several skin depths for the frequencies of interest.
- 6.84.** For the parallel-plate resonator of Fig. 6.70, assume that the dielectric is slightly lossy, having a conductivity  $\sigma_a \ll \omega\epsilon$ .
- (a) Assuming the plates to be perfect conductors, show that the  $Q$  of the resonator is given by  $Q_1 = \omega\epsilon/\sigma_a$ .
- (b) If, in addition to the slightly lossy dielectric, the plates are made up of slightly lossy conductors, show that the  $Q$  of the resonator is given by

$$\frac{1}{Q} = \frac{1}{Q_1} + \frac{1}{Q_2}$$

where  $Q_1$  is as given in part (a) and  $Q_2$  is equal to  $l/2\delta$  as derived in Example 6-32.

- 6.85. Show that the units of  $\sqrt{Ne^2/m\epsilon_0}$  are (seconds) $^{-1}$  and that  $e^2/4\pi^2m\epsilon_0$  is equal to 80.6.
- 6.86. The maximum plasma frequency of the plane ionosphere considered in Example 6-33 is 10 MHz.
- (a) What is the minimum value of  $\theta_0$  at which a signal of frequency 20 MHz can be incident on the ionosphere in order to get reflected and not to penetrate the ionosphere?
- (b) What is the maximum frequency of a signal incident on the ionosphere at an angle  $\theta_0 = 30^\circ$  so that it will be reflected?
- 6.87. In Fig. 6.92, a satellite signal of frequency  $f = 20$  MHz passes through a hypothetical plane slab ionosphere of uniform plasma frequency  $f_N = 12$  MHz. The earth's magnetic field and the effect of electron collisions with heavy particles are to be neglected. Find the true elevation angle of the satellite as seen from the receiver.

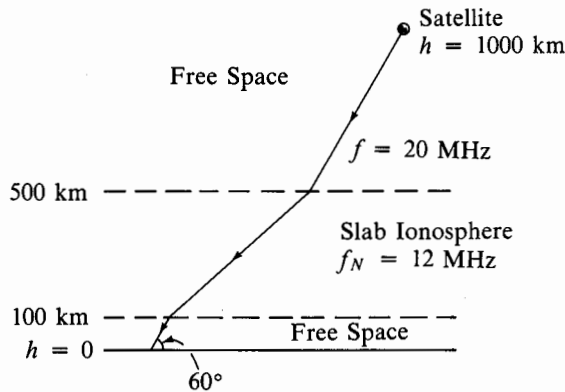


Fig. 6.92. For Problem 6.87.

- 6.88. A technique of locating the position of an aircraft is by measuring its ranges from a system of satellites of known locations. The apparent range between a satellite and the aircraft is obtained by measuring the time delay of a pulsed continuous wave signal and multiplying it by the velocity of light in free space. The range is an apparent value because the time delay is determined by the group velocity of the signal in the intervening medium which is not free space. For a signal of frequency  $f$  much larger than the maximum plasma frequency in the ionosphere and neglecting earth's magnetic field, show that the apparent range is greater than the true range by the amount  $(40.3/f^2) \int_A^S N ds$ , where  $\int_A^S N ds$  is the integrated electron density in a column of cross section  $1 \text{ m}^2$  from the aircraft ( $A$ ) to the satellite ( $S$ ) and  $f$  is in hertz. For  $\int_A^S N ds = 10^{18}$  electrons/ $\text{m}^2$ , find the excess range for two frequencies: (a) 140 MHz, (b) 1,600 MHz.

- 6.89. Two Hertzian dipoles situated at the origin and carrying currents of the same frequency are oriented along the  $x$  and  $z$  axes, respectively. The dipoles are of the same length and their currents are equal in magnitude and in phase. Discuss the polarization of the radiation field due to the dipole arrangement at (a) a point along the  $x$  axis, (b) a point along the  $z$  axis, (c) a point along the  $y$  axis, and (d) a point along the line  $x = 0, y = z$ . Repeat for the dipole currents equal in magnitude but differing in phase by  $\pi/2$ .
- 6.90. The oscillating version of the static magnetic dipole consists of a circular loop of wire of radius  $a$  carrying current varying sinusoidally with time. For circumference of the loop small compared to the wavelength, the current can be considered to be uniform and in phase around the loop so that it is given by  $I(t) = I_0 \cos \omega t$ . Assume the dipole to be centered at the origin and lying in the  $xy$  plane with the current flowing in the  $\phi$  direction.
- (a) Find the time-varying magnetic vector potential due to the oscillating magnetic dipole for  $r \gg a$ .
- (b) Obtain the electromagnetic fields due to the oscillating magnetic dipole.
- (c) Show that the radiation fields due to the oscillating magnetic dipole are given by

$$\vec{E} = \frac{\beta^2 \eta \bar{I}_0 \pi a^2}{4\pi r} \sin \theta e^{-j\beta r} \mathbf{i}_\theta$$

$$\vec{H} = -\frac{\beta^2 \bar{I}_0 \pi a^2}{4\pi r} \sin \theta e^{-j\beta r} \mathbf{i}_\phi$$

- 6.91. Fig. 6.93 shows an oscillating electric quadrupole consisting of three time-varying charges given by

$$Q_1(t) = Q_2(t) = Q_0 \sin \omega t$$

$$Q_3(t) = -2Q_0 \sin \omega t$$

The charges are connected by filamentary wires.

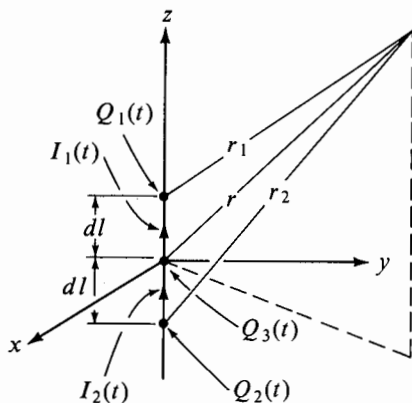


Fig. 6.93. For Problem 6.91.

- (a) Write the expressions for the currents  $I_1(t)$  and  $I_2(t)$  such that the continuity equation is satisfied.
- (b) Find the time-varying magnetic vector potential due to the oscillating quadrupole, in the limit that  $dl \rightarrow 0$  keeping  $Q_0(dl)^2$  constant.

- (c) Find the electromagnetic fields due to the oscillating quadrupole.  
 (d) Find the radiation fields due to the oscillating quadrupole. Verify by deriving them directly from the radiation fields due to the oscillating dipole given by Eqs. (6-339) and (6-340).
- 6.92.** Find the radiation resistance of a straight copper wire of length 1 cm carrying current of frequency 100 MHz. Compare the radiation resistance with the ohmic resistance of the wire (taking into account skin effect) if it has a cylindrical cross section of radius 1 mm. Repeat for a frequency of 300 MHz.
- 6.93.** A half-wave dipole is a center-fed, straight wire antenna having a length equal to half the wavelength. The current distribution along the half-wave dipole is given by

$$\bar{I}(z) = \bar{I}_0 \cos \frac{\pi z}{L} \quad \text{for} \quad -\frac{L}{2} < z < \frac{L}{2}$$

as shown in Fig. 6.94.

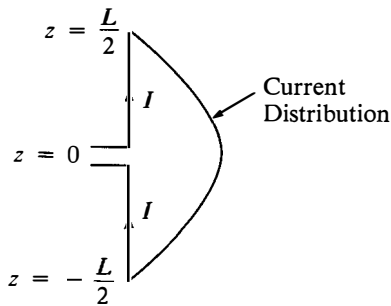


Fig. 6.94. For Problem 6.93.

- (a) Show that the radiation fields of the half-wave dipole are

$$\bar{E}_\theta = \frac{j\eta\bar{I}_0 e^{-j(\pi/L)r} \cos[(\pi/2) \cos \theta]}{2\pi r \sin \theta}$$

$$\bar{H}_\phi = \frac{j\bar{I}_0 e^{-j(\pi/L)r} \cos[(\pi/2) \cos \theta]}{2\pi r \sin \theta}$$

- (b) Show that the radiation resistance of the half-wave dipole in free space is 73 ohms, given that

$$\int_{\theta=0}^{\pi/2} \frac{\cos^2[(\pi/2) \cos \theta]}{\sin \theta} d\theta = 0.609$$

- (c) Sketch the normalized radiation intensity pattern.  
 (d) Show that the directivity of the half-wave dipole is 1.64.
- 6.94.** Two identical short dipoles form an array as shown in Fig. 6.95. Show that the radiation fields due to the array are given by the radiation fields due to one of the dipoles multiplied by the factor  $2 \cos[(\beta d \sin \theta \cos \phi)/2]$ . Plot the normalized

radiation intensity patterns in three planes: (a)  $\phi = \pi/2$ , (b)  $\phi = 0$ , and (c)  $\theta = \pi/2$  for  $d = \lambda/2$ .

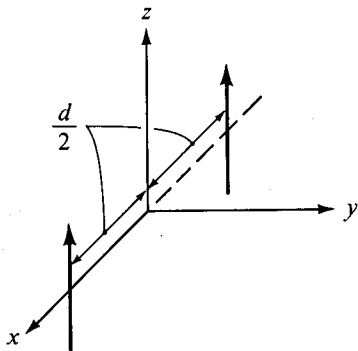


Fig. 6.95. For Problem 6.94.